Aus dem Medizinischen Zentrum für Innere Medizin
des Universitätsklinikums Gießen und Marburg GmbH, Standort Gießen

Medizinische Klinik und Poliklinik II

Leiter: Prof. Dr. W. Seeger

Rechtsventrikuläre Funktion bei pulmonaler Hypertonie - Diagnostik und klinische Relevanz

Kumulative Habilitationsschrift
zur Erlangung der Venia Legendi
des Fachbereichs Medizin
der Justus-Liebig-Universität Gießen

vorgelegt von

Dr. med. Khodr Tello

Gießen 2020

Diese Schrift ist meiner Frau Silke, meinen Töchtern Samira und Hanna und meinen Eltern gewidmet

Inhalt

1 Einleitung

1.1 Einführung

Eine der ersten Schriften über die Bedeutung des rechten Ventrikels stammt aus dem Jahr 1616 von Sir William Harvey. Darin urteilt er: „[D]er rechte Ventrikel ist hauptsächlich da, um Blut durch die Lungen zu pumpen und nicht um diese zu ernähren“ (1,2). Der rechte Ventrikel (RV) galt dennoch lange Zeit als „entbehrlich“ für die gesamte Herzfunktion und wurde als eine lediglich passive Leitung für den Blutfluss zwischen systemischem und pulmonalem Kreislauf angesehen. In der Medizinforschung wurde der RV über Jahrzehnte vernachlässigt und galt als die „vergessene Kammer“. Einige experimentelle Studien legten nahe, dass eine vollständige Zerstörung der freien RV-Wand keine nachweisbare Beeinträchtigung der globalen Herzleistung aufwies, und stützten damit diese Annahme (3). Der RV wurde daher lange Zeit für die Aufrechterhaltung der normalen Hämodynamik als weitaus unbedeutender angesehen als der linke Ventrikel (LV). Es dauerte bis in die 70er Jahre des letzten Jahrhunderts, bis seine Bedeutung und insbesondere seine kontraktile Funktion für die globale Zirkulation aufgezeigt werden konnte. Die rechtsventrikuläre Funktion erwies sich beispielsweise in einer der ersten Studien mit Fokussierung auf den RV als eminent wichtig für die Prognose nach Herztransplantationen und deren Assoziation mit dem pulmonalvaskulären Widerstand (4). Weitere embryologische und physiologische Untersuchungen fokussierten sich daraufhin zunehmend auf den RV. Sie erbrachten interessanterweise, dass der LV und der RV unterschiedliche embryonale Ursprünge haben und dass Adaptationen als Folge von chronischer Druck- und Volumenbelastung auf unterschiedlichen transkriptionellen und translationalen Vorgängen basieren. Dies beinhaltet unterschiedliche Proteinexpressionslevel bezüglich des Metabolismus, unterschiedliche kontraktile Elemente und verschiedene Mechanismen des Remodellings (5). In den letzten Jahrzehnten wurde es daher zunehmend evident, dass die Bedeutung des RV auf das Überleben bezogen der des LV nicht untergeordnet ist und dass vielmehr eine lebenswichtige gegenseitige Abhängigkeit besteht.

Etwa fünf Prozent der westlichen Bevölkerung leiden an Rechtsherzversagen mit unterschiedlichen Ursachen. Das Rechtsherzversagen ist definiert als ein klinisches Syndrom mit Atemnot, Beinödemen, Belastungsluftnot und Fatigue, resultierend aus strukturellen oder funktionellen Störungen des RV mit der Folge einer inadäquaten Füllung oder eines inadäquaten Auswurfs (6). Rechtsherzversagen ist Folge einer Änderung der Vorlast, der Inotropie/Lusitropie oder der Nachlast. Einige Erkrankungen können daher durch akute oder chronische Druck- und Volumenbelastung die Rechtsherzfunktion erheblich beeinträchtigen, zum Beispiel die Lungenarterienembolie, das Linksherzversagen, angeborene Herzerkrankungen, Pulmonal- und Trikuspidalklappenerkrankungen sowie RV-Kardiomyopathien. Eine Erkrankung, die aufgrund ihres progressiven Verlaufs und struktureller Veränderungen der Lungengefäße die Nachlast stetig erhöht, ist die Pulmonal-arterielle Hypertonie (PAH).

PAH und andere Formen der präkapillären Pulmonalen Hypertonie (PH) sind derzeit durch einen mittleren pulmonal-arteriellen Druck (engl. Mean Pulmonary Artery Pressure, mPAP) von ≥ 25 mmHg definiert (7). Eine kürzlich vorgeschlagene neue Definition, die als Grenzwert einen mPAP > 20 mmHg und begleitend einen Lungengefäßwiderstand (engl. Pulmonary Vascular Resistance, PVR) ≥ 3 Wood Units (WU) (8) vorsieht, muss in zukünftigen Richtlinien noch bestätigt werden. Diese neue Einteilung wird jedoch aller Voraussicht nach Einzug in die nationalen und internationalen Leitlinien halten. Der hohe mPAP, der die Erkrankung des Lungenhochdruckes maßgeblich definiert, ist mit strukturellen Veränderungen der Lungengefäße verbunden und bedingt mit einem erhöhten PVR eine hohe Nachlast für den RV (9). Die Prognose der PH wird entscheidend von der Funktion des RV bestimmt (10). Dabei spielt die Adaptation des RV an die gebotene höhere Druck- und Widerstandsbelastung eine große Rolle. Vorspannung, Nachlast und Kontraktilität sind äußerst bedeutend bei der Anpassung

des RV an die erhöhten Druck- und Widerstandsverhältnisse als grundlegende pathophysiologische Charakteristika der PH. Die Vorlast ist definiert als die anfängliche Dehnung der Myozyten vor der Kontraktion, repräsentiert die Wandspannung während der Diastole und hängt entscheidend mit der ventrikulären Füllung zusammen. Kontraktilität ist die intrinsische Fähigkeit des Herzmuskels, sich unabhängig von der Vorspannung zu kontrahieren. Eine Änderung der Vorspannung wirkt sich jedoch auch in einem bestimmten Maß auf die Kontraktionskraft aus. Die rechtsventrikuläre Nachlast bedingt wesentlich die RV-Wandspannung, die während des RV-Auswurfs auftritt. Nach dem Gesetz von Laplace ist die Wandspannung proportional zum Druck während des RV-Auswurfs, multipliziert mit dem Radius des rechtsventrikulären Cavums, geteilt durch die Wanddicke. Der RV-Druck während des Auswurfs wird dabei durch mehrere Komponenten bestimmt: den mittleren Widerstand des pulmonalvaskulären Gefäßbettes, dessen arterielle Compliance und die arteriellen Wellenreflexionen, die aus dem pulsierenden arteriellen Blutfluss resultieren.

Aus dem Laplace-Gesetz und abgeleiteter Wandspannung geht hervor, dass bei hypertrophiertem Ventrikel sowie entsprechend großer Muskeldicke und niedrigem rechtsventrikulären Radius eine niedrigere Muskelspannung genügt, um einen adäquaten Druck zu erzeugen. Bei ausgeprägter Füllung und dementsprechender Vordehnung des Ventrikels kommt es jedoch zu einer Steigerung der Kontraktilität, bei der das überschüssige Volumen mit erhöhtem Druck ausgeworfen wird. Die Dehnung vergrößert den Radius des Ventrikels, sodass sich bei gleicher Muskelspannung eigentlich ein niedrigerer Druck erzeugen ließe. Die Erklärung für diesen Vorgang liefert der Frank-Starling-Mechanismus. Die Fähigkeit des Ventrikels, die Kraft der Kontraktion an Veränderungen der ventrikulären Füllung anzupassen, bildet eine der Hauptsäulen der Herzphysiologie. Der deutsche Physiologe Otto Frank beschrieb erstmalig, dass der Druck maßgeblich von der initialen diastolischen Spannung abhängt, konnte jedoch keinen Beleg dafür erbringen, wie die gesteigerte Kontraktionskraft generiert wird und ob sie von der initialen Spannung oder aber der Länge der Sarkomere/Vordehnung der Myozyten abhängt (11). Dass die Kontraktionskraft maßgeblich von letzterem bestimmt wird, konnte erstmals von Starling und seinen Mitarbeitern belegt werden (12). Somit erklärt der Frank-Starling-Mechanismus die Fähigkeit des Ventrikels, auf veränderte Füllungszustände mit veränderter Kontraktionskraft zu reagieren. Überdies werden grundlegende Adaptationen des Ventrikels als Reaktion auf die Nachlast durch eine große Frank-Starling-Reserve bedingt, bei der eine Zunahme der Nachlast auch mit einer Zunahme der Vorlast einhergeht (13). Dieses Phänomen wird als „Vorlastreserve“ bezeichnet. Eine fortschreitende RV-Dilatation tritt auf, wenn eine Zunahme der Nachlast durch den Frank-Starling-Mechanismus nicht kompensiert werden kann und sich die ventrikuläre Funktion und das Verhältnis aus Kontraktilität und Nachlast zugunsten der Nachlast verschlechtert. Um das Schlagvolumen (SV) zu erhalten, kommt es zur sogenannten „heterometrischen Adaptation“ des RV und zur RV-Dilatation. Der Erweiterung der rechtsventrikulären Volumina als Maladaptationsmechanismus geht die RV-pulmonal-arterielle Entkopplung voraus. Dabei wird die überproportional ansteigende Nachlast nicht mehr durch eine höhere Kontraktilität des RV kompensiert.

Bei PH ist die Reaktion beziehungsweise Adaptation des RV auf die Zunahme der Nachlast (als RV-arterielle Kopplung, engl. RV-Arterial Coupling) die Hauptdeterminante für die Prognose der Patienten (14). Sie resultiert aus einem komplexen Zusammenspiel von neuroendokrinen und parakrinen Signalen und einer erhöhten Nachlast, die in der Folge zu rechtsventrikulärer Myokardischämie, Entzündung und Fibrose sowie zum Verlust von Myozyten führt (15,16).

In diesem Sinne ist es für die PH von zentraler Bedeutung, einerseits die Nachlast zu senken, die zur Belastung des RV führt, anderseits jedoch auch therapeutisch die Maladaptation des RV anzugehen und beispielsweise die rechtsventrikuläre Funktion durch eine Senkung der Nachlast und eine Erhöhung der Kontraktilität zu verbessern. Derzeit sind 14 PAH-spezifische Medikamente verfügbar,

die auf vier PAH-relevante molekulare Signalwege abzielen: spannungsabhängige L-Typ-Calciumkanäle, Endothelin, Prostacyclin/cAMP und Stickoxid/cGMP (7). Bislang sind keine Medikamente verfügbar, für die bei chronischer Anwendung eine direkte Verbesserung der rechtsventrikulären Kontraktilität mit verbesserter Prognose belegt wäre.

Es hat jedoch inzwischen eine Verschiebung weg von dem Dogma gegeben, nur die Wirkungen dieser zugelassenen Arzneimittel auf das Lungengefäßsystem zu berücksichtigen, hin zur Untersuchung möglicher direkter Wirkungen auf den RV und seiner Interaktion mit dem Lungenarteriensystem. Um die direkten Wirkungen bestehender und zukünftiger Therapien auf die RV-Funktion zu bewerten, müssen zunächst die verschiedenen und vielfältigen invasiven und non-invasiven Methoden zur Erfassung der RV-Funktion, ihre Vor- und Nachteile und ihre Rolle im Zusammenhang mit PAH eingehend untersucht werden.

1.2 Kontraktile RV-Funktion und RV-arterielle Kopplung

Die Erfassung der RV-Funktion ist für die Nachsorge und Behandlung von Patienten mit PH von entscheidender Bedeutung. Die Echokardiografie ist allgemein zugänglich, nichtinvasiv und bietet eine umfassende Beurteilung der systolischen und diastolischen RV-Funktion. Darüber hinaus ist die kardiale Magnetresonanztomographie (kMRT, engl. Cardiac Magnetic Resonance Imaging, cMRI) ein zunehmend wichtiges Instrument zur Überwachung der RV-Funktion bei PH. Echokardiografie und kMRT bieten jedoch aufgrund der Abhängigkeit der erfassten Parameter von der Nachlast im besten Fall nur indirekte Werte für die RV-Kontraktilität. Zur Beurteilung der nachlastunabhängigen Kontraktilität stehen Techniken zur Verfügung, die über Druck-Volumen-Beziehungen im RV die Kontraktilität mittels dafür vorgesehener Druck-Volumen-Katheter (Konduktanz-Katheter) direkt messen (10). Obwohl die Durchführbarkeit dieser Techniken beim Menschen gezeigt worden ist (17,18), weisen sie große Nachteile auf, die sie für den täglichen klinischen Gebrauch unpraktisch machen. Dazu gehören die Komplexität der Datenerfassung und Analyse, die invasive Natur der Messungen und die erheblichen Gerätekosten. Um jedoch ein klares Verständnis von der RV-Physiologie zu erhalten, mögliche Ersatzuntersuchungen für den Konduktanz-Katheter zu identifizieren und Arzneimittelwirkungen auf den RV zu bewerten, sind Erfassungen der Kontraktilität, der Nachlast und der RV-arteriellen Kopplung, die aus der Druck-Volumen-Beziehung herrühren, derzeit unerlässlich. Die Informationen zur RV-Funktion, die durch Druck-Volumen-Schleifen, Echokardiografie und kMRT bereitgestellt werden, werden nachstehend ausführlich beschrieben.

<u>Druck-Volumen-Schleifen: physiologische Ansätze zur Messung der RV-arteriellen Kopplung</u>

Der Ventrikel weist eine elastische Struktur auf, die sich während des Herzzyklus entlang eines Zeitverlaufs kontrahiert (und entspannt) und mittels einer zeitlich variierenden Elastizität charakterisiert ist (19). Basierend auf diesem Prinzip kann die ventrikuläre Kontraktilität durch die Erzeugung mehrerer Druck-Volumen-Schleifen während der Lastmanipulation bestimmt werden, wie zuerst für den LV beschrieben (19) und anschließend für den RV übernommen (20,21) (Abbildung 2). Das maximale endsystolische Verhältnis von Druck und Volumen wird für jede einzelne Druck-Volumen-Schleife bestimmt. Dies ist der einzige Punkt der Druck-Volumen-Beziehung, der für auswerfende und nichtauswerfende Herz-Schläge in der Systole typisch ist, und daher der optimale Punkt, der sich von einer isolierten aktiven Muskel-Kraft-Längen-Beziehung eines Muskels für eine Druck-Volumen-Beziehung des Ventrikels adaptieren lässt. Dabei korrespondiert Druck mit Kraft und Volumen mit Länge. Eine lineare Regressionslinie, die diese Druck-Volumen-Punkte verbindet, wird dann verwendet, um die endsystolische Druck-Volumen-Beziehung zu bestimmen. Die Steigung dieser Linie ist die endsystolische Elastizität (engl. End-Systolic Elastance, Ees) und ein weitgehend lastunabhängiges Maß für die Kontraktilität des Ventrikels.

Im frühen Verlauf der PH erhöht der RV die Kontraktilität als Reaktion auf die erhöhte Nachlast (Abbildung 1). Diese Anpassung wird als homöometrische Anpassung bezeichnet und ist erstmals von Anrep (22) beschrieben worden. Zu den Mechanismen, die zur Erhöhung der Kontraktilität führen, gehören autokrine und parakrine Reaktionen auf Muskel-Dehnung, Veränderungen der Myofilamenteigenschaften (23) und Muskelhypertrophie. Um das Zusammenspiel zwischen RV-Kontraktilität und arterieller Nachlast (RV-arterielle Kopplung) zu bewerten, wird Ees relativ zur arteriellen Elastizität (engl arterial elastance, Ea) ausgedrückt. Ea ist ein zusammenfassendes Maß für die Nachlast, das sowohl ohmsche (resistive) als auch pulsierende Lastkomponenten berücksichtigt. Andere Messungen der Nachlast umfassen die der Ventrikelwandspannung und der Lungenarterien-Impedanz. Die Messung dieser Variablen ist jedoch aufwendig und erfordert die Messung der Wanddicke, des maximalen Drucks und Volumens (für die Ventrikelwandspannung) oder gleichzeitige Messungen von Druck und Fluss (24). Die Vereinfachung der arteriellen Last mittels Definition einer sogenannten „effektiven Ea“ ist erstmals von Sunagawa et al. vorgeschlagen worden (25,26). Ea ist als ein stationärer arterieller Parameter definiert, der die Hauptelemente der Gefäßlast ($Ea = RT / [ts + \tau (1-e-td/\tau)]$) enthält, wobei RT der mittlere Gesamtwiderstand, ts und td systolische und diastolische Zeitintervalle und τ die Zeitkonstante des diastolischen Druckabfalls (Produkt aus Widerstand und Compliance) sind. Dieser Parameter kann auch durch das Verhältnis des endsystolischen Drucks (engl. End-Systolic Pressure, ESP) zum SV (ESP/SV) abgeschätzt werden, das aus einer Druck-Volumen-Schleife ermittelt wird. Wichtig ist, dass diese vereinfachte Version gemeinsame Einheiten mit Ees (mmHg/l) aufweist und die Beurteilung der RV-arteriellen Kopplung als Verhältnis der Elastizitäten ermöglicht. Die Sunagawa-Methode ist sowohl im systemischen als auch im pulmonalen Kreislauf validiert worden (27,28). Aus Druck-Volumen-Schleifen abgeleitete Ea bieten daher eine sehr nützliche Methode zur Beurteilung der jeweiligen arteriellen Last und ihrer Auswirkung auf den Ventrikel. Zu betonen ist jedoch, dass Ees und Ea den Nachteil haben, dass sie die Herzfrequenz nicht berücksichtigen, obwohl sich die Herzfrequenz auf die Vorlast (durch Ändern der diastolischen Dauer), die Nachlast (durch Beeinflussung der Impedanz) und die Kontraktilität (Kraft-Frequenz-Beziehung) auswirkt.

Durch eine Erhöhung der Ees bleibt die Kopplung (das Verhältnis der Ees zu Ea) bei steigender Nachlast zunächst erhalten. Das ideale Kopplungsverhältnis für einen optimalen Energietransfer vom Ventrikel zum arteriellen System wird allgemein mit 1,5–2,0 angenommen. Diese Annahme basiert jedoch auf Untersuchungen von isolierten LV des Hundes. Es beschreibt das optimale Verhältnis von Ees/Ea bei maximaler Schlagarbeit (engl. Stroke Work, SW) (25). De Tombe et al. (1993) (29) zeigten, dass die maximale SW in isolierten Hundeherzen im Durchschnitt bei $Ea/Ees = 0,80 \pm 0,16$ ($Ees/Ea \sim 1,25$) liegt, während die maximale ventrikuläre Effizienz (SW/myokardialer Sauerstoffverbrauch) bei $Ea / Ees = 0,70 \pm 0,15$ ($Ees / Ea \sim 1,4$) liegt. In jüngerer Zeit haben Axell und Mitarbeiter (2017) die „Ees/Ea“-Schwelle bei maximaler RV-SW unter Verwendung eines Tiermodells auf 0,68 festgelegt, wobei Werte unter dieser Schwelle auf eine RV-Dysfunktion hinweisen (30). Mit fortschreitender PH kommt es zu einer Dilatation des RV, um das SV und folglich das Herzzeitvolumen aufrechtzuerhalten, was als „heterometrische Anpassung“ bezeichnet wird. Es ist noch unklar, warum es bei einigen PH-Patienten primär zu einer homöometrischen und bei anderen schon sehr früh zu einer heterometrischen Anpassung kommt. Eine mögliche Erklärung ist, dass die homöometrische Anpassung aufgrund der Auswirkungen der chronischen Drucküberlastung und der neurohormonalen Aktivierung auf die intrinsische Kardiomyozytenfunktion mit unterschiedlichem individuellen zeitlichem Muster versagt. Gegenwärtige Methoden zur Bestimmung des Zeitpunkts einer RV-Maladaptation während der Nachsorge bei Patienten mit PH umfassen u.a. die Überwachung der ventrikulären Masse und des Volumens (31). Die Entkopplung des RV-arteriellen Verhältnisses könnte jedoch viel früher beginnen, bevor die ventrikuläre Dilatation und die Reduktion des Masse/Volumen-Verhältnisses offensichtlich sind.

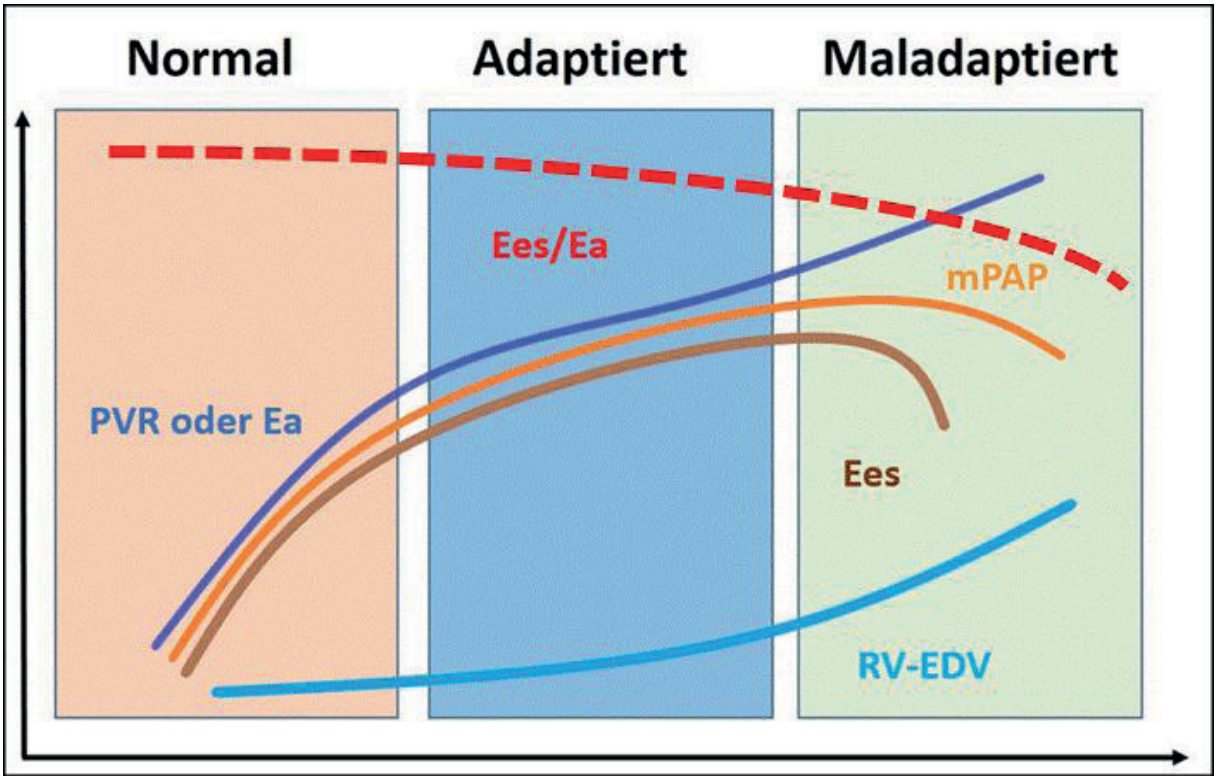

Abbildung 1: Grafische Darstellung des rechtsventrikulären Adaptationsprozesses bei pulmonaler Hypertonie. Bei fortschreitender Erkrankung und steigender Nachlast (Pulmonal-vaskulärer Widerstand (PVR) und arterieller Elastizität (Ea)) kommt es zu einer kompensatorischen Erhöhung der lastunabhängigen Kontraktilität (Endsystolische Elastizität (Ees)) (homöometrische Adaptation). Dabei wird zunächst das Verhältnis Ees/Ea und damit die rechtsventrikuläre-arterielle Kopplung erhalten. Es wird angenommen, dass die Steigerung der Kontraktilität primär durch Muskelhypertrophie erreicht wird. Bei fehlender Adaptation der Kontraktilität an die steigende Nachlast kommt es zu einer RV-arteriellen „Entkopplung", bei der Ea Ees übersteigt. Weitere Adaptationsmechanismen kommen dann zum Tragen, vornehmlich die rechtsventrikuläre Dilatation (heterometrische Dilatation), um das SV zu erhalten. Adaptiert nach (10)

Ees: Endsystolische Elastizität; Ea: arterielle Elastizität; PVR: Pulmonary Vascular Resistance (pulmonal-vaskulärer Widerstand); mPAP: mean Pulmonary Artery Pressure (mittlerer pulmonal-arterieller Druck); RV-EDV: rechtsventrikuläres enddiastolisches Volumen

1.3 Methodik: Konstruktion und Bewertung von RV-Druck-Volumen-Schleifen

Die erste Arbeitsgruppe, die RV-Druck-Volumen-Schleifen von menschlichen Freiwilligen mit normaler hämodynamischer Funktion konstruierte, verwendete Abdrücke von menschlichen und tierischen rechten Ventrikeln und platzierte sie in ihrer anatomischen Position auf dem Herzkatheter-Tisch, um das RV-Volumen abzuschätzen (21). Eine andere Gruppe verwendete die Ventrikulografie zur Bestimmung des Volumens und kombinierte sie mit der Druckmessung, um Druck-Volumen-Schleifen zu erzeugen (32).

Mit der Entwicklung des Druck-Volumen-Katheters und seiner Validierung für die Messung des RV-Volumens (33) wurde die Erforschung von RV-Druck-Volumen-Schleifen weiter verbreitet, da die Bewertung einfacher und direkter durchzuführen ist als in früheren Methoden beschrieben. Der

Konduktanz-Katheter misst gleichzeitig Druck und Volumen. Das Volumen wird gemessen, indem ein elektrisches Feld zwischen der proximalen und der distalen Elektrode des Katheters angelegt wird, wenn die Katheterspitze (mittels Echokardiografie oder Radiografie) adäquat in der RV-Spitze positioniert wird. Die elektrische Leitfähigkeit wird von den übrigen Elektroden kontinuierlich gemessen, Änderungen der Leitfähigkeit spiegeln Änderungen des Segmentvolumens wider. Der Katheter wird entweder über kMRT oder mit hypertoner Kochsalzlösung volumenkalibriert, wobei die kMRT-Methode weiter verbreitet ist.

Der Katheter wurde in mehreren Studien eingesetzt (Tabelle 1). Diese Studien umfassten Patienten mit idiopathischer oder mit systemischer Sklerose assoziierter PAH (17,18), systemischer Sklerose ohne PH (18), chronisch thromboembolischer pulmonaler Hypertonie (CTEPH) (30), (34), Fallot-Tetralogie (35) und Herzinsuffizienz mit erhaltener Ejektionsfraktion (36) sowie mit Zustand nach Lungenresektion (37). Der Hauptunterschied zwischen diesen Studien besteht in der Methode zur Beurteilung der RV-arteriellen Kopplung. In vier der Studien (Hsu et al., 2016; Latus et al., 2013; Rommel et al., 2018; Tedford et al., 2013) wurde Ees unter Verwendung einer sogenannten Multi-Beat-Methode mit kontrollierter Reduktion der Vorlast entweder durch Ballonokklusion der Vena cava inferior oder durch das Valsalva-Manöver bestimmt. Dabei wurden mehrere Herzschläge nach Ballonokklusion oder in der zweiten Phase des Valsalva-Manövers aufgenommen, die als Grundlage der Berechnung von Ees verwendet werden (Abbildung 2). Die Valsalva-Methode wurde erstmals 2013 beschrieben. Es zeigte sich, dass in der zweiten Phase des Manövers die RV-Vorlast signifikant reduziert wird (38). Anschließend wurde diese Methode durch die Multibeat-Messung von Druck-Volumen-Schleifen mit Vena-cava-Ballonokklusion validiert (18). In den verbleibenden Studien (Axell et al., 2017; McCabe et al., 2014; Wink et al., 2016) wurde der Konduktanz-Katheter verwendet, um ESP als einen der wesentlichen Werte zum Erhalt von Ees exakt zu messen. Dieser Wert ist unabdingbar für die Bestimmung der Kopplung nach der sogenannten „Single-Beat-Methode“ (39). Diese Methode hat den Vorteil, dass lediglich ein Herzschlag zur Ermittlung von Ees und Ea benötigt wird und dementsprechend auf die invasive Ballonokklusion der Vena cava verzichtet werden kann. Bei der Single-Beat-Methode wird Ea als ESP/SV und Ees als (Pmax – ESP)/SV berechnet, wobei Pmax als der maximale theoretische Druck geschätzt wird, der sich durch das Klemmen der Pulmonalklappe und damit in einem nichtauswerfenden Herzschlag aufbauen würde. Frühe und späte Abschnitte der RV-Druckkurve werden mittels der Methode der kleinsten Quadrate in eine Sinuswelle extrapoliert (Abbildung 2B). Pmax wird als Maximum der Sinuswelle bestimmt.

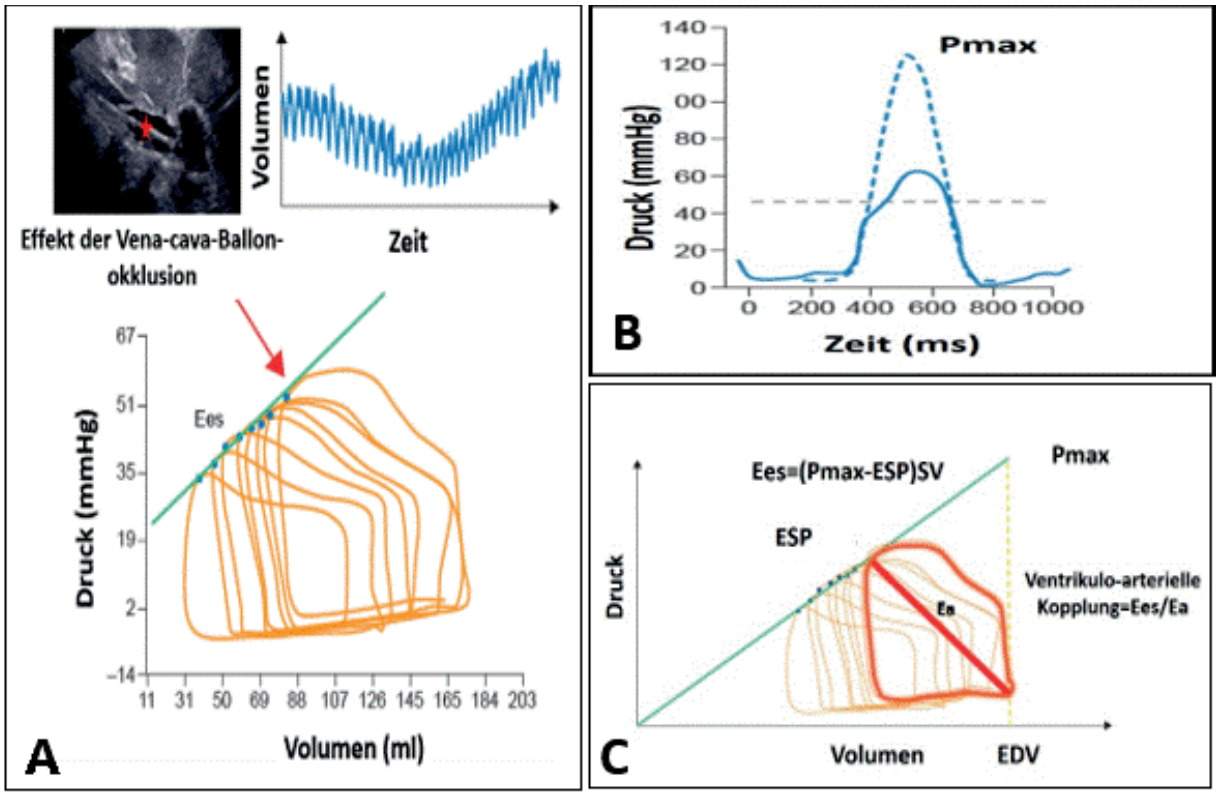

Abbildung 2: Darstellung verschiedener Methoden der Erfassung der lastunabhängigen Kontraktilität mittels Multi-Beat-Methode (A) und Single-Beat-Methode (B und C). **A**: Durch Vorlastreduktion und Vena-Cava-Ballon-Okklusion (mit rotem Sternchen markierter Ballon in der Vena cava) erfolgt eine Volumenreduktion und eine Volumenverschiebung nach links. Die Steigung in den endsystolischen Druck-Volumen-Relationen (ESPVR) ergibt die endsystolische Elastizität (Ees). **B**: Die Druck/Zeit-Kurve des rechten Ventrikels dient als Grundlage zur Berechnung des sogenannten Pmax, den theoretisch maximal möglichen Druck bei geschlossener Pulmonalklappe. Durch Extrapolation der isovolumetrischen Druckbereiche mittels Methode der kleinsten Quadrate in eine Sinuskurve (gestrichelte Linie) erfolgt die Herleitung des Pmax. **C**: Der Pmax dient in der sogenannten Single-Beat-Methode als Druckpunkt, um die Ees, definiert als Steigung zwischen Pmax und endsystolischem Druck, aus einem einzelnen Herzschlag zu berechnen. Ea: arterielle Elastizität; EDV: enddiastolisches Volumen; ESP: endsystolischer Druck, SV: Schlagvolumen. Abbildung adaptiert aus (40) mit Erlaubnis.

Die Single-Beat-Methode wurde zuerst für den LV beschrieben (41) und später für den RV übernommen (39). Ihre Haupteinschränkung ist die Tatsache, dass sie bei normotensiven Hunden für den RV validiert worden ist. Es bleibt daher unklar, ob sie ein zuverlässiges Maß für die Kontraktilität des RV beim Menschen ist. Inuzuka et al. verglichen die Single-Beat-Messung mit der direkten Multi-Beat-Messung von Ees über die Vorspannungsreduktion beim Menschen. Die Ergebnisse zeigten nur eine geringe Korrelation zwischen der Single-Beat- und der Multi-Beat-Methode (42).

1.4 Beurteilung der diastolischen Funktionsstörung des rechten Ventrikels

Untersuchungen aus jüngerer Zeit zeigen, dass die diastolische RV-Funktion für die Prognose der PH-Patienten von besonderer Bedeutung ist und dass eine erhöhte diastolische RV-Steifheit signifikant mit Ereignissen wie Mortalität und Lungentransplantation assoziiert ist (14,43). Beispielsweise wurde bei Patienten, die drei Monate lang eine PAH-spezifische Therapie erhalten haben, eine signifikant geringere diastolische RV-Steifheit im Vergleich zu den Werten vor der Behandlung gefunden (44).

Über den LV ist bekannt, dass eine diastolische Dysfunktion und Steifheit Hauptursachen für Herzversagen sind. Dabei ist das Herzversagen bei erhaltener Auswurffraktion (engl. Heart Failure With Preserved Ejection Fraction, HFpEF) hinlänglich bezüglich einer Diagnostik und Therapie untersucht worden (45). Daher ist ein wesentlicher Bestandteil der routinemäßigen Untersuchung von Patienten mit Herzversagen die Beurteilung der linksventrikulären diastolischen Funktion mittels Echokardiografie.

Bezüglich der rechtsventrikulären diastolischen Funktion gibt es derzeit keine valide nichtinvasive Methode, die die RV-Steifheit ausreichend beschreibt. Die diastolische RV-Funktion wird physiologisch typischerweise aus der enddiastolischen Druck-Volumen-Beziehung (engl. End-Diastolic Pressure Volume Relationship, EDPVR) quantifiziert. Unter idealen Bedingungen würde die EDPVR aus Druck-Volumen-Schleifen mit mehreren Schlägen und Vorlastreduzierung gemessen. Die Werte Endsystolisches Volumen (ESV)/Beginn-diastolischer Druck (engl., Begin-Diastolic Pressure, BDP) und Enddiastolisches Volumen (EDV)/Enddiastolischer Druck (engl. End-Diastolic Pressure, EDP) werden aus jeder einzelnen Druck-Volumen-Schleife bestimmt und dann an eine EDPVR angepasst (46). Aufgrund der Invasivität der Druck-Volumen-Messungen und der hohen Kosten werden alternative Wege in Betracht gezogen. Dazu wird beispielsweise die EDPVR aus einem einzelnen Herzschlag berechnet. RV-Druckpunkte aus der Rechtsherzkatheter-Messung werden zur Bestimmung des BDP und des EDP verwendet, während die kMRT zur Bestimmung von ESV und EDV herangezogen wird. Im LV ist die EDPVR mithilfe von Exponential- und Kubikgleichungen beschrieben worden. Aktuelle Studien zur diastolischen Funktion des RV verwenden eine Exponentialanpassung, um die diastolische Steifheit des RV (engl. End-Diastolic Elastance, Eed) zu beschreiben (14,43,44). Die Ableitung des EDPVR ist ein Maß für die RV-Steifheit oder die Druckänderung bei gegebener Volumenänderung und wird von den Eigenschaften des Myokards, der Ventrikelstruktur und der extrazellulären Matrix beeinflusst (47).

Um den Pathomechanismus des RV-Versagens zu verstehen, ist es wichtig, zwischen volumenabhängigen Änderungen der diastolischen RV-Steifheit und allgemeinen Änderungen der Ventrikelsteifheit zu unterscheiden. In einem Pulmonalarterien-Banding-Modell der Rechtsherzinsuffizienz bei Ratten erhöht eine anhaltende Drucküberlastung des RV die intrinsische Steifheit der freien Wand, orientiert Myofasern und Kollagenfasern in Längsrichtung um (von basal zum Apex) und erhöht die intrinsische Steifheit der Myofasern (48). Diese Veränderungen in der Biomechanik der freien RV-Wand sind mit erhöhten Werten der diastolischen RV-Steifheit in den hämodynamischen Messungen verbunden. Ein möglicher molekularer Mechanismus für eine erhöhte diastolische Steifheit ist neben Matrixveränderungen/Fibrose der Ventrikelwand eine Veränderung der Titinphosphorylierung, die die Steifheit von RV-Sarkomeren reguliert (46). Zusätzliche Veränderungen auf zellulärer Ebene, die möglicherweise zu Veränderungen der diastolischen Steifheit beitragen können, umfassen eine Erhöhung der Kalzium-Empfindlichkeit (Ca^{2+}) aufgrund einer verminderten Phosphorylierung von Troponin I und/oder eine verminderte Clearance von diastolischem Ca^{2+} (49).

Die diastolische RV-Steifheit ist ein potenzieller Frühindikator für RV-Versagen und Krankheitsprogression (50), da sie eine zentrale Bedeutung bei der Anpassung an eine erhöhte Nachlast bei PH hat. Patienten mit PAH, die mehr als fünf Jahre überlebt hatten, zeigten eine erhöhte diastolische Steifheit im Vergleich zu Patienten ohne PH; dieser Unterschied war aber nach Normalisierung der Wandstärke nicht mehr erkennbar (51). Patienten mit PAH, die weniger als fünf Jahre überlebt hatten, hatten eine Zunahme der diastolischen RV-Steifheit, die nicht durch eine Zunahme der Wandstärke erklärt wurde, was darauf hindeutet, dass die intrinsische Myokardsteifheit in verschiedenen Stadien der PAH eine entscheidende Rolle spielen kann.

1.5 Echokardiografie des rechten Ventrikels

Die Echokardiografie ist eines der wichtigsten Screening-Instrumente bei der Beurteilung der PH (7) und wird zur Beurteilung der RV-Funktion in der täglichen klinischen Routine verwendet. Als indirektes Maß für die RV-Funktion hat sich die Größe des rechten Vorhofs als prognostisch relevant erwiesen (52,53). Die systolische Exkursion der Trikuspidalklappenebene (engl. Tricuspidal Annular Plane Excursion, TAPSE) wird häufig als Marker für die RV-Funktion verwendet. In einer Studie mit 47 Patienten mit PAH war TAPSE mit Überleben assoziiert (54). Jedoch konnte in einer anschließenden Studie mit 777 Patienten mit präkapillärer PH (insbesondere Patienten mit funktioneller Klasse III–IV der New York Heart Association (NYHA) und RV Dilatation) kein Zusammenhang mit Mortalität gezeigt werden. Obwohl TAPSE einfach zu messen ist, spiegelt dieser Parameter vorwiegend die basolaterale longitudinale RV-Funktion wider und ist sowohl volumen- als auch lastabhängig (52). Der RV-Fractional-Area-Change (FAC) ist ebenso ein im 2D-Echo zu bestimmendes Maß, das die endsystolische (engl. End-Systolic Area, ESA) mit der enddiastolischen Fläche (engl. End-Diastolic Area, EDA) ins Verhältnis setzt (EDA-ESA/EDA). FAC zeigte ebenso Assoziationen zur Prognose von PH-Patienten (52) und ist ein einfach zu ermittelnder Parameter. Ein weiterer valider und einfach zu messender Wert der RV-myokardialen Leistung ist der „RV Myocardial Performance Index“, ein zusammengesetztes Maß für die systolische und diastolische Funktion. Werte von ≥ 0,64 (52) und > 0,88 (55) sind prognostisch relevant.

Neben den traditionellen und gut etablierten direkten und indirekten Messungen der RV-Funktion wurden in den letzten Jahren einige sehr interessante neue Echokardiografie-Techniken eingeführt. Aufgrund der komplexen Geometrie des RV kann die 2D-Echokardiografie den Einfluss- und Ausflusstrakt nicht in einer Aufnahme erfassen. Dagegen bietet die Echtzeit-3D-Echokardiografie ein vielversprechendes Instrument zur Quantifizierung der RV-Funktion, da sie die komplexe RV-Struktur inklusive des Ausflusstrakts erfasst, welcher 25 Prozent des RV-Volumens ausmacht. Darüber hinaus wurde die 3D-Echokardiographie gegen den Goldstandard der kMRT-bestimmten Volumetrie validiert. Zudem liegen mittlerweile Referenzwerte für die Volumetrie vor (56,57). Ein weiteres nützliches Instrument zur Erfassung der rechtsventrikulären Funktion ist der sogenannte longitudinale Strain, also die Messung der longitudinalen Deformation des Myokards im B-Bild mit der sogenannten Speckle-Tracking-Methode. Dabei werden verschiedene Punkte (engl. Speckles) im B-Bild über den kardialen Zyklus verfolgt (engl. Tracking). Im 3D Echo können zudem die Deformationen in der radiären und der zirkumferenziellen Ebene gemessen werden. Es konnte gezeigt werden, dass die echokardiografisch ermittelte 3D-RV-Ejectionsfraktion (EF), der Strain der freien Wand und die FAC das Outcome bei PH vorhersagen (58). Darüber hinaus hat eine kürzlich durchgeführte Metaanalyse gezeigt, dass mittels 3D- und 2D-Echokardiografie gemessener longitudinaler RV-Strain bei PH-Patienten ein Überlebensprädiktor sein kann (59).

1.6 Echokardiografische Surrogate für die RV-arterielle Kopplung

Guazzi et al. schlagen einen einfachen Ansatz zur Bewertung der RV-Kontraktilität in vivo vor. Die Längsbewegung des basolateralen Segmentes des RV, repräsentiert durch die TAPSE, wird dabei gegen die Kraft aufgetragen, die zur Überwindung der auferlegten Last erzeugt wird (dargestellt durch pulmonal-arteriellen systolischen Druck [engl. Pulmonary Artery Systolic Pressure, PASP]) (60). Sie maßen die Beziehung zwischen TAPSE und PASP bei Patienten mit Herzinsuffizienz mit verringerter EF (engl. Heart Failure With Reduced Ejection Fraction, HFrEF) oder erhaltener EF (HFpEF). Das TAPSE/PASP-Verhältnis war dabei ein signifikanter prognostischer Indikator. Die Autoren beschreiben zudem das PASP/ESA Verhältnis als Maß für die Ees. Dies basiert auf der Annahme, dass PASP mit ESP korreliert und V0 (Schnittpunkt der Ees an der X-Achse der Druck-Volumenbeziehung) vernachlässigbar

ist. Dadurch wird Ees von der ursprünglichen Gleichung (Pmax – ESP/SV) vereinfacht zu PASP/ESA. Dabei setzen die Autoren ESA mit ESV gleich. Ea wird dementsprechend zu PASP/SV vereinfacht. Die genannten hergeleiteten Parameter wurden mit TAPSE/PASP verglichen. Es zeigte sich, dass das TAPSE/PASP-Verhältnis bei Patienten mit HFpEF eine signifikante Korrelation mit dem vorgeschlagenen Surrogat der Kopplung (Kontraktilität = PASP/ESA; Nachlast = PASP/SV) aufweist. Die Autoren verwenden daher das TAPSE/PASP-Verhältnis zur Beschreibung der RV-arteriellen Kopplung bei diesen Patienten (61). Eine Validierung mit Druck-Volumen-Kathetern und ein Vergleich mit direkt ermittelten Ees/Ea-Werten ist nicht erfolgt. Mit abnehmendem TAPSE/PASP-Wert wurden erhöhte Werte kardialer Belastungsmarker (Brain Natriuretic Peptide, BNP) und eine Verschlechterung der systemischen und pulmonalen Hämodynamik, der aeroben Belastungskapazität und der Atemeffizienz beobachtet (61). Die Autoren berichten auch über eine signifikante Korrelation zwischen TAPSE und PASP sowie der Compliance der Lungenarterien.

In den letzten Jahren wurden mehrere echokardiografische Indizes der RV-Funktion vorgeschlagen, um die RV-arterielle Kopplung bei Patienten präziser zu beschreiben, einschließlich des Verhältnisses von RV-FAC zu mPAP (gemessen im Rechtsherzkatheter) (62), der FAC zur ESA (63) und des Verhältnisses von TAPSE zur Pulmonalarterien-Akzelerationszeit (engl. Pulmonary Artery Acceleration Time, PAAT) in der Flusskurve der Pulmonalarterie (64). Keines dieser vorgeschlagenen echokardiografischen Surrogate wurde jedoch direkt mit dem Goldstandard der per Druck-Volumen-Katheter generierten Kontraktilität verglichen. Kürzlich wurde ein echokardiografisches Surrogat für die RV-arterielle Kopplung vorgeschlagen, das auf dem SV und dem ESV basiert und im 3D-Echo gemessen wird. Das Maß korrelierte gut mit der RV-arteriellen Kopplung, die aus kombinierten kMRT- und hämodynamischen Messungen berechnet wurde (65), wobei aber die letztere kMRT-basierte Methode ebenso nicht mit Druck-Volumen-Schleifen validiert wurde (weitere Einzelheiten im folgenden Abschnitt zu kMRT-Surrogaten). Interessanterweise wurde die Echtzeit-3D-Echokardiografie auch in Kombination mit hochsensitiven RV-Druckmessungen verwendet. Dabei nutzten die Autoren spezielle Druck-Katheter für den RV und führten gleichzeitig Volumenmessungen des RV mittels 3D-Echokardiografie durch, um Druck-Volumen-Schleifen während der routinemäßigen Herzkathetermessung bei Patienten mit angeborener Herzkrankheit zu erzeugen (66). Dabei konnte die Gruppe Druck-Volumen-Schleifen semi-invasiv erzeugen.

1.7 Kardiales MRT (kMRT)

Die kardiale MRT wird derzeit als Goldstandardtechnik zur Bewertung von RV-Volumen und -Funktion angesehen und wird für die Nachsorge von Patienten mit PH empfohlen (7). Volumenmessungen einschließlich des SV, des RV-EDV und des RV-ESV spiegeln den RV-Anpassungsprozess wider, haben prognostischen Wert und sind leicht zu bestimmen (67,68). Es konnte gezeigt werden, dass RV-EF und das Verhältnis von SV zu ESV einen prognostischen Wert bei Patienten mit PH haben (14,69,70). Ein niedriger SV-Index zu Studienbeginn und eine Verringerung des SV-Index sind mit einer erhöhten Mortalität assoziiert (68). Die Erfassung der RV-Masse ist ebenfalls von großer Bedeutung. Das Masse-Volumen-Verhältnis liefert einen wertvollen prognostischen Parameter, da geringere Masse-Volumen-Verhältnisse (exzentrische Hypertrophie) mit einer schlechteren NYHA-Funktionsklasse verbunden sind und eine klinische Verschlechterung vorhersagen (71). Darüber hinaus ist kürzlich gezeigt worden, dass die RV-Masse das Outcome bei PAH vorhersagt (72).

Die kMRT liefert ferner wichtige Informationen bezüglich des Zusammenspiels des RV mit dem LV, der „interventricular dependence“. Unter normalen Umständen ist die Auswirkung des rechten auf den LV zu vernachlässigen. Bei chronischer Überlastung durch einen erhöhten RV-Druck führen RV-Hypertrophie und -Dilatation jedoch zu einer Verschiebung des Septums zur linken Seite und zu einer zusätzlichen Kompression des LV. Zusätzlich wird die linksventrikuläre Füllung durch ein verringertes

RV-SV ebenfalls beeinträchtigt (73), was mittels einer kMRT-Volumetrie zeitnah ermittelt werden kann.

Ein weiteres hinlänglich untersuchtes diagnostisches Instrument ist das „Delayed Enhancement“, eine bekannte und etablierte Technik in der kMRT. Es ist festgestellt worden, dass ein spätes Gadolinium-Enhancement am RV-Insertionspunkt signifikant mit einem erhöhten mPAP assoziiert ist und das Überleben bei PAH vorhersagt (74). Zudem ist ein Zusammenhang mit einer verringerten regionalen Kontraktilität (75) dargestellt worden. Dies sind Daten, die zukünftig den Weg für einen Einsatz des „Delayed Enhancements“ in der Diagnostik der PH im kMRT ebnen könnten. Während das „Delayed Enhancement“ lokalisierte myokardiale Veränderungen darstellt, identifiziert das sogenannte T1-Mapping eher diffuse myokardiale Veränderungen, indem native RV T1-basierend auf T1-Zeiten vor und nach dem Kontrast gemessen werden (76). Das T1-Mapping wird als ein Marker für Fibrose beschrieben (77) und könnte die Früherkennung einer myokardialen Beteiligung bei PH ermöglichen (78). In neueren Publikationen wird eine Assoziation des T1-Mappings mit der Lungenarteriensteifheit (engl. Pulmonary Artery Stiffness, PA-Stiffness) (79) aufgezeigt. Das T1-Mapping ist jedoch kein Indikator, der eine prognostische Aussage unabhängig von der Größe und Funktion des RV bei Patienten mit PAH ermöglicht (80).

Ein mittlerweile etabliertes und hochinteressantes Maß der im MRT ermittelten RV-Funktion ist MRT-Strain, ein neues Maß zur Erfassung der regionalen Deformation des Herzmuskels. Dabei werden analog zur Speckle-Tracking-Methode der Echokardiografie während des kardialen Zyklus sogenannte Voxels im MRT-Bild verfolgt. Dies erlaubt eine Analyse der Myokardverformung. Diese Technik ist vorteilhaft, da sie in der Routine-Erfassung einer RV-MRT-Diagnostik zugänglich und keine weitere Bildbearbeitung notwendig ist.

1.8 Surrogate der kardialen MRT für die RV-arterielle Kopplung

Sanz und Kollegen beschrieben 2012 (81) eine Methode zur Vereinfachung der Kontraktilitätsmessungen ohne Durchführung von Druck-Volumen-Kathetermessungen und nur basierend auf MRT. Analog zur Methode von Guazzi und Kollegen bezüglich der RV-arteriellen Kopplung in der Echokardiografie (60) vernachlässigt diese Methode V0. Die Methode beschreibt somit Ees als das Verhältnis von ESP zu ESV. Zusätzlich zu dieser Annahme werden ESP durch mPAP ersetzt und Ea als mPAP/SV berechnet. Dadurch wird die Methode deutlich vereinfacht, da nun reine Rechtsherzkatheter-Daten und MRT-Volumetrie ausreichend für eine Bestimmung der RV-arteriellen Kopplung sind. Allerdings haben Trip et al. (82) gezeigt, dass erstens V0 bei PAH nicht vernachlässigbar ist und von der RV-Dilatation abhängt und zweitens Ees, gemessen als mPAP/ESV (wobei V0 vernachlässigt wird), signifikant niedriger ist als Ees, gemessen als (Pmax–mPAP)/(EDV – ESV).

Die kardiale MRT wurde interessanterweise bei der ersten Beurteilung von Druck-Volumen-Schleifen bei Patienten mit PAH verwendet (n=6). Volumenmessungen aus der kMRT wurden mit Druckmessungen aus einer konventionellen Rechtsherzkatheter-Untersuchung synchronisiert (83).

1.9 Prognostische Relevanz von Parametern der RV-Funktion

Die Bedeutung des RV für die Prognose bei PH ist unstrittig und gilt als die Hauptdeterminante des Überlebens. Durch die zahlreichen Untersuchungsmodalitäten des RV ist es jedoch von besonderer Wichtigkeit, die verschiedenen Parameter der direkten oder indirekten RV-Funktion zu definieren, die eine prognostische Aussage erlauben. In den konventionellen Untersuchungstechniken gibt es einige Parameter, die invasiv oder non-invasiv bestimmt werden und mit Prognose bei Rechtsherzinsuffizienz assoziiert sind. Echokardiografische Prädiktoren des Überlebens sind beispielsweise die Größe des RV (84), Zeichen eines Perikardergusses (85), die TAPSE (84), die maximale Geschwindigkeit im Gewebedoppler, das sogenannte Systolic Tissue Doppler Imaging (Gewebedoppler) (TDI) (86), der

rechtsventrikuläre Strain, sowohl im 3D- als auch im 2D-Echo gemessen (87), die Dyssynchronität (88), der Tei-Index (89) und die Größe des rechten Vorhofes (90). Eine invasive Untersuchung, die auch Aufschluss über die rechtskardiale Leistung gibt, ist die Rechtsherzkatheter-Untersuchung. Prädiktoren des Überlebens, die aus der Rechtsherzkatheter-Untersuchung abgeleitet werden, sind das Herzzeitvolumen, der Druck im rechten Vorhof (91), der PVR und der pulmonal-arterielle Druck (92). Als non-invasives Instrument mit umfassender Evaluierung der rechtskardialen Form, Struktur und Funktion ist die kardiale MRT hochinteressant. Einige länger untersuchte Parameter wie die RV-EF (69) und das SV (68) sowie neuerdings auch die RV-Masse (72) erlauben sehr genaue Aussagen über die RV-Funktion und die Prognose bei Patienten mit PH.

In welchem Ausmaß Surrogate der RV-arteriellen Kopplung für die Prognose bei PH-Patienten entscheidend sind, ist bislang nicht ausreichend untersucht. Die RV-arterielle Kopplung bietet eine ganzheitliche Charakterisierung des Zusammenspiels zwischen Ventrikel und pulmonalem Gefäßbett. Daher liegt es nahe, dass die bestmögliche Kopplung auch mit Prognose assoziiert sein sollte, da sie sowohl Nachlastparameter als auch die RV-Kontraktilität beinhaltet, die jeweils unabhängig mit Prognose assoziiert sind. Allerdings ist derzeit unklar, obwohl die Bedeutung der RV-arteriellen Kopplung unbestritten ist, ob Parameter, die diese charakterisieren, mit Prognose oder Mortalität assoziiert sind.

Das echokardiografisch ermittelte TAPSE/PASP-Verhältnis zeigt bei HFpEF-Patienten eine Assoziation mit Outcome (61). Das SV/ESV-Verhältnis, gemessen mit volumetrischen Parametern im MRT, konnte ebenso Outcome vorhersagen (14,70). Beiden Parametern ist gemein, dass bislang eine Validierung und ein Vergleich mit direkter Messung der Ees beziehungsweise Ea und Ees/Ea nicht erfolgt ist. Aufgrund der Invasivität, der hohen Kosten und der schwierigen Durchführung ist das Ees/Ea-Verhältnis bislang nicht auf mögliche prognostische Assoziationen bei Patienten mit PH hin untersucht worden.

1.10 Die Bedeutung der Rechtes Atrium-Rechter Ventrikel-Achse bei Pulmonaler Hypertonie

Ein wesentliches Symptom bei Rechtsherzversagen ist der venöse Rückstrom, der das klinische Bild mit erweiterten Halsvenen, Aszites oder Beinödemen wesentlich prägt. Bislang gibt es viele weitreichende Untersuchungen bezüglich der systolischen RV-Funktion und des RV-Versagens. Allerdings ist es bislang unklar, warum einige Patienten trotz erhaltener systolischer RV-Funktion einen venösen Rückstau haben und andere beispielsweise bei reduzierter systolischer Funktion keinen ausgeprägten venösen Rückstau aufweisen. Die Erklärung könnte in der bislang unterschätzten diastolischen Funktion des RV liegen, welche möglicherweise eine der Hauptdeterminanten des venösen Rückstaus darstellt. Steigen bei diastolischer RV-Steifheit die RV-EDP Werte wesentlich an, führt dieses während der Kontraktion des rechten Atriums (RA) zu einem Rückstau bis in die Vena cava inferior und die Halsvenen. Vielversprechende Daten legen jedoch auch den Schluss nahe, dass die RA-Funktion per se ein nicht zu vernachlässigender Faktor ist und bei diastolischer und systolischer Dysfunktion des RV eine entscheidende Rolle als anatomische Brücke zwischen Venen und RV spielen könnte. Die Vorhoffunktion ist komplex und umfasst mehrere Komponenten, bestehend aus einer Reservoir-Phase während der atrialen Füllung, einer Conduit-Phase während passiver Entleerung des Atriums in den Ventrikel und einer Pump-Phase (auch „Booster“-Phase) während der atrialen Systole. All diese Phasen spielen eine entscheidende Rolle für die gesamte Herzfunktion. Aufgrund des relativ neuen Forschungsfeldes im Bereich der RA-Funktion sind die Begriffe nicht einheitlich und werden teilweise unterschiedlich verwendet. In dieser Schrift wird, angelehnt an die meisten Publikationen für die Conduit-Phase, der Begriff „passive“ Phase verwendet und für die Pump- oder Booster-Phase der Begriff „aktive“ Phase benutzt (siehe Abbildung 3).

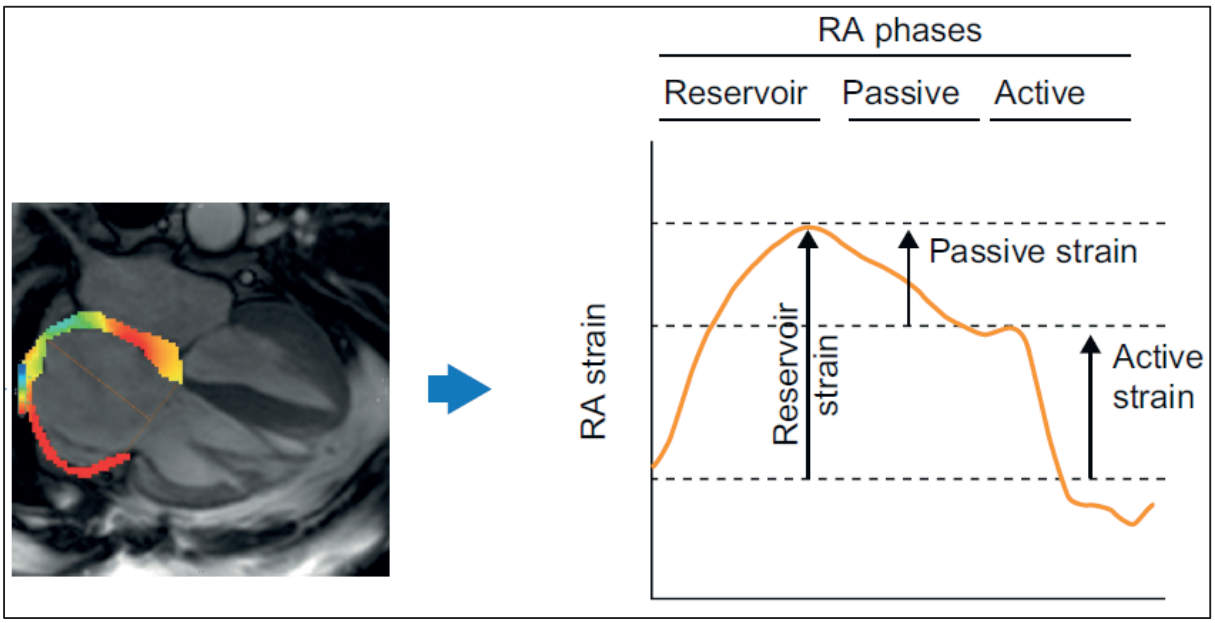

Abbildung 3: Schematische Darstellung eines abgeleiteten RA-Strains aus der kardialen Bildgebung– Beispiel für MRT-Feature-Tracking von RA-Reservoir, passiver und aktiver Phase. RA: rechtes Atrium. Abbildung aus Anlage I mit Erlaubnis

Eine verminderte RA-Funktion manifestiert sich bei PH hauptsächlich, wenn der RV versagt. Ein erweiterter rechter Vorhof ist häufig bei Patienten mit PAH und gilt als wichtiger Parameter in der Risikostratifizierung dieser Patienten (7). Allerdings ist die Beurteilung der RA-Dilatation alleine womöglich nicht ausreichend, um die Komplexität der wichtigen Pathophysiologie im Grenzbereich zwischen rechtem Vorhof und RV zu erfassen. Eine detaillierte Beurteilung der RA-Funktion wird zwangsläufig zu einem besseren Verständnis der RV-Funktion und insbesondere der RA-RV Achse in der PH beitragen. Das echokardiografische RA-Speckle-Tracking hat zu bemerkenswerten Ergebnissen bei der Beurteilung der RA-Deformation und -Funktion bei Patienten mit PH geführt (93). Es wird vermutet, dass die RA-Reservoir-Funktion eine Schlüsselrolle beim Fortschreiten der PH spielt. Die RA-Deformation lässt sich auch im MRT valide mithilfe des beschriebenen Feature-Trackings messen. Die RA-Funktion unterteilt sich dabei in die sogenannte Reservoir-Funktion und diese wiederum in die aktive und passive Phase. Beide Phasen kann man sowohl im MRT als auch in der Echokardiografie messen. Inwiefern die diastolische oder die systolische RV-Funktion, gemessen mit dem Goldstandard der Druck-Volumen-Schleifen des RV, entscheidend sind für den Verlust der RA-Funktion, ist derzeit nicht bekannt.

Studie	Ees (mmHg/ml)	Ea (mmHg/ml)	Ees/Ea
Single-Beat-Methode			
McCabe et al (34)			
Normal-Kontrollen (n=7)	0.44±0.20	0.30±0.10	1.46±0.30
CTED (n=7)	0.59±0.15	0.52±0.24	1.27±0.36
CTEPH (n=7)	1.13±0.43	1.92±0.70	0.60±0.18
Axell et al (94)			
CTED (n=10)	nicht angegeben	0.47±0.18	2.29±1.68
CTEPH (n=10)	nicht angegeben	1.10±0.52	0.72±0.59
Wink et al. (37)			
Patienten mit Lungenresektion (n=10)	0.30±0.08	0.49±0.15	0.64±0.21
Multi-Beat-Methode			
Tedford et al. (18)			
SSc mit PAH (n=7)	0.8±0.3	0.9±0.4	1.0±0.5
IPAH (n=5)	2.3±1.1	1.2±0.5	2.1±1.0
SSc ohne PAH (n=7)	0.9±0.6	0.4±0.1	2.3±1.2
Latus et al. (35)			
Fallot Tetralogy (n=24)	0.24±0.18	0.50±0.28	~0.3
Hsu et al. (17)			
IPAH (n=9, in Ruhe)	0.99±0.34	1.18±0.82	1.12±0.59
SSc-PAH (n=15, in Ruhe)	0.45±0.14	1.30±1.05	0.46±0.17
Rommel et al. (36)			
Kontrolle (n=9, Baseline-Daten)	0.47±0.08	0.35±0.04	~1.3
HFpEF (n=24, Baseline-Daten)	0.83±0.55	0.42±0.15	~1.6

Tabelle 1: Auswahl an Studien über rechtsventrikuläre-pulmonal-arterielle Kopplung.

Ees: End-systolic elastance; Ea: arterial elastance, CTED: Chronic Thromboembolic Disease (deutsch: chronisch thromboembolische Erkrankung); CTEPH: Chronic Thromboembolic Pulmonary Hypertension (deutsch: chronische thromboembolische Pulmonale Hypertonie); PAH: Pulmonal-arterielle Hypertonie; SSc: Systemische Sklerodermie; IPAH: Idiopathische pulmonal-arterielle Hypertonie; HFpEF: Heart failure with preserved ejection fraction. Tabelle adaptiert aus (40) mit Erlaubnis.

2 Zielsetzung

Die Forschung über die Adaptation des RV an erhöhte Nachlast hat in den letzten Jahren an Bedeutung gewonnen. Insbesondere die Adaptation bei chronischer Druck- und Volumenbelastung ist in den letzten Jahrzehnten vorangetrieben worden. Ein Großteil des dabei publizierten Wissens bezüglich des RV ist an Forschung im LV angelehnt oder wird direkt übernommen. Dies erfolgt, obwohl viele Ergebnisse der Forschungsarbeiten zeigen, dass der LV und der RV unterschiedliche embryonale Ursprünge haben und teilweise unterschiedlich auf eine erhöhte Nach- oder Vorlast reagieren. Auf die Kontraktilität und die RV-arterielle Kopplung bezogen, gibt es zudem einige invasive und nichtinvasive Surrogate, vornehmlich ermittelt aus der Rechtsherzkatheter-Untersuchung, der Echokardiografie und der MRT, die bislang nicht mit dem Goldstandard der Druck-Volumen-Schleifen verglichen worden sind. Diese Surrogate werden derzeit ohne Validierung in der Literatur als Ausdruck der RV-arteriellen Kopplung verwendet und ohne Diskussion als lastunabhängig betitelt. Es wäre von großem klinischen und wissenschaftlichen Vorteil, Parameter zu etablieren, die non-invasiv mit vorhandenen Mitteln der MRT/der Echokardiografie als Instrumente der Bildgebung mit verlässlicher diagnostischer Information eine Aussage über die Kontraktilität beziehungsweise die enddiastolische Steifheit des RV treffen können. Der Zeitpunkt, an dem die Nachlast die Kontraktilität übersteigt und der RV zu einer Maladaptation übergeht, der sogenannte Punkt der „RV-arteriellen Entkopplung“, ist derzeit unklar. Genauso unklar ist es, ob das Verhältnis von Ees zu Ea an diesem Übergang zur Maladaptation des RV tatsächlich dem des LV entspricht. Publikationen beziehen sich bezüglich Ees und Ea weitgehend auf den linksventrikulären Status und übernehmen die Absolutwerte für den RV. Über viele bildgebende Parameter aus Echokardiografie, MRT und Rechtsherzkatheter-Untersuchung ist bekannt, dass sie eine Aussage über die Prognose erlauben. Das Ees/Ea-Verhältnis ist physiologisch hochinteressant und wichtig, um die Abhängigkeit der RV-Adaptation von der steigenden Nachlast zu verstehen. Allerdings ist bislang in keiner Studie ein direkter Zusammenhang zwischen RV-arterieller Kopplung, gemessen mittels Goldstandard, und klinischer Verschlechterung der Patienten oder gar Prognose gezeigt worden. Somit bleibt die klinische Relevanz derzeit noch fraglich. Die RA-Funktion ist für die RV-Funktion bedeutend. Die RA-Fläche ist mit der Prognose assoziiert. Inwiefern die RA-Funktion mit lastunabhängigen Parametern assoziiert ist, ist bislang ungeklärt.

Vor dem Hintergrund dieses begrenzten Wissensstandes zu rechtsventrikulären und rechtsatrialen Funktion bei PH ergaben sich folgende Ziele dieser Habilitationsschrift:

- Validierung vorhandener Surrogate der RV-arteriellen Kopplung mit dem Goldstandard der Druck-Volumen-Erfassung des RV (inkl. Rechtsherzkatheter-Untersuchung, MRT und Echokardiografie)
- Vergleich der RV-arteriellen Kopplung mit nichtinvasiven Messmethoden im kMRT als non-invasiver Goldstandard der RV-Funktion und Etablierung neuer nichtinvasiver Parameter
- Definition des Punktes der RV-arteriellen Entkopplung für den RV
- Erfassung der klinischen Relevanz von lastunabhängigen Parametern
- Evaluation der Assoziation der RA-Funktion mit lastunabhängigen Parametern der RV-Funktion

3 Ergebnisse und Diskussion

3.1 Der Ersatz des endsystolischen Druckes durch den mittleren pulmonal-arteriellen Druck führt zur Unterschätzung der RV-arteriellen Kopplung (Anlage A)

Um die komplexe, teure und aufwendige Messung mittels Druck- und Volumenkatheter zu umgehen, ist eine Methode vorgeschlagen worden, die lediglich auf Daten der Rechtsherzkatheter-Untersuchung beruht (82). Der ESP wird dabei durch den mPAP ersetzt. Eine direkte Erfassung des für die Berechnung der Ees wichtigen ESP wird damit überflüssig (siehe Abbildung 2 und 4). Die Erfassung der rechtsventrikulären Druck/Zeit-Kurve genügt gemäß dieses Ansatzes, um die isovolumetrischen Kontraktions- und Relaxationsabschnitte zu bestimmen und dadurch mittels Methode der kleinsten Quadrate den Pmax zu berechnen und die Ees als Steigung zwischen mPAP und Pmax zu definieren (siehe Einleitung und Abbildung 2). Diese Methode hätte viele Vorteile, insbesondere die Vermeidung eines zusätzlichen Katheters außer dem Rechtsherzkatheter und die Möglichkeit der Erfassung der lastunabhängigen Parameter im klinischen Routinebetrieb. Die Methode basiert gänzlich auf Druckerfassung zur Beschreibung der Kontraktilitätsparameter, da das nötige SV aus den Katheterdaten berechnet wird. Einige Gruppen haben sich ausschließlich auf diese Methode verlassen, um die lastunabhängige Kontraktilität zu beschreiben (82). Dies ist jedoch möglicherweise nicht korrekt, da sich die Form der RV-Druck-Volumen-Schleifen mit zunehmendem pulmonal-arteriellen Druck ändert, sodass ESP näher am systolischen RV-Druck als am mPAP liegt (21). Chemla und Kollegen (95) beschrieben eine signifikante Korrelation zwischen dem ESP und dem mPAP. Dies lieferte die Grundlage für den Vorschlag, dass mPAP ESP bei der Single-Beat-Methode zur Erfassung von Ees ersetzt und somit die Bewertung der RV-arteriellen Kopplung vereinfacht wird. Diese Korrelation basierte jedoch auf Daten von nur 15 Patienten, von denen keiner eine PAH hatte (fünf Patienten hatten eine PH als Folge einer Linksherzerkrankung). Zusätzlich ist der ESP aus der Druckkurve der Lungenarterie abgeschätzt und nicht direkt im RV gemessen worden. Eine Durchsicht der aktuellen und der älteren Literatur ergab, dass die mittlerweile häufig verwendete Methode bislang nie mit dem Goldstandard validiert worden ist.

In der vorliegenden Studie haben wir somit den Fehler quantifiziert, Ees mithilfe von mPAP zu erfassen statt mit ESP. Wir haben bei 20 Patienten mit PAH RV-Volumina und RV-Drücke mit einem Konduktanz-Katheter (4F, CD Leycom, Hengelo, Niederlande) gemessen. Die Studie ist von der Ethikkommission der Universitätsklinik Gießen genehmigt worden. Alle Patienten haben eine schriftliche Einverständniserklärung abgegeben: 13 Frauen und 7 Männer im Alter von 51 ± 15 Jahren (Mittelwert ± SD (Standardabweichung)), alle mit der Diagnose PAH (Nizza-Gruppe 1). Die Diagnose beruht auf einem im Rechtsherzkatheter gemessenen mPAP von ≥ 25 mmHg und einem PVR von > 3 WU nach den aktuellen Empfehlungen (7).

17 Patienten hatten eine idiopathische PAH, ein Patient eine portopulmonale Hypertonie, ein Patient eine „Humanes Immundefizienz Virus“-(HIV)-assoziierte PAH und ein Patient eine mit systemischer Sklerose assoziierte PAH. Basierend auf hämodynamischen Messungen lagen der PVR bei 5,9 [4,3–8,6 (Interquartilbereich)] WU, der mPAP bei 41±11 mmHg, der PAWP bei 7±2 mmHg und die gemischt-venöse Sättigung bei 69 %±6 %. Die Patienten waren in NYHA-Funktionsklasse III (n = 12) oder II (n = 8).

Abbildung 4 zeigt eine starke Korrelation zwischen mPAP und ESP. Die Beziehung zwischen mPAP und ESP wurde durch ein lineares Regressionsmodell als ESP = 1,65 × mPAP – 7,79 (r = 0,932; r2 = 0,868; P

< 0,001) beschrieben. Das Bland-Altman-Diagramm zeigte obendrein eine Unterschätzung des ESP durch mPAP insbesondere bei Druckwerten über 50 mmHg.

Der Vergleich von Ees, Ea und Ees/Ea, berechnet unter Verwendung von mPAP statt ESP, ergab signifikante Unterschiede (alle P < 0,001, Wilcoxon-Test): Ees wurde berechnet als 0,87 ± 0,44 im Vergleich zu 0,62 ± 0,38 mmHg/ml; Ea wurde berechnet als 0,52 ± 0,25 im Vergleich zu 0,76 ± 0,39 mmHg/ml; Ees/Ea ergab 1,84 ± 0,78 im Vergleich zu 0,89 ± 0,49. Diese Unterschiede unterstreichen die Wichtigkeit der Validierung verschiedener Kontraktilitätsmessungen.

Zusammenfassend kann daher mPAP kein Ersatz für RV-ESP bei der Bewertung der RV-Kontraktilität und der RV-arteriellen Kopplung sein. Obwohl die geringe Stichprobengröße unserer Studie berücksichtigt werden muss, legen unsere Ergebnisse nahe, dass der ESP durch die Gleichung ESP = 1,65 × mPAP – 7,79 ohne direkte Messungen vorsichtig geschätzt werden kann.

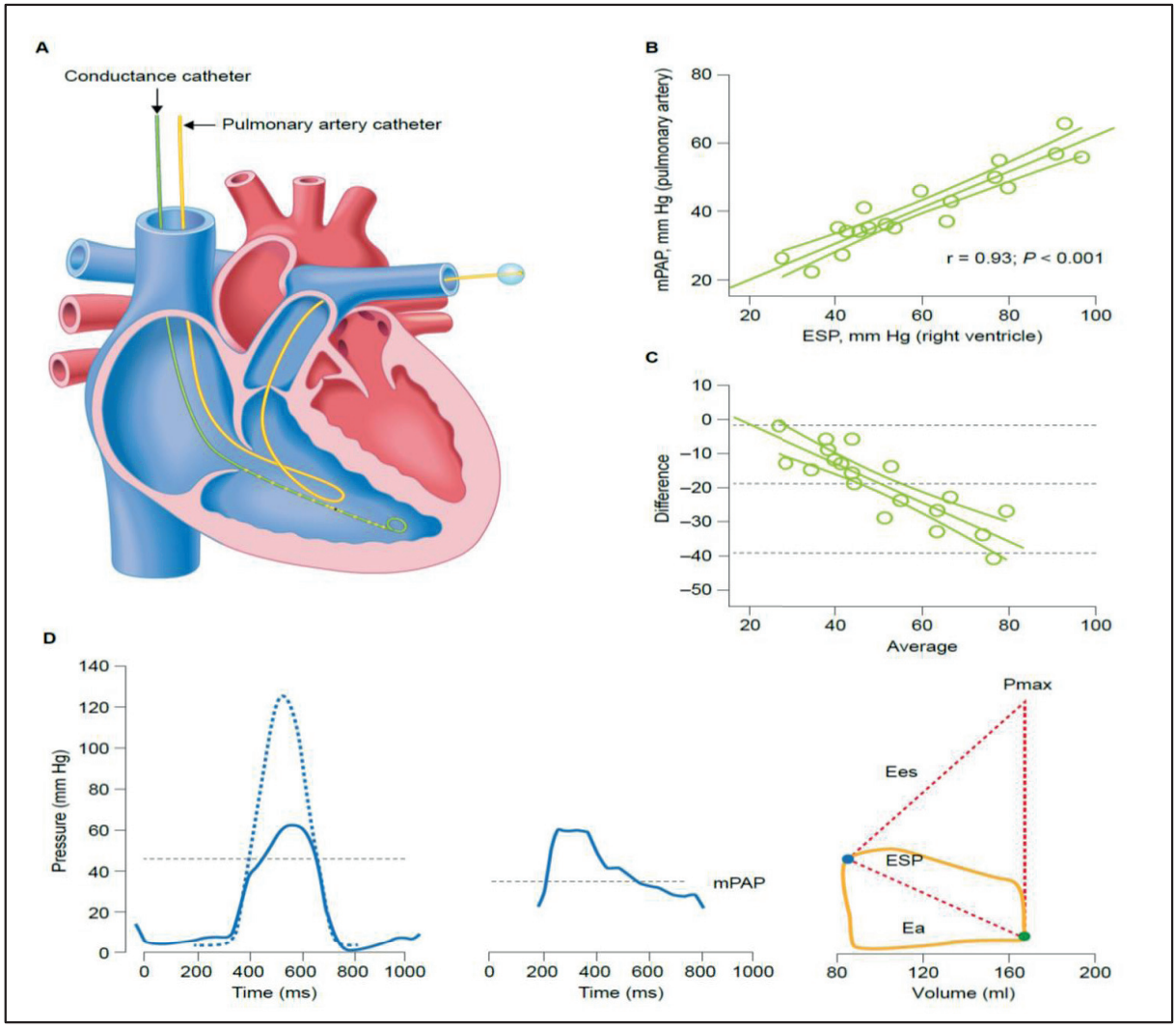

Abbildung 4: Bewertung des mittleren pulmonal-arteriellen Druckes (mPAP) als Ersatz für den endsystolischen Druck (ESP) bei der Beurteilung der rechtsventrikulären Kontraktilität bei PAH. **A**: Positionierung des Konduktanz-Katheters und des Rechtsherzkatheters zur Messung von ESP bzw

mPAP **B**: Korrelation von ESP (gemessen über Konduktanz-Katheter) mit mPAP. **C**: Bland-Altman-Diagramm, das eine Unterschätzung des ESP basierend auf mPAP zeigt, insbesondere bei hohen Drücken (> 50 mmHg). **D**: Zwei beispielhafte ursprüngliche Messungen der rechtsventrikulären Druckkurve und des mPAP, Schätzung des theoretischen Maximaldruckes (Pmax) und Berechnung der endsystolischen Elastizität (Ees) und der arteriellen Elastizität (Ea) bei einem Patienten. Abbildung aus Anlage A mit Erlaubnis.

3.2 Validierung echokardiografischer Parameter als Surrogate der RV-arteriellen Kopplung (Anlage B)

Nichtinvasive Parameter der RV-arteriellen Kopplung sind von enormer Bedeutung für den klinischen Alltag. Sollten durch MRT oder Echokardiografie hergeleitete Parameter tatsächlich Parameter der RV-arteriellen Kopplung widerspiegeln, wäre dadurch eine Abschätzung oder gar Messung von lastunabhängigen Parametern im Routine-Klinikalltag möglich.

Einer der Parameter, die als Surrogate vorgeschlagen worden sind, ist das TAPSE/PASP-Verhältnis. Erstmals von Guazzi und Kollegen ins Gespräch gebracht (60), ist dieser Parameter laut den Erstbeschreibern ein Ausdruck des Kraft/Längen-Verhältnisses des Ventrikels. Die Kraft-Längen-Beziehung ist die Grundlage für die Erfassung der Kontraktilität in ihren Ursprüngen und repräsentiert die Kontraktilitätserfassung eines Muskelstreifens. Daran angelehnt werden einige Parameter zur Ermittlung der Kontraktilität beschrieben, wie auch das TAPSE/PASP-Verhältnis. Dabei repräsentieren TAPSE die Länge und PASP die Kraft.

Weitere Parameter sind in den letzten Jahren veröffentlicht worden, die als Surrogate der RV-arteriellen Kopplung gelten, wie RV-FAC/mPAP (invasiv gemessen) (62,96,97), RV-FAC/RV/ESA (98), TAPSE/PAAT (99) und SV/ESA (angelehnt an PASP/ESA als Surrogat für Ees (100,101) und PASP/SV als Surrogat für Ea) (102) (siehe Einleitung). Die genannten Parameter sind aufgrund theoretischer Überlegung des Kraft/Längen-Verhältnisses ermittelt und als Surrogate beschrieben, keiner davon ist jedoch mit dem Goldstandard der Druck-Volumen-Schleifen validiert worden. Ziel unseres Projektes war es somit, die genannten Parameter mit dem Goldstandard der Druck-Volumen-Schleifen zunächst im Single-Beat-Verfahren zu untersuchen. Weil die diastolische RV-Funktion mit Outcome und Schwere der PAH assoziiert ist (46,51), wurde auch die Beziehung dieser Parameter zu Eed erfasst.

Einen Tag vor der invasiven Messung der pulmonalen Hämodynamik und der Erfassung der Single-Beat-RV-Druckvolumenmessung führten wir bei 52 Patienten mit PAH oder CTEPH eine Echokardiografie und eine kMRT des RV durch. Die Beziehungen der vorgeschlagenen Surrogate zu Ees/Ea und Eed wurden durch Spearman-Korrelation, multivariate logistische Regression und „Receiver Operating Characteristic"-Analysen (ROC-Analysen) bewertet. Assoziationen mit Prognose wurden durch Kaplan-Meier-Analysen hergestellt. Die aktuelle Analyse umfasste Patienten mit PAH und CTEPH, die prospektiv zwischen Januar 2016 und Juni 2018 in die Studie „Right-Heart-1" (Nummer NCT03403868 bei Clinical Trails.gov) und in das Gießener PH-Register (103) aufgenommen wurden. Die Patienten wurden gemäß den aktuellen Empfehlungen diagnostiziert (7). Alle Patienten erhielten gezielte PAH-Therapien auf der Grundlage der klinischen Bewertung und des besten Versorgungsstandards. Alle teilnehmenden Patienten gaben eine schriftliche Einverständniserklärung zur Aufnahme in die Studie ab. Für die Überlebensanalyse wurde eine separate Gruppe von 193 Patienten mit idiopathischer PAH retrospektiv als externe Validierungskohorte analysiert. Die Studienkohorte wurde prospektiv bis zum 20. März 2019 verfolgt. Wir bewerteten die klinische Verschlechterung in der Studienkohorte und das Gesamtüberleben in der externen Validierungskohorte. Die klinische Verschlechterung wurde wie folgt definiert:

a) eine Verringerung der Belastungsfähigkeit (–15 % im Vergleich zum 6-Minuten-Gehtest zu Studienbeginn)
b) Verschlechterung der Funktionsklasse nach New York Heart Association (NYHA)
c) klinische Verschlechterung, die eine Krankenhauseinweisung erfordert
d) Notwendigkeit neuer PAH-Therapien bzw. intravenöser Diuretika
e) Lungentransplantation
f) Tod

Ees/Ea, Ea (Abbildung 5) und Eed korrelierten mit TAPSE/PASP, FAC/mPAP, RV-FAC/ESA und SV/ESA. Keines der Surrogate korrelierte mit Ees.

In der univariaten logistischen Regressionsanalyse waren TAPSE/PASP, FAC/mPAP, RV-FAC/ESA und SV/ESA mit bei 0,805 dichotomisiertem Ees/Ea (auf Grundlage der Ergebnisse von Anlage F) assoziiert. In der multivariaten Analyse war nur TAPSE/PASP (Beta-Koeffizient: 2,154) assoziiert. Unter Verwendung von ROC-Analysen und des Youden-Index ermittelten wir einen Grenzwert für TAPSE/PASP von 0,31 mm/mmHg zur Vorhersage einer RV-arteriellen Entkopplung (definiert als Ees/Ea < 0,805, angelehnt an Anlage F).

In der Studienkohorte wurden 26 klinische Verschlechterungsereignisse während einer mittleren Nachbeobachtungszeit von 13 Monaten (Interquartilbereich: 5,3–24,8 Monate) beobachtet. Die Kaplan-Meier-Analyse ergab, dass Patienten mit PH und TAPSE/PASP < 0,31 mm/mmHg signifikant mehr Ereignisraten hatten als Patienten mit höherem TAPSE/PASP (log Rang P = 0,019) (Anlage B). Dies wurde durch eine multivariate Cox-Regressionsanalyse gestützt, die Alter, Geschlecht und TAPSE/PASP umfasste. TAPSE/PASP zeigte eine Hazard-Ratio von 2,73 (95-Prozent-Konfidenzintervall: 1,14–6,54) als Prädiktor für eine klinische Verschlechterung.

In der externen Validierungskohorte zeigten Patienten mit idiopathischer PAH und TAPSE/PASP < 0,31 mm/mmHg ein signifikant schlechteres Gesamtüberleben als Patienten mit höherem TAPSE/PASP (log Rang P = 0,003) (siehe auch Anlage H). TAPSE/PASP prognostizierte auch die Gesamtmortalität (Hazard-Ratio: 1,85; 95-Prozent-Konfidenzintervall: 1,16–2,95) in einer multivariaten Cox-Regressionsanalyse einschließlich Funktionsklasse, Alter, Geschlecht und PVR (siehe Anlage B).

Zusammenfassend zeigen die vorliegenden Ergebnisse, dass das echokardiografische TAPSE/PASP-Verhältnis ein klinisch relevanter und valider Ersatz für invasiv gemessene Ees/Ea zur Beurteilung der RV-arteriellen Kopplung ist und Informationen zur diastolischen RV-Steifheit (Eed) liefert, jedoch nicht zur RV-Kontraktilität (Ees).

Sowohl TAPSE als auch PASP können leicht durch eine Standard-Echokardiografie-Untersuchung am Krankenbett gemessen werden. Weitere Studien sind jedoch erforderlich, um den möglichen prognostischen Mehrwert von TAPSE/PASP für schwere PH zu bewerten, auch im Vergleich zu den bereits publizierten prognostisch relevanten Kriterien zur Risikostratifizierung (7). Die umfassende und anspruchsvolle Methodik begrenzte die Größe der Studienkohorte. Der relativ kurze prospektive Beobachtungszeitraum, die Stichprobengröße der Studienkohorte und die retrospektive Analyse der externen Validierungskohorte schränken die Interpretation der Ergebnisse ein. Der prognostische Wert der identifizierten TAPSE/PASP-Grenze muss in einer großen prospektiven Studie noch bestätigt werden. Weitere Einschränkungen bestehen durch die Art der verwendeten Methodik („Single-Beat-Methode“, siehe Einleitung). Der Goldstandard der Erfassung der RV-arteriellen Kopplung ist die Multi-Beat-Methode.

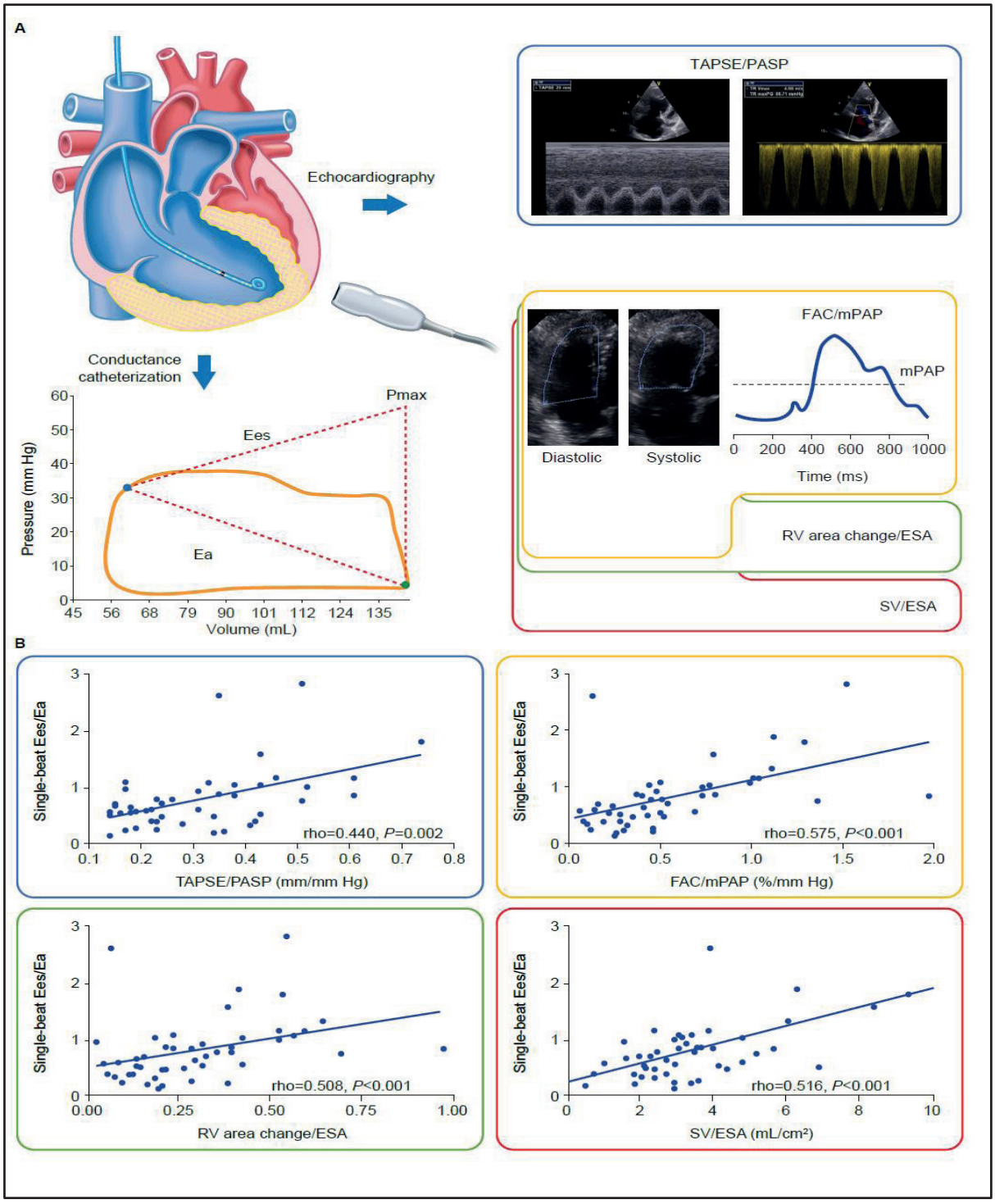

Abbildung 5 Surrogate für RV-arterielle Kopplung und ihre Assoziation mit Single-Beat-Ees/Ea bei Patienten mit PH. **A**: Surrogate wurden mit Single-Beat-Druck-Volumen-Schleifen verglichen. **B**: TAPSE/PASP, FAC/mPAP, RV-FAC/ESA und SV/ESA (alle mit Ausnahme von mPAP [Rechtsherzkatheter] und SV [kardiale Magnetresonanztomografie] durch Echokardiografie gemessen) zeigten signifikante Assoziationen mit invasiv gemessenen Single-Beat-Ees/Ea Werten.

Ea: arterielle Elastizität; Ees: endsystolische Elastizität; ESA: endsystolische Fläche; FAC: Fractional Area Shortening; mPAP: mittlerer Pulmonalarteriendruck; PASP: systolischer pulmonal-arterieller Druck; Pmax: maximaler Druck eines isovolumischen Schlags; RV: rechtsventrikulär; SV: Schlagvolumen; TAPSE: Tricuspidal Annular Plane Excursion. Abbildung aus Anlage B mit Erlaubnis.

3.3 TAPSE/PASP differenziert zwischen Schwere der Lungenerkrankungen (Anlage C)

Die PH als Folge chronischer Lungenerkrankungen (engl. PH-Lung-Disease, PH-LD) ist häufig leicht bis mittelschwer, wobei viele Patienten einen mPAP von < 35 mmHg aufweisen. Ein geringer Prozentsatz der Patienten, die zur Untersuchung in speziellen Zentren überwiesen worden sind, kann eine schwere PH mit einem mPAP im Bereich der PAH aufweisen (104). Die RV-Funktion ist jedoch häufig auch bei leichter bis mittelschwerer PH-LD eingeschränkt und stellt eine wichtige Determinante für das Überleben und den Funktionsstatus bei PH-LD dar (105). Wir untersuchten daher die funktionelle Signifikanz und prognostische Relevanz des TAPSE/PASP-Verhältnisses bei PH-LD als Surrogat der RV-arteriellen Kopplung.

Wir analysierten Patienten mit PH-LD und idiopathischer PAH, die prospektiv in das Gießener PH-Register aufgenommen wurden (103). Die Diagnose der PH-LD wurde von einem multidisziplinären Board zwischen Dezember 2004 und März 2012 vor der Aufnahme in das Gießener PH-Register gestellt. Die Follow-up-Daten wurden bis Februar 2018 aus dem Gießener PH-Register abgerufen. Die Analyse umfasste Patienten mit vollständigen echokardiografischen (Tag 1) und invasiven hämodynamischen Daten (Tag 2) sowie vollständiger Nachsorge. Die Untersuchung wurde von der Ethikkommission der Medizinischen Fakultät der Universität Gießen bewilligt (AZ 186/16, 266/11). Alle teilnehmenden Patienten gaben eine schriftliche Einverständniserklärung ab.

Wie kürzlich vorgeschlagen (104) wurde PH-LD durch einen mPAP von > 21 mmHg (21–24 mmHg mit pulmonalem Gefäßwiderstand (PVR) ≥ 3 WU oder nur ≥ 25 mmHg) definiert. Eine schwere PH-LD ist mit einem mPAP von ≥ 35 mmHg oder mPAP ≥ 25 mmHg mit niedrigem Herzindex (< 2,0 L min/m^2) definiert. Insgesamt wurden 172 Patienten mit PH-LD eingeschlossen (Alter: 58 ± 26 Jahre; mPAP: 34 (28–41) mmHg; PVR: 5,5 (3,8–7,9) WU; Herzindex: 2,5 ± 0,7 l min/m^2). 78 (45,3 %) Patienten hatten eine PH aufgrund einer chronisch obstruktiven Lungenerkrankung (PH-COPD), die bei 21 (12,2 %) Patienten als schwerwiegend eingestuft wurde. Die restlichen 94 (54,7 %) Patienten hatten eine PH aufgrund einer interstitiellen Lungenerkrankung (PH-ILD), die bei 44 (25,6 %) Patienten als schwerwiegend eingestuft wurde. Die Lungenfunktion war zwischen schwerer und nicht schwerer PH-ILD nicht unterschiedlich (TLC (Totale Lungenkapazität): p = 0,699; VC (Vitalkapazität): p = 0,838; unabhängiger t-Test). Es gab keine Korrelationen zwischen TLC oder VC und dem TAPSE/PASP-Verhältnis bei schwerer und nicht schwerer PH-ILD.

Die ROC-Analyse ergab einen Cut-off von 0,26 mm/mmHg für TAPSE/PASP mit einer Sensitivität von 80,6 % und einer Spezifität von 71,2 % zur Unterscheidung zwischen schwerer und nicht schwerer PH-LD, die TAPSE oder PASP allein überlegen war. Logistische multivariate Analysen (angepasst an Alter und Geschlecht) zeigten eine signifikante Assoziation zwischen TAPSE/PASP und den hämodynamischen Phänotypen (dichotomisiert bei 0,26 mm/mmHg; OR: 9,37; 95-Prozent-CI: 4,56–19,26; p < 0,001). Darüber hinaus zeigte die ROC-Analyse, dass TAPSE/PASP auch in der Lage ist, zwischen schwerer und nicht schwerer PH-COPD sowie schwerer und nicht schwerer PH-ILD zu unterscheiden (Abbildung 6). Dies wurde durch eine logistische multivariate Analyse gestützt (multivariates OR für PH-COPD: 18,60; 95-Prozent-CI: 4,45–77,75; p < 0,001; und PH-ILD: 8,44; 95-Prozent-Konfidenzintervall: 3,34–21,36; p < 0,001). Interessanterweise sagte das TAPSE/PASP-Verhältnis das Überleben sowohl bei PH-COPD als auch bei PH-ILD voraus (Abbildung 6).

In der vorliegenden Studie zeigte das TAPSE/PASP-Verhältnis als echokardiografisches Surrogat der RV-arteriellen Kopplung seinen klinischen Nutzen bei der PH-LD. Die adäquate RV-Adaptation kann jedoch von Patient zu Patient variieren und vom Vorliegen von Komorbiditäten abhängen, wie dies beispielsweise bei Patienten mit systemischer Sklerose gezeigt wurde (23). Die Auswirkungen chronischer Infektionen, wie häufig bei schweren Lungenerkrankungen auftretend, auf die RV-arterielle Kopplung bei PH-LD-Patienten müssen jedoch weiter untersucht werden.

Zusammenfassend ist das TAPSE/PASP-Verhältnis eine einfache und klinisch relevante Messung zur Unterscheidung der hämodynamischen Phänotypen von Patienten mit PH-LD. Das TAPSE/PASP-Verhältnis könnte sich als wichtiges nichtinvasives Instrument zur Bewertung zukünftiger therapeutischer Interventionen bei Patienten mit PH-LD erweisen.

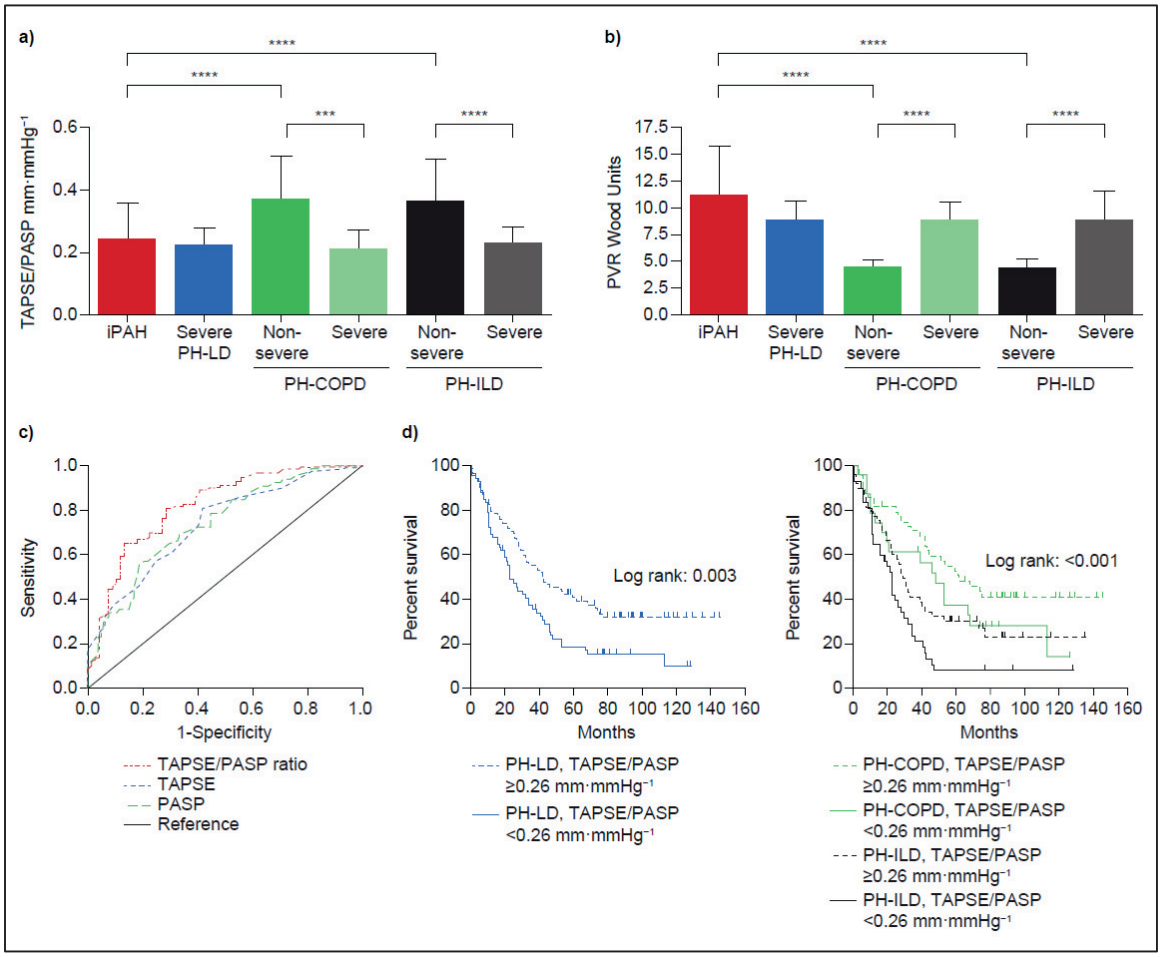

Abbildung 6: Verhältnis von Tricuspidal Annular Plane Excursion (TAPSE) zu systolischem Pulmonalarteriendruck (PASP) als Indikator für den hämodynamischen Schweregrad und die Prognose bei Pulmonaler Hypertonie infolge einer chronischen Lungenerkrankung (PH-LD). **a)** TAPSE/PASP-Verhältnis und **b)** pulmonaler Gefäßwiderstand (PVR) bei Patienten mit idiopathischer Pulmonalarterieller Hypertonie (iPAH) und Patienten mit Pulmonaler Hypertonie aufgrund einer chronisch obstruktiven Lungenerkrankung (PH-COPD) oder einer interstitiellen Lungenerkrankung (PH-ILD) stratifiziert nach hämodynamischem Schweregrad (Balkendiagramme zeigen Median und Interquartilbereich; **** $p < 0{,}0001$; *** $p < 0{,}001$; Unterschiede zwischen den Gruppen wurden mit dem Kruskal-Wallis-Test analysiert). **c)** ROC-Analyse des Verhältnisses TAPSE/PASP (Fläche unter der Kurve (engl. Area Under the Curve, AUC): 0,825; $p < 0{,}001$), TAPSE (AUC: 0,736; $p < 0{,}001$) und PASP (AUC: 0,739; $p < 0{,}001$) zur Unterscheidung zwischen schwerer und nicht schwerer PH-LD. **d)** Kaplan-Meier-Überlebenskurven bei Patienten mit PH-LD und durch das TAPSE/PASP-Verhältnis stratifizierte Teilgruppen mit PH-ILD und PH-COPD. Abbildung aus Anlage C mit Erlaubnis.

3.4 Validierung vorhandener Surrogate der RV-arteriellen Kopplung mit dem Goldstandard Multi-Beat (Anlage D)

Vorhandene Surrogate der RV-arteriellen Kopplung basieren teilweise auf nichtinvasiven echokardiografischen Untersuchungen (vor allem TAPSE/PASP) und MRT-Bildgebung (SV/ESV) des Herzens. Die invasiv ermittelten Surrogate basieren einerseits auf der sogenannten Single-Beat-Methode (siehe Einleitung), bei der einerseits teilweise mPAP als Ersatz für ESP verwendet wird (siehe Einleitung und Anlage A). Andererseits basieren die Ees/Ea-Messungen auf dem aktuell akzeptierten Goldstandard mit Vorlastreduktion und Generierung multipler Druck-Volumen-Schleifen und der direkten Erfassung der Ees (Abbildung 2). In einem Bericht der American Thoracic Society (6) wird die Notwendigkeit einer Studie zum Vergleich der vorhandenen Methoden zur Berechnung oder Messung von Ees hervorgehoben. Die prognostische Relevanz der RV-arteriellen Kopplung, die mit der Goldstandard-Multibeat-Methode gemessen worden ist, blieb bisher ebenfalls undefiniert.

Wir untersuchten daher die RV-pulmonal-arterielle Kopplung unter Verwendung der Multi-Beat-Methode, um Ees/Ea bei Patienten mit schwerer PH (PAH oder CTEPH) zu bestimmen, und bewerteten ihre prognostische Relevanz durch Aufzeichnung klinischer Ereignisse während des Follow-up. Wir verglichen zudem die Multi-Beat-Methode mit vereinfachten Surrogat-Methoden zur Bewertung der RV-pulmonal-arteriellen Kopplung, einschließlich Single-Beat von Ees/Ea, Volumenmethode beziehungsweise kMRT-Methode (SV/ESV) und TAPSE/PASP-Verhältnis aus der Echokardiografie.

Wir analysierten Patienten mit PAH und CTEPH (diagnostiziert nach den aktuellen Empfehlungen (14)), die zwischen Februar 2017 und Dezember 2018 prospektiv an der „Right-Heart-1“-Studie (15) (ClinicalTrials.gov-Kennung: NCT03403868) und dem Gießener PH-Register (16) teilnahmen. Alle Patienten wurden an Tag 1 einer kMRT-Bildgebung und einer Echokardiografie des rechten Herzens sowie an Tag 2 einer Druckvolumen- und einer Swan-Ganz-Katheter-Untersuchung unterzogen. Nur Patienten mit vollständigen Multi-Beat-, Single-Beat-, kMRT- und echokardiografischen Auswertungen wurden in die Endanalyse aufgenommen. Alle teilnehmenden Patienten erteilten ihre schriftliche Einwilligung zur Aufnahme in die „Right-Heart-1“-Studie. Die Untersuchung entspricht den in der Deklaration von Helsinki dargelegten Grundsätzen und wurde von der Ethikkommission der Medizinischen Fakultät der Universität Gießen genehmigt (Genehmigung Nr. 108/15).

Folgende Methoden wurden evaluiert:

Multibeat-Methode:

Wenn die Druck-Volumen-Schleifen eine deutliche Überlappung als Zeichen stabiler Messverhältnisse aufwiesen, begannen wir, die Vorlast zu verringern (Abbildung 2, siehe Einleitung). Zu diesem Zweck wurden ein Führungsdraht und ein Ballon (Amplatzer-24-mm-Sizing-Balloon II, St. Jude Medical [jetzt Abbott], Belgien) über eine 10F-Einführschleuse in die rechte Vena femoralis eingeführt. Unter Kontrolle transthorakaler echokardiografischer Kontrolle wurde die Vena cava inferior für mindestens zehn Sekunden verschlossen. Multi-Beat Ees wurde durch eine Steigung in den endsystolischen Druck-Volumen-Punkten bestimmt (Abbildung 2).

Single-Beat-Methode.

Single-Beat-Ees wurde wie von Brimioulle et al. (39) beschrieben berechnet (siehe Einleitung, Abbildung 2). Jede RV-Druckkurve wurde visuell analysiert, um die erste Ableitung des Drucks über die Zeit (dP/dt) während der isovolumetrischen Kontraktion und der isovolumetrischen Relaxation zu erhalten (Abbildung 2). Die Sinuswellenextrapolation wurde sodann verwendet, um den theoretischen

isovolumetrischen Maximaldruck (Pmax) zu berechnen. Um eine zuverlässige Messung von Pmax zu gewährleisten, wurden alle Messungen von zwei erfahrenen Prüfern unabhängig voneinander durchgeführt, die hinsichtlich der klinischen Daten verblindet waren.

Druck-basierte Methoden zur Berechnung von RV-arterieller Kopplung

Drei publizierte Methoden wurden berechnet.

Druckmethode # 1:

Diese Methode basierte auf Standardmessungen des Rechtsherzkatheters und der RV-Druckkurve, der Berechnung von Pmax und der Annahme, dass der mPAP gleich ESP ist (82). Ees gemäß Druckmethode # 1 wurde als (Pmax – mPAP)/SV berechnet. Ea wurde als mPAP/SV berechnet. Die RV-arterielle Kopplung (Ees/Ea) wurde somit als (Pmax-mPAP)/mPAP berechnet.

Druckmethode # 2. Obwohl eine starke Korrelation zwischen mPAP und ESP besteht, wurde von unserer Gruppe festgestellt, dass mPAP ESP unterschätzt (106). Um dies zu beheben, kann ESP mit $ESP_{berechnet}$ = 1,65 × mPAP – 7,79 geschätzt werden. Wir haben daher Ees als (Pmax – $ESP_{berechnet}$)/SV angenommen; dementsprechend wurde Ea als $ESP_{berechnet}$/SV abgeleitet. Die RV-arterielle Kopplung wurde als (Pmax-$ESP_{berechnet}$)/$ESP_{berechnet}$

Druckmethode # 3. Der ESP wird in einigen Publikationen durch den systolischen RV-Druck (engl. Systolic Right Ventricular Pressure, sRVP) abgeschätzt (14). Ees wird als (Pmax – sRVP)/SV berechnet und Ea als sRVP/SV geschätzt. Die RV-arterielle Kopplung wird sodann als (Pmax-sRVP)/sRVP berechnet.

Volumenbasierte Methode zur Beurteilung der RV-arteriellen Kopplung

SV/ESV gilt als vereinfachte Methode zur Kalkulation von Ees/Ea ((ESP/ESV) / (ESP/SV) = SV/ESV) (14,81) (siehe Einleitung).

Echokardiografische Methode:

Als echokardiografische Methode zur Erfassung wurde die TAPSE/PASP-Ratio verwendet (60) (Anlage B).

Das mittlere Ees/Ea unterschied sich nicht signifikant zwischen Multi-Beat- und Single-Beat-Methode (P = 0,557) oder zur Druckmethode # 2 (P = 0,788). Es zeigte sich jedoch ein signifikanter Unterschied zwischen mittlerem Multi-Beat Ees/Ea im Vergleich zu den Druckmethoden # 1 und # 3 (beide P < 0,001). Wie in Abbildung 7 gezeigt, korrelierten alle vereinfachten Methoden zur Schätzung von Ees/Ea signifikant mit Multi-Beat Ees/Ea. In der Bland- und Altman-Analyse bestand nur ein sehr geringer Bias zwischen Multi-Beat Ees/Ea und Ees/Ea, welches durch die Single-Beat-Methode oder die Druckmethode # 2 bestimmt wurde, was eine hervorragende Genauigkeit für diese beiden vereinfachten Methoden zeigt. Die Abweichung im Vergleich zu Ees/Ea mit Multi-Beat war für die Druckmethoden # 1 und # 3 und für die Volumenmethode in unterschiedlichem Maße erhöht. Die Übereinstimmungsgrenzen zwischen Single-Beat- und Multi-Beat Ees/Ea lagen relativ nahe beieinander, was für die Single-Beat-Methode eine akzeptable Genauigkeit anzeigt.

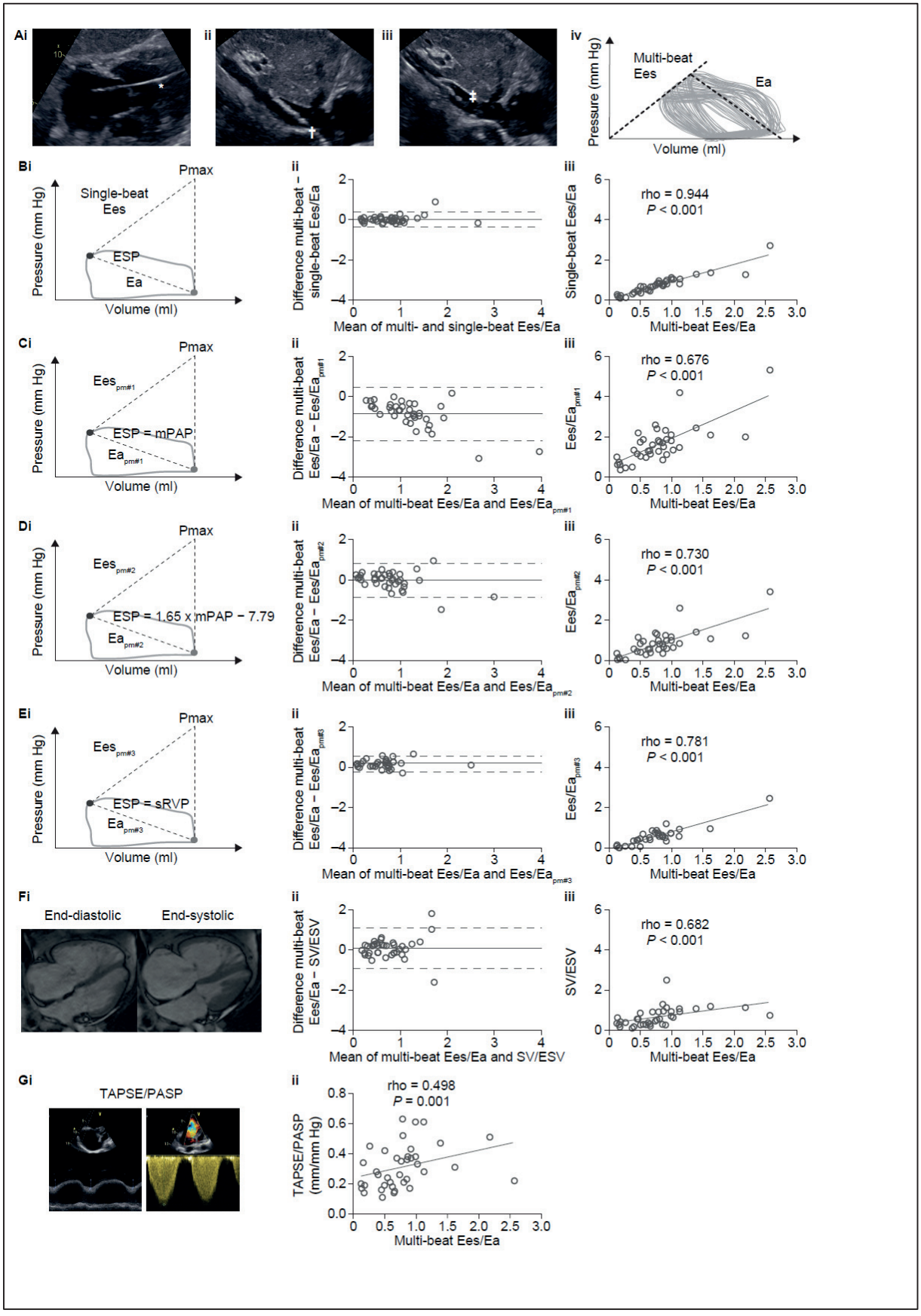
Ai
ii
iii
iv
Multi-beat Ees
Ea
Pressure (mm Hg)
Volume (ml)
Bi
Pmax
Single-beat Ees
ESP
Ea
ii
Difference multi-beat – single-beat Ees/Ea
Mean of multi- and single-beat Ees/Ea
iii
Single-beat Ees/Ea
rho = 0.944
P < 0.001
Multi-beat Ees/Ea
Ci
Ees pm#1
ESP = mPAP
Ea pm#1
Difference multi-beat Ees/Ea – Ees/Ea pm#1
Mean of multi-beat Ees/Ea and Ees/Ea pm#1
Ees/Ea pm#1
rho = 0.676
Di
Ees pm#2
ESP = 1.65 x mPAP – 7.79
Ea pm#2
Difference multi-beat Ees/Ea – Ees/Ea pm#2
Mean of multi-beat Ees/Ea and Ees/Ea pm#2
Ees/Ea pm#2
rho = 0.730
Ei
Ees pm#3
ESP = sRVP
Ea pm#3
Difference multi-beat Ees/Ea – Ees/Ea pm#3
Mean of multi-beat Ees/Ea and Ees/Ea pm#3
Ees/Ea pm#3
rho = 0.781
Fi
End-diastolic
End-systolic
Difference multi-beat Ees/Ea – SV/ESV
Mean of multi-beat Ees/Ea and SV/ESV
SV/ESV
rho = 0.682
Gi
TAPSE/PASP
TAPSE/PASP (mm/mm Hg)
rho = 0.498
P = 0.001

Abbildung 7: Vergleich der Methoden zur Beurteilung der rechtsventrikulären (RV)-pulmonal-arteriellen Kopplung bei Patienten mit PH. **(A)** (i): Bei der Goldstandard-Multi-Beat-Methode wurden RV-Druck und -Volumen mit einem Konduktanz-Katheter (markiert mit *; CD Leycom, Niederlande) während des abnehmenden venösen Rückflusses durch Ballonverschluss der Vena cava inferior gemessen ([ii] entleerter und [iii] aufgeblasener Ballon, angegeben mit † bzw. ‡; Amplatzer-24-mm-Größenballon II, St. Jude Medical [jetzt Abbott], Belgien); (iv) Endsystolische Elastizität (Ees) wurde durch die Steigung erhalten, die an den endsystolischen Abschnitten der Druck-Volumen-Schleifen angebracht war; die arterielle Elastizität (Ea) wurde als endsystolischer Druck (ESP)/Schlagvolumen (SV) berechnet. **(B–G)** (i) Vereinfachte Methoden zur Beurteilung der RV-arteriellen Kopplung umfassen **(B)** die Single-Beat-Methode (mit Berechnung von Ees aus dem theoretischen isovolumetrischen Maximaldruck [Pmax] und ESP) (39), (C–E) an die Single-Beat-Methode angepasste Druckmethoden, wobei die ESP unter Verwendung von drei verschiedenen Annahmen geschätzt wird (**[C]** Druckmethode # 1: ESP = mittlerer pulmonal-arterieller Druck [mPAP] (9); **[D]** Druckmethode # 2: ESP = 1,65 × mPAP – 7,79 (19); **[E]** Druckmethode # 3: ESP = systolischer RV-Druck [sRVP] (14)), **(F)** das auf kardialen Magnetresonanz-Bildgebungsdaten basierende Volumenverfahren (Ees/Ea = SV/Endsystolisches Volumen [ESV]) (81) und **(G)** die echokardiografische Methode (Ees/Ea = Tricuspidal Annular Plane Excursion [TAPSE]/systolischer pulmonal-arterieller Druck [PASP]) (60). **(B–F)** (ii) Bland-Altman-Plots wurden verwendet, um den Übereinstimmungsgrad zwischen der Multi-Beat-Methode und **(B)** der Single-Beat-Methode zu bewerten (Bias: 0,009; Übereinstimmungsgrenzen [limits of agreement, LOA]: – 0,353, 0,371], **(C)** pm # 1 (Bias: – 0,858; LOA: – 2,190, 0,475), **(D)** pm # 2 (Bias: – 0,023; LOA: – 0,874, 0,828), **(E)** pm # 3 (Bias: 0,207; LOA: – 0,232, 0,579) und **(F)** die Volumenmethode (Bias: 0,085; LOA: – 0,905, 1,075). Die durchgezogene Linie repräsentiert den Bias, die gestrichelten Linien repräsentieren die LOA. **(B–F)** (iii) Korrelationen zwischen der Multi-Beat-Methode und der **(B)** Single-Beat-, **(C-E)** -Druck- und **(F)** –Volumenmethode(n) wurden unter Verwendung des Spearman-Rho-Koeffizienten bewertet. **(G)** (ii) Die Korrelation zwischen der Multi-Beat-Methode und der echokardiografischen TAPSE/PASP Methode wurde ebenso analysiert. Abbildung aus Anlage D mit Erlaubnis.

Die vorliegenden Ergebnisse zeigen zusammenfassend, dass Single-Beat-Ees/Ea im Vergleich zu Multi-Beat Ees/Ea für die Beurteilung der RV-arteriellen Kopplung bei Patienten mit schwerer PH eine ausgezeichnete Genauigkeit mit akzeptabler Präzision aufweist. Andere indirekte Schätzungen von Ees/Ea unter Verwendung einer ausschließlichen Druck- oder Volumenanalyse waren mit einer schlechteren Genauigkeit und/oder einem größeren Präzisionsverlust verbunden.

Die Single-Beat-Methode erwies sich aufgrund instabiler Pmax-Berechnungen wegen ungenauer Definitionen von isovolumetrischen Abschnitten der RV-Druckkurve manchmal als schwierig zu reproduzieren (27, 28). Daher könnten Unsicherheiten bei der Pmax-Berechnung sowie die unvollständige Linearität der endsystolischen Druck-Volumen-Beziehungen Gründe für Unterschiede zwischen der Single-Beat- und der Multi-Beat-Methode sein. Ein solch evidenter Unterschied trat jedoch in der vorliegenden Studie nicht auf. Eine mögliche Erklärung für die gute Übereinstimmung zwischen den beiden Methoden in unserer Studie könnte sein, dass wir jede RV-Druckkurve direkt visuell analysiert haben, anstatt automatisierte Kalkulationen anzuwenden. Unsere Daten deuten darauf hin, dass die Ergebnisse von Studien mit schwerer PH, die entweder über Multi-Beat- (4, 5, 29) oder Single-Beat-Methode (7, 15) bestimmt worden sind, vergleichbar sind. Obwohl die Korrelation zwischen Single-Beat- und Multi-Beat Ees/Ea hoch signifikant gewesen ist und die Bland- und Altman-Analyse keine Bias aufgewiesen hat, ist jedoch anzumerken, dass die LOA zwischen –0,35 und +0,37 gelegen haben. Ausgehend von einem Punkt der RV-arteriellen Entkopplung von 0,805, mittels Multi-

Beat gemessen (Anlage F), könnten identische Single-Beat Messungen in einem Bereich von 0,455 bis 1,175 liegen, was eine nicht zu vernachlässigende Spanne wäre.

Die vorliegende Studie ist durch ihre kleine Stichprobe von nur 38 Patienten limitiert. Jedoch sind die untersuchten Methoden komplex und invasiv. Eine weitere Einschränkung besteht darin, dass bei gesunden Kontrollen nicht gemessen worden ist. Die Invasivität der Multi- und Single-Beat-Messungen von Ees/Ea wäre jedoch ein wesentliches ethisches Hindernis für eine solche Studie.

Zusammenfassend bestätigen die vorliegenden Ergebnisse die „klassische“ Single-Beat-Methode. Druckbasierte Methoden und die einfacheren nichtinvasiven Methoden zur Beurteilung der RV-arteriellen Kopplung zeigten unterschiedliche Genauigkeit und Präzision, könnten jedoch in der täglichen klinischen Praxis nützlich sein. Zukünftige neu zu entwickelnde nichtinvasive Messungen der RV-arteriellen Kopplung können entweder durch Multi- oder Single-Beat-Messungen von Ees/Ea validiert werden.

3.5 Vergleich von Ees/Ea und Eed mit Strain aus kardialem MRT (Anlage E)

Aus der kMRT-Bildgebung abgeleitete Surrogate der RV-Kontraktilität wie RV-EF und SV/ESV helfen dabei, den Beginn der RV-Dilatation vorherzusagen, und sind prognostisch relevant (14,107,108). Darüber hinaus ist das sogenannte kMRT-Feature-Tracking eine neuartige Methode zur Quantifizierung der Myokarddeformation, in Strain-Bildgebung gemessen. Dabei wird die Deformation des Myokards in der longitudinalen, radiären und zirkumferentiellen Ebene gemessen. Es konnte gezeigt werden, dass Strain, mit Feature Tracking gemessen, mit der RV-Ejektionsfraktion bei PH assoziiert ist (109) und bei dilatierter Kardiomyopathie eine stärkere Assoziation mit der Mortalität aufweist als die linksventrikuläre Ejektionsfraktion (110). Das physiologische Korrelat des RV-Strains muss jedoch noch definiert werden, da bislang unklar ist, ob RV-Strain-Messungen bei chronischer RV-Überlastung mit direkten Messungen der diastolischen RV-Steifheit (Eed), Ees und der Nachlast zusammenhängen (Ea) oder mit dem Ees/Ea-Verhältnis, das die RV-arterielle Kopplung darstellt. kMRT-basierte Surrogate dieser Variablen wären von großem klinischem Nutzen, da sie in die klinische Routine integriert werden könnten sowie eine komplexe und invasive Messung vermieden werden könnte.

Das Ziel ist daher gewesen, die Assoziation des kMRT-RV-Strains mit invasiv gemessenen Parametern aus Druck-Volumen-Schleifen zu definieren und den klinischen Nutzen der Strain-Analyse bei PH-Patienten zu bewerten. Darüber hinaus wurden neben den konventionellen Parametern der pulmonalen Hämodynamik (mPAP, PVR, Herzzeitvolumen (HZV)) auch Parameter der PA-Stiffness, der Pulmonalarterien-Compliance (PA-Compliance) und der PA-Dehnbarkeit (PA-distensibility) wie beschrieben (111) untersucht.

Wir analysierten Patienten mit PAH und CTEPH (diagnostiziert gemäß den aktuellen Richtlinien (112)), die zwischen Januar 2016 und April 2018 prospektiv an der „Right-Heart-I“-Studie (ClinicalTrials.gov: NCT03403868) und dem PH-Register in Gießen (113) teilnahmen. Alle Patienten wurden an Tag 1 einer kMRT-Bildgebung und an Tag 2 einer Druck-Volumen- und Swan-Ganz-Katheter-Untersuchung unterzogen. Alle Patienten erhielten gezielte Therapien bezüglich der PH, die auf klinischen Gründen und dem besten Behandlungsstandard beruhten. Es wurden insgesamt 38 Patienten eingeschlossen.

Der radiäre Strain der RV-Kurzachse korrelierte mit der RV-Dilatation (RV-EDV/(Body-Surface-Area, Körperoberfläche), BSA; Abbildung 8B). Der longitudinale Strain in der Längsachse korrelierte auch mit der Hypertrophie (RV-Masse/BSA) und der RV-EF (8B). Der zirkumferentielle Strain der Kurzachse (8B)

und der longitudinale Strain der langen Achse waren mit der PA-Stiffness assoziiert (Anlage E). Darüber hinaus zeigte der longitudinale Strain der langen Achse eine signifikante Korrelation mit der PA-distensibility (rho = – 0,406, p = 0,019).

Der longitudinale RV-Strain der langen Achse korrelierte mit dem mPAP und dem PVR (Abbildung 8C). Der zirkumferentielle Strain der kurzen Achse und der radiäre Strain der langen Achse korrelierten mit dem Herzindex beziehungsweise dem PVR (Abbildung 8C).

Ees/Ea zeigte Korrelationen mit dem longitudinalen RV-Strain der langen Achse (Abbildung 8D). Eed zeigte eine nichtlineare Assoziation mit dem radiären Strain der kurzen Achse (Abbildung 8D). Es konnte keine Korrelation von Ees mit Strain nachgewiesen werden.

Als sehr interessanter Marker erwies sich die Ratio aus dem globalen longitudinalen Strain zu EDV/BSA. Mit einer AUC von 0,908 in der ROC-Analyse sagt dieser von unserer Gruppe neu definierte Parameter eine RV-Steifheit als Surrogat der Eed voraus (AUC = 0,908; p < 0,001; Abbildung 9). Zu weiteren Assoziationen in den Ergebnissen wird auf Anlage E verwiesen.

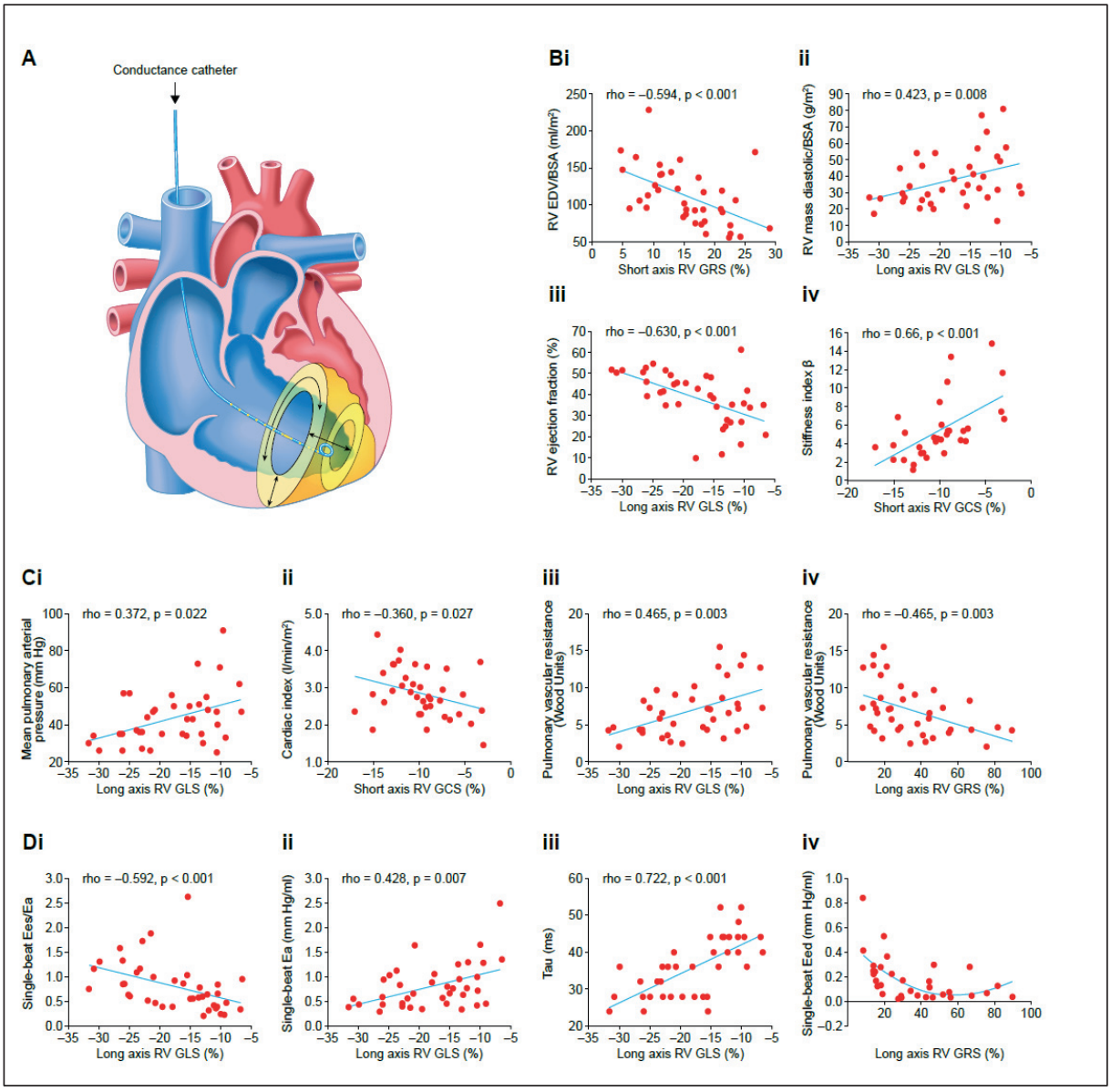

Abbildung 8: Assoziation von RV Global Strain mit kMRT RV-Maladaptation, invasiver pulmonaler Hämodynamik und Druck-Volumen-Schleifen

(A) In der Studie wurden Konduktanz-Katheterdaten mit kMRT-Daten zur Erfassung der radiären, longitudinalen und zirkumferentiellen RV-Bewegung verglichen, schematische Darstellung . **(B)** (i–iii) RV-Maladaptation (RV-Masse (diastolisch) und-EDV) und (iv) PA-Stiffness (angegeben als Stiffness-index β, siehe Anlage E) waren mit Strain-Werten assoziiert. **(C)** Wichtige Parameter der pulmonalen Hämodynamik und **(D)** Parameter aus Druck-Volumen-Schleifen waren mit dem Strain assoziiert. BSA: Körperoberfläche; Ea: arterielle Elastizität; EDV: enddiastolisches Volumen; Eed: enddiastolische Elastizität; GCS: globaler zirkumferentieller Strain (engl. Global Circumferential Strain); GLS: globaler

longitudinaler Strain; GRS: globaler radiärer Strain; RV: rechtsventrikulär. Abbildung aus Anlage E mit Erlaubnis

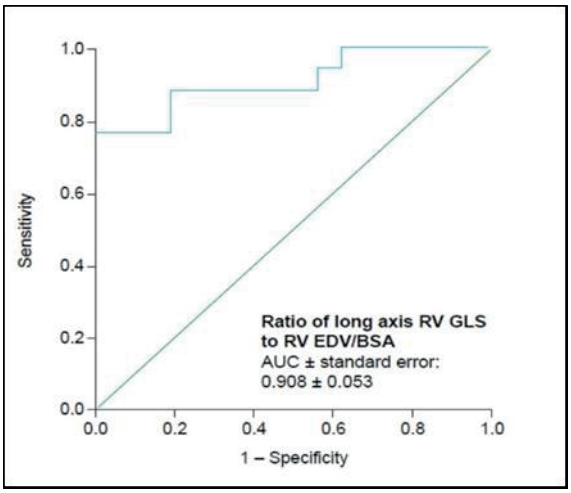

Abbildung 9: Assoziation des globalen longitudinalen RV Strains (GLS)/EDV-Ratio aus der kardialen Magnetresonanztomografie mit der diastolischen RV-Steifheit. Abbildung aus Anlage E mit Erlaubnis.

Die Ratio aus RV GLS/EDV/BSA sagte die diastolische RV-Steifheit (Eed dichotomisiert bei 0,124 mmHg/ml) bei der ROC-Analyse voraus. AUC = Fläche unter der Kurve (Area under the curve); BSA = Körperoberfläche (Body Surface Area); EDV = enddiastolisches Volumen; Eed = enddiastolische Elastizität; GLS = globaler longitudinaler Strain; RV = rechtsventrikulär.

Unsere Daten belegen erstmals eine signifikante Assoziation von durch kMRT-Bildgebung abgeleiteten RV-Strain-Parametern mit Ees/Ea, Ea und Eed. Wir konnten zeigen, dass die mittels kMRT-Feature-Tracking gemessene Strain-Werte signifikant mit der diastolischen RV-Funktion und Eed sowie der Nachlast assoziiert sind. Darüber hinaus spiegelte der kMRT-RV-Strain die RV-arterielle Kopplung wider und war mit RV-Dilatation und -Hypertrophie sowie konventionellen invasiven hämodynamischen Parametern assoziiert. Unsere Daten besagen, dass der kMRT-RV-Strain ein vielversprechender Indikator für die RV-arterielle Entkoppelung (angelehnt an Anlage F) und die diastolische RV-Steifheit ist. Dies erweitert das ohnehin schon erhebliche Anwendungsspektrum für kMRT zur Beurteilung der RV-Funktion bei der Nachsorge von Patienten mit PH. Darüber hinaus tragen unsere Ergebnisse dazu bei, die Wissenslücke in Bezug auf die Physiologie der RV-Belastung bei chronischer Drucküberlastung wie bei PH zu schließen.

Interessanterweise korrelierte die Ees nicht mit RV-Strain. Dies könnte darin begründet liegen, dass erstens in unserer Kohorte von Patienten mit chronischer Drucküberlastung der maximale Anstieg der Ees als Reaktion auf die erhöhte Nachlast bereits erreicht worden sein kann. Dies wird durch frühere Studien von Ees zur Adaptation des RV während der chronischen Drucküberlastung gestützt (114). Zweitens waren unsere Patienten möglicherweise in einem Zustand relativer RV-arterieller Entkopplung (Patientencharakteristika siehe Anlage E), in dem Eed und Ea weiter zunehmen, aber die Ees-Erhöhung erschöpft ist. Zunahmen von Ea und Eed in Kombination mit einem unveränderlichen Ees erklären möglicherweise, warum Strain-Werte mit dem Ees/Ea-Verhältnis korreliert sind, nicht jedoch mit Ees. Die Ergebnisse stehen in Einklang mit Daten, die zuvor von Guihaire et al. publiziert worden sind (114). Darin zeigt sich in einem Schweinemodell mit chronischer RV-Druckbelastung, dass die üblichen RV-Funktionsparameter eher mit der RV-arteriellen Kopplung als mit der ventrikulären

Kontraktilität assoziiert sind. Die Assoziation der Strain-Messung aus der kMRT mit der lastunabhängigen Messung von Eed in unserer Studie zeigt, dass die kMRT-Strain-Analyse ein vielversprechendes Instrument für die Nachuntersuchung von Patienten mit PH ist und das Potenzial hat, invasive Messungen von Eed und RV-arterieller Kopplung in Zukunft gegebenenfalls überflüssig zu machen. Der neue vorgeschlagene Parameter (globaler longitudinaler Strain (GLS)/EDV/BSA) zur non-invasiven Diagnostik der RV-Steifheit ist vielversprechend bei der Abschätzung der diastolischen RV-Funktion. Dies ist eine wichtige Beobachtung, da die diastolische RV-Funktion mit klinischer Verschlechterung der PH-Patienten assoziiert ist (43).

3.6 Definition des Punktes der RV-arteriellen Entkopplung (Anlage F)

RV-Versagen kann als Dyspnoe-/Müdigkeitssyndrom mit Einschränkung der Belastbarkeit und eventueller systemischer Stauung definiert werden, die durch die Unfähigkeit des RV verursacht wird, sich an eine erhöhte Nachlast unter Erhalt einer adäquaten Auswurfleistung anzupassen. Eine optimale RV-arterielle Kopplung beziehungsweise Ees/Ea-Ratio, die einen notwendigen Fluss mit einem minimalen Energieaufwand ermöglicht, tritt bei einem Ees/Ea-Verhältnis zwischen 1,5 und 2,2 (10) auf. Das Ausmaß der RV-arteriellen Entkopplung, bei dem ein RV-Versagen auftritt, ist jedoch nicht genau bekannt. Alle Untersuchungen diesbezüglich sind aus Untersuchungen des LV hergeleitet (10).

Daher kombinierten wir die kMRT des RV mit invasiver Druck-Volumen-Messung mittels Konduktanz-Katheter, um den Wert von Ees/Ea zu bestimmen, unterhalb dessen wesentliche Maladaptationsprozesse des RV beginnen. Wir erfassten zudem die Assoziation von RV-arterieller Entkopplung und diastolischer RV-Steifheit (Eed) mit kMRT-Indizes der RV-Maladaptation wie RV-Masse (68), RV-Masse/Volumen-Verhältnis (115), RV-EF (69), T1- und T2-Mapping (116) sowie die Assoziation von RV-arterieller Entkopplung mit aus kMRT hergeleiteten Parametern der PA-Stiffness (117), um die Pathophysiologie des RV-Versagens näher zu beleuchten.

Der Einschluss der Patienten erfolgte im Rahmen der Right-Heart-1-Studie (NCT03403868) zwischen Januar 2016 und Juli 2018. Das Prozedere der Untersuchung unterschied sich nicht von dem diesbezüglich zuvor beschriebenen Prozedere der Right-Heart-1-Studie.

Um die Reserve von Ees/Ea nach maladaptiven RV-Änderungen zu untersuchen, verglichen wir Druck-Volumen-Schleifen mit kMRT-Parametern wie RV-Dilatation, -Hypertrophie und -Funktion (Abbildung 10). Unsere Daten zeigen, dass Ees/Ea im RV-EDV/BSA-Tertil 3 gegenüber 1 erheblich vermindert ist und sich über die Tertile der RV-Hypertrophie (RV-Masse/BSA) und der EF bis zu einem Median von 0,56 verschlechtert (Abbildung 10). Darüber hinaus zeigen unsere Daten ein ähnliches Muster für Eed mit einer erheblichen Beeinträchtigung bei fortgeschrittener RV-Maladaptation (Abbildung 10). Unsere Ergebnisse belegen somit, dass Ees/Ea und Eed während des ersten Krankheitsverlaufs eine Reserve aufweisen, bis eine RV-arterielle Entkopplung auftritt. Diese Reserve beginnt beim vom LV adaptierten Optimum von Ees/Ea zwischen 1,5 und 2,0 bis zur RV-arteriellen Entkopplung von 0,8.

Um einen präzisen Cut-off von Ees/Ea zu erhalten, der die maladaptiven RV-Änderungen am besten unterscheidet, wurde die ROC-Kurvenanalyse mit Youden-Index verwendet (118). Für diese ROC-Analyse wurde die RV-Maladaption als RV-EF < 35 % definiert, da dieser Wert notwendigerweise mit einem Anstieg von EDV und ESV bei erhaltenem SV verbunden ist und mit einer erhöhten Mortalität bei Patienten mit PH in Verbindung steht (14,69,70,107).

Dadurch konnte erstmals eine RV-arterielle Entkopplung als Absolutwert von 0,805 für den RV definiert werden (Anlage F). Die Relevanz von Ees/Ea als Maß für die RV-arterielle Kopplung wurde durch die

Assoziation mit RV-Dilatation, Funktion, Masse, EF sowie Dehnbarkeit und Kapazität der Lungenarterien gestützt (siehe Anlage F). Es wurde bereits gezeigt, dass Patienten mit PAH, die gezielte Therapien erhalten, möglicherweise mehrere Jahre stabil bleiben, schließlich jedoch eine RV-Dilatation und EF-Minderung erleiden, was eine klinische Verschlechterung und verringerte Überlebensrate zur Folge hat (10,107,119). Da der Übergang von Adaptation zu Maladaptation und zu offensichtlichem Rechtsherzversagen fließend sein kann und Grenzwerte für Volumina schwer zu definieren sind, um diese Übergänge zu charakterisieren, haben wir uns entschlossen, Maladaptation oder Versagen als RV EF < 35 % zu definieren.

In vielen Studien wurden bereits Patienten mit PH in Bezug auf eine Ees- und Ea-Erfassung untersucht (Tabelle 1). Dies ist jedoch die erste Studie, die den Punkt der RV-arteriellen Entkopplung erfasst, an dem es zur RV-Dilatation kommt. Dies könnte in Zukunft bei verbesserter und schnellerer Erfassung des Ees/Ea-Verhältnisses zu einer schnelleren Diagnose des beginnenden RV-Versagens führen, da ein Abfallen des Ees/Ea-Verhältnisses von 1,5 bis 2,0 auf 0,8 erfolgt, bis eine Dilatation auftritt. Dies inkludiert, dass eine ausgeprägte Reserve der RV-arteriellen Kopplung besteht, bis Maladaptation auftritt (Abbildung 10).

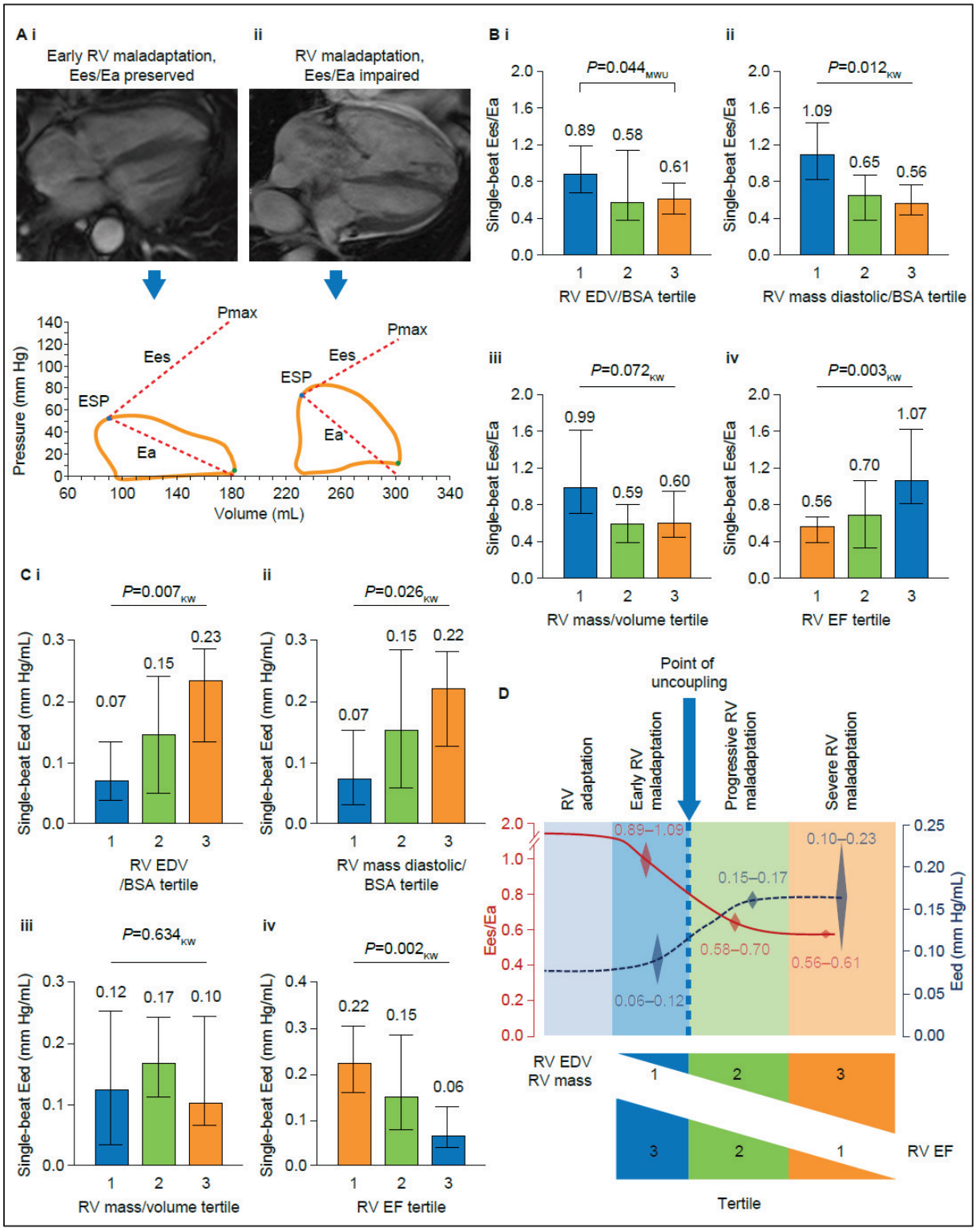

Abbildung 10:

Reserve der RV-arteriellen Kopplung (Ees/Ea), geschichtet nach maladaptiven RV-Veränderungen bei Patienten mit Pulmonaler Hypertonie

(A) Repräsentative Bilder der kardialen Magnetresonanztomografie und der Druck-Volumen-Schleifen für Patienten mit (i) erhaltenem Ees/Ea, frühen Anzeichen von maladaptiven RV-Veränderungen und (ii) beeinträchtigtem Ees/Ea und schwerer RV-Maladaptation. **(B)** Ees/Ea und **(C)** Eed, aufgeteilt nach

Tertilen von (i) RV-EDV/BSA, (ii) RV-Masse (diastolisch)/BSA, (iii) RV-Masse/Volumen-Verhältnis und (iv) RV-EF, die eine signifikante Reduktion von Ees/Ea in RV-EDV/BSA-Tertil 3 gegenüber 1 und über alle Tertile von RV-Masse (diastolisch)/BSA und eine signifikante Erhöhung von RV-EF hinweg zeigen. Zusätzlich zeigt sich eine signifikante Erhöhung von Eed über alle Tertile von RV-Maladaptationsparametern mit Ausnahme des RV-Masse/Volumen-Verhältnisses. Die Unterschiede zwischen den Tertilen wurden unter Verwendung der unabhängigen Stichproben per Kruskal-Wallis- oder Mann-Whitney-U-Test analysiert. **(D)** Im Verlauf der PH passt sich der RV zunächst der erhöhten Nachlast an. Mit fortschreitender Erkrankung kommt es zu einer RV-arteriellen Entkopplung mit schwerer RV-Maladaptation. Unsere Daten zeigen, dass Ees/Ea eine beträchtliche Reserve aufweist, die von Medianwerten von 0,89 bis 1,09 bei früher Maladaptation auf 0,56 bis 0,61 bei schwerer RV-Maladaptation abfällt. BSA gibt die Körperoberfläche an (Body Surface Area); Ea: arterielle Elastizität; EDV: enddiastolisches Volumen; Eed: enddiastolische Elastizität; Ees: endsystolische Elastizität; EF: Ejection Fraction; ESP: Endsystolischer Druck; KW: Kruskal-Wallis-Test; MWU: Mann-Whitney-U-Test; Pmax: theoretischer maximaler isovolumischer Druck, berechnet aus einer nichtlinearen Extrapolation des frühen und des späten Teils der RV-Druckkurve; RV: rechtsventrikulär. Abbildung mit Erlaubnis aus Anlage F.

3.7 **Assoziation von diastolischer RV-Steifheit mit erhöhter ventilatorischer Ineffizienz (Anlage G)**

Kurzatmigkeit ist eines der Hauptsymptome der PAH. Die Belastungsintoleranz bei der PAH ist multifaktoriell und neben einer zirkulatorischen Limitation spielt auch eine pathologische ventilatorische Antwort eine Rolle. Unter Belastung zeigen PAH-Patienten eine ineffiziente Hyper-/Totraumventilation welches in einem Anstieg des Verhältnisses der Ventilation (VE) zu Kohlendioxid-Ausatmung (VCO_2) (VE/VCO_2) während eines kardiopulmonalen Belastungstests resultiert (120,121). Es hat sich in der Tat gezeigt, dass die VE/VCO_2-Steigung unter Belastung ein wichtiger Prädiktor für das Outcome von PAH ist (122). Dies wurde daher als ein Parameter in die Risikostratifizierung zur Verlaufsbeurteilung der PAH aufgenommen (123). Andererseits beruht das derzeitige pathophysiologische Verständnis von PAH auf der Anpassung der rechtsventrikulären Funktion an die Nachlast (10,124,125). Inwiefern ineffiziente Hyper-/Totraumventilation bei der PAH mit der rechtsventrikulären Funktion und Adaptation des RV zusammenhängt, ist derzeit unbekannt. Wir untersuchten daher die RV-Funktion durch invasive Bestimmung von Ees, Ea und Eed und bezogen die Ergebnisse auf die VE/VCO_2-Steigung und andere Spiroergometrie-Parameter, von denen bekannt ist, dass sie prognostisch relevant sind, beispielsweise die maximale Sauerstoffaufnahme (VO_2peak) und den O_2-Puls, definiert als Verhältnis aus VO_2 und Herzfrequenz.

In diese Analyse wurden Patienten der „Right-Heart-1"-Studie zwischen Januar 2016 und Juli 2018 eingeschlossen. Das Prozedere unterschied sich vom zuvor beschriebenen Prozedere der Studie darin, dass alle Patienten einer Spiroergometrie-Untersuchung unterzogen worden sind (bzgl. Belastungsprotokoll siehe Anlage G).

Die aus Druck-Volumen-Schleifen abgeleiteten Parameter Ea und Eed korrelierten mit der VE/VCO_2-Steigung und dem $PETCO_2$ (Partiales Endtidales CO_2). Zusätzlich zeigte Ea mit dem O_2-Puls eine Korrelation. VE/VCO_2-Steigung und $PETCO_2$ korrelierten ebenfalls mit PVR. Es gab keine Korrelationen zwischen Ees/Ea oder Ees und Spiroergometrie-Parametern. Es gab ebenso keine Korrelation zwischen Parametern, die aus den Konduktanzwerten gewonnen wurden und dem Peak-VO_2. Interessanterweise zeigte sich, dass die VE/VCO_2-Steigung, $PETCO_2$ und der Peak O_2-Puls eine Korrelation mit der PA-Stiffness aufweisen. VE/VCO_2-Nadir Werte zeigten noch signifikantere Korrelationen mit Ea, Eed, PA-Stiffness, PVR und BNP als VE/VCO_2-Steigung (Anlage G). Eed und Ea zeigten starke Assoziationen mit VE/VCO_2-Grenzwerten, die nach aktuellen Leitlinien für die Risikobewertung von PAH-Patienten verwendet werden.

Wie in Abbildung 11 dargestellt, zeigt die Auftragung von VE/VCO_2 als Funktion von $PaCO_2$ eine charakteristische Verschiebung der Kurve nach links, was auf eine Zunahme der Chemosensitivität bei PAH-Patienten mit hoher Eed gehabt hindeutet (basierend auf einer zuvor beschriebenen Grenze für Eed (Anlage F)). Darüber hinaus war VE/VCO_2 in Ruhe und unter Belastung bei Patienten bei hoher Eed deutlich höher als bei niedriger Eed (Abbildung 11b).

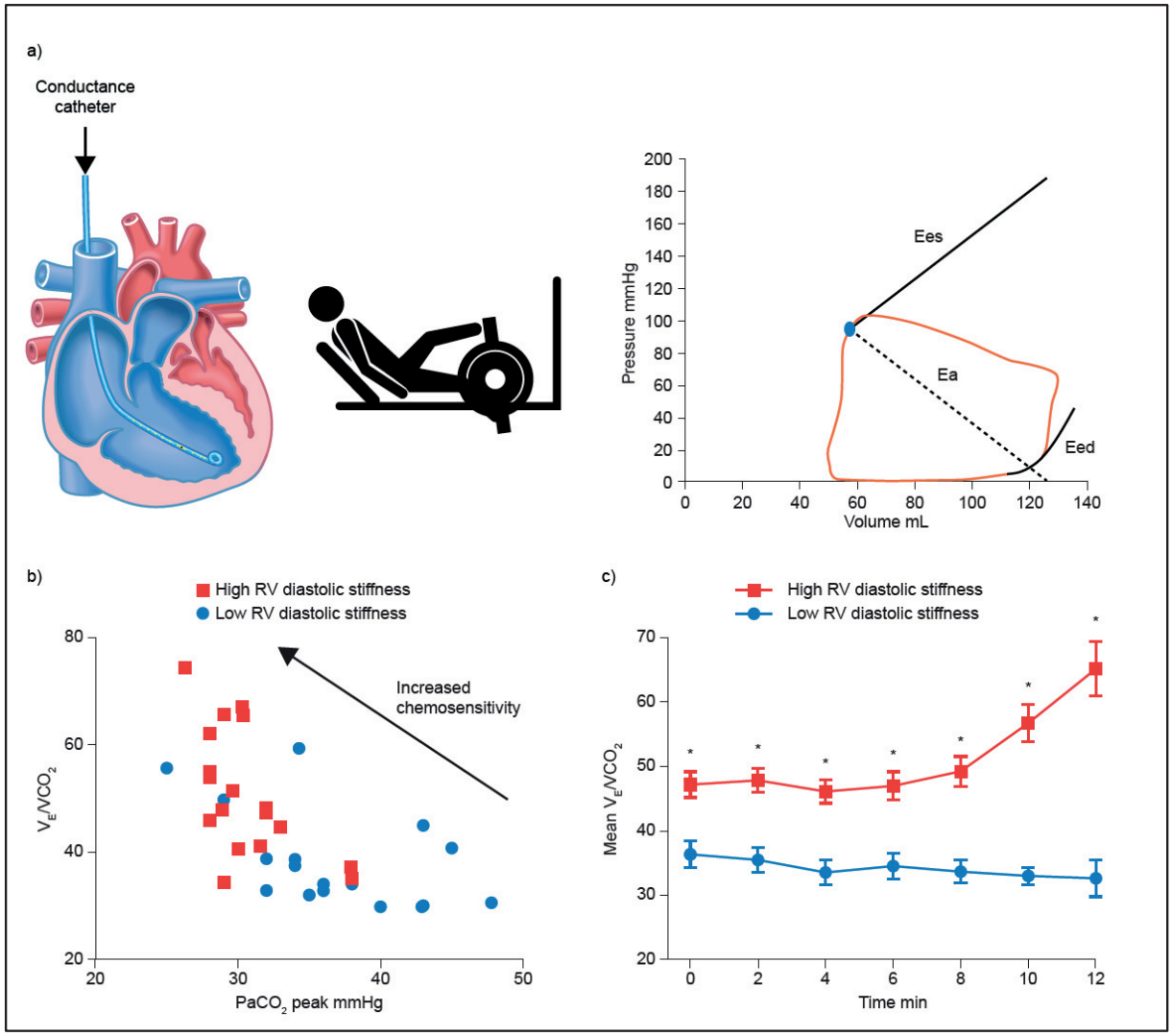

Abbildung 11: Pathophysiologisches Konzept der Assoziation von erhöhter diastolischer rechtsventrikulärer Steifheit mit erhöhter Chemosensitivität bei PAH

a) Es wurden Daten aus Konduktanz-Katheter und Spiroergometrie zur Analyse verwendet, schematische Darstellung. **b)** Patienten mit hoher Eed haben niedrigere $PaCO_2$- und höhere VE/VCO_2-Werte. Dies ist ein Hinweis auf erhöhte Chemosensitivität **c)** VE/VCO_2 ist in Ruhe und unter Belastung bei Patienten mit hoher Eed deutlich höher. Eine hohe diastolische RV-Steifheit wurde definiert als Eed > 0,124 mmHg/ml wie zuvor beschrieben (Anlage F). Fehlerbalken zeigen den Standardfehler des Mittelwerts an. * $p < 0{,}01$ (mit ungepaartem t-Test analysiert). Ea: arterielle Elastizität; Eed: enddiastolische Elastizität; Ees: endsystolische Elastizität; $PaCO_2$: kapillärer Kohlendioxid-Partialdruck;

RV: rechtsventrikulär; VE/VCO_2: Minutenvolumen/Kohlendioxidabgabe (Ventilationsäquivalent für Kohlendioxid). Abbildung aus Anlage G mit Erlaubnis.

In der vorliegenden Studie zeigten sowohl die rechtsventrikuläre diastolische Steifheit als auch erhöhte Nachlast des RV eine Assoziation mit ineffizienter Ventilation bei möglicherweise erhöhter Chemosensitivität bei Patienten mit PAH, während die RV-Kontraktilität (Ees), isoliert oder gekoppelt an Nachlast (Ees/Ea), keine Assoziation aufwies. Eine erhöhte Aktivität des sympathischen Nervensystems sagt eine schlechte Prognose für PAH voraus (126). Ein Anstieg der VE/VCO_2-Steigung wurde ebenfalls als Prädiktor für eine schlechte Prognose bei PAH identifiziert, wenn auch bei einiger Variabilität zwischen PAH-Subtypen [3, 4]. Insofern spielen die Mechanismen, die zu erhöhter Chemosensitivität führen, eine bedeutende Rolle. Diese Mechanismen sind bei PAH weitgehend unbekannt. Es zeigte sich zum Beispiel, dass eine Vorhofseptostomie den Tonus des sympathischen Nervensystems bei PAH reduziert trotz des bestehenden Rechts-Links-Shunts und Hypoxämie. Dies könnte mit einem reversiblen Bainbridge-Reflex erklärt werden (127), der bedingt, dass bei Dehnung des Myokards wie bei erhöhter diastolischer Steifheit die Chemosensitivität zunimmt. Unsere Ergebnisse belegen deutlich, dass die diastolische Steifheit eine Assoziation mit Hyperventilation/ineffizienter Ventilation und damit erhöhter Chemosensitivität zeigt und unterstützen damit andere Studien, die die diastolische Steifheit als eine der Hauptdeterminanten für die Prognose bei PAH ausmachten (43). Eine aktuelle weitere Studie erklärt eindrücklich, dass der venöse Rückstrom bei Patienten mit PH primär mit der erhöhten Eed zusammenhängt und zum Krankheitsprogress führt (128). Dabei könnte die Eed im Stadium der chronischen Druck- und Volumenüberlastung die Hauptdeterminante der Symptomatik sein und sollte damit therapeutisch ein Hauptziel darstellen. Somit ist eine der möglichen Erklärungen für die Ergebnisse der vorliegenden Studie, dass eine erhöhte Steifheit der rechten Herzkammer bei Patienten mit PAH die Hyperventilation/ineffiziente Ventilation und Kurzatmigkeit entscheidend triggert.

3.8 TAPSE/PASP als prognostischer Marker (Anlage H)

Das TAPSE/PASP-Verhältnis wurde als ein wichtiger klinischer und prognostischer Parameter bei Patienten mit und ohne PH und Herzinsuffizienz validiert (PH) [7–11] und als unabhängiger Prädiktor des Outcomes bei Patienten mit kombinierter prä- und postkapillärer PH identifiziert (60,61). Das TAPSE/PASP-Verhältnis wurde im Hinblick auf die Prognose bei PAH-Patienten noch nicht hinreichend untersucht. Das Ziel war es einerseits, die prognostischen Werte des TAPSE/PASP-Verhältnisses in PAH zu untersuchen, andererseits die Beziehung zwischen TAPSE und PASP auf der einen sowie zu hämodynamischen Parametern auf der anderen Seite.

Wir analysierten Patienten mit PAH, die zwischen November 2003 und Juli 2014 in das Gießener PH-Register aufgenommen wurden (103) (Anlage H). Die Analyse umfasste Patienten mit vollständiger Echokardiografie und invasiven hämodynamischen Daten zum Zeitpunkt der Registrierung und vollständigen Follow-up-Daten. Diese wurden bis Mai 2017 aus dem PH-Register Gießen abgerufen. Alle Patienten erhielten gezielt PAH-Therapien, die auf dem besten Behandlungsstandard beruhten. Die Untersuchung wurde von der Ethikkommission der Medizinischen Fakultät der Universität Gießen gebilligt (AZ 186/16, 266/11).

Die mittlere Nachbeobachtungszeit ± SD betrug 81,3 ± 55,7 Monate [Median [IQR]: 72,5 [89,4] Monate, in denen 145 (50,0 %) der Patienten gestorben sind. Die mediane [IQR] Nachbeobachtungszeit in TAPSE/PASP-Tertilen 1, 2 und 3 betrug 64,0 [89,5] Monate, 85,0 [85,5] Monate und 73,5 [106,3] Monate. In einer multivariaten Analyse ist TAPSE/PASP mit Mortalität assoziiert (Anlage H). Die prognostische Signifikanz des TAPSE/PASP-Verhältnisses wurde bestätigt durch Kaplan-Meier-Analysen, die im mittleren und hohen TAPSE/PASP-Bereich bezüglich des Überlebens insgesamt

deutlich besser ausfielen als im niedrigen Tertil (Abbildung 12). Das 5-Jahres-Gesamtüberleben lag bei 58,1 %, 73,0% und 70,0 %, aufsteigend von niedrigen zu hohen TAPSE/PASP-Tertilen (Abbildung 12).

Das TAPSE/PASP-Verhältnis korrelierte signifikant mit der PAC und zeigte eine hyperbelartige Beziehung zu PVR (Abbildung 13).

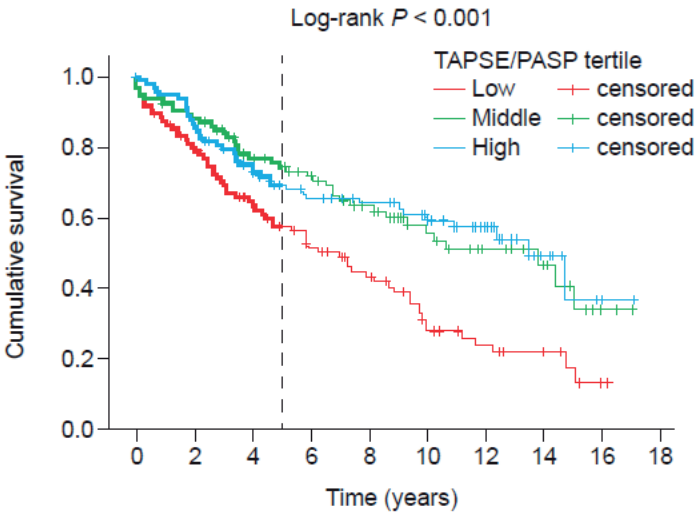

Number at risk	1 year	3 years	5 years
Low tertile	83	64	50
Middle tertile	93	81	63
High tertile	85	66	50

Abbildung 12: Kaplan-Meier-Überlebenskurven in Abhängigkeit von Tertilen des TAPSE/PASP-Verhältnisses in Patienten mit PAH (n = 290). Bereiche der Tertilen sind low: <0,19mm/mmHg, middle: 0,19-0,32mm/mmHg, high> 0,32 mm/mmHg. PASP: pulmonal-arterieller systolischer Druck; TAPSE: Tricuspidal Annular Plane Excursion. Abbildung aus Anlage H mit Erlaubnis.

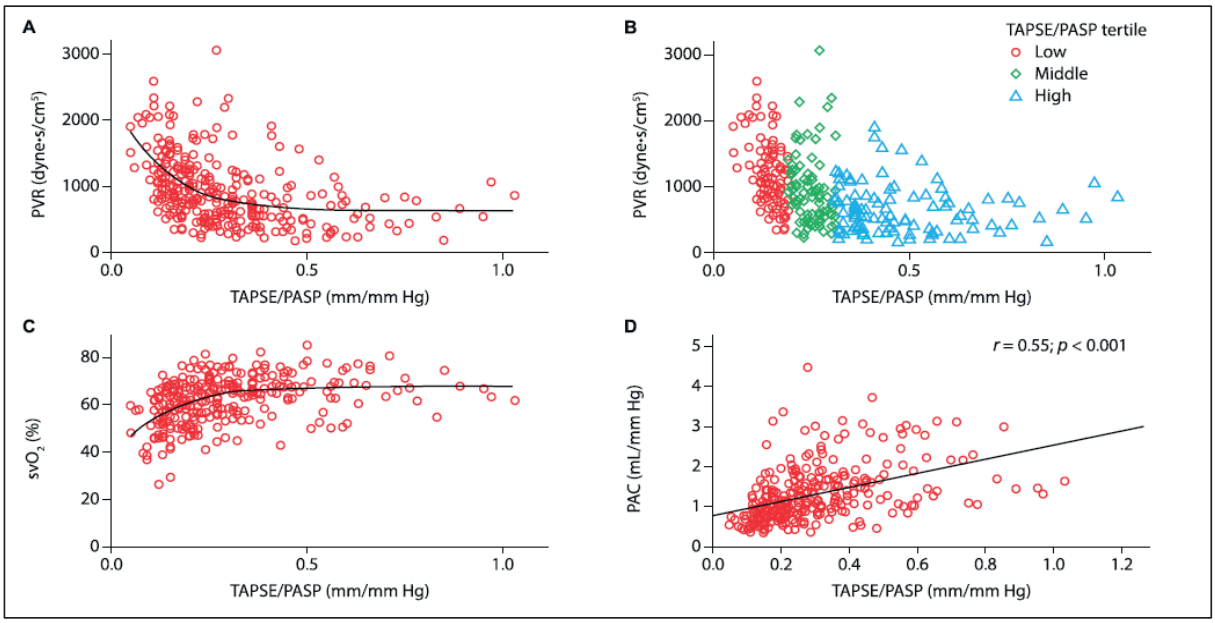

Abbildung 13: Beziehung des TAPSE/PASP-Verhältnisses zu PVR, SvO_2 und PAC. Streudiagramme zeigen **(A)** PVR gegen TAPSE/PASP, **(B)** PVR versus TAPSE/PASP nach TAPSE/PASP-Tertilen, **(C)** SvO_2 versus TAPSE/PASP, **(D)** Spearman-Korrelation von PAC mit TAPSE/PASP. PAC: Pulmonal-arterielle Compliance; PASP: Pulmonal-arterieller systolischer Druck; PVR: Pulmonary Vascular Resistance; SvO_2: gemischt-venöse Sauerstoffsättigung; TAPSE: Tricuspidal Annular Plane Systolic Excursion. Abbildung aus Anlage H mit Erlaubnis.

Zusammenfassend haben wir eine komplette Analyse des TAPSE/PASP-Verhältnisses in einer großen Kohorte von Patienten mit PAH vorgelegt. Neue Erkenntnisse unserer Studie umfassen erstens, dass das TAPSE/PASP-Verhältnis ein aussagekräftiger prognostischer Parameter bei Patienten mit PAH ist, sowie zweitens, dass TAPSE/PASP mit Pulmonalarterien-Compliance (PAC) korreliert und eine hyperbelartige Assoziation mit PVR hat. Unsere Daten führen das TASPE/PASP-Verhältnis als unabhängigen prognostischen echokardiografischen Parameter bei Patienten mit PAH ein. Obwohl mehrere echokardiografische Parameter der RV-Funktion mit Überleben assoziiert sind, zeigen unsere Daten, dass im direkten Vergleich das TAPSE/PASP-Verhältnis möglicherweise konventionellen Parametern überlegen ist. Dies könnte darin begründet sein, dass TAPSE/PASP die RV-arterielle Kopplung widerspiegelt (Anlage B) und als nachlastunabhängiger Parameter angesehen werden kann. Das wäre der entscheidende Unterschied zu anderen echokardiografischen Parametern der RV-Funktion, die allesamt als lastabhängig gelten. Unsere Daten belegen, dass das TAPSE/PASP-Verhältnis mit dem Schweregrad der Trikuspidalklappeninsuffizienz (TI) zusammenhängt (Anlage H). Dieser Befund ist von klinischer Bedeutung, da eine schwere TI per se bei Patienten mit PAH prognostisch bedeutend ist (129). Die TAPSE-Werte werden bei schwerer TI wegen des Pendelvolumens allerdings überbewertet (84); somit kann die TAPSE bei schwerer TI nur bedingt als Parameter der RV-Funktion verwendet werden. Die Ratio der TAPSE zu PASP stellt sich demgegenüber als robusterer Parameter dar. Korrelation und Assoziationen mit aus Druck- und Volumenkathetern erbrachten Daten der RV-arteriellen Kopplung konnten von unserer Gruppe bereits gezeigt werden (Anlage B). Die deutliche

lineare Korrelation zu PAC und die hyperbelartige Beziehung zu PVR legen den Schluss nahe, dass diese Nachlastparameter in das TAPSE/PASP-Verhältnis eingehen.

Weitere Studien sind nötig, um die Funktion dieser Ratio genau zu definieren. Allerdings stellt dieser Parameter einen leicht zu bestimmenden Wert dar, der prognostische Aussagen über die RV-Funktion erlaubt.

3.9 Klinische Relevanz von Ees/Ea (Multi-Beat-Methode) (Anlage D)

Wie in den vorherigen Abschnitten dargestellt, ist die RV-arterielle Kopplung ein wichtiger funktioneller Parameter, der, gemessen mit echokardiografischen Surrogaten (TAPSE/PASP, Anlage B, Anlage H) und kMRT-abgeleiteten Surrogaten (SV/ESV, (14,81)) eine prognostische Bedeutung hat. Der Goldstandard der Erfassung der RV-arteriellen Kopplung ist die Multi-Beat-Methode (siehe Einleitung). Interessanterweise sind die Parameter, die aus dieser Methode gewonnen werden und RV-arterielle Kopplung beschreiben, bislang nicht auf prognostische Relevanz hin untersucht worden.

Um diese Wissenschaftslücke zu schließen und die prognostisch-klinische Relevanz zu erfassen, untersuchten wir in einem Teilprojekt unserer „Right-Heart-1“-Studie 38 Patienten mit PAH mit der Multi-Beat-Methode. Eingeschlossen wurden Patienten mit PAH im Zeitraum von Februar 2017 bis Dezember 2018. Während der Untersuchungen gab es keinerlei Komplikationen. Alle Untersuchungen wurden unter Supervision des Verfassers (Qualifikation: Internistische Intensivmedizin und Pneumologie) und eines weiteren Internisten durchgeführt. Nur Patienten, bei denen eine adäquate Messung des Ees und der Ea unter Vorlastsenkung durchgeführt werden konnten, wurden eingeschlossen. In die Analyse gingen auch Daten von Patienten ein, die eine Vena-cava-Okklusion mittels Ballon-Okklusion ablehnten, jedoch der Valsalva-Methode zustimmten, um die Vorlast zu senken.

Die prognostische Relevanz von Multi-Beat Ees/Ea wurde durch prospektive Bewertung klinischer Verschlechterungsereignisse ab dem Zeitpunkt der Multi-Beat-Messung bis März 2019 bestimmt. Die klinische Verschlechterung wurde wie folgt definiert: Verringerung der Belastbarkeit (– 15 % im Vergleich mit dem Basis-6-Minuten-Gehtest), Verschlechterung der Funktionsklasse nach NYHA oder klinische Verschlechterung, die eine Krankenhauseinweisung erfordert, Notwendigkeit neuer PAH-Therapien, Lungentransplantation oder Tod.

Insgesamt wurden neun klinische Verschlechterungsereignisse während einer mittleren Nachbeobachtungszeit von sechs [2,8–11,3] Monaten (acht Krankenhauseinweisungen [einschließlich sechs Eskalationen einer spezifischen PAH-Therapie] und ein Fall einer Verschlechterung der Funktionsklasse) beobachtet. Unter Verwendung von ROC-Analysen und des Youden-Index ermittelten wir einen Cut-off von 0,70 für Multi-Beat Ees/Ea, um eine klinische Verschlechterung zu unterscheiden (AUC: 0,736; P = 0,035; Sensitivität: 62,1 %; Spezifität: 89,9 %) (Anlage D). In der multivariaten Cox-Regressionsanalyse (angepasst an Alter und Geschlecht) war Ees/Ea, das bei 0,70 dichotomisiert wurde, signifikant mit einer klinischen Verschlechterung assoziiert (multivariate Hazard-Ratio: 10,87; 95-Prozent-Konfidenzintervall: 1,34 bis 90,91; p = 0,010). Dies wurde durch Kaplan-Meier-Analysen gestützt, die eine signifikant höhere klinische Verschlechterungsrate bei Patienten mit Ees/Ea unter 0,70 im Vergleich zu Patienten mit höheren Ees/Ea-Werten zeigten (log-rank P = 0,005; Abbildung 14).

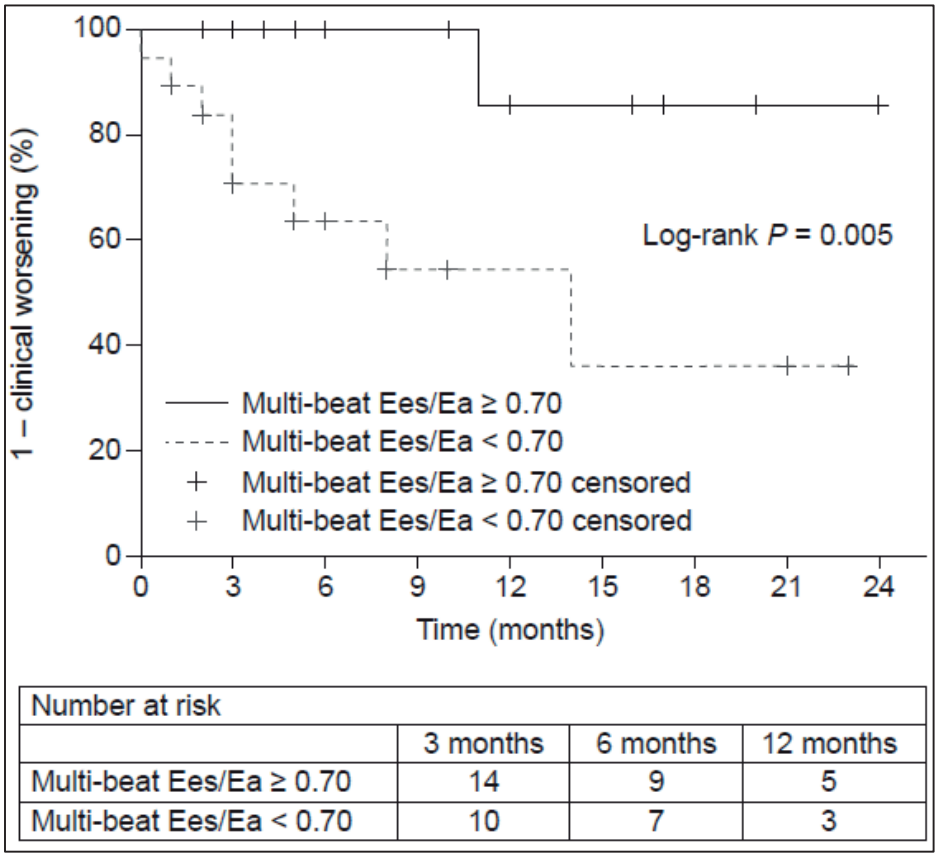

Number at risk			
	3 months	6 months	12 months
Multi-beat Ees/Ea ≥ 0.70	14	9	5
Multi-beat Ees/Ea < 0.70	10	7	3

Abbildung 14: Kaplan-Meier-Analyse der Zeit bis zur klinischen Verschlechterung bei Patienten mit Pulmonaler Hypertonie, die bei einem Verhältnis von endsystolischer/arterieller Elastizität (Ees/Ea) von 0,70 dichotomisiert wurden. Der Cut-Off wurde aus Analysen der Receiver Operating Characteristics (ROC) und des Youden-Index (Fläche unter der ROC-Kurve: 0,736; p = 0,035; Sensitivität: 62,1 %; Spezifität: 89,9 %) abgeleitet. Abbildung aus Anlage D mit Erlaubnis.

Zusammenfassend wurde in der vorliegenden Studie gezeigt, dass Multi-Beat Ees/Ea ein unabhängiger Prädiktor für das Outcome ist mit einem Cut-Off von 0,7, um eine klinische Verschlechterung zu unterscheiden. Dies stimmt mit unserer vorherigen Feststellung überein, dass eine RV-Dilatation mit einer prognostisch relevanten Abnahme der EF unter 35 % auftritt, wenn das Single-Beat Ees/Ea-Verhältnis von normalen Werten von 1,5 bis 2,0 auf unter 0,8 abgenommen hat. Somit scheint der kritische Bereich der RV-arteriellen Entkopplung im Bereich 0,7 bis 0,8 zu liegen. Damit ist erstmals eine prognostische Relevanz der Ees/Ea-Messung gezeigt sowie eine Absolutgrenze ermittelt worden, ab der die RV-arterielle Entkopplung beginnt und prognostisch ungünstig wird.

Zukünftige Studien sind nötig, um mit einem größeren Patientenkollektiv die Studienergebnisse zu bestätigen und gegebenenfalls Ees/Ea in Zusammenhang zu Mortalität zu setzen.

3.10 Evaluation der RA-Funktion bei Pulmonaler Hypertonie (Anlage I)

Eine echokardiografische 2D-Speckle-Tracking-Studie ergab, dass die Funktionen des RA-Reservoirs und der passiven Phase bei schwerer PH unabhängig von RA-Größe und -Druck beeinträchtigt sind, was auf ein RV-Versagen zurückzuführen ist (130). Daher ist der Einfluss des RV-Versagens auf den

rechten Vorhof ein wesentlicher Bestandteil der Pathophysiologie der PH. Die Beurteilung der RA-Funktion wiederum scheint für ein besseres Verständnis der RV-Funktion bei PH von wesentlicher Bedeutung zu sein. Das Bewusstsein für die Bedeutung der RA-RV-Achse in der PH wächst. Mehrere echokardiografische Speckle-Tracking-Studien haben über Deformation und Funktion der RA bei Patienten mit PH berichtet (93,131,132). Dabei wurde vermutet, dass die RA-Reservoir-Funktion eine Schlüsselrolle bei der Progression der PH spielt. Daher bestand der Zweck dieser Studie darin, die RA-Funktion mittels kMRT im so genannten „Feature Tracking" zu evaluieren und mit lastunabhängigen Parametern der RV-Funktion in Beziehung zu setzen, einschließlich Goldstandardbestimmungen der Kontraktilität, gemessen als Ees, der arteriellen Last, gemessen als Ea, und der diastolischen Steifheit, gemessen als Eed.

Die Patienten wurden prospektiv zwischen Januar 2016 und Dezember 2018 eingeschlossen. Patienten mit Vorhofflattern oder -flimmern wurden ausgeschlossen. Alle Patienten erhielten einen Tag vor Rechtsherzkatheter-Untersuchung und Druck-Volumen-Katheter-Untersuchung ein kMRT zur Erfassung der verschiedenen RA-Phasen und zur Beschreibung der RA-Funktion.

Die RA-Strain-Analyse wurde aus dem Vierkammerblick erfasst. Endokardkonturen wurden manuell in endsystolischen Bildern mit anschließendem automatischem „Feature Tracking" während des gesamten Herzzyklus durchgeführt. Die Qualität des automatischen Trackings wurde visuell überprüft. Bei unzureichendem automatischem „Tracking" wurden manuelle Anpassungen an der Anfangskontur vorgenommen und der Algorithmus wiederholt. Es wurden keine RA-Segmente von der Analyse ausgeschlossen. Das Tracking wurde dreimal wiederholt. Für die Analyse wurden Durchschnittswerte verwendet wie in einer vergleichbaren Studie beschrieben (133). Um die Intra- und Inter-(Observer-)Beobachter-Reproduzierbarkeit des RA-Reservoir-Strains zu testen, wurden zehn zufällig ausgewählte Analysen zweimal vom selben Beobachter beziehungsweise von einem zweiten wiederholt. Wie zuvor beschrieben (134) wurden der RA-Reservoir-Strain und der aktive RA-Strain durch Messen der entsprechenden Spitzen-Strain-Werte bewertet (Abbildung 3). Der passive RA-Strain wurde als Differenz zwischen dem RA-Reservoir-Strain und dem aktiven RA-Strain berechnet.

Insgesamt wurden 54 Patienten mit PH eingeschlossen. Die meisten hatten eine idiopathische PAH, waren in der Funktionsklasse III nach NYHA (Anlage I). Ein erheblicher Teil der Patienten erhielt eine duale oder dreifach kombinierte gezielte PH-Therapie. Fünf Patienten hatten keine spezifische PH-Therapie. Von ihnen hatte einer eine operable CTEPH. Die verbleibenden vier Patienten mit CTEPH wurden zuvor als inoperabel eingestuft, erhielten bereits lösliche Guanylatcyclase-Stimulatoren und wurden für die Ballonangioplastie evaluiert. Der Intraclass-Korrelationskoeffizient für die Übereinstimmung zwischen den verschiedenen Beobachtern betrug 0,86 (95-Prozent-CI: 0,417–0,970; p = 0,05) mit einem Variationskoeffizienten von elf Prozent in Bezug auf die RA-Reservoirs-Funktion. Die meisten Patienten wiesen eine RA- und RV-Dilatation auf (Anlage I).

Das Reservoir, der aktive und der passive Strain korrelierten signifikant mit der diastolischen RV-Funktion [Eed und EDP); Abbildung 15], zeigten jedoch keine Assoziation mit RV-Kontraktilität, Ees oder Nachlast, Ea oder mPAP.

Zusätzlich zeigte der RA-Reservoir-Strain signifikante Korrelationen mit dem RA-Druck (engl. Right Atrial Pressure, RAP), dem Herzindex, BNP und dem RA-Volumen (Anlage I). Darüber hinaus wurden signifikante Korrelationen mit der RV-Dilatation (RV-EDV), der RV-Hypertrophie (RV-Masse) und der RV-EF beobachtet. Zudem ergaben sich signifikante Korrelationen des passiven und aktiven RA-Strains mit RAP, Herzindex, BNP, RA-Maximalvolumen, RV-EDV und -Masse sowie RV-EF (siehe Anlage I). Das

RA-Reservoir, passiver und aktiver Strain waren sämtlich signifikant mit dem Durchmesser der Vena cava inferior assoziiert (Anlage I).

In einer univariaten linearen Regressionsanalyse zeigte der B-Koeffizient, dass ein Anstieg von Eed und EDP signifikant mit einer Verringerung der RA-Reservoir-Funktion verbunden war. In entsprechenden multivariaten Modellen entdeckten wir, dass ein erhöhter EDP mit einer verringerten Funktion des RA-Reservoirs verbunden war (Anlage I) und dass ein Anstieg des EDP mit einer Verringerung des passiven RA-Strains verbunden war. Darüber hinaus war ein erhöhter Eed-Wert unabhängig mit einem verringerten aktiven RA-Strain verbunden (Anlage I).

Die vorliegenden Ergebnisse zeigen, dass bei chronischer PH die RA-Funktion maßgeblich von der diastolischen RV-Funktion abhängt. Unsere Daten legen nahe, dass eine Beeinträchtigung der RV-Lusitropie die RA-Deformation direkt beeinflusst, was wiederum eine Ursache für einen erhöhten venösen Rückfluss sein kann. Die beobachtete Assoziation zwischen der diastolischen RV-Steifheit und der phasischen RA-Funktion steht daher im Einklang mit der Tatsache, dass die myokardiale RV-Steifheit zu einem verringerten passiven Zufluss und einem diastolischen Rückfluss führt, wodurch die frühe diastolische Füllung beeinträchtigt wird und ein großer Anteil der RV-Füllung von der atrialen Kontraktion abhängt (135,136). Wenn die Vorhoffunktion beeinträchtigt ist, kommt es zu einem erhöhten venösen Rückfluss und einer anschließenden klinischen Verschlechterung mit den Anzeichen eines RV-Versagens. Unsere Daten zeigen signifikante Korrelationen der phasischen RA-Funktion mit der RA-Größe und dem Durchmesser der Vena cava inferior (Anlage I), was darauf hindeutet, dass ein Verlust der Reservoir-Funktion zu einem Rückfluss der Venen führt. Dies wird durch aktuelle Daten von Marcus und Mitarbeitern gestützt, die einen Zusammenhang zwischen venösem Rückfluss während der atrialen Kontraktion und diastolischer RV-Steifheit zeigen (128).

Unsere Daten belegen damit erneut, dass die diastolische RV-Funktion im Stadium der chronischen Druckbelastung des RV eine bedeutende, gar entscheidende Rolle für die Gesamtfunktion des RV-Funktion und die Symptomatik bei PH spielt, wie auch in Anlage G gezeigt. Dabei zeigt die aktuelle Studie einen direkten Zusammenhang zwischen der eingeschränkten diastolischen Funktion und der eingeschränkten RA-Funktion, die eine für Patienten direkte klinische Konsequenz mit venösem Rückstau, Halsvenenstau, Aszites und gegebenenfalls Beinödemen zur Folge hat. Somit wären zukünftige Studien notwendig, die gezielt auf die diastolische Funktion zielen und diese angehen.

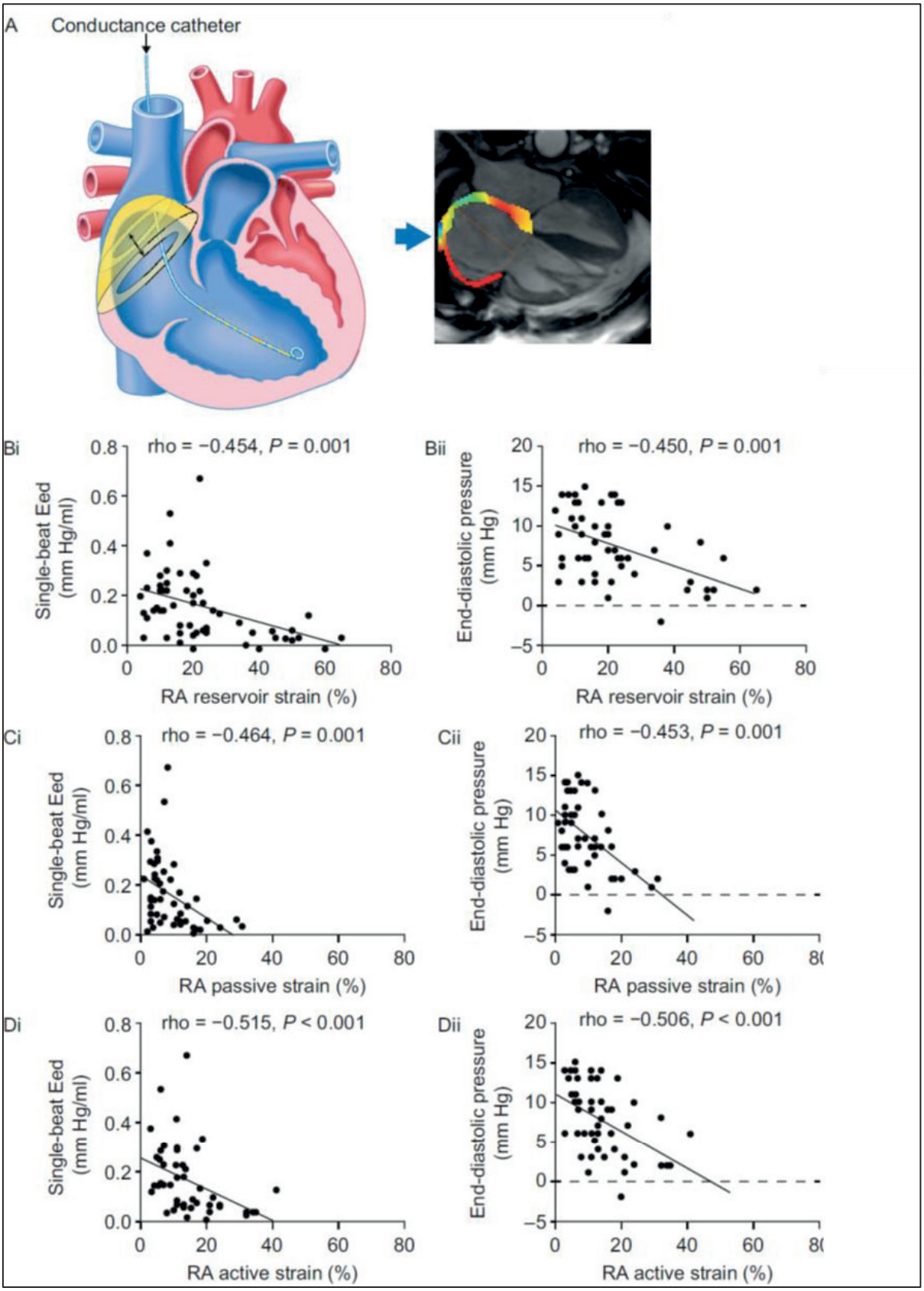

Abbildung 15: Assoziation der RA-Phasenfunktion mit der diastolischen RV-Funktion. Schematische Darstellung des RA-Strains in Kombination mit einem Druck-Volumen-Katheter. Korrelation von RA-

Reservoir-Strain (B), passivem Strain (C) und aktivem Strain (D) mit Eed (i) und enddiastolischem Druck (ii). Eed: End-diastolic Elastance; RA: Rechtes Atrium. Abbildung aus Anlage I mit Erlaubnis.

4 Zusammenfassung

Der rechte Ventrikel (RV) spielt für die Prognose der PH eine bedeutende Rolle. Die rechtsventrikuläre Funktion wurde in den letzten Jahrzehnten unterschätzt, auch und gerade aufgrund der Annahme, sie habe lediglich eine Konduitfunktion, welche dazu dient, den Blutfluss von den Venen in die Lungenarterien zu gewährleisten. Aus dieser vereinfachten Annahme resultierte eine deutliche Unterbewertung der rechtskardialen Funktion. Offensichtlich ist, dass die kontraktile Funktion des rechten Ventrikels Voraussetzung für eine Adaptation an jegliche Erhöhung des Lungenwiderstandes und für eine Herzzeitvolumensteigerung bei körperlicher Belastung ist. Die pulmonale Hypertonie (PH) stellt eine Erkrankung dar, bei der die rechtskardiale Funktion zur Überwindung der erhöhten Nachlast von besonderer Bedeutung ist. Um die dadurch auftretende Wandspannung zu senken, kommt es zunächst zu einer kompensatorischen Hypertrophie und Steigerung der rechtsventrikuläre Elastizität (Ees; Maß der lastunabhängigen Kontraktilität). Letzteres dient auch insbesondere dazu, das Verhältnis aus Ees und Ea (pulmonalarterielle Elastizität; zusammenfassendes Maß der Nachlast) in der kompensierten Phase im Gleichgewicht zu halten. Übersteigt die Ea die Ees wesentlich, kommt es zur RV-pulmonalarteriellen Entkopplung mit RV-Dilatation, erhöhtem RV-Volumen, reduzierter RV-Auswurfleistung und systemischem Rückstau.

Daraus ergibt sich, dass die Messung der kontraktilen Funktion des RV im Verlauf der PH unverzichtbar ist. Konventionelle Messungen der RV-Funktion wie echokardiografische Parameter und MRT-abgeleitete Funktionsparameter, als auch indirekt abgeleitete Parameter aus dem Rechtsherzkatheter, sind nachlastabhängig und repräsentieren nicht die intrinsische lastunabhängige Kontraktilität des rechten Ventrikels. Adaptiert an den linken Ventrikel wurden Katheter, die Druck und Volumen zur gleichen Zeit zur Erstellung von Druck-Volumen-Schleifen messen, auch für den rechten Ventrikel verwendet, um die lastunabhängige Kontraktilität und die diastolische Steifheit (Eed; enddiastolische Elastizität) zu messen. Über eine sogenannte Single-beat-Methode, basierend auf einem einzelnen Herzschlag, oder eine Multi-beat-Methode, basierend auf einer Vorlastreduktion und Erfassungen mehrerer Druck-Volumen-Schleifen, können die Kontraktilität und diastolische Funktion aus den Druck-Volumen-Beziehungen berechnet werden

Da diese Katheter in der Messung aufwendig und teuer sind, wurden Surrogate beschrieben, die die komplexe Messung ersetzen sollen. Vereinfachte Parameter, abgeleitet aus dem Rechtsherzkatheter, dem Druck-Volumen-Katheter, MRT oder Echokardiografie, wurden empfohlen. Dabei sind diese Messungen bislang nicht mit dem Goldstandard validiert worden.

Bezüglich dieser Validierung der vorgeschlagenen Methoden mit dem Goldstandard, der Erfassung mehrerer Druck-Volumen-Schleifen mittels Multi-Beat Methode, konnten wir zeigen, dass

- der Ersatz des endsystolischen Druckes (ESP) durch pulmonalarteriellen Mitteldruck (mPAP), wie von vielen Arbeitsgruppen verwendet, zu falschen Werten der Kontraktilität führt, da der mPAP den ESP gerade in hohen Druckbereichen unterschätzt.

- die in der Echokardiografie vorgeschlagene TAPSE/PASP-Ratio (Tricuspidal Annular Plane Excursion/pulmonalarterieller systolischer Druck) mit der Prognose bei PAH assoziiert ist, mit der in der Single-beat-Methode gemessenen Ees/Ea-Ratio korreliert und unter den vorgeschlagenen Surrogat-Parametern der Echokardiografie die besten Vorhersagen der RV-pulmonalarteriellen Kopplung erlaubt. Die TAPSE/PASP-Ratio erlaubt zudem hämodynamische Charakterisierung und Prognoseabschätzung bei PH im Kontext chronischer Lungenerkrankungen.

- die Single-beat-Methode, mittels Druck-Volumen-Katheter gemessen, die beste Surrogat-Methode zur Berechnung der Ees/Ea-Ratio im Vergleich zu verschiedenen aus Echokardiografie und MRT abgeleiteten Parametern darstellt, validiert an der Multi-Beat Ees/Ea.

Weiterhin ist es von enormer Wichtigkeit, nichtinvasive Methoden der kardialen Deformationsmessung (Strain im sogenannten Feature-Tracking) mit Parametern der RV-pulmonalarteriellen Kopplung zu vergleichen um neue nicht-invasive Parameter der Erfassung der diastolischen Funktion zu eruieren. Wir konnten zeigen, dass

- der globale longitudinale Strain (GLS) mit Ees/Ea assoziiert ist.

- das Verhältnis von GLS zu EDV(BSA) (körperoberflächenbezogenes RV enddiastolisches Volumen) ein sehr guter Parameter ist, die diastolische Steifheit (Eed) nichtinvasiv vorherzusagen.

Der Punkt, an dem die Nachlast (Ea) die rechtsventrikuläre Elastizität (Ees) wesentlich übersteigt und sich eine RV-pulmonalarterielle Entkopplung einstellt, ist bislang an Publikationsergebnisse des LV angelehnt worden und für den rechten Ventrikel nicht bekannt. Unsere Ergebnisse haben diesen Punkt erstmalig definiert und belegen, dass

- die RV-arterielle Entkopplung bei einem Ees/Ea-Wert unterhalb von 0,805 beginnt, mit der Folge einer RV-Dilatation und Reduktion der RV-EF.

- Ees/Ea-Werte unterhalb von 0,7 mit einer schlechten klinischen Prognose verbunden sind.

Untersuchungen haben gezeigt, dass die diastolische Steifheit entscheidend den Rückfluss des venösen Blutes aus dem RV in die Venen vorantreibt. Allerding war bislang die Funktion des rechten Vorhofs (RA) vernachlässigt worden. Wir konnten hinsichtlich dieser Aspekte der RV-Funktion bei PH zeigen, dass

- die diastolische RV-Steifheit (Eed) bei PH-Patienten mit erhöhter ventilatorischer Ineffizienz assoziiert ist.

- die aktive RA-Funktion entscheidend von der diastolischen Funktion des RV abhängt und eine Einschränkung dieser Funktion zu einem vermehrten systemischen Rückstau führt.

Zusammenfassend bestätigt die vorliegende Arbeit die Bedeutung der systolischen und diastolischen Funktion der RA-RV Achse bei PH. Die Erweiterung des Arsenals zur präzisen (invasiven) wie auch zur non-invasiven Erfassung dieser Achse kann in Zukunft genutzt werden, um spezifisch auf die RV-Funktion zielende Therapieansätze zu entwickeln.

5 Abkürzungsverzeichnis

AUC	Area Under The Curve
BDP	Begin-diastolic Pressure
BNP	Brain Natriuretic Peptide
BSA	Body Surface Area
COPD	Chronic Obstructive Pulmonary Disease
CTED	Chronic Thrombembolic Disease
CTEPH	Chronic Thrombembolic Pulmonary Hypertension
Ea	Arterial Elastance
EDA	End-diastolic Area
EDP	End-diastolic Pressure
EDPVR	End-diastolic Pressure Volume Relationship
EDV	End-diastolic Volume
Eed	End-diastolic Elastance
Ees	End-systolic Elastance
EF	Ejection Fraction
ESA	End-systolic Area
ESP	End-systolic Pressure
ESV	Endsystolisches Volumen
FAC	Fractional Area Change
FEV1	Einsekundenkapazität
FVC	Forcierte Vitalkapazität
GCS	Global Circumferential Strain
GLS	Global Longitudinal Strain
GRS	Global Radial Strain
HFpEF	Heart Failure with Preserved Ejection Fraction
HIV	Human Immunodeficiency Virus
HZV	Herzzeitvolumen
kMRT	Kardiales MRT
LOA	Limits of Agreement
LV	Linker Ventrikel
mPAP	Mean Pulmonary Artery Pressure
NYHA	New York Heart Association
PAAT	Pulmonary Artery Acceleration Time
PAC	Pulmonary Artery Compliance
PAH	Pulmonal-arterielle Hypertonie
PASP	Pulmonal-arterieller Systolischer Druck
PETCO2	Partiales End-Tidales CO2
PH	Pulmonale Hypertonie
PH-ILD	Pulmonary Hypertension-Interstitial Lung Disease
PH-LD	Pulmonale Hypertonie-Lung Disease
PVR	Pulmonary Vascular Resistance
RA	Rechtes Atrium
RAP	Right Atrial Pressure
ROC	Receiver Operating Characteristic
RV	Rechter Ventrikel
sRVP	Systolic Right Ventricular Pressure
Ssc	Systemic Scleroderma
SV	Schlagvolumen

SW	Stroke Work
TAPSE	Tricuspidal Annular Plane Excursion
TDI	Tissue Doppler Imaging
TI	Trikuspidalklappeninsuffizienz
TLC	Total Lung Capacity
VC	Vitalkapazität
VE	Minutenvolumen
WU	Wood Units

6 Literatur

1. Harvey. Exercitatio Anatomica de Motu Cordis et Sanguinis in Animalibus. . Frankfurt 1628.
2. Kyriakos Anastasiadis SW, Polychronis Antonitsis. Failing Right Heart, 2015.
3. Starr I JW, Meade RH. The absence of conspicuous increments of venous pressure after severe damage to the RV of the dog, with discussion of the relation between clinical congestive heart failure and heart disease. Am Heart J 1943;26:291–301.
4. Griepp RB, Stinson EB, Dong E, Jr., Clark DA, Shumway NE. Determinants of operative risk in human heart transplantation. American journal of surgery 1971;122:192-7.
5. Friehs I, Cowan DB, Choi YH et al. Pressure-overload hypertrophy of the developing heart reveals activation of divergent gene and protein pathways in the left and right ventricular myocardium. American journal of physiology Heart and circulatory physiology 2013;304:H697-708.
6. Lahm T, Douglas IS, Archer SL et al. Assessment of Right Ventricular Function in the Research Setting: Knowledge Gaps and Pathways Forward. An Official American Thoracic Society Research Statement. American journal of respiratory and critical care medicine 2018;198:e15-e43.
7. Galie N, Humbert M, Vachiery JL et al. 2015 ESC/ERS Guidelines for the diagnosis and treatment of pulmonary hypertension: The Joint Task Force for the Diagnosis and Treatment of Pulmonary Hypertension of the European Society of Cardiology (ESC) and the European Respiratory Society (ERS): Endorsed by: Association for European Paediatric and Congenital Cardiology (AEPC), International Society for Heart and Lung Transplantation (ISHLT). European heart journal 2016;37:67-119.
8. Simonneau G, Montani D, Celermajer DS et al. Haemodynamic definitions and updated clinical classification of pulmonary hypertension. The European respiratory journal 2019;53.
9. Humbert M, Guignabert C, Bonnet S et al. Pathology and pathobiology of pulmonary hypertension: state of the art and research perspectives. The European respiratory journal 2019;53.
10. Vonk Noordegraaf A, Westerhof BE, Westerhof N. The Relationship Between the Right Ventricle and its Load in Pulmonary Hypertension. Journal of the American College of Cardiology 2017;69:236-243.
11. Frank O. Zur Dynamik des Herzmuskels. Ztschr Biol 1895;32:370.
12. Patterson SW, Piper H, Starling EH. The regulation of the heart beat. The Journal of physiology 1914;48:465-513.
13. Ross J, Jr. Afterload mismatch and preload reserve: a conceptual framework for the analysis of ventricular function. Progress in cardiovascular diseases 1976;18:255-64.
14. Vanderpool RR, Pinsky MR, Naeije R et al. RV-pulmonary arterial coupling predicts outcome in patients referred for pulmonary hypertension. Heart (British Cardiac Society) 2015;101:37-43.
15. Gomez-Arroyo J, Sandoval J, Simon MA, Dominguez-Cano E, Voelkel NF, Bogaard HJ. Treatment for pulmonary arterial hypertension-associated right ventricular dysfunction. Annals of the American Thoracic Society 2014;11:1101-15.

16. Voelkel NF, Gomez-Arroyo J, Abbate A, Bogaard HJ, Nicolls MR. Pathobiology of pulmonary arterial hypertension and right ventricular failure. The European respiratory journal 2012;40:1555-65.
17. Hsu S, Houston BA, Tampakakis E et al. Right Ventricular Functional Reserve in Pulmonary Arterial Hypertension. Circulation 2016;133:2413-22.
18. Tedford RJ, Mudd JO, Girgis RE et al. Right ventricular dysfunction in systemic sclerosis-associated pulmonary arterial hypertension. Circulation Heart failure 2013;6:953-63.
19. Suga H, Sagawa K, Shoukas AA. Load independence of the instantaneous pressure-volume ratio of the canine left ventricle and effects of epinephrine and heart rate on the ratio. Circulation research 1973;32:314-22.
20. Maughan WL, Shoukas AA, Sagawa K, Weisfeldt ML. Instantaneous pressure-volume relationship of the canine right ventricle. Circulation research 1979;44:309-15.
21. Redington AN, Gray HH, Hodson ME, Rigby ML, Oldershaw PJ. Characterisation of the normal right ventricular pressure-volume relation by biplane angiography and simultaneous micromanometer pressure measurements. British heart journal 1988;59:23-30.
22. von Anrep G. On local vascular reactions and their interpretation. The Journal of physiology 1912;45:318-27.
23. Hsu S, Kokkonen-Simon KM, Kirk JA et al. Right Ventricular Myofilament Functional Differences in Humans With Systemic Sclerosis-Associated Versus Idiopathic Pulmonary Arterial Hypertension. Circulation 2018;137:2360-2370.
24. Chesler NC, Roldan A, Vanderpool RR, Naeije R. How to measure pulmonary vascular and right ventricular function. Conference proceedings : Annual International Conference of the IEEE Engineering in Medicine and Biology Society IEEE Engineering in Medicine and Biology Society Annual Conference 2009;2009:177-80.
25. Sunagawa K, Maughan WL, Sagawa K. Effect of regional ischemia on the left ventricular end-systolic pressure-volume relationship of isolated canine hearts. Circulation research 1983;52:170-8.
26. Sunagawa K, Maughan WL, Sagawa K. Optimal arterial resistance for the maximal stroke work studied in isolated canine left ventricle. Circulation research 1985;56:586-95.
27. Morimont P, Lambermont B, Ghuysen A et al. Effective arterial elastance as an index of pulmonary vascular load. American journal of physiology Heart and circulatory physiology 2008;294:H2736-42.
28. Ghuysen A, Lambermont B, Kolh P et al. Alteration of right ventricular-pulmonary vascular coupling in a porcine model of progressive pressure overloading. Shock (Augusta, Ga) 2008;29:197-204.
29. De Tombe PP, Jones S, Burkhoff D, Hunter WC, Kass DA. Ventricular stroke work and efficiency both remain nearly optimal despite altered vascular loading. The American journal of physiology 1993;264:H1817-24.
30. Axell RG, Messer SJ, White PA et al. Ventriculo-arterial coupling detects occult RV dysfunction in chronic thromboembolic pulmonary vascular disease. Physiol Rep 2017;5.
31. Badagliacca R, Poscia R, Pezzuto B et al. Right ventricular remodeling in idiopathic pulmonary arterial hypertension: adaptive versus maladaptive morphology. The Journal of heart and lung transplantation : the official publication of the International Society for Heart Transplantation 2015;34:395-403.
32. Brown KA, Ditchey RV. Human right ventricular end-systolic pressure-volume relation defined by maximal elastance. Circulation 1988;78:81-91.
33. Dickstein ML, Yano O, Spotnitz HM, Burkhoff D. Assessment of right ventricular contractile state with the conductance catheter technique in the pig. Cardiovascular research 1995;29:820-6.
34. McCabe C, White PA, Hoole SP et al. Right ventricular dysfunction in chronic thromboembolic obstruction of the pulmonary artery: a pressure-volume study using the conductance catheter. Journal of applied physiology (Bethesda, Md : 1985) 2014;116:355-63.

35. Latus H, Binder W, Kerst G, Hofbeck M, Sieverding L, Apitz C. Right ventricular-pulmonary arterial coupling in patients after repair of tetralogy of Fallot. The Journal of thoracic and cardiovascular surgery 2013;146:1366-72.
36. Rommel KP, von Roeder M, Oberueck C et al. Load-Independent Systolic and Diastolic Right Ventricular Function in Heart Failure With Preserved Ejection Fraction as Assessed by Resting and Handgrip Exercise Pressure-Volume Loops. Circulation Heart failure 2018;11:e004121.
37. Wink J, de Wilde RB, Wouters PF et al. Thoracic Epidural Anesthesia Reduces Right Ventricular Systolic Function With Maintained Ventricular-Pulmonary Coupling. Circulation 2016;134:1163-1175.
38. Wang Z, Yuan LJ, Cao TS, Yang Y, Duan YY, Xing CY. Simultaneous beat-by-beat investigation of the effects of the Valsalva maneuver on left and right ventricular filling and the possible mechanism. PloS one 2013;8:e53917.
39. Brimioulle S, Wauthy P, Ewalenko P et al. Single-beat estimation of right ventricular end-systolic pressure-volume relationship. American journal of physiology Heart and circulatory physiology 2003;284:H1625-30.
40. Tello K, Seeger W, Naeije R et al. Right heart failure in pulmonary hypertension: Diagnosis and new perspectives on vascular and direct right ventricular treatment. Br J Pharmacol 2019.
41. Takeuchi M, Igarashi Y, Tomimoto S et al. Single-beat estimation of the slope of the end-systolic pressure-volume relation in the human left ventricle. Circulation 1991;83:202-12.
42. Inuzuka R, Hsu S, Tedford RJ, Senzaki H. Single-Beat Estimation of Right Ventricular Contractility and Its Coupling to Pulmonary Arterial Load in Patients With Pulmonary Hypertension. Journal of the American Heart Association 2018;7.
43. Trip P, Rain S, Handoko ML et al. Clinical relevance of right ventricular diastolic stiffness in pulmonary hypertension. The European respiratory journal 2015.
44. Vanderpool RR, Desai AA, Knapp SM et al. How prostacyclin therapy improves right ventricular function in pulmonary arterial hypertension. European Respiratory Journal 2017;50:1700764.
45. Pieske B, Tschope C, de Boer RA et al. How to diagnose heart failure with preserved ejection fraction: the HFA-PEFF diagnostic algorithm: a consensus recommendation from the Heart Failure Association (HFA) of the European Society of Cardiology (ESC). European heart journal 2019;40:3297-3317.
46. Rain S, Handoko ML, Trip P et al. Right ventricular diastolic impairment in patients with pulmonary arterial hypertension. Circulation 2013;128:2016-25, 1-10.
47. Burkhoff D, Mirsky I, Suga H. Assessment of systolic and diastolic ventricular properties via pressure-volume analysis: a guide for clinical, translational, and basic researchers. American journal of physiology Heart and circulatory physiology 2005;289:H501-12.
48. Hill MR, Simon MA, Valdez-Jasso D, Zhang W, Champion HC, Sacks MS. Structural and mechanical adaptations of right ventricle free wall myocardium to pressure overload. Annals of biomedical engineering 2014;42:2451-65.
49. Rain S, Bos Dda S, Handoko ML et al. Protein changes contributing to right ventricular cardiomyocyte diastolic dysfunction in pulmonary arterial hypertension. Journal of the American Heart Association 2014;3:e000716.
50. Alaa M, Abdellatif M, Tavares-Silva M et al. Right ventricular end-diastolic stiffness heralds right ventricular failure in monocrotaline-induced pulmonary hypertension. American journal of physiology Heart and circulatory physiology 2016;311:H1004-h1013.
51. Trip P, Rain S, Handoko ML et al. Clinical relevance of right ventricular diastolic stiffness in pulmonary hypertension. The European respiratory journal 2015;45:1603-12.
52. Grapsa J, Pereira Nunes MC, Tan TC et al. Echocardiographic and Hemodynamic Predictors of Survival in Precapillary Pulmonary Hypertension: Seven-Year Follow-Up. Circulation Cardiovascular imaging 2015;8.

53. Grapsa J, Gibbs JS, Cabrita IZ et al. The association of clinical outcome with right atrial and ventricular remodelling in patients with pulmonary arterial hypertension: study with real-time three-dimensional echocardiography. European heart journal cardiovascular Imaging 2012;13:666-72.
54. Forfia PR, Fisher MR, Mathai SC et al. Tricuspid annular displacement predicts survival in pulmonary hypertension. American journal of respiratory and critical care medicine 2006;174:1034-41.
55. Yeo TC, Dujardin KS, Tei C, Mahoney DW, McGoon MD, Seward JB. Value of a Doppler-derived index combining systolic and diastolic time intervals in predicting outcome in primary pulmonary hypertension. The American journal of cardiology 1998;81:1157-61.
56. Grewal J, Majdalany D, Syed I, Pellikka P, Warnes CA. Three-dimensional echocardiographic assessment of right ventricular volume and function in adult patients with congenital heart disease: comparison with magnetic resonance imaging. Journal of the American Society of Echocardiography : official publication of the American Society of Echocardiography 2010;23:127-33.
57. Maffessanti F, Muraru D, Esposito R et al. Age-, body size-, and sex-specific reference values for right ventricular volumes and ejection fraction by three-dimensional echocardiography: a multicenter echocardiographic study in 507 healthy volunteers. Circulation Cardiovascular imaging 2013;6:700-10.
58. Jone PN, Patel SS, Cassidy C, Ivy DD. Three-dimensional Echocardiography of Right Ventricular Function Correlates with Severity of Pediatric Pulmonary Hypertension. Congenital heart disease 2016;11:562-569.
59. Hulshof HG, Eijsvogels TMH, Kleinnibbelink G et al. Prognostic value of right ventricular longitudinal strain in patients with pulmonary hypertension: a systematic review and meta-analysis. European heart journal cardiovascular Imaging 2018.
60. Guazzi M, Bandera F, Pelissero G et al. Tricuspid annular plane systolic excursion and pulmonary arterial systolic pressure relationship in heart failure: an index of right ventricular contractile function and prognosis. American journal of physiology Heart and circulatory physiology 2013;305:H1373-81.
61. Guazzi M, Dixon D, Labate V et al. RV Contractile Function and its Coupling to Pulmonary Circulation in Heart Failure With Preserved Ejection Fraction: Stratification of Clinical Phenotypes and Outcomes. JACC Cardiovascular imaging 2017.
62. Prins KW, Archer SL, Pritzker M et al. Interleukin-6 is independently associated with right ventricular function in pulmonary arterial hypertension. The Journal of heart and lung transplantation : the official publication of the International Society for Heart Transplantation 2018;37:376-384.
63. French S, Amsallem M, Ouazani N et al. EXPRESS: Non-invasive Right Ventricular Load Adaptability Indices in Patients with Scleroderma-Associated Pulmonary Arterial Hypertension. Pulmonary circulation 2018:2045894018788268.
64. Levy PT, El Khuffash A, Woo KV, Singh GK. Right Ventricular-Pulmonary Vascular Interactions: An Emerging Role for Pulmonary Artery Acceleration Time by Echocardiography in Adults and Children. Journal of the American Society of Echocardiography : official publication of the American Society of Echocardiography 2018.
65. Aubert R, Venner C, Huttin O et al. Three-Dimensional Echocardiography for the Assessment of Right Ventriculo-Arterial Coupling. Journal of the American Society of Echocardiography : official publication of the American Society of Echocardiography 2018;31:905-915.
66. Herberg U, Gatzweiler E, Breuer T, Breuer J. Ventricular pressure-volume loops obtained by 3D real-time echocardiography and mini pressure wire-a feasibility study. Clinical research in cardiology : official journal of the German Cardiac Society 2013;102:427-38.
67. Swift AJ, Capener D, Johns C et al. Magnetic Resonance Imaging in the Prognostic Evaluation of Patients with Pulmonary Arterial Hypertension. American journal of respiratory and critical care medicine 2017.

68. van Wolferen SA, Marcus JT, Boonstra A et al. Prognostic value of right ventricular mass, volume, and function in idiopathic pulmonary arterial hypertension. European heart journal 2007;28:1250-7.
69. Baggen VJ, Leiner T, Post MC et al. Cardiac magnetic resonance findings predicting mortality in patients with pulmonary arterial hypertension: a systematic review and meta-analysis. European radiology 2016;26:3771-3780.
70. Brewis MJ, Bellofiore A, Vanderpool RR et al. Imaging right ventricular function to predict outcome in pulmonary arterial hypertension. International journal of cardiology 2016;218:206-211.
71. Badagliacca R, Poscia R, Pezzuto B et al. Right ventricular concentric hypertrophy and clinical worsening in idiopathic pulmonary arterial hypertension. The Journal of heart and lung transplantation : the official publication of the International Society for Heart Transplantation 2016.
72. Simpson CE, Damico RL, Kolb TM et al. Ventricular Mass as a Prognostic Imaging Biomarker in Incident PAH. The European respiratory journal 2019.
73. Gan C, Lankhaar JW, Marcus JT et al. Impaired left ventricular filling due to right-to-left ventricular interaction in patients with pulmonary arterial hypertension. American journal of physiology Heart and circulatory physiology 2006;290:H1528-33.
74. Freed BH, Gomberg-Maitland M, Chandra S et al. Late gadolinium enhancement cardiovascular magnetic resonance predicts clinical worsening in patients with pulmonary hypertension. Journal of cardiovascular magnetic resonance : official journal of the Society for Cardiovascular Magnetic Resonance 2012;14:11.
75. "Recent advances in targeting the prostacyclin pathway in pulmonary arterial hypertension." Irene M. Lang and Sean P. Gaine. Eur Respir Rev 2015; 24: 630-641. European respiratory review : an official journal of the European Respiratory Society 2016;25:99.
76. Mewton N, Liu CY, Croisille P, Bluemke D, Lima JA. Assessment of myocardial fibrosis with cardiovascular magnetic resonance. Journal of the American College of Cardiology 2011;57:891-903.
77. Iles L, Pfluger H, Phrommintikul A et al. Evaluation of diffuse myocardial fibrosis in heart failure with cardiac magnetic resonance contrast-enhanced T1 mapping. Journal of the American College of Cardiology 2008;52:1574-80.
78. Spruijt OA, Vissers L, Bogaard HJ, Hofman MB, Vonk-Noordegraaf A, Marcus JT. Increased native T1-values at the interventricular insertion regions in precapillary pulmonary hypertension. The international journal of cardiovascular imaging 2016;32:451-9.
79. Jankowich M, Abbasi SA, Vang A, Choudhary G. Right Ventricular Fibrosis is Related to Pulmonary Artery Stiffness in Pulmonary Hypertension: A Cardiac Magnetic Resonance Imaging Study. American journal of respiratory and critical care medicine 2019.
80. Saunders LC, Johns CS, Stewart NJ et al. Diagnostic and prognostic significance of cardiovascular magnetic resonance native myocardial T1 mapping in patients with pulmonary hypertension. Journal of cardiovascular magnetic resonance : official journal of the Society for Cardiovascular Magnetic Resonance 2018;20:78.
81. Sanz J, Garcia-Alvarez A, Fernandez-Friera L et al. Right ventriculo-arterial coupling in pulmonary hypertension: a magnetic resonance study. Heart (British Cardiac Society) 2012;98:238-43.
82. Trip P, Kind T, van de Veerdonk MC et al. Accurate assessment of load-independent right ventricular systolic function in patients with pulmonary hypertension. The Journal of heart and lung transplantation : the official publication of the International Society for Heart Transplantation 2013;32:50-5.
83. Kuehne T, Yilmaz S, Steendijk P et al. Magnetic resonance imaging analysis of right ventricular pressure-volume loops: in vivo validation and clinical application in patients with pulmonary hypertension. Circulation 2004;110:2010-6.

84. Ghio S, Klersy C, Magrini G et al. Prognostic relevance of the echocardiographic assessment of right ventricular function in patients with idiopathic pulmonary arterial hypertension. International journal of cardiology 2010;140:272-8.
85. Fine NM, Chen L, Bastiansen PM et al. Outcome prediction by quantitative right ventricular function assessment in 575 subjects evaluated for pulmonary hypertension. Circulation Cardiovascular imaging 2013;6:711-21.
86. Ernande L, Cottin V, Leroux PY et al. Right isovolumic contraction velocity predicts survival in pulmonary hypertension. Journal of the American Society of Echocardiography : official publication of the American Society of Echocardiography 2013;26:297-306.
87. Haeck ML, Scherptong RW, Marsan NA et al. Prognostic value of right ventricular longitudinal peak systolic strain in patients with pulmonary hypertension. Circulation Cardiovascular imaging 2012;5:628-36.
88. Badagliacca R, Poscia R, Pezzuto B et al. Right ventricular dyssynchrony in idiopathic pulmonary arterial hypertension: Determinants and impact on pump function. The Journal of heart and lung transplantation : the official publication of the International Society for Heart Transplantation 2015;34:381-389.
89. Tei C, Dujardin KS, Hodge DO et al. Doppler echocardiographic index for assessment of global right ventricular function. Journal of the American Society of Echocardiography : official publication of the American Society of Echocardiography 1996;9:838-47.
90. Haddad F, Doyle R, Murphy DJ, Hunt SA. Right ventricular function in cardiovascular disease, part II: pathophysiology, clinical importance, and management of right ventricular failure. Circulation 2008;117:1717-31.
91. Humbert M, Sitbon O, Chaouat A et al. Survival in patients with idiopathic, familial, and anorexigen-associated pulmonary arterial hypertension in the modern management era. Circulation 2010;122:156-63.
92. Benza RL, Miller DP, Gomberg-Maitland M et al. Predicting survival in pulmonary arterial hypertension: insights from the Registry to Evaluate Early and Long-Term Pulmonary Arterial Hypertension Disease Management (REVEAL). Circulation 2010;122:164-72.
93. Bhave NM, Visovatti SH, Kulick B, Kolias TJ, McLaughlin VV. Right atrial strain is predictive of clinical outcomes and invasive hemodynamic data in group 1 pulmonary arterial hypertension. The international journal of cardiovascular imaging 2017;33:847-855.
94. Axell RG, Messer SJ, White PA et al. Ventriculo-arterial coupling detects occult RV dysfunction in chronic thromboembolic pulmonary vascular disease. Physiol Rep 2017;5:e13227.
95. Chemla D, Hebert JL, Coirault C, Salmeron S, Zamani K, Lecarpentier Y. Matching dicrotic notch and mean pulmonary artery pressures: implications for effective arterial elastance. The American journal of physiology 1996;271:H1287-95.
96. Prins KW, Weir EK, Archer SL et al. Pulmonary pulse wave transit time is associated with right ventricular-pulmonary artery coupling in pulmonary arterial hypertension. Pulmonary circulation 2016;6:576-585.
97. Richter MJ, Ghofrani HA, Gall H. Beyond interleukin-6 in right ventricular function: Evidence for another biomarker. J Heart Lung Transplant 2018;37:674-675.
98. French S, Amsallem M, Ouazani N et al. Non-invasive right ventricular load adaptability indices in patients with scleroderma-associated pulmonary arterial hypertension. Pulmonary circulation 2018;8:2045894018788268.
99. Levy PT, El Khuffash A, Woo KV, Hauck A, Hamvas A, Singh GK. A novel noninvasive index to characterize right ventricle pulmonary arterial vascular coupling in children. J Am Coll Cardiol Img 2018; Dec 6 [E-pub ahead of print], http://dx.doi.org/10.1016/j.jcmg.2018.09.022
100. Claessen G, La Gerche A, Voigt JU et al. Accuracy of echocardiography to evaluate pulmonary vascular and rv function during exercise. J Am Coll Cardiol Img 2016;9:532-43.

101. Pratali L, Allemann Y, Rimoldi SF et al. RV contractility and exercise-induced pulmonary hypertension in chronic mountain sickness: a stress echocardiographic and tissue Doppler imaging study. J Am Coll Cardiol Img 2013;6:1287-97.
102. Guazzi M, Dixon D, Labate V et al. RV contractile function and its coupling to pulmonary circulation in heart failure with preserved ejection fraction: stratification of clinical phenotypes and outcomes. J Am Coll Cardiol Img 2017;10:1211-1221.
103. Gall H, Felix JF, Schneck FK et al. The Giessen Pulmonary Hypertension Registry: Survival in pulmonary hypertension subgroups. The Journal of heart and lung transplantation : the official publication of the International Society for Heart Transplantation 2017.
104. Nathan SD, Barbera JA, Gaine SP et al. Pulmonary hypertension in chronic lung disease and hypoxia. The European respiratory journal 2019;53.
105. Prins KW, Rose L, Archer SL et al. Disproportionate Right Ventricular Dysfunction and Poor Survival in Group 3 Pulmonary Hypertension. American journal of respiratory and critical care medicine 2018;197:1496-1499.
106. Tello K, Richter MJ, Axmann J et al. More on Single-Beat Estimation of Right Ventriculo-Arterial Coupling in Pulmonary Arterial Hypertension. American journal of respiratory and critical care medicine 2018.
107. van de Veerdonk MC, Kind T, Marcus JT et al. Progressive right ventricular dysfunction in patients with pulmonary arterial hypertension responding to therapy. Journal of the American College of Cardiology 2011;58:2511-9.
108. Vanderpool RR, Rischard F, Naeije R, Hunter K, Simon MA. Simple functional imaging of the right ventricle in pulmonary hypertension: Can right ventricular ejection fraction be improved? International journal of cardiology 2016;223:93-94.
109. Oyama-Manabe N, Sato T, Tsujino I et al. The strain-encoded (SENC) MR imaging for detection of global right ventricular dysfunction in pulmonary hypertension. The international journal of cardiovascular imaging 2013;29:371-8.
110. Romano S, Judd RM, Kim RJ et al. Feature-Tracking Global Longitudinal Strain Predicts Death in a Multicenter Population of Patients With Ischemic and Nonischemic Dilated Cardiomyopathy Incremental to Ejection Fraction and Late Gadolinium Enhancement. JACC Cardiovascular imaging 2018;11:1419-1429.
111. Stevens GR, Garcia-Alvarez A, Sahni S, Garcia MJ, Fuster V, Sanz J. RV dysfunction in pulmonary hypertension is independently related to pulmonary artery stiffness. JACC Cardiovascular imaging 2012;5:378-87.
112. Galie N, Humbert M, Vachiery JL et al. 2015 ESC/ERS Guidelines for the diagnosis and treatment of pulmonary hypertension: The Joint Task Force for the Diagnosis and Treatment of Pulmonary Hypertension of the European Society of Cardiology (ESC) and the European Respiratory Society (ERS): Endorsed by: Association for European Paediatric and Congenital Cardiology (AEPC), International Society for Heart and Lung Transplantation (ISHLT). Eur Heart J 2016;37:67-119.
113. Gall H, Felix JF, Schneck FK et al. The Giessen Pulmonary Hypertension Registry: Survival in pulmonary hypertension subgroups. The Journal of heart and lung transplantation : the official publication of the International Society for Heart Transplantation 2017;36:957-967.
114. Guihaire J, Haddad F, Noly PE et al. Right ventricular reserve in a piglet model of chronic pulmonary hypertension. The European respiratory journal 2014.
115. Badagliacca R, Poscia R, Pezzuto B et al. Right ventricular concentric hypertrophy and clinical worsening in idiopathic pulmonary arterial hypertension. J Heart Lung Transplant 2016;35:1321-1329.
116. Garcia-Alvarez A, Garcia-Lunar I, Pereda D et al. Association of myocardial T1-mapping CMR with hemodynamics and RV performance in pulmonary hypertension. J Am Coll Cardiol Img 2015;8:76-82.

117. Sanz J, Kariisa M, Dellegrottaglie S et al. Evaluation of pulmonary artery stiffness in pulmonary hypertension with cardiac magnetic resonance. J Am Coll Cardiol Img 2009;2:286-95.
118. Ruopp MD, Perkins NJ, Whitcomb BW, Schisterman EF. Youden Index and optimal cut-point estimated from observations affected by a lower limit of detection. Biom J 2008;50:419-30.
119. van de Veerdonk MC, Marcus JT, Westerhof N et al. Signs of right ventricular deterioration in clinically stable patients with pulmonary arterial hypertension. Chest 2015;147:1063-71.
120. Weatherald J, Sattler C, Garcia G, Laveneziana P. Ventilatory response to exercise in cardiopulmonary disease: the role of chemosensitivity and dead space. The European respiratory journal 2018;51.
121. Dumitrescu D, Sitbon O, Weatherald J, Howard LS. Exertional dyspnoea in pulmonary arterial hypertension. European respiratory review : an official journal of the European Respiratory Society 2017;26.
122. Groepenhoff H, Vonk-Noordegraaf A, Boonstra A, Spreeuwenberg MD, Postmus PE, Bogaard HJ. Exercise testing to estimate survival in pulmonary hypertension. Med Sci Sports Exerc 2008;40:1725-32.
123. Galie N, Humbert M, Vachiery JL et al. 2015 ESC/ERS Guidelines for the diagnosis and treatment of pulmonary hypertension: The Joint Task Force for the Diagnosis and Treatment of Pulmonary Hypertension of the European Society of Cardiology (ESC) and the European Respiratory Society (ERS): Endorsed by: Association for European Paediatric and Congenital Cardiology (AEPC), International Society for Heart and Lung Transplantation (ISHLT). The European respiratory journal 2015;46:903-75.
124. Vonk Noordegraaf A, Chin KM, Haddad F et al. Pathophysiology of the right ventricle and of the pulmonary circulation in pulmonary hypertension: an update. The European respiratory journal 2018.
125. Naeije R, Manes A. The right ventricle in pulmonary arterial hypertension. European respiratory review : an official journal of the European Respiratory Society 2014;23:476-87.
126. Ciarka A, Doan V, Velez-Roa S, Naeije R, van de Borne P. Prognostic significance of sympathetic nervous system activation in pulmonary arterial hypertension. American journal of respiratory and critical care medicine 2010;181:1269-75.
127. Ciarka A, Vachiery JL, Houssiere A et al. Atrial septostomy decreases sympathetic overactivity in pulmonary arterial hypertension. Chest 2007;131:1831-7.
128. Marcus JT, Westerhof BE, Groeneveldt JA, Bogaard HJ, de Man FS, Vonk Noordegraaf A. Vena cava backflow and right ventricular stiffness in pulmonary arterial hypertension. The European respiratory journal 2019;54.
129. Chen L, Larsen CM, Le RJ et al. The prognostic significance of tricuspid valve regurgitation in pulmonary arterial hypertension. The clinical respiratory journal 2018;12:1572-1580.
130. Querejeta Roca G, Campbell P, Claggett B, Solomon SD, Shah AM. Right Atrial Function in Pulmonary Arterial Hypertension. Circ Cardiovasc Imaging 2015;8:e003521; discussion e003521.
131. Sakata K, Uesugi Y, Isaka A et al. Evaluation of right atrial function using right atrial speckle tracking analysis in patients with pulmonary artery hypertension. Journal of echocardiography 2016;14:30-8.
132. Fukuda Y, Tanaka H, Ryo-Koriyama K et al. Comprehensive Functional Assessment of Right-Sided Heart Using Speckle Tracking Strain for Patients with Pulmonary Hypertension. Echocardiography (Mount Kisco, NY) 2016;33:1001-8.
133. von Roeder M, Kowallick JT, Rommel KP et al. Right atrial-right ventricular coupling in heart failure with preserved ejection fraction. Clinical research in cardiology : official journal of the German Cardiac Society 2019.
134. Leng S, Dong Y, Wu Y et al. Impaired Cardiovascular Magnetic Resonance-Derived Rapid Semiautomated Right Atrial Longitudinal Strain Is Associated With Decompensated

Hemodynamics in Pulmonary Arterial Hypertension. Circulation Cardiovascular imaging 2019;12:e008582.
135. Andersen S, Nielsen-Kudsk JE, Vonk Noordegraaf A, de Man FS. Right Ventricular Fibrosis. Circulation 2019;139:269-285.
136. Burlew BS, Weber KT. Cardiac fibrosis as a cause of diastolic dysfunction. Herz 2002;27:92-8.

7 Liste der Anhänge

Anlage A	More on Single-Beat Estimation of Right Ventriculoarterial Coupling in Pulmonary Arterial Hypertension. **Tello K**, Richter MJ, Axmann J, Buhmann M, Seeger W, Naeije R, Ghofrani HA, Gall H. Am J Respir Crit Care Med. 2018 Sep 15;198(6):816-818
Anlage B	Validation of the Tricuspid Annular Plane Systolic Excursion/Systolic Pulmonary Artery Pressure Ratio for the Assessment of Right Ventricular-Arterial Coupling in Severe Pulmonary Hypertension. **Tello K**, Wan J, Dalmer A, Vanderpool R, Ghofrani HA, Naeije R, Roller F, Mohajerani E, Seeger W, Herberg U, Sommer N, Gall H, Richter MJ. Circ Cardiovasc Imaging. 2019 Sep;12(9)
Anlage C	A simple echocardiographic estimate of right ventricular-arterial coupling to assess severity and outcome in pulmonary hypertension on chronic lung disease. **Tello K**, Ghofrani HA, Heinze C, Krueger K, Naeije R, Raubach C, Seeger W, Sommer N, Gall H, Richter MJ. Eur Respir J. 2019 Sep 12;54(3)
Anlage D	Evaluation and Prognostic Relevance of Right Ventricular-Arterial Coupling in Pulmonary Hypertension. Richter MJ, Peters D, Ghofrani HA, Naeije R, Roller F, Sommer N, Gall H, Grimminger F, Seeger W, **Tello K**. Am J Respir Crit Care Med. 2020 Jan 1;201(1):116-119
Anlage E	Cardiac Magnetic Resonance Imaging-Based Right Ventricular Strain Analysis for Assessment of Coupling and Diastolic Function in Pulmonary Hypertension. **Tello K**, Dalmer A, Vanderpool R, Ghofrani HA, Naeije R, Roller F, Seeger W, Wilhelm J, Gall H, Richter MJ. JACC Cardiovasc Imaging. 2019 Nov;12(11 Pt 1):2155-2164
Anlage F	Reserve of Right Ventricular-Arterial Coupling in the Setting of Chronic Overload. **Tello K**, Dalmer A, Axmann J, Vanderpool R, Ghofrani HA, Naeije R, Roller F, Seeger W, Sommer N, Wilhelm J, Gall H, Richter MJ. Circ Heart Fail. 2019 Jan;12(1)
Anlage G	Impaired right ventricular lusitropy is associated with ventilatory inefficiency in pulmonary arterial hypertension. **Tello K**, Dalmer A, Vanderpool R, Ghofrani HA, Naeije R, Roller F, Seeger W, Dumitrescu D, Sommer N, Brunst A, Gall H, Richter MJ. Eur Respir J. 2019 Nov 21;54(5)
Anlage H	Relevance of the TAPSE/PASP ratio in pulmonary arterial hypertension. **Tello K**, Axmann J, Ghofrani HA, Naeije R, Narcin N, Rieth A, Seeger W, Gall H, Richter MJ. Int J Cardiol. 2018 Sep 1;266:229-235
Anlage I	Right ventricular function correlates of right atrial strain in pulmonary hypertension: a combined cardiac magnetic resonance and conductance catheter study. **Tello K**, Dalmer A, Vanderpool R, Ghofrani HA, Naeije R, Roller F, Seeger W, Wiegand M, Gall H, Richter MJ. Am J Physiol Heart Circ Physiol. 2020 Jan 1;318(1):H156-H164

8 Anhänge

Anlage A

More on Single-Beat Estimation of Right Ventriculoarterial Coupling in Pulmonary Arterial Hypertension.

Tello K, Richter MJ, Axmann J, Buhmann M, Seeger W, Naeije R, Ghofrani HA, Gall H. Am J Respir Crit Care Med. 2018 Sep 15;198(6):816-818

10. Torres-Atencio I, Ainsua-Enrich E, de Mora F, Picado C, Martín M. Prostaglandin E2 prevents hyperosmolar-induced human mast cell activation through prostanoid receptors EP2 and EP4. *PLoS One* 2014;9:e110870.

More on Single-Beat Estimation of Right Ventriculoarterial Coupling in Pulmonary Arterial Hypertension

To the Editor:

Right ventricular (RV) function is the main determinant of symptomatology and outcome in pulmonary arterial hypertension (PAH) (1). However, guidelines for the diagnosis and treatment of PAH do not advise on how best to measure RV function in these patients (2).

It has been better realized in recent years that RV adaptation in severe PAH is essentially homeometric, with an increase in contractility matching the increased afterload (1). As recently reviewed (3), the gold standard measure of RV contractility is end-systolic elastance (Ees), which is reasonably assumed equal to maximum elastance and defined by an end-systolic pressure (ESP) versus end-systolic volume relationship (1, 3). To assess the adequacy of RV contractility adaptation to afterload, Ees is expressed relative to arterial elastance (Ea), defined by an ESP versus stroke volume (SV) relationship (1, 3). The optimal coupling of the RV to afterload allowing for flow output at a minimal energy cost occurs at an Ees/Ea ratio of around 1.5 (3). When the Ees/Ea ratio decreases to 1 or below, the homeometric adaptation of the RV is exhausted. The RV then uses a dimensional or "heterometric" adaptation (Starling's law of the heart) to maintain flow output in response to metabolic demand (3).

Because of the major prognostic relevance of RV function, there is interest in an earlier and robust diagnosis of RV–arterial uncoupling and definition of critical Ees and Ees/Ea values associated with a risk for clinical deterioration. But how accurate are these measurements as currently performed in expert PAH centers?

Methods for assessment of RV–arterial coupling and their prognostic value were recently reviewed in detail by Tabima and colleagues (4). Ees can be measured from a family of pressure–volume loops at decreasing venous return (5) or by a single-beat method relying on the determination of a maximum pressure from nonlinear extrapolation of early and late isovolumic portions (before maximal and after minimal dP/dt, respectively) of the RV pressure curve (Figure 1) (6, 7). Ees is then equal to (maximum pressure − ESP)/SV, and Ea is equal to ESP/SV (3, 4).

Recent studies of RV–arterial coupling in severe PAH have assumed that mean pulmonary artery pressure (mPAP) would be an acceptable surrogate of ESP (3). However, this assumption is based on measurements in a small cohort of 15 patients, none of whom had PAH (five had pulmonary hypertension due to left heart disease), and with ESP measured at the PAP dicrotic notch (8). Although mPAP may be close to RV ESP in healthy individuals, the shape of RV pressure–volume loops in patients with severe PAH changes with increasing PAP, so that ESP becomes closer to RV systolic pressure than to mPAP (9).

In the present study, we quantified the error associated with Ees estimation using mPAP instead of ESP by measuring RV volumes and pressures with a conductance catheter (4F, CD Leycom) in 20 consecutive patients with PAH. The study was approved by the Institutional Review Board of the University of Giessen (#2015/108). All the patients gave written informed consent. There were 13 women and 7 men, aged 51 ± 15 years (mean ± SD). The diagnosis of PAH rested on a step-by-step approach to exclude pulmonary hypertension due to cardiac or pulmonary diseases and right heart catheterization showing mPAP >25 mm Hg and pulmonary vascular resistance >3 Wood units, in agreement with current recommendations (2). Results are expressed as mean ± SD when normally distributed (assessed by Kolmogorov-Smirnov test), and otherwise as median (interquartile range).

Seventeen patients had idiopathic PAH, one had portal hypertension–associated PAH, one had HIV-associated PAH, and one had systemic sclerosis–associated PAH. On the basis of hemodynamic measurements, pulmonary vascular resistance was 5.9 (interquartile range, 4.3–8.6) Wood units, mPAP was 41 ± 11 mm Hg, wedged PAP was 7 ± 2 mm Hg, and mixed venous oxygen saturation was 69 ± 6%. The patients were in New York Heart Association functional class III ($n = 12$) or II ($n = 8$).

As shown in Figure 1, there was a strong correlation between mPAP and ESP. The relationship between mPAP and ESP was described by a linear regression model as ESP = 1.65 × mPAP – 7.79 ($r = 0.932$; $r^2 = 0.868$; $P < 0.001$). However, this relationship differed from the line of identity with underestimation of ESP by mPAP in proportion to pulmonary hypertension severity. Pressure-dependent bias (indicating insufficient accuracy) and large limits of agreement (indicating insufficient precision) were confirmed on a Bland–Altman plot (10).

The comparison of Ees, Ea, and Ees/Ea calculated using mPAP versus ESP revealed significant differences (all $P < 0.001$, Wilcoxon signed rank test): Ees was calculated as 0.87 ± 0.44 versus 0.62 ± 0.38 mm Hg/ml (median difference, 0.18; range, 0.03–0.56), Ea was calculated as 0.52 ± 0.25 versus 0.76 ± 0.39 mm Hg/ml (median difference, −0.18; range, −0.56 to −0.02), and Ees/Ea was calculated as 1.84 ± 0.78 versus 0.89 ± 0.49 (median difference, 0.90; range, 0.20–1.85). These differences emphasize the importance of validating different contractility measurements.

Thus, mPAP cannot be a surrogate for RV ESP in the evaluation of RV contractility and RV–arterial coupling. Although the small sample size of our study must be considered, our results suggest that ESP can be cautiously estimated by the equation ESP = 1.65 × mPAP − 7.79 in the absence of direct measurements.

The study is funded by the German Research Foundation, Bonn, Germany (Collaborative Research Center 1213, "Pulmonary Hypertension and Cor Pulmonale" and Excellence Cluster "Cardio-Pulmonary System").

Author Contributions: K.T., M.J.R., W.S., H.A.G., and H.G. designed the study; K.T., M.J.R., J.A., and H.G. performed patient recruitment, care and follow-up; K.T., M.J.R., M.B., R.N., and H.G. performed data collection, maintenance, and analysis; M.J.R., J.A., M.B., W.S., R.N., H.A.G., and H.G. performed critical revision of the manuscript; and K.T. drafted the manuscript.

Originally Published in Press as DOI: 10.1164/rccm.201802-0283LE on May 14, 2018

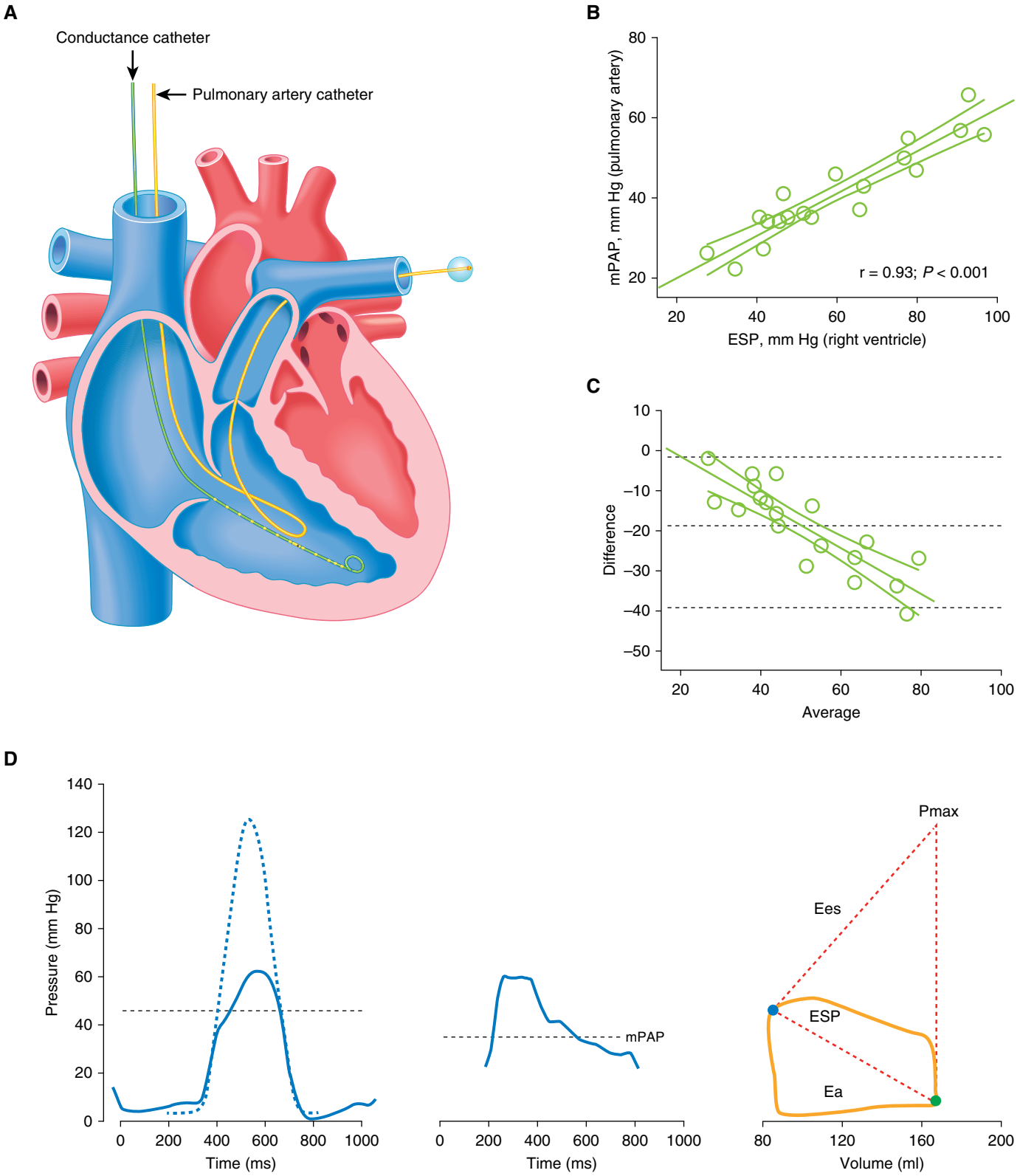

Figure 1. Evaluation of mean pulmonary artery pressure (mPAP) as a replacement for end-systolic pressure (ESP) in the assessment of right ventricular contractility in pulmonary arterial hypertension. (*A*) Positioning of conductance and pulmonary artery catheters for measurement of ESP and mPAP, respectively. (*B*) Correlation of ESP (measured via conductance catheter) with mPAP. (*C*) Bland–Altman plot showing underestimation of ESP based on mPAP, especially at high (>50 mm Hg) pressures. (*D*) Original measurements of right ventricular pressure curve and mPAP, estimation of theoretical isovolumetric maximum pressure (Pmax), and calculation of end-systolic elastance (Ees) and arterial elastance (Ea) in one patient.

The single-beat method was validated in an animal model with only mild to moderate pulmonary hypertension (6), and soon thereafter applied to patients with PAH (7). It has since been used in several clinical studies as an alternative to multiple beat approaches in PAH (1, 3, 4). Whether this is equally accurate requires further investigation in larger populations with differing severities of PAH. Neither single- nor multiple-beat methodologically rigorous measurements of Ees/Ea have yet been demonstrated to have independent prognostic relevance in PAH. The use of a true gold standard will be indispensable for the validation of imaging or catheterization surrogates of RV–arterial coupling, and selecting the RV function measurements that are most relevant to patients' outcomes. ■

Author disclosures are available with the text of this letter at www.atsjournals.org.

Acknowledgment: Editorial assistance was provided by Claire Mulligan, Ph.D. (Beacon Medical Communications Ltd, Brighton, UK), funded by the University of Giessen.

Khodr Tello, M.D.
Manuel J. Richter, M.D.
Jens Axmann
Universities of Giessen and Marburg Lung Centre, member of the German Centre for Lung Research
Giessen, Germany

Martin Buhmann, Ph.D.
Justus-Liebig-University Giessen
Giessen, Germany

Werner Seeger, M.D.
Universities of Giessen and Marburg Lung Centre, member of the German Centre for Lung Research
Giessen, Germany

Robert Naeije, M.D., Ph.D.
Erasme University Hospital
Brussels, Belgium

Hossein Ardeschir Ghofrani, M.D.
Universities of Giessen and Marburg Lung Centre, member of the German Centre for Lung Research
Giessen, Germany
Kerckhoff Heart, Rheuma and Thoracic Center
Bad Nauheim, Germany
and
Imperial College London
London, United Kingdom

Henning Gall, M.D., Ph.D.
Universities of Giessen and Marburg Lung Centre, member of the German Centre for Lung Research
Giessen, Germany

References

1. Vonk-Noordegraaf A, Haddad F, Chin KM, Forfia PR, Kawut SM, Lumens J, *et al*. Right heart adaptation to pulmonary arterial hypertension: physiology and pathobiology. *J Am Coll Cardiol* 2013; 62(25 Suppl):D22–D33.
2. Galiè N, Humbert M, Vachiery JL, Gibbs S, Lang I, Torbicki A, *et al*. 2015 ESC/ERS Guidelines for the diagnosis and treatment of pulmonary hypertension: The Joint Task Force for the Diagnosis and Treatment of Pulmonary Hypertension of the European Society of Cardiology (ESC) and the European Respiratory Society (ERS): endorsed by: Association for European Paediatric and Congenital Cardiology (AEPC), International Society for Heart and Lung Transplantation (ISHLT). *Eur Respir J* 2015;46:903–975.
3. Vonk Noordegraaf A, Westerhof BE, Westerhof N. The relationship between the right ventricle and its load in pulmonary hypertension. *J Am Coll Cardiol* 2017;69:236–243.
4. Tabima DM, Philip JL, Chesler NC. Right ventricular-pulmonary vascular interactions. *Physiology (Bethesda)* 2017;32:346–356.
5. Maughan WL, Shoukas AA, Sagawa K, Weisfeldt ML. Instantaneous pressure-volume relationship of the canine right ventricle. *Circ Res* 1979;44:309–315.
6. Brimioulle S, Wauthy P, Ewalenko P, Rondelet B, Vermeulen F, Kerbaul F, *et al*. Single-beat estimation of right ventricular end-systolic pressure-volume relationship. *Am J Physiol Heart Circ Physiol* 2003;284: H1625–H1630.
7. Kuehne T, Yilmaz S, Steendijk P, Moore P, Groenink M, Saaed M, *et al*. Magnetic resonance imaging analysis of right ventricular pressure-volume loops: in vivo validation and clinical application in patients with pulmonary hypertension. *Circulation* 2004;110:2010–2016.
8. Chemla D, Hébert JL, Coirault C, Salmeron S, Zamani K, Lecarpentier Y. Matching dicrotic notch and mean pulmonary artery pressures: implications for effective arterial elastance. *Am J Physiol* 1996;271: H1287–H1295.
9. Redington AN, Rigby ML, Shinebourne EA, Oldershaw PJ. Changes in the pressure-volume relation of the right ventricle when its loading conditions are modified. *Br Heart J* 1990;63:45–49.
10. Bland JM, Altman DG. Statistical methods for assessing agreement between two methods of clinical measurement. *Lancet* 1986;1:307–310.

The Light at the End of the Long Pulmonary Hypertension Tunnel Brightens

To the Editor:

Pulmonary vascular research has evolved from investigations of the physiology of circulatory responses to an intense mining of the genetic, cellular, and molecular mechanisms that drive the various forms of the disease. The breakthrough in the field was the documentation that continuous prostacyclin infusion therapy improved function and prevented early death in 41 patients with idiopathic pulmonary arterial hypertension (PAH) (1). This first effective treatment moved the field away from being hopeless and set the tone for the future. Soon after, the development of oral drugs led the way to embrace multidrug treatment regimens. The success and ease of delivery of oral drugs have generated the desire to screen patients to start treatment early. Now, the scientific pressure is to transcend vasodilator drugs to discover more precise therapies based on pathobiology. Animal model studies (2–5) continue to uncover new mechanisms of pulmonary vascular remodeling, and these new mechanisms and pathways challenge clinical investigators to seek proof of efficacy in properly designed patient trials. The threshold to move from the bench to the patient has been significantly lowered. In a recent editorial in the *Journal*, Martin Wilkins (6) emphasized that "the best model of PAH is the patient with the disease." Further evolution is necessary—and the chances that this evolution will take place have improved with the

Originally Published in Press as DOI: 10.1164/rccm.201802-0325LE on June 26, 2018

Anlage B

Validation of the Tricuspid Annular Plane Systolic Excursion/Systolic Pulmonary Artery Pressure Ratio for the Assessment of Right Ventricular-Arterial Coupling in Severe Pulmonary Hypertension.

Tello K, Wan J, Dalmer A, Vanderpool R, Ghofrani HA, Naeije R, Roller F, Mohajerani E, Seeger W, Herberg U, Sommer N, Gall H, Richter MJ. Circ Cardiovasc Imaging. 2019 Sep;12(9)

Circulation: Cardiovascular Imaging

ORIGINAL ARTICLE

Validation of the Tricuspid Annular Plane Systolic Excursion/Systolic Pulmonary Artery Pressure Ratio for the Assessment of Right Ventricular-Arterial Coupling in Severe Pulmonary Hypertension

See Editorial by Bashline and Simon

Khodr Tello, MD
Jun Wan, PhD
Antonia Dalmer, MD
Rebecca Vanderpool, PhD
Hossein A. Ghofrani, MD
Robert Naeije, MD, PhD
Fritz Roller, MD
Emad Mohajerani, MD
Werner Seeger, MD
Ulrike Herberg, MD, PhD
Natascha Sommer, MD, PhD
Henning Gall, MD, PhD
Manuel J. Richter, MD

BACKGROUND: The ratios of tricuspid annular plane systolic excursion (TAPSE)/echocardiographically measured systolic pulmonary artery pressure (PASP), fractional area change/invasively measured mean pulmonary artery pressure, right ventricular (RV) area change/end-systolic area, TAPSE/pulmonary artery acceleration time, and stroke volume/end-systolic area have been proposed as surrogates of RV-arterial coupling. The relationship of these surrogates with the gold standard measure of RV-arterial coupling (invasive pressure-volume loop-derived end-systolic/arterial elastance [Ees/Ea] ratio) and RV diastolic stiffness (end-diastolic elastance) in pulmonary hypertension remains incompletely understood. We evaluated the relationship of these surrogates with invasive pressure-volume loop-derived Ees/Ea and end-diastolic elastance in pulmonary hypertension.

METHODS: We performed right heart echocardiography and cardiac magnetic resonance imaging 1 day before invasive measurement of pulmonary hemodynamics and single-beat RV pressure-volume loops in 52 patients with pulmonary arterial hypertension or chronic thromboembolic pulmonary hypertension. The relationships of the proposed surrogates with Ees/Ea and end-diastolic elastance were evaluated by Spearman correlation, multivariate logistic regression, and receiver operating characteristic analyses. Associations with prognosis were evaluated by Kaplan-Meier analysis.

RESULTS: TAPSE/PASP, fractional area change/mean pulmonary artery pressure, RV area change/end-systolic area, and stroke volume/end-systolic area but not TAPSE/pulmonary artery acceleration time were correlated with Ees/Ea and end-diastolic elastance. Of the surrogates, only TAPSE/PASP emerged as an independent predictor of Ees/Ea (multivariate odds ratio: 18.6; 95% CI, 0.8–96.1; *P*=0.08). In receiver operating characteristic analysis, a TAPSE/PASP cutoff of 0.31 mm/mm Hg (sensitivity: 87.5% and specificity: 75.9%) discriminated RV-arterial uncoupling (Ees/Ea <0.805). Patients with TAPSE/PASP <0.31 mm/mm Hg had a significantly worse prognosis than those with higher TAPSE/PASP.

CONCLUSIONS: Echocardiographically determined TAPSE/PASP is a straightforward noninvasive measure of RV-arterial coupling and is affected by RV diastolic stiffness in severe pulmonary hypertension.

CLINICAL TRIAL REGISTRATION: URL: https://www.clinicaltrials.gov. Unique identifier: NCT03403868.

Key Words: acceleration ■ echocardiography ■ hypertension ■ magnetic resonance imaging ■ pressure

https://www.ahajournals.org/journal/circimaging

CLINICAL PERSPECTIVE

The gold standard for assessment of right ventricular (RV)-arterial coupling is measurement of the end-systolic/arterial elastance (Ees/Ea) ratio from invasive pressure-volume loops. However, this approach is technically demanding, expensive, and unpractical at the bedside, and noninvasive surrogates of Ees/Ea are therefore being sought. The ratio of tricuspid annular plane systolic excursion/systolic pulmonary artery pressure (TAPSE/PASP, measured by echocardiography) has been used as a surrogate of Ees/Ea but has not yet been validated against invasive pressure-volume loop-derived Ees/Ea. The current study is the first to evaluate the relationship of TAPSE/PASP and other proposed surrogates of Ees/Ea with invasive pressure-volume loop-derived Ees/Ea and RV diastolic stiffness (end-diastolic elastance). In 52 patients with severe pulmonary hypertension, TAPSE/PASP and other echocardiographic surrogates were correlated with Ees/Ea and end-diastolic elastance but only TAPSE/PASP emerged as an independent predictor of Ees/Ea in multivariate analysis. TAPSE/PASP <0.31 mm/mm Hg predicted RV-arterial uncoupling (defined as Ees/Ea <0.805) in the study cohort and was associated with a poor prognosis in both the study cohort and an external validation cohort of 193 patients. These results show that TAPSE/PASP is a clinically relevant, straightforward, noninvasive measure of RV-arterial coupling that also provides information on RV diastolic stiffness in severe pulmonary hypertension. Both TAPSE and PASP are easily measured by a standard bedside echocardiographic examination. Further studies are needed to evaluate the possible added value of TAPSE/PASP in current risk assessment strategies for severe pulmonary hypertension.

Right ventricular (RV) function is the main determinant of symptomatology and outcome in severe pulmonary hypertension (PH).[1,2] The RV adapts to increased afterload in PH by increasing contractility to preserve RV-arterial coupling and flow output response to peripheral demand. When this homeometric (ie, contractility) adaptation is exhausted, the RV relies on a heterometric (ie, dimension or Starling law) adaptation, resulting in increased filling pressures, dilatation, negative ventricular interaction, and systemic congestion.[3] The gold standard metric of contractility is pressure-volume loop-derived end-systolic elastance (Ees), and RV-arterial coupling is assessed as a ratio of end-systolic to arterial elastances (Ees/Ea).[1–3] We recently showed that RV-arterial coupling has considerable reserve, as the Ees/Ea ratio has to decrease from 1.5 to 2 to 0.8 before the RV volume increases above normal and right heart failure may be diagnosed.[4] Thus the Ees/Ea metric could help to anticipate and possibly prevent right heart failure in severe PH.[1,2]

However, measuring Ees and Ea via pressure-volume loops is invasive, technically demanding, and expensive. Therefore, simpler noninvasive surrogates are being sought. One surrogate is the Doppler echocardiography measurement of the tricuspid annular plane systolic excursion (TAPSE)/systolic pulmonary artery pressure (PASP) ratio.[5] TAPSE/PASP is a potent independent predictor of precapillary PH and prognosis in heart failure,[5–10] with a prognostic cutoff value of 0.36 mm/mm Hg.[11] TAPSE/PASP is also an independent predictor of outcome in pulmonary arterial hypertension (PAH).[12] Initially regarded as an indirect assessment of the ventricular length-tension relationship,[5] TAPSE/PASP has been considered a surrogate of Ees/Ea based on the assumption that TAPSE estimates contractility and PASP estimates afterload.[6–12] To what extent this assumption is correct has not yet been investigated.

We, therefore, assessed the relationship of echocardiographic TAPSE/PASP with Ees/Ea in severe PH. We also evaluated other suggested surrogates, including the ratios of RV fractional area change (FAC) to mean pulmonary artery pressure (mPAP, invasively measured),[13–15] RV area change to RV end-systolic area (ESA),[16] TAPSE to pulmonary artery acceleration time (PAAT),[17] and stroke volume (SV) to ESA (derived by dividing PASP/ESA as a surrogate of Ees[18,19] by PASP/SV as a surrogate of Ea).[9] Because RV diastolic function may be altered independently of Ees or Ees/Ea and is associated with disease severity and outcome in PAH,[20,21] we also assessed the relationship of the surrogates with end-diastolic elastance (Eed).

METHODS

The raw data that underpin this study are available from the corresponding author on reasonable request.

Study Design and Patients

The current analysis included 52 consecutive patients with PAH and chronic thromboembolic PH who were prospectively enrolled into the Right Heart I study and the Giessen PH Registry[22] between January 2016 and June 2018 (study cohort; Figure I in the Data Supplement). Forty-two of the patients have been reported previously[4,23,24] and were reanalyzed for the present study. The patients were diagnosed according to current guidelines,[25] with a multidisciplinary board (including pulmonologists and radiologists) assessing each diagnosis before enrollment. All patients underwent right heart echocardiography and cardiac magnetic resonance imaging 1 day before pressure-volume/Swan-Ganz

catheterization and received targeted PAH therapies based on clinical evaluation and best standard of care. All participating patients gave written informed consent for enrollment into the Right Heart I study.

Only for survival analysis, a separate group of 193 patients with idiopathic PAH (from a previously reported cohort of 290 patients with PAH)[12] was analyzed retrospectively as an external validation cohort.

The investigation conforms with the principles of the Declaration of Helsinki and was approved by the ethics committee of the Faculty of Medicine at the University of Giessen (Approval No. 108/15). All authors had full access to all the data in the study and take responsibility for its integrity and the data analysis.

Imaging

Doppler echocardiography was performed according to current guidelines,[26] using Vivid E9 and Vivid S5 systems (GE Healthcare, Wauwatosa, WI). RV area change/ESA was calculated as (end-diastolic area–ESA)/ESA.[16] Cardiac magnetic resonance imaging of RV volumes was performed with the Avanto 1.5 Tesla scanner system (Siemens Healthineers, Erlangen, Germany; gradient strength and slew rate: SQ-Engine (45mT/m @ 200 T/m/s).[27]

Right Heart Catheterization

All patients underwent right heart catheterization by insertion of a Swan-Ganz catheter via the internal jugular vein using an 8F introducer sheath. Pressure values were continuously assessed. Cardiac index was measured using the direct or indirect Fick method as available. Pulmonary vascular resistance was calculated as (mPAP–pulmonary artery wedge pressure)/cardiac output.

Pressure-Volume Catheterization

We inserted a 4F pressure-volume catheter (CA-Nr 41063, CD Leycom, Zoetermeer, the Netherlands) via the same 8F introducer sheath as above, and positioned the tip of the catheter in the RV apex with guidance from transthoracic echocardiography and online pressure-volume loops.[4] An intracardiac analyzer (Inca, CD Leycom, Zoetermeer, the Netherlands) was used to display real-time, beat-to-beat pressure-volume loops. Ees and Ea were calculated using the RV single-beat method.[28] RV Eed was calculated from a curvilinear adjustment of end-systolic and end-diastolic pressure/volume ratios to generate a β-coefficient of stiffness.[20,29] We calibrated volume measurements with cardiac magnetic resonance imaging.

Outcomes

The study cohort was followed prospectively until March 20, 2019. We evaluated clinical worsening in the study cohort and overall survival in the external validation cohort. Clinical worsening was defined as any of the following: (1) a reduction in exercise capacity (–15% compared with the baseline 6-minute walk test); (2) worsening in World Health Organization functional class; or (3) clinical deterioration requiring hospital admission (need for new PAH therapies, intravenous diuretics, lung transplantation, or death).

Statistical Analyses

Adherence to a gaussian distribution was determined using the Kolmogorov-Smirnov test and visual assessment of histograms. Variables with a non-normal distribution were ln-transformed and then rechecked with the Kolmogorov-Smirnov test. Differences in echocardiographic parameters dichotomized at an Ees/Ea cutoff of 0.805 (defined as the threshold at which RV-arterial uncoupling begins)[4] were evaluated using the independent *t* test or independent Mann-Whitney *U* test. Interobserver and intraobserver variability of echocardiographic measurements were assessed in 10 randomly selected patients using intraclass correlation coefficients. Coefficient of variation was defined as the SD of the difference between the 2 measurements (or observers) divided by their mean value times 100.[30] TAPSE/PASP (measured echocardiographically) was compared with TAPSE/invasive systolic pulmonary arterial pressure (assessed by right heart catheterization) using Bland-Altman analysis.[31]

Associations of surrogates for RV-arterial coupling (TAPSE/PASP, FAC/mPAP, RV area change/ESA, TAPSE/PAAT, and SV/ESA, all measured by echocardiography except mPAP [right heart catheterization] and SV [cardiac magnetic resonance]) with pressure-volume variables (Ees, Ees/Ea, Eed, and Ea) were measured with Spearman rank correlation coefficient; trend lines were least-squares fits of straight-line models. The relationship of Eed with TAPSE/PASP was also evaluated by stratifying data according to TAPSE/PASP tertile, as done previously[9,12]; between-group differences were analyzed with the Kruskal-Wallis test. For these analyses, $P<0.05$ was considered statistically significant.

To determine which surrogate is most strongly related to Ees/Ea, all surrogates were included in a univariate logistic binary regression analysis as continuous variables. Surrogates that were significant in the univariate analysis were added into a multivariate model ($P<0.10$ was considered statistically significant for this analysis). Multicollinearity was assessed using the variance inflation factor. Receiver operating characteristic curves were used to identify the most powerful surrogate for discriminating RV-arterial uncoupling (Ees/Ea <0.805). Area under the curves were compared using the methodology of Delong and coworkers.[32] Cox proportional-hazards regression models and Kaplan-Meier analyses with log-rank tests were used to assess the prognostic relevance of the TAPSE/PASP ratio. For the multivariate prognostic models, variable selection was based on clinical significance.

MedCalc version 18.11.6 (MedCalc Software, Belgium) was used to compare receiver operating characteristic area under the curves. SPSS, version 23.0 (IBM, Armonk, NY) was used for all other statistical analyses.

RESULTS

Study Cohort

Most of the 52 included patients presented with idiopathic PAH (Table 1). Pulmonary hemodynamics were impaired, and most of the patients presented in World Health Organization functional class III (n=28). Pressure-volume loop measurements, surrogates for RV-arterial coupling, and other echocardiographic and cardiac magnetic resonance data are shown in Table 2. Cardiac

Table 1. Clinical Characteristics of the Study Cohort

	Patients With PH (n=52)
Male/female	26/26
Age, y	54±14
PH subtype	
Idiopathic pulmonary arterial hypertension	34 (65)
Heritable pulmonary arterial hypertension	2 (4)
Pulmonary arterial hypertension associated with	9 (17)
HIV infection	1
Portal hypertension	4
Connective tissue disease	3
Congenital heart disease	1
Chronic thromboembolic PH	6 (12)
Pulmonary veno-occlusive disease	1 (2)
Treatment	
Phosphodiesterase type 5 inhibitor	26 (50)
Endothelin receptor antagonist	30 (58)
Soluble guanylate cyclase stimulator	16 (31)
Prostanoid	14 (27)
Combination therapy	
Dual therapy	16 (31)
Triple therapy	13 (25)
World Health Organization functional class*	
I	3 (6)
II	17 (34)
III	28 (56)
IV	2 (4)
Right heart catheterization	
Mean pulmonary artery pressure, mm Hg	47 [35–54]
Right atrial pressure, mm Hg	8±4
Pulmonary vascular resistance, Wood Units	6.9 [4.4–10.2]
Cardiac index, L/min per m^2	2.8±0.7
Pulmonary artery wedge pressure, mm Hg	9±3

Values represent n, n/n, n (%), mean±SD or median [interquartile range]. PH indicates pulmonary hypertension.
*n=50.

Table 2. RV Pressure-Volume Loop Measurements and Echocardiographic and Cardiac Magnetic Resonance Imaging-Derived Parameters in the Study Cohort

	Patients With PH (n=52)
RV pressure-volume loop measurements	
Ea, mm Hg/mL	0.77 [0.46–1.09]
Ees, mm Hg/mL	0.49 [0.32–0.73]
Ees/Ea ratio	0.70 [0.47–1.02]
Eed, mm Hg/mL	0.14 [0.06–0.24]
Surrogates for RV-arterial coupling and contractility	
TAPSE/PASP, mm/mm Hg*	0.28 [0. 19–0.42]
FAC/mPAP, %/mm Hg†	0.45 [0.25–0.77]
RV area change/ESA†	0.26 [0.14–0.41]
TAPSE/PAAT, mm/ms†	0.27[0.25–0.37]
PASP/ESA, mm Hg/cm^2	3.0 [1.4–5.8]
SV/ESA, mL/cm^2†	3.5 [2.3–4.1]
Cardiac magnetic resonance measurements	
RV end-diastolic volume/body surface area, mL/m^2	111 [88–144]
RV mass diastolic/body surface area, g/m^2	38 [28–52]
RV ejection fraction, %	37±13
SV, mL	71 [59–95]
Echocardiographic data	
TAPSE, mm	21 [18–25]
PASP, mm Hg*	75±24
Right atrial size, cm^2†	21 [17–26]
RV basal diameter, cm†	4.9 [4.3–5.4]
RV systolic free wall myocardial velocity, cm/s‡	12 [10–13]
FAC, %†	21±11
PAAT, ms†	74 [59–89]
ESA, cm^2†	24 [19–30]

Values represent mean±SD or median [interquartile range]. Ea indicates arterial elastance; Eed, end-diastolic elastance; Ees, end-systolic elastance; ESA, end-systolic area; FAC, fractional area change; mPAP, mean pulmonary artery pressure (assessed by right heart catheterization); PAAT, pulmonary artery acceleration time; PASP, systolic pulmonary artery pressure; PH, pulmonary hypertension; RV, right ventricular; SV, stroke volume (assessed by cardiac magnetic resonance); and TAPSE, tricuspid annular plane systolic excursion.
*n=45.
†n=47.
‡n=50.

magnetic resonance measurements revealed substantial RV dilatation and hypertrophy, with decreased ejection fraction. Echocardiography revealed a preserved TAPSE and RV systolic free wall myocardial velocity, substantially elevated PASP, impaired FAC, and high right atrial and RV dimensions. Patients with Ees/Ea <0.805 showed significantly increased right atrial and RV dilatation, impaired TAPSE, and lower values for all surrogates of RV-arterial coupling except TAPSE/PAAT compared with patients with Ees/Ea ≥0.805 (Table I in the Data Supplement).

Intraclass correlation coefficients for interobserver and intraobserver comparisons in key echocardiographic measurements are shown in Table II in the Data Supplement. The overall agreement between TAPSE/PASP (echocardiographic) and TAPSE/systolic pulmonary arterial pressure (invasive) was good (mean bias: 0.0176 mm/mm Hg; 95% CI, −0.0087 to 0.043 mm/mm Hg; Figure II in the Data Supplement).

Surrogates of RV-Arterial Coupling and Their Association With Pressure-Volume Loop Measurements

Ees/Ea, Ea, and Eed were correlated with TAPSE/PASP, FAC/mPAP, RV area change/ESA, and SV/ESA (Figures 1 and 2) but not with TAPSE/PAAT (transformed or not; data not shown). None of the surrogates were corre-

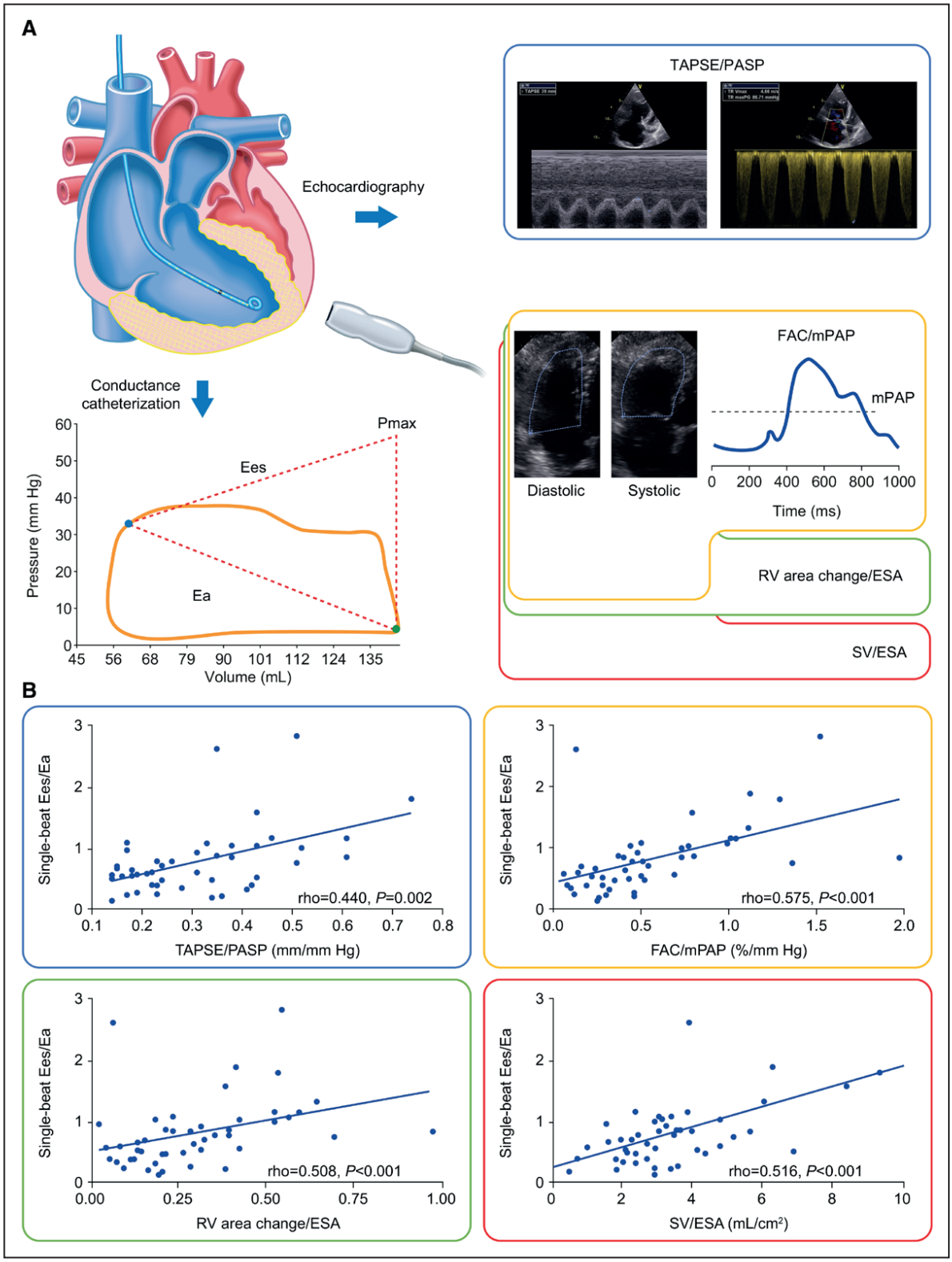

Figure 1. Surrogates for right ventricle (RV)-arterial coupling and their association with single-beat end-systolic elastance (Ees)/arterial elastance (Ea) in patients with pulmonary hypertension.

A, Surrogates were compared with data obtained from invasively measured single-beat pressure-volume loops in the study cohort. **B**, Tricuspid annular plane systolic excursion (TAPSE)/systolic pulmonary artery pressure (PASP), fractional area change (FAC)/mean pulmonary artery pressure (mPAP), RV area change/end-systolic area (ESA), and stroke volume (SV)/ESA (all measured by echocardiography except mPAP [right heart catheterization] and SV [cardiac magnetic resonance]) showed significant associations with invasively measured single-beat Ees/Ea. No association of Ees/Ea with TAPSE/pulmonary artery acceleration time (ρ=–0.016; *P*=0.926) and PASP/ESA (ρ=–0.015; *P*=0.924) was evident. Pmax indicates maximum pressure of an isovolumic beat.

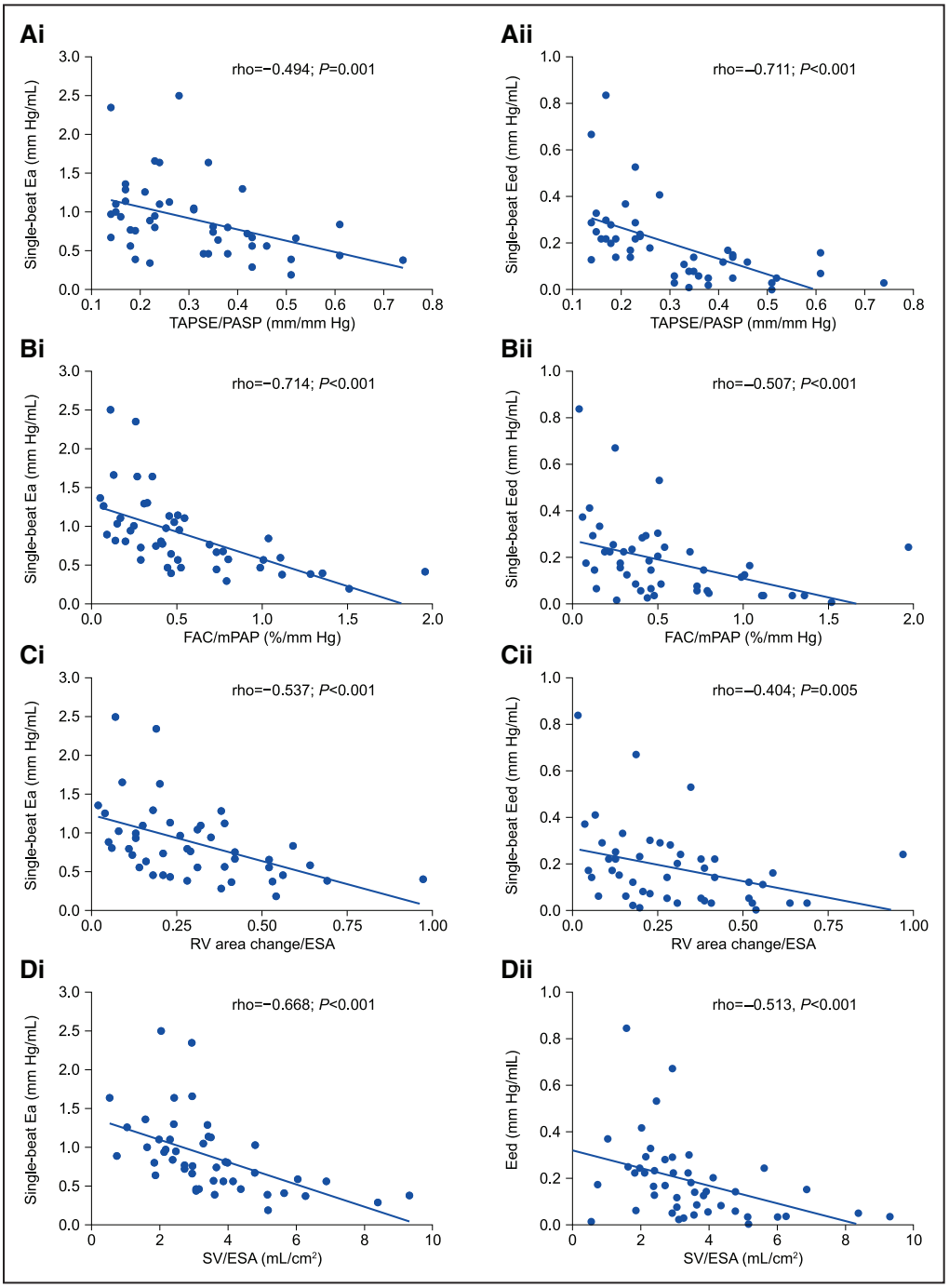

Figure 2. Association of surrogates for right ventricle (RV)-arterial coupling with RV single-beat arterial elastance (Ea) and end-diastolic elastance (Eed) in patients with pulmonary hypertension.

A, Tricuspid annular plane systolic excursion (TAPSE)/systolic pulmonary artery pressure (PASP), (**B**) Fractional area change (FAC)/mean pulmonary artery pressure (mPAP), (**C**) RV area change/end-systolic area (ESA), and (**D**) stroke volume (SV)/ESA (all measured by echocardiography except mPAP [right heart catheterization] and SV [cardiac magnetic resonance]) showed significant associations with **i**, Ea and **ii**, Eed in the study cohort. Ea and Eed showed no significant association with TAPSE/pulmonary artery acceleration time (ρ=–0.072, *P*=0.631 and ρ=–0.051, *P*=0.734, respectively) and PASP/ESA (ρ=0.118, *P*=0.452 and ρ=0.085, *P*=0.589, respectively).

lated with Ees. Eed increased substantially from TAPSE/PASP tertile 3 to tertile 1 (Figure 3).

Relevance of Surrogates for Prediction of RV-Arterial Coupling and Prognosis

In univariate logistic regression analysis, TAPSE/PASP, FAC/mPAP, RV area change/ESA, and SV/ESA were associated with Ees/Ea dichotomized at 0.805 (Table 3). Using multivariate analysis, only TAPSE/PASP (β-coefficient: 2.154) remained associated (Table 3). Using receiver operating characteristic analyses and the Youden index, we identified cutoffs of 0.31 mm/mm Hg for TAPSE/PASP, 0.71%/mm Hg for FAC/mPAP, and 2.93 mL/cm² for SV/ESA to discriminate RV-arterial uncoupling (Ees/Ea <0.805; Figure 4). We found no significant differences in area

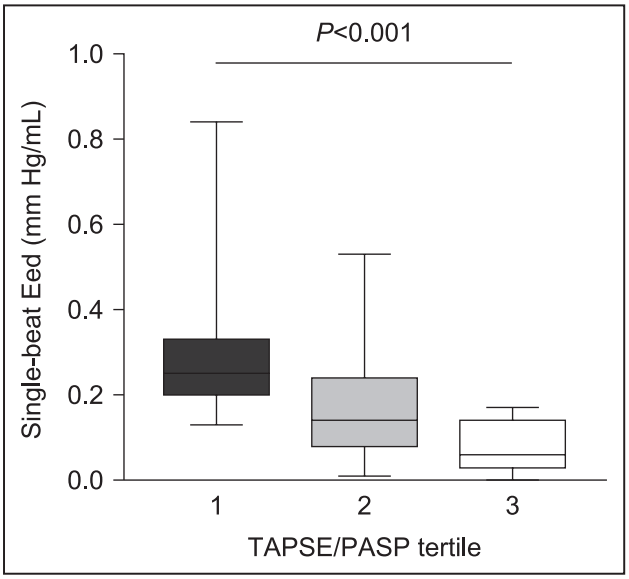

Figure 3. Stratification of end-diastolic elastance (Eed) according to tricuspid annular plane systolic excursion (TAPSE)/systolic pulmonary artery pressure (PASP) tertile in patients with pulmonary hypertension. Eed showed significant differences across tertiles of the echocardiographic TAPSE/PASP ratio in the study cohort (Kruskal-Wallis test). Boxes show median and interquartile range; whiskers show minimum to maximum.

under the curve between the surrogates (TAPSE/PASP versus FAC/mPAP, *P*=0.5334; TAPSE/PASP versus SV/ESA, *P*=0.3405; and FAC/mPAP versus SV/ESA, *P*=0.7462).

In the study cohort, 26 clinical worsening events were observed during a median follow-up time of 13 (interquartile range: 5.3–24.8) months. Kaplan-Meier analysis revealed that patients with PH and TAPSE/PASP <0.31 mm/mm Hg had a significantly worse prognosis than those with higher TAPSE/PASP (log-rank *P*=0.019; Figure 5A). This was supported by multivariate Cox regression analysis including age, sex, and TAPSE/PASP dichotomized at 0.31 mm/mm Hg; TAPSE/PASP showed a hazard ratio of 2.73 (95% CI, 1.14–6.54) as a predictor of clinical worsening.

In the external validation cohort, patients with idiopathic PAH and TAPSE/PASP <0.31 mm/mm Hg showed significantly worse overall survival than those with higher TAPSE/PASP (log-rank *P*=0.003; Figure 5B). TAPSE/PASP also predicted overall mortality (hazard ratio: 1.85; 95% CI, 1.16–2.95) in multivariate Cox regression analysis including World Health Organization functional class, age, sex, pulmonary vascular resistance, and TAPSE/PASP dichotomized at 0.31 mm/mm Hg.

DISCUSSION

The present results show that the echocardiographic TAPSE/PASP ratio is a clinically relevant and valid surrogate of invasively measured Ees/Ea to assess RV-arterial coupling and provides information on RV diastolic stiffness but not RV contractility.

Several other ratios have been proposed to estimate RV-arterial coupling. FAC/mPAP showed relationships with pulsatile RV afterload[14] and biomarkers of RV dysfunction.[13,15] RV area change/ESA was introduced as a surrogate for RV-arterial coupling in a small cohort of patients with scleroderma-associated PAH.[16] In that study, neither RV area change/ESA nor TAPSE/PASP had prognostic relevance.[16] TAPSE/PAAT was introduced as a substitute for TAPSE/PASP in children in whom a sufficient quality of Doppler velocity signal of tricuspid regurgitation could not be obtained,[33] and relied on the argument that PAAT would be a better measure of pulmonary vascular impedance (or afterload) than PASP.[34] However, none of these surrogates was evaluated against the gold standard Ees/Ea metric for RV-arterial coupling. Only echocardiographic TAPSE/PASP and TAPSE/PAAT were evaluated against simplified calculations of Ees/Ea based on single RV pressure curve analysis[7,17] or echocardiographic SV/ESA.[9] The present study shows that only TAPSE/PASP is independently related to invasively measured Ees/Ea.

All considered surrogates of RV-arterial coupling except TAPSE/PAAT were associated with RV afterload (Ea) and diastolic stiffness (Eed) but not RV contractility (Ees). The observed associations with Ea provide

Table 3. Logistic Binary Regression Analysis of the Association of Surrogates for RV-Arterial Coupling and Contractility with Ees/Ea Dichotomized at 0.805 in the Study Cohort

	Univariate Analysis			Multivariate Analysis		
	Odds Ratio	95% CI	*P* Value	Odds Ratio	95% CI	*P* Value
TAPSE/PASP	27.0	3.5–205.9	0.001	8.6	0.8–96.1	0.080
FAC/mPAP	4.2	1.5–11.5	0.005	9.0	0.2–318.0	0.251
RV area change/ESA	2.8	1.1–7.1	0.028	6.9	0.2–250.0	0.292
TAPSE/PAAT	3.4	0.4–33.0	0.288	…	…	…
PASP/ESA	1.1	0.6–2.0	0.882	…	…	…
SV/ESA	1.9	1.2–3.1	0.010	1.1	0.7–2.0	0.632

Displayed parameters were measured by echocardiography except mPAP (right heart catheterization) and SV (cardiac magnetic resonance). Ea indicates arterial elastance; Ees, end-systolic elastance; ESA, end-systolic area; FAC, fractional area change; mPAP, mean pulmonary artery pressure; PAAT, pulmonary artery acceleration time; PASP, systolic pulmonary artery pressure; RV, right ventricular; SV, stroke volume; and TAPSE, tricuspid annular plane systolic excursion.

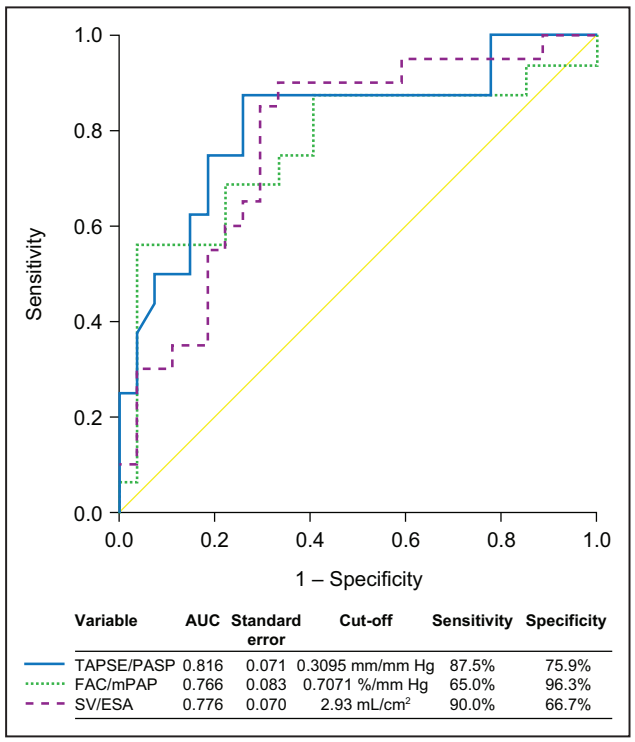

Variable	AUC	Standard error	Cut-off	Sensitivity	Specificity
TAPSE/PASP	0.816	0.071	0.3095 mm/mm Hg	87.5%	75.9%
FAC/mPAP	0.766	0.083	0.7071 %/mm Hg	65.0%	96.3%
SV/ESA	0.776	0.070	2.93 mL/cm^2	90.0%	66.7%

Figure 4. Receiver operating characteristic curve analysis of tricuspid annular plane systolic excursion (TAPSE)/systolic pulmonary artery pressure (PASP), fractional area change (FAC)/mean pulmonary artery pressure (mPAP), and stroke volume (SV)/end-systolic area (ESA) for discriminating right ventricle (RV)-arterial uncoupling in patients with pulmonary hypertension.
TAPSE, PASP, FAC, and ESA were assessed by echocardiography in the study cohort; mPAP was assessed by right heart catheterization; and SV by cardiac magnetic resonance. RV-arterial uncoupling was defined as single-beat end-systolic elastance (Ees)/arterial elastance (Ea) <0.805. Diagonal segments were produced by ties. AUC indicates area under the curve.

the missing link between the physiological concept of assessing RV load adaptability indirectly via echocardiography and the direct invasive measurement. It is unclear whether RV systolic and diastolic dysfunction can evolve separately in heart failure or severe PH because some studies showed tight correlations between Ees and Eed[35,36] while others found Ees and Eed to be dissociated.[20,21] The correlation of surrogates with Eed but not Ees in our study is compatible with dissociated adaptation of inotropic and lusitropic function in severe PH.

The absence of correlations between surrogates of RV-arterial coupling and Ees agrees with the previously reported association of echocardiographic indices of RV function with RV-arterial coupling but not contractility in an experimental model of chronic pressure overload.[37] The absence of a correlation between TAPSE/PAAT and Ees/Ea is more surprising, as PAAT is a better measure of afterload than PASP.[38] This is possibly explained by the curvilinearity of the relationship between PAAT and PASP, with a smaller range of PAAT than PASP covered in the present study making PAAT less sensitive to the observed range of RV afterload.

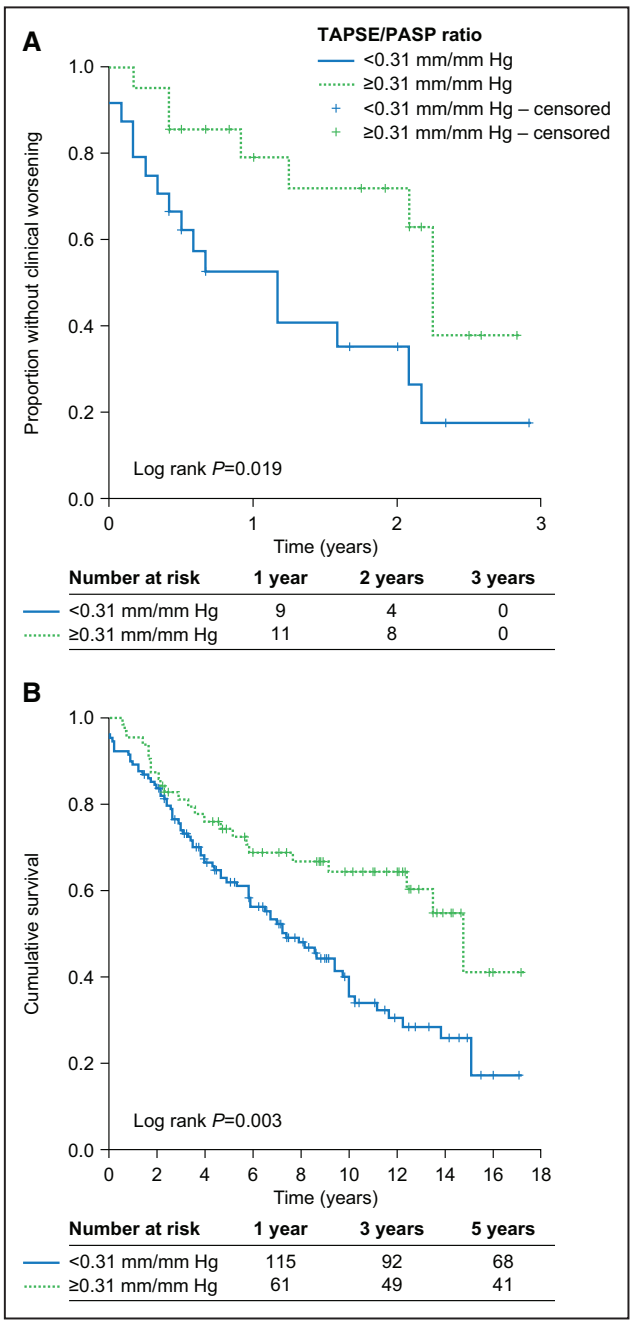

Figure 5. Kaplan-Meier plots of outcomes in patients stratified by tricuspid annular plane systolic excursion (TAPSE)/systolic pulmonary artery pressure (PASP).
Stratification by echocardiographic TAPSE/PASP (≥0.31 mm/mm Hg and <0.31 mm/mm Hg) revealed significant differences in **A**, clinical worsening in patients with pulmonary hypertension (study cohort; estimates of mean and median time to clinical worsening are shown in Table III in the Data Supplement), and (**B**) overall survival in patients with idiopathic pulmonary arterial hypertension (external validation cohort; subset of a previously published cohort[12]).

Based on our receiver operating characteristic and univariate analyses of TAPSE/PASP, FAC/mPAP, and SV/ESA to significantly discriminate RV-arterial uncoupling, all these surrogates might be used in the clinic based on local preferences. Nevertheless, the information content of TAPSE/PASP is superior as this metric was the only independent predictor of gold standard Ees/Ea in severe PH.

In the present study, the TAPSE/PASP cutoff value for prediction of RV-arterial uncoupling (Ees/Ea <0.805)[4] was 0.31, which is lower than the cutoff value of 0.36 previously associated with survival in heart failure.[11] This difference may be related to better-preserved contractility adaptation to higher levels of afterload in severe PH compared with heart failure. In addition, our study showed the prognostic and clinical relevance of the proposed cutoff in PAH and, therefore, highlighted the association between clinical utility and RV pathophysiology.

Limitations

We used the single-beat method to estimate Eed, Ees, and Ea; it is unclear if the multiple-beat approach would yield similar results, although there is a recent report of agreement between the 2 approaches.[39] Limitations of echocardiographic analysis include observer dependency, reliability, and 2-dimensional plane measurement. In general, echocardiographic measurements have shown favorable interobserver and intraobserver variability in PH,[40] but some variability must be considered in clinical practice. Moreover, as RV dysfunction progresses, TAPSE reaches a minimum and shows no further decrease.[41] Most of the patients in our cohort were already in a state of uncoupling (median Ees/Ea: 0.70). Other reasons for the somewhat unexpected absence of correlation between TAPSE and Ees in our study may be that TAPSE is afterload-dependent, plane-dependent, and falsely increased in the presence of severe tricuspid regurgitation. The reliability of TAPSE as a parameter of RV function (and therefore the utility of TAPSE/PASP) may thus be reduced in the later stages of RV failure or after heart surgery. In addition, echocardiographic PASP is influenced by the quality of acquisition and signal of the peak tricuspid regurgitation velocity.[42] An important limitation is the partial dependency of the Eed calculation[29] as well as the TAPSE/PASP ratio on volume, which might explain the higher correlation of TAPSE/PASP with Eed than with Ees/Ea. The comprehensive and demanding methodology limited the size of the study cohort. The relatively short prospective observational period, the study cohort sample size, and the retrospective analysis of the external validation cohort limit the interpretation of the results; the prognostic value of the identified TAPSE/PASP cutoff must be confirmed in a large prospective study.

Conclusions

The echocardiographic TAPSE/PASP ratio is a straightforward surrogate of invasively measured Ees/Ea to assess RV-arterial coupling. Both TAPSE and PASP are easily measured by a standard bedside echocardiographic examination. Further studies are needed to evaluate the possible added value of TAPSE/PASP in current risk assessment strategies for severe PH.

ARTICLE INFORMATION

Received February 20, 2019; accepted July 2, 2019.

The Data Supplement is available at https://www.ahajournals.org/doi/suppl/10.1161/CIRCIMAGING.119.009047.

Correspondence

Khodr Tello, MD, Department of Internal Medicine, Justus-Liebig-University Giessen, Klinikstrasse 32, 35392 Giessen, Germany. Email khodr.tello@innere.med.uni-giessen.de

Affiliations

Department of Internal Medicine (K.T., A.D., H.A.G., E.M., W.S., N.S., H.G., M.J.R.) and Department of Radiology (F.R.), Justus-Liebig-University Giessen, Universities of Giessen and Marburg Lung Center (UGMLC), Member of the German Center for Lung Research (DZL), Germany. Department of Pulmonary and Critical Care Medicine, National Pulmonary Embolism & Pulmonary Vascular Diseases Research Group, National Clinical Research Center for Respiratory Diseases, China-Japan Friendship Hospital, Beijing, China (J.W.). University of Arizona, Tucson (R.V.). Department of Pneumology, Kerckhoff Heart, Rheuma and Thoracic Center, Bad Nauheim, Germany (H.A.G.). Department of Medicine, Imperial College London, United Kingdom (H.A.G.). Erasme University Hospital, Brussels, Belgium (R.N.). Department of Pediatric Cardiology, University of Bonn, Germany (U.H.).

Acknowledgments

We thank Claire Mulligan, PhD, (Beacon Medical Communications Ltd, Brighton, United Kingdom) for editorial support, funded by the University of Giessen.

Sources of Funding

This work was funded by the Excellence Cluster Cardio-Pulmonary System (ECCPS) and the Collaborative Research Center (SFB) 1213—Pulmonary Hypertension and Cor Pulmonale, grant number SFB1213/1, project B08 (German Research Foundation, Bonn, Germany).

Disclosures

Dr Tello has received speaking fees from Actelion and Bayer. Dr Ghofrani has received consultancy fees from Bayer, Actelion, Pfizer, Merck, GSK, and Novartis; fees for participation in advisory boards from Bayer, Pfizer, GSK, Actelion, and Takeda; lecture fees from Bayer HealthCare, GSK, Actelion, and Encysive/Pfizer; industry-sponsored grants from Bayer HealthCare, Aires, Encysive/Pfizer, and Novartis; and sponsored grants from the German Research Foundation, Excellence Cluster Cardiopulmonary Research, and the German Ministry for Education and Research. Dr Naeije has relationships with drug companies including AOPOrphan Pharmaceuticals, Actelion, Bayer, Reata, Lung Biotechnology Corporation, and United Therapeutics. In addition to being an investigator in trials involving these companies, relationships include consultancy service, research grants, and membership of scientific advisory boards. Dr Seeger has received speaker/consultancy fees from Pfizer and Bayer Pharma AG. Dr Sommer has received fees from Actelion. Dr Gall has received fees from Actelion, AstraZeneca, Bayer, BMS, GSK, Janssen-Cilag, Lilly, MSD, Novartis, OMT, Pfizer, and United Therapeutics. Dr Richter has received support from United Therapeutics and Bayer; speaker fees from Bayer, Actelion, Mundipharma, Roche, and OMT; and consultancy fees from Bayer. The other authors report no conflicts.

REFERENCES

1. Lahm T, Douglas IS, Archer SL, Bogaard HJ, Chesler NC, Haddad F, Hemnes AR, Kawut SM, Kline JA, Kolb TM, Mathai SC, Mercier O, Michelakis ED, Naeije R, Tuder RM, Ventetuolo CE, Vieillard-Baron A, Voelkel NF, Vonk-Noordegraaf A, Hassoun PM; American Thoracic Society Assembly on Pulmonary Circulation. Assessment of right ventricular function in the

research setting: knowledge gaps and pathways forward. an official american thoracic society research statement. *Am J Respir Crit Care Med.* 2018;198:e15–e43. doi: 10.1164/rccm.201806-1160ST
2. Vonk Noordegraaf A, Chin KM, Haddad F, Hassoun PM, Hemnes AR, Hopkins SR, Kawut SM, Langleben D, Lumens J, Naeije R. Pathophysiology of the right ventricle and of the pulmonary circulation in pulmonary hypertension: an update. *Eur Respir J.* 2019;53:1801900. doi: 10.1183/13993003.01900-2018
3. Vonk Noordegraaf A, Westerhof BE, Westerhof N. The relationship between the right ventricle and its load in pulmonary hypertension. *J Am Coll Cardiol.* 2017;69:236–243. doi: 10.1016/j.jacc.2016.10.047
4. Tello K, Dalmer A, Axmann J, Vanderpool R, Ghofrani HA, Naeije R, Roller F, Seeger W, Sommer N, Wilhelm J, Gall H, Richter MJ. Reserve of right ventricular-arterial coupling in the setting of chronic overload. *Circ Heart Fail.* 2019;12:e005512. doi: 10.1161/CIRCHEARTFAILURE.118.005512
5. Guazzi M, Bandera F, Pelissero G, Castelvecchio S, Menicanti L, Ghio S, Temporelli PL, Arena R. Tricuspid annular plane systolic excursion and pulmonary arterial systolic pressure relationship in heart failure: an index of right ventricular contractile function and prognosis. *Am J Physiol Heart Circ Physiol.* 2013;305:H1373–H1381. doi: 10.1152/ajpheart.00157.2013
6. Bosch L, Lam CSP, Gong L, Chan SP, Sim D, Yeo D, Jaufeerally F, Leong KTG, Ong HY, Ng TP, Richards AM, Arslan F, Ling LH. Right ventricular dysfunction in left-sided heart failure with preserved versus reduced ejection fraction. *Eur J Heart Fail*. 2017;19:1664–1671. doi: 10.1002/ejhf.873
7. Gerges M, Gerges C, Pistritto AM, Lang MB, Trip P, Jakowitsch J, Binder T, Lang IM. Pulmonary hypertension in heart failure. epidemiology, right ventricular function, and survival. *Am J Respir Crit Care Med.* 2015;192:1234–1246. doi: 10.1164/rccm.201503-0529OC
8. Gorter TM, van Veldhuisen DJ, Voors AA, Hummel YM, Lam CSP, Berger RMF, van Melle JP, Hoendermis ES. Right ventricular-vascular coupling in heart failure with preserved ejection fraction and pre- vs. post-capillary pulmonary hypertension. *Eur Heart J Cardiovasc Imaging.* 2018;19:425–432. doi: 10.1093/ehjci/jex133
9. Guazzi M, Dixon D, Labate V, Beussink-Nelson L, Bandera F, Cuttica MJ, Shah SJ. RV Contractile function and its coupling to pulmonary circulation in heart failure with preserved ejection fraction: stratification of clinical phenotypes and outcomes. *JACC Cardiovasc Imaging.* 2017;10(10 pt B):1211–1221. doi: 10.1016/j.jcmg.2016.12.024
10. Guazzi M, Naeije R, Arena R, Corrà U, Ghio S, Forfia P, Rossi A, Cahalin LP, Bandera F, Temporelli P. Echocardiography of right ventriculoarterial coupling combined with cardiopulmonary exercise testing to predict outcome in heart failure. *Chest.* 2015;148:226–234. doi: 10.1378/chest.14-2065
11. Guazzi M. Use of TAPSE/PASP ratio in pulmonary arterial hypertension: An easy shortcut in a congested road. *Int J Cardiol.* 2018;266:242–244. doi: 10.1016/j.ijcard.2018.04.053
12. Tello K, Axmann J, Ghofrani HA, Naeije R, Narcin N, Rieth A, Seeger W, Gall H, Richter MJ. Relevance of the TAPSE/PASP ratio in pulmonary arterial hypertension. *Int J Cardiol.* 2018;266:229–235. doi: 10.1016/j.ijcard.2018.01.053
13. Prins KW, Archer SL, Pritzker M, Rose L, Weir EK, Sharma A, Thenappan T. Interleukin-6 is independently associated with right ventricular function in pulmonary arterial hypertension. *J Heart Lung Transplant.* 2018;37:376–384. doi: 10.1016/j.healun.2017.08.011
14. Prins KW, Weir EK, Archer SL, Markowitz J, Rose L, Pritzker M, Madlon-Kay R, Thenappan T. Pulmonary pulse wave transit time is associated with right ventricular-pulmonary artery coupling in pulmonary arterial hypertension. *Pulm Circ.* 2016;6:576–585. doi: 10.1086/688879
15. Richter MJ, Ghofrani HA, Gall H. Beyond interleukin-6 in right ventricular function: evidence for another biomarker. *J Heart Lung Transplant*. 2018;37:674–675. doi: 10.1016/j.healun.2017.12.002
16. French S, Amsallem M, Ouazani N, Li S, Kudelko K, Zamanian RT, Haddad F, Chung L. Non-invasive right ventricular load adaptability indices in patients with scleroderma-associated pulmonary arterial hypertension non-invasive right ventricular load adaptability indices in patients with scleroderma-associated pulmonary arterial hypertension. *Pulm Circ.* 2018;8:2045894018788268. doi: 10.1177/2045894018788268
17. Levy PT, El Khuffash A, Woo KV, Hauck A, Hamvas A, Singh GK. A novel noninvasive index to characterize right ventricle pulmonary arterial vascular coupling in children [published online December 6, 2018]. *J Am Coll Cardiol Img*. doi: 10.1016/j.jcmg.2018.09.022
18. Claessen G, La Gerche A, Voigt JU, Dymarkowski S, Schnell F, Petit T, Willems R, Claus P, Delcroix M, Heidbuchel H. Accuracy of echocardiography to evaluate pulmonary vascular and RV function during exercise. *JACC Cardiovasc Imaging.* 2016;9:532–543. doi: 10.1016/j.jcmg.2015.06.018
19. Pratali L, Allemann Y, Rimoldi SF, Faita F, Hutter D, Rexhaj E, Brenner R, Bailey DM, Sartori C, Salmon CS, Villena M, Scherrer U, Picano E, Sicari R. RV contractility and exercise-induced pulmonary hypertension in chronic mountain sickness: a stress echocardiographic and tissue Doppler imaging study. *JACC Cardiovasc Imaging.* 2013;6:1287–1297. doi: 10.1016/j.jcmg.2013.08.007
20. Rain S, Handoko ML, Trip P, Gan CT, Westerhof N, Stienen GJ, Paulus WJ, Ottenheijm CA, Marcus JT, Dorfmüller P, Guignabert C, Humbert M, Macdonald P, Dos Remedios C, Postmus PE, Saripalli C, Hidalgo CG, Granzier HL, Vonk-Noordegraaf A, van der Velden J, de Man FS. Right ventricular diastolic impairment in patients with pulmonary arterial hypertension. *Circulation*. 2013;128:2016–2025, 2021. doi: 10.1161/CIRCULATIONAHA.113.001873
21. Trip P, Rain S, Handoko ML, van der Bruggen C, Bogaard HJ, Marcus JT, Boonstra A, Westerhof N, Vonk-Noordegraaf A, de Man FS. Clinical relevance of right ventricular diastolic stiffness in pulmonary hypertension. *Eur Respir J.* 2015;45:1603–1612. doi: 10.1183/09031936.00156714
22. Gall H, Felix JF, Schneck FK, Milger K, Sommer N, Voswinckel R, Franco OH, Hofman A, Schermuly RT, Weissmann N, Grimminger F, Seeger W, Ghofrani HA. The giessen pulmonary hypertension registry: survival in pulmonary hypertension subgroups. *J Heart Lung Transplant.* 2017;36:957–967. doi: 10.1016/j.healun.2017.02.016
23. Tello K, Dalmer A, Vanderpool R, Ghofrani HA, Naeije R, Roller F, Seeger W, Wilhelm J, Gall H, Richter MJ. Cardiac magnetic resonance imaging-based right ventricular strain analysis for assessment of coupling and diastolic function in pulmonary hypertension [published online March 8, 2019]. *J Am Coll Cardiol Img*. doi: 10.1016/j.jcmg.2018.12.032
24. Tello K, Richter MJ, Axmann J, Buhmann M, Seeger W, Naeije R, Ghofrani HA, Gall H. More on single-beat estimation of right ventriculoarterial coupling in pulmonary arterial hypertension. *Am J Respir Crit Care Med.* 2018;198:816–818. doi: 10.1164/rccm.201802-0283LE
25. Galiè N, Humbert M, Vachiery JL, Gibbs S, Lang I, Torbicki A, Simonneau G, Peacock A, Vonk Noordegraaf A, Beghetti M, Ghofrani A, Gomez Sanchez MA, Hansmann G, Klepetko W, Lancellotti P, Matucci M, McDonagh T, Pierard LA, Trindade PT, Zompatori M, Hoeper M. 2015 ESC/ERS Guidelines for the diagnosis and treatment of pulmonary hypertension: The Joint Task Force for the Diagnosis and Treatment of Pulmonary Hypertension of the European Society of Cardiology (ESC) and the European Respiratory Society (ERS): endorsed by: Association for European Paediatric and Congenital Cardiology (AEPC), International Society for Heart and Lung Transplantation (ISHLT). *Eur Respir J.* 2015;46:903–975. doi: 10.1183/13993003.01032-2015
26. Rudski LG, Lai WW, Afilalo J, Hua L, Handschumacher MD, Chandrasekaran K, Solomon SD, Louie EK, Schiller NB. Guidelines for the echocardiographic assessment of the right heart in adults: a report from the American Society of Echocardiography endorsed by the European Association of Echocardiography, a registered branch of the European Society of Cardiology, and the Canadian Society of Echocardiography. *J Am Soc Echocardiogr.* 2010;23:685–713; quiz 786. doi: 10.1016/j.echo.2010.05.010
27. Hundley WG, Bluemke DA, Finn JP, Flamm SD, Fogel MA, Friedrich MG, Ho VB, Jerosch-Herold M, Kramer CM, Manning WJ, Patel M, Pohost GM, Stillman AE, White RD, Woodard PK; American College of Cardiology Foundation Task Force on Expert Consensus Documents. ACCF/ACR/AHA/NASCI/SCMR 2010 expert consensus document on cardiovascular magnetic resonance: a report of the American College of Cardiology Foundation Task Force on Expert Consensus Documents. *Circulation*. 2010;121:2462–508. doi: 10.1161/CIR.0b013e3181d44a8f
28. Brimioulle S, Wauthy P, Ewalenko P, Rondelet B, Vermeulen F, Kerbaul F, Naeije R. Single-beat estimation of right ventricular end-systolic pressure-volume relationship. *Am J Physiol Heart Circ Physiol*. 2003;284:H162 5H1630. doi: 10.1152/ajpheart.01023.2002
29. Vanderpool RR, Puri R, Osorio A, Wickstrom K, Desai A, Black S, Garcia JGN, Yuan J, Rischard F. Express: surfing the right ventricular pressure waveform: methods to assess global, systolic and diastolic RV function from a clinical right heart catheterization [published online April 2, 2019]. *Pulm Circ*. doi: 10.1177/2045894019850993
30. van der Zwaan HB, Geleijnse ML, McGhie JS, Boersma E, Helbing WA, Meijboom FJ, Roos-Hesselink JW. Right ventricular quantification in clinical practice: two-dimensional vs. three-dimensional echocardiography compared with cardiac magnetic resonance imaging. *Eur J Echocardiogr.* 2011;12:656–664. doi: 10.1093/ejechocard/jer107
31. Giavarina D. Understanding bland altman analysis. *Biochem Med (Zagreb).* 2015;25:141–151. doi: 10.11613/BM.2015.015

32. DeLong ER, DeLong DM, Clarke-Pearson DL. Comparing the areas under two or more correlated receiver operating characteristic curves: a nonparametric approach. *Biometrics.* 1988;44:837–845.
33. Levy PT, El Khuffash A, Woo KV, Singh GK. Right ventricular-pulmonary vascular interactions: an emerging role for pulmonary artery acceleration time by echocardiography in adults and children. *J Am Soc Echocardiogr.* 2018;31:962–964. doi: 10.1016/j.echo.2018.04.004
34. Rudski L, Gargani L, Naeije R, Bossone E. Authors' reply: pulmonary flow wave morphology characteristics of pulmonary hypertension. *J Am Soc Echocardiogr.* 2018;31:964–965. doi: 10.1016/j.echo.2018.04.017
35. Vanderpool RR, Desai AA, Knapp SM, Simon MA, Abidov A, Yuan JX, Garcia JGN, Hansen LM, Knoper SR, Naeije R, Rischard FP. How prostacyclin therapy improves right ventricular function in pulmonary arterial hypertension. *Eur Respir J.* 2017;50:1700764. doi: 10.1183/13993003.00764-2017
36. Vanderpool RR, Pinsky MR, Naeije R, Deible C, Kosaraju V, Bunner C, Mathier MA, Lacomis J, Champion HC, Simon MA. RV-pulmonary arterial coupling predicts outcome in patients referred for pulmonary hypertension. *Heart.* 2015;101:37–43. doi: 10.1136/heartjnl-2014-306142
37. Guihaire J, Haddad F, Boulate D, Decante B, Denault AY, Wu J, Hervé P, Humbert M, Dartevelle P, Verhoye JP, Mercier O, Fadel E. Non-invasive indices of right ventricular function are markers of ventricular-arterial coupling rather than ventricular contractility: insights from a porcine model of chronic pressure overload. *Eur Heart J Cardiovasc Imaging.* 2013;14:1140–1149. doi: 10.1093/ehjci/jet092
38. Kitabatake A, Inoue M, Asao M, Masuyama T, Tanouchi J, Morita T, Mishima M, Uematsu M, Shimazu T, Hori M, Abe H. Noninvasive evaluation of pulmonary hypertension by a pulsed Doppler technique. *Circulation.* 1983;68:302–309. doi: 10.1161/01.cir.68.2.302
39. Inuzuka R, Hsu S, Tedford RJ, Senzaki H. Single-beat estimation of right ventricular contractility and its coupling to pulmonary arterial load in patients with pulmonary hypertension. *J Am Heart Assoc*. 2018;7:e007929. doi: 10.1161/JAHA.117.007929
40. Sato T, Tsujino I, Ohira H, Oyama-Manabe N, Yamada A, Ito YM, Goto C, Watanabe T, Sakaue S, Nishimura M. Validation study on the accuracy of echocardiographic measurements of right ventricular systolic function in pulmonary hypertension. *J Am Soc Echocardiogr.* 2012;25:280–286. doi: 10.1016/j.echo.2011.12.012
41. Kind T, Mauritz GJ, Marcus JT, van de Veerdonk M, Westerhof N, Vonk-Noordegraaf A. Right ventricular ejection fraction is better reflected by transverse rather than longitudinal wall motion in pulmonary hypertension. *J Cardiovasc Magn Reson.* 2010;12:35. doi: 10.1186/1532-429X-12-35
42. Amsallem M, Sternbach JM, Adigopula S, Kobayashi Y, Vu TA, Zamanian R, Liang D, Dhillon G, Schnittger I, McConnell MV, Haddad F. Addressing the controversy of estimating pulmonary arterial pressure by echocardiography. *J Am Soc Echocardiogr.* 2016;29:93–102. doi: 10.1016/j.echo.2015.11.001

Anlage C

A simple echocardiographic estimate of right ventricular-arterial coupling to assess severity and outcome in pulmonary hypertension on chronic lung disease.

Tello K, Ghofrani HA, Heinze C, Krueger K, Naeije R, Raubach C, Seeger W, Sommer N, Gall H, Richter MJ. Eur Respir J. 2019 Sep 12;54(3)

A simple echocardiographic estimate of right ventricular–arterial coupling to assess severity and outcome in pulmonary hypertension on chronic lung disease

To the Editor:

The adaptation of right ventricular (RV) systolic function to afterload is a major determinant of outcome in pulmonary hypertension [1]. The gold standard measurement of RV–pulmonary arterial (PA) coupling is the ratio of end-systolic to arterial elastances (E_{es}/E_a) which is optimal for RV flow output at minimal energy cost at values between 1.5 and 2 [2]. Progressive RV–PA uncoupling is associated with maintained RV dimensions down to E_{es}/E_a values of around 0.8 [3]. Thus, the evaluation of RV–PA coupling would theoretically allow monitoring of the transition from compensated to decompensated RV function in pulmonary hypertension. However, measuring RV–PA coupling at the bedside is technically demanding and invasive. Therefore, simpler imaging surrogates are being evaluated. One of those is the ratio of tricuspid annular plane systolic excursion (TAPSE) as a surrogate of contractility and systolic pulmonary artery pressure (PASP) as a surrogate of afterload, both measured using echocardiography (M-mode for TAPSE and Doppler assessment of the maximum velocity of tricuspid regurgitation for PASP) [4]. The TAPSE/PASP ratio has emerged as a potent predictor of outcome in heart failure [5] as well as in pulmonary arterial hypertension (PAH) [6].

Pulmonary hypertension secondary to chronic lung diseases (PH-LD) is most often mild to moderate, with many patients having a mean pulmonary artery pressure (PAP) <35 mmHg. A small percentage of patients referred for evaluation in dedicated centres may have severe pulmonary hypertension with mean PAP in the range reported in PAH [7]. However, RV function is often altered even in mild-to-moderate PH-LD, and is an important determinant of survival and functional status in PH-LD [7, 8]. We therefore explored the functional significance and prognostic relevance of the TAPSE/PASP ratio in PH-LD.

We analysed patients with PH-LD and idiopathic PAH (iPAH) enrolled in the prospectively recruiting Giessen PH Registry [9]. The diagnosis of PH-LD was established by a multidisciplinary board before enrolment in the Giessen PH registry [9] between December 2004 and March 2012. Follow-up data were retrieved from the Giessen PH Registry up to February 2018. The analysis included consecutive patients with complete echocardiographic (day 1) and invasive haemodynamic data (day 2) and complete follow-up. The patients with iPAH (n=193) were a subset of a previously reported cohort of 290 patients with PAH [6]. The investigation was approved by the ethics committee of the Faculty of Medicine at the University of Giessen (Approval No. 186/16, 266/11). All participating patients gave written informed consent.

As recently updated [7], PH-LD was defined by a mean PAP of ⩾21 mmHg (21–24 mmHg with pulmonary vascular resistance (PVR) ⩾3 Wood Units, or ⩾25 mmHg alone), with mean PAP ⩾35 mmHg alone or mean PAP ⩾25 mmHg with low cardiac index (<2.0 $L \cdot min^{-1} \cdot m^{-2}$) sub-defining severe PH-LD.

@ERSpublications
The ratio of tricuspid annular plane systolic excursion to systolic pulmonary artery pressure is a simple echocardiographic parameter that reflects haemodynamic severity and predicts survival in pulmonary hypertension due to lung diseases. http://bit.ly/2KgLAbR

Cite this article as: Tello K, Ghofrani HA, Heinze C, *et al.* A simple echocardiographic estimate of right ventricular-arterial coupling to assess severity and outcome in pulmonary hypertension on chronic lung disease. *Eur Respir J* 2019; 54: 1802435 [https://doi.org/10.1183/13993003.02435-2018].

Normally distributed data were expressed as mean±SD; non-normally distributed data were expressed as median (interquartile range). Receiver operating characteristic (ROC) analyses and the Youden Index were used to determine thresholds for discrimination of PH-LD severity. Logistic regression models were built to assess the ability of the TAPSE/PASP ratio to discriminate severe and non-severe PH-LD and to predict survival. In all analyses, $p<0.05$ was considered significant.

In total, 172 patients with PH-LD were included (age: 58±26 years; mean PAP: 34 (28–41) mmHg; PVR: 5.5 (3.8–7.9) Wood Units; cardiac index: 2.5±0.7 $L \cdot min^{-1} \cdot m^{-2}$). 78 (45.3%) patients had pulmonary hypertension due to chronic obstructive pulmonary disease (PH-COPD), which was classified as severe in 21 (12.2%) patients. The remaining 94 (54.7%) patients had pulmonary hypertension due to interstitial lung disease (PH-ILD), which was classified as severe in 44 (25.6%) patients. The patients with PH-COPD had a reduced forced expiratory volume in 1 s (FEV_1) of 51±23% predicted and a FEV_1/forced vital capacity (FVC) ratio of 57±14%. The FEV_1/FVC ratio was higher in severe *versus* non-severe PH-COPD while FEV_1 was not different (FEV_1/FVC: 63±12% pred *versus* 55±15% pred, p=0.049; FEV_1: p=0.088; independent t-test). We found no correlation between FEV_1/FVC or FEV_1 and the TAPSE/PASP ratio in severe and non-severe PH-COPD (data not shown). The patients with PH-ILD had reduced total lung capacity (TLC; 71±21% pred) and vital capacity (VC; 61±22% pred). Neither parameter differed between severe and non-severe PH-ILD (TLC: p=0.699; VC: p=0.838; independent t-test). There were no correlations between TLC or VC and the TAPSE/PASP ratio in severe and non-severe PH-ILD (data not shown).

In the patients with severe PH-LD, TAPSE/PASP ratios and PVR values were in the same range as those observed in the patients with iPAH and significantly lower and higher, respectively, than those observed in the patients with non-severe PH-LD (figure 1a).

ROC analysis identified a cut-off of 0.26 $mm \cdot mmHg^{-1}$ for TAPSE/PASP with a sensitivity of 80.6% and a specificity of 71.2% to discriminate between severe and non-severe PH-LD, which was superior to TAPSE or PASP alone (figure 1b). Logistic multivariate analysis (adjusting for age and sex) showed a significant ability of the TAPSE/PASP ratio (dichotomised at 0.26 $mm \cdot mmHg^{-1}$; OR: 9.37; 95% CI: 4.56–19.26; p<0.001) to discriminate the haemodynamic phenotypes. In addition, ROC analysis showed that TAPSE/PASP is also able to discriminate between severe and non-severe PH-COPD and severe and non-severe PH-ILD (figure 1c). This was supported by logistic multivariate analysis (multivariate OR for PH-COPD: 18.60; 95% CI: 4.45–77.75; p<0.001; and PH-ILD: 8.44; 95% confidence interval: 3.34–21.36; p<0.001). Interestingly, the TAPSE/PASP ratio predicted survival in PH-COPD as well as in PH-ILD (figure 1d).

Previous studies reported only mild-to-moderate alterations in lung function tests in patients with severe PH secondary to COPD [10, 11], and better lung function in severe PH-COPD compared with non-severe PH-COPD [12, 13]. This is supported by our data showing a higher FEV_1/FVC ratio in COPD with severe *versus* non-severe PH, and agrees with the notion of a predominantly vascular phenotype in these patients [11].

Afterload dependent progression of RV function from adaptation over maladaptation and eventually to failure is determining the symptomatic status and prognosis irrespectively of the underlying pulmonary hypertension subgroup [14]. In the present study, the TAPSE/PASP ratio, as an afterload dependent echocardiographic surrogate of RV–PA coupling, showed its clinical utility in PH-LD. This is in line with the previously described prognostic relevance and association to PVR in PAH [6] as well as in heart failure [15]. However, the adequacy of RV adaptation may vary from one patient to another and depend on the presence of co-morbidities, as has been shown for example in patients with systemic sclerosis [1, 2]. Nevertheless, the impact of chronic infections or an inflammatory state on RV–PA coupling in PH-LD patients need further investigation.

Limitations to the present findings are the absence of invasive validation of the TAPSE/PASP ratio, the high proportion of patients with severe PH-LD (probably related to the fact that the UGMLC is a national tertiary referral centre for pulmonary hypertension), and the currently unclear therapeutic relevance. Other parameters such as FAC and global longitudinal strain, have not been investigated in our study but might also be associated with contractility/coupling and outcome. In addition, variability in load condition might influence the TASPE/PASP ratio due to its afterload dependency.

In conclusion, the TAPSE/PASP ratio is a straightforward and clinically relevant measurement to differentiate between the haemodynamic phenotypes of patients with PH-LD. The TAPSE/PASP ratio might prove to be an important non-invasive tool for the evaluation of future therapeutic interventions in patients with PH-LD.

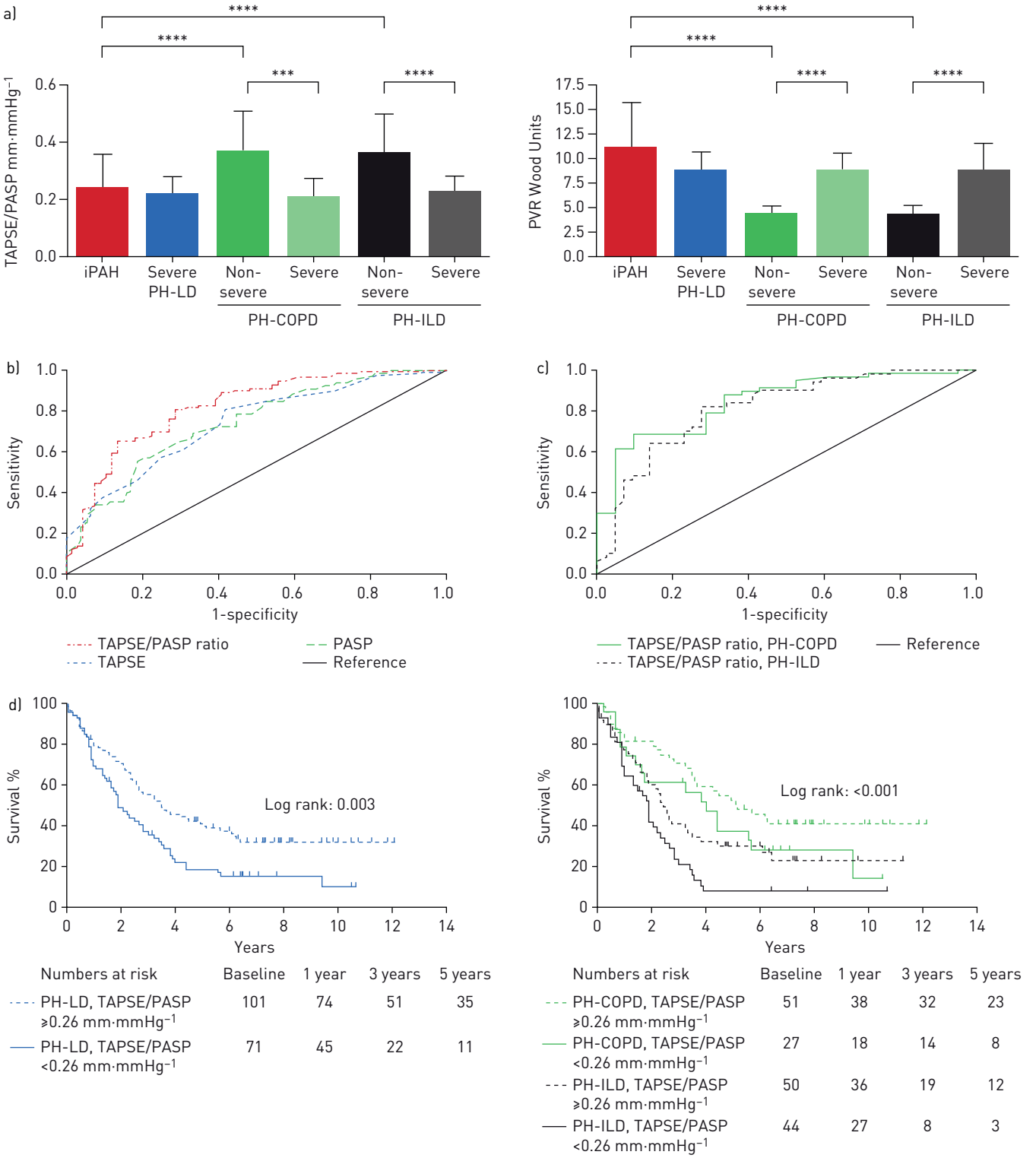

Numbers at risk	Baseline	1 year	3 years	5 years
PH-LD, TAPSE/PASP ≥0.26 mm·mmHg^{-1}	101	74	51	35
PH-LD, TAPSE/PASP <0.26 mm·mmHg^{-1}	71	45	22	11

Numbers at risk	Baseline	1 year	3 years	5 years
PH-COPD, TAPSE/PASP ≥0.26 mm·mmHg^{-1}	51	38	32	23
PH-COPD, TAPSE/PASP <0.26 mm·mmHg^{-1}	27	18	14	8
PH-ILD, TAPSE/PASP ≥0.26 mm·mmHg^{-1}	50	36	19	12
PH-ILD, TAPSE/PASP <0.26 mm·mmHg^{-1}	44	27	8	3

FIGURE 1 The tricuspid annular plane systolic excursion (TAPSE)/ systolic pulmonary artery pressure (PASP) ratio as an indicator of haemodynamic severity and prognosis in pulmonary hypertension secondary to chronic lung disease (PH-LD). a) TAPSE/PASP ratio and pulmonary vascular resistance (PVR) in patients with idiopathic pulmonary arterial hypertension (iPAH) and patients with pulmonary hypertension due to chronic obstructive pulmonary disease (PH-COPD) or interstitial lung disease (PH-ILD) stratified by haemodynamic severity (bar charts show median and interquartile range; ****p<0.0001; ***p<0.001; between-group differences were analysed with the Kruskal-Wallis test). b) Receiver operating characteristic analyses of the TAPSE/PASP ratio (area under the curve (AUC): 0.825; p<0.001), TAPSE (AUC: 0.736; p<0.001) and PASP (AUC: 0.739; p<0.001) for discriminating between severe and non-severe PH-LD (diagonal segments were produced by ties). c) Receiver operating characteristic analyses of the TAPSE/PASP ratio for discriminating between severe and non-severe PH-COPD (AUC: 0.847; p<0.001) and PH-ILD (AUC: 0.815; p<0.001) (diagonal segments were produced by ties). d) Kaplan–Meier survival curves in patients with PH-LD and subsets with PH-ILD and PH-COPD stratified by the TAPSE/PASP ratio.

Khodr Tello[1], Hossein A. Ghofrani[1,2,3], Charlotte Heinze[1], Karsten Krueger[4], Robert Naeije[5], Christina Raubach[1], Werner Seeger[1], Natascha Sommer[1], Henning Gall[1,6] and Manuel J. Richter[1,6]
[1]Dept of Internal Medicine, Justus-Liebig-University Giessen, Universities of Giessen and Marburg Lung Center (UGMLC), Member of the German Center for Lung Research (DZL), Giessen, Germany. [2]Dept of Pneumology, Kerckhoff Heart, Rheuma and Thoracic Center, Bad Nauheim, Germany. [3]Dept of Medicine, Imperial College London, London, UK. [4]Institute of Sports Science, Department of Exercise and Health, Leibniz University Hannover, Hannover, Germany. [5]Erasme University Hospital, Brussels, Belgium. [6]These authors have contributed equally to this work.

Correspondence: Manuel J. Richter, Dept of Internal Medicine, Justus-Liebig-University Giessen, Universities of Giessen and Marburg Lung Center (UGMLC), Member of the German Center for Lung Research (DZL), Klinikstrasse 33, 35392 Giessen, Germany. E-mail manuel.richter@innere.med.uni-giessen.de

Received: 21 Dec 2018 | Accepted after revision: 24 April 2019

Acknowledgements: Editorial assistance was provided by Claire Mulligan (Beacon Medical Communications Ltd, Brighton, UK), funded by the University of Giessen.

Conflict of interest: H.A. Ghofrani reports that this work was funded by the Excellence Cluster Cardio-Pulmonary System (ECCPS) and the Collaborative Research Center (SFB) 1213, Pulmonary Hypertension and Cor Pulmonale, grant number SFB1213/1, project B08 (German Research Foundation, Bonn, Germany), and received editorial support, funded by the University of Giessen; personal fees for consultancy and advisory board work from Bayer and Pfizer, personal fees for consultancy, advisory board work and lectures from Actelion and GSK, personal fees for consultancy from Merck, grants and personal fees for consultancy from Novartis, grants and personal fees for lectures from Bayer HealthCare and Encysive/Pfizer, grants from Aires, German Research Foundation, Excellence Cluster Cardiopulmonary Research and German Ministry for Education and Research, personal fees for advisory board work from Takeda, outside the submitted work. C. Heinze has nothing to disclose. K. Krüger has nothing to disclose. R. Naeije reports grants and personal fees for consultancy and advisory board work from AOPOrphan Pharmaceuticals, Actelion, Bayer, Reata, Lung Biotechnology Corporation and United Therapeutics, outside the submitted work. C. Raubach has nothing to disclose. W. Seeger reports that this work was funded by the Excellence Cluster Cardio-Pulmonary System (ECCPS) and the Collaborative Research Center (SFB) 1213, Pulmonary Hypertension and Cor Pulmonale, grant number SFB1213/1, project B08 (German Research Foundation, Bonn, Germany), and received editorial support, funded by the University of Giessen; personal fees for lectures and consultancy from Pfizer and Bayer Pharma AG, outside the submitted work. N. Sommer reports personal fees from Actelion, outside the submitted work. H. Gall reports that this work was funded by the Excellence Cluster Cardio-Pulmonary System (ECCPS) and the Collaborative Research Center (SFB) 1213, Pulmonary Hypertension and Cor Pulmonale, grant number SFB1213/1, project B08 (German Research Foundation, Bonn, Germany), and received editorial support, funded by the University of Giessen; personal fees from Actelion, AstraZeneca, Bayer, BMS, GSK, Janssen-Cilag, Lilly, MSD, Novartis, OMT, Pfizer andUnited Therapeutics, outside the submitted work. M.J. Richter reports that this work was funded by the Excellence Cluster Cardio-Pulmonary System (ECCPS) and the Collaborative Research Center (SFB) 1213, Pulmonary Hypertension and Cor Pulmonale, grant number SFB1213/1, project B08 (German Research Foundation, Bonn, Germany), and received editorial support, funded by the University of Giessen; grants from United Therapeutics, grants and personal fees for lectures and consultancy from Bayer, personal fees for lectures from Actelion, Mundipharma, Roche and OMT, outside the submitted work. K. Tello reports that this work was funded by the Excellence Cluster Cardio-Pulmonary System (ECCPS) and the Collaborative Research Center (SFB) 1213, Pulmonary Hypertension and Cor Pulmonale, grant number SFB1213/1, project B08 (German Research Foundation, Bonn, Germany), and received editorial support, funded by the University of Giessen; personal fees for lectures from Actelion and Bayer, outside the submitted work.

Support statement: Funded by the Deutsche Forschungsgemeinschaft (DFG, German Research Foundation), Projektnummer 268555672, SFB 1213, Project B08. Funding information for this article has been deposited with the Crossref Funder Registry.

References

1 Vonk Noordegraaf A, Chin KM, Haddad F, *et al.* Pathophysiology of the right ventricle and of the pulmonary circulation in pulmonary hypertension: an update. *Eur Respir J* 2019; 53: 1801900.
2 Vonk Noordegraaf A, Westerhof BE, Westerhof N. The relationship between the right ventricle and its load in pulmonary hypertension. *J Am Coll Cardiol* 2017; 69: 236–243.
3 Tello K, Dalmer A, Axmann J, *et al.* Reserve of right ventricular-arterial coupling in the setting of chronic overload. *Circ Heart Fail* 2019; 12: e005512.
4 Guazzi M, Bandera F, Pelissero G, *et al.* Tricuspid annular plane systolic excursion and pulmonary arterial systolic pressure relationship in heart failure: an index of right ventricular contractile function and prognosis. *Am J Physiol Heart Circ Physiol* 2013; 305: H1373–H1381.
5 Guazzi M, Dixon D, Labate V, *et al.* RV contractile function and its coupling to pulmonary circulation in heart failure with preserved ejection fraction: stratification of clinical phenotypes and outcomes. *JACC Cardiovasc Imaging* 2017; 10: 10 Pt B, 1211–1221.
6 Tello K, Axmann J, Ghofrani HA, *et al.* Relevance of the TAPSE/PASP ratio in pulmonary arterial hypertension. *Int J Cardiol* 2018; 266: 229–235.
7 Nathan SD, Barbera JA, Gaine SP, *et al.* Pulmonary hypertension in chronic lung disease and hypoxia. *Eur Respir J* 2019; 53: 1801914.
8 Prins KW, Rose L, Archer SL, *et al.* Disproportionate right ventricular dysfunction and poor survival in group 3 pulmonary hypertension. *Am J Respir Crit Care Med* 2018; 197: 1496–1499.
9 Gall H, Felix JF, Schneck FK, *et al.* The Giessen Pulmonary Hypertension Registry: survival in pulmonary hypertension subgroups. *J Heart Lung Transplant* 2017; 36: 957–967.

10 Seeger W, Adir Y, Barbera JA, *et al.* Pulmonary hypertension in chronic lung diseases. *J Am Coll Cardiol* 2013; 62: Suppl. 25, D109–D116.
11 Kovacs G, Agusti A, Barbera JA, *et al.* Pulmonary vascular involvement in chronic obstructive pulmonary disease. is there a pulmonary vascular phenotype? *Am J Respir Crit Care Med* 2018; 198: 1000–1011.
12 Chaouat A, Bugnet AS, Kadaoui N, *et al.* Severe pulmonary hypertension and chronic obstructive pulmonary disease. *Am J Respir Crit Care Med* 2005; 172: 189–194.
13 Boerrigter BG, Bogaard HJ, Trip P, *et al.* Ventilatory and cardiocirculatory exercise profiles in COPD: the role of pulmonary hypertension. *Chest* 2012; 142: 1166–1174.
14 Sanz J, Sanchez-Quintana D, Bossone E, *et al.* Anatomy, function, and dysfunction of the right ventricle: JACC State-of-the-Art Review. *J Am Coll Cardiol* 2019; 73: 1463–1482.
15 Guazzi M, Naeije R. Pulmonary hypertension in heart failure: pathophysiology, pathobiology, and emerging clinical perspectives. *J Am Coll Cardiol* 2017; 69: 1718–1734.

Anlage D

Evaluation and Prognostic Relevance of Right Ventricular-Arterial Coupling in Pulmonary Hypertension.

Richter MJ, Peters D, Ghofrani HA, Naeije R, Roller F, Sommer N, Gall H, Grimminger F, Seeger W, **Tello K**. Am J Respir Crit Care Med. 2020 Jan 1;201(1):116-119

response to parenteral antibiotic administration: lack of association in cystic fibrosis. *Chest* 2003;123:1495–1502.
4. Mogayzel PJ Jr, Naureckas ET, Robinson KA, Brady C, Guill M, Lahiri T, *et al*.; Cystic Fibrosis Foundation Pulmonary Clinical Practice Guidelines Committee. Cystic Fibrosis Foundation pulmonary guideline: pharmacologic approaches to prevention and eradication of initial *Pseudomonas aeruginosa* infection. *Ann Am Thorac Soc* 2014; 11:1640–1650.
5. Etherington C, Hall M, Conway S, Peckham D, Denton M. Clinical impact of reducing routine susceptibility testing in chronic *Pseudomonas aeruginosa* infections in cystic fibrosis. *J Antimicrob Chemother* 2008;61:425–427.
6. Somayaji R, Parkins MD, Shah A, Martiniano SL, Tunney MM, Kahle JS, *et al*.; Antimicrobial Resistance in Cystic Fibrosis InternationalWorking Group. Antimicrobial susceptibility testing (AST) and associated clinical outcomes in individuals with cystic fibrosis: a systematic review. *J Cyst Fibros* 2019;18:236–243.
7. Sanders DB, Bittner RC, Rosenfeld M, Hoffman LR, Redding GJ, Goss CH. Failure to recover to baseline pulmonary function after cystic fibrosis pulmonary exacerbation. *Am J Respir Crit Care Med* 2010; 182:627–632.
8. VanDevanter DR, Flume PA, Morris N, Konstan MW. Probability of IV antibiotic retreatment within thirty days is associated with duration and location of IV antibiotic treatment for pulmonary exacerbation in cystic fibrosis. *J Cyst Fibros* 2016;15:783–790.
9. Zemanick E, Burgel PR, Taccetti G, Holmes A, Ratjen F, Byrnes CA, *et al*.; On behalf of the Antimicrobial Resistance International Working Group in Cystic Fibrosis. Antimicrobial resistance in cystic fibrosis: a Delphi approach to defining best practices. *J Cyst Fibros* 2019;0: S1569–1993.

Evaluation and Prognostic Relevance of Right Ventricular–Arterial Coupling in Pulmonary Hypertension

To the Editor:

Right ventricular (RV) function is the main determinant of symptomatology and prognosis in pulmonary hypertension (PH) (1). The gold standard method for evaluation of RV function in PH relies on the measurement of the end-systolic/arterial elastance ratio (Ees/Ea) calculated from a family of pressure–volume relationships across multiple cardiac cycles at decreasing preload by either balloon inflation in the inferior vena cava or a Valsalva maneuver (2). The prognostic relevance of RV–arterial coupling measured using this multibeat method remains undefined. A simplified single-beat method was developed in which RV pressure measurements were combined with integration of pulmonary arterial flow to calculate relative changes in volume (3). The single-beat method has been implemented in clinical studies (4) but has not been validated against the multibeat method in humans with PH. Even simpler surrogates have been developed, based on the exclusive analysis of a single RV pressure–time curve (pressure method) (5), cardiac magnetic resonance imaging of end-diastolic volume and end-systolic volume (ESV; volume method) (6), or echocardiography-derived parameters (7).

We investigated RV–arterial coupling, using the multibeat method to determine Ees/Ea (ClinicalTrials.gov: NCT03403868) in 38 patients with severe PH (19 female and 19 male; age [mean ± SD]: 55 ± 13 years; 36 with pulmonary arterial hypertension [PAH] and two with chronic thromboembolic PH; mean pulmonary artery pressure [mPAP]: 47 ± 15 mm Hg; median pulmonary vascular resistance: 7 [interquartile range, 5–11] Wood Units; cardiac index: 2.6 ± 0.7 l/min/m^2) and assessed its prognostic relevance by recording clinical events during follow-up.

The single-beat method to assess Ees/Ea was originally validated for the right ventricle by Brimioulle and coworkers in anesthetized dogs (3). It sometimes proved difficult to reproduce owing to unstable calculations of the theoretical isovolumetric maximum pressure (Pmax) from imprecise definitions of isovolumetric portions of the RV pressure curve. Thus, uncertainties in Pmax calculations and imperfect linearity of end-systolic pressure (ESP)–volume relationships could be reasons for disagreement between single-beat and multiple-beat methods. However, such a disagreement did not occur in the present study: single-beat Ees/Ea accurately reflected multibeat Ees/Ea. Our data suggest that the results of studies in severe PH that reported on either multibeat (2) or single-beat (4) methods to determine Ees/Ea can be considered comparable (Figure 1).

To ensure reliable measurement of Pmax, all measurements were performed independently by two experienced examiners who were blinded to the clinical data. A third observer in the University Hospital in Bonn, Germany, analyzed 19 of the patients with an intraclass correlation coefficient of 0.95, a coefficient of variance of 12%, and a 95% confidence interval of 0.89–0.98 ($P < 0.001$). To reduce uncertainty in Pmax calculations, a method based on the second derivative of the pressure waveform has recently shown promise, reducing interobserver variability compared with the established first-derivative method and yielding nonsignificant interobserver differences (8).

Although the correlation between single-beat and multibeat Ees/Ea was highly significant and the Bland–Altman analysis showed no bias in our study, the limits of agreement ranged from −0.35 to +0.37, suggesting a range of error relative to Ees/Ea thresholds defining RV–arterial uncoupling (Ees/Ea < 0.8) (4) and predicting poor prognosis (Ees/Ea < 0.7, as shown in the present study).

It was assumed that mPAP would be a reasonable estimate of ESP (5). However, as mPAP increases from normal values to the level seen in severe PH, the RV pressure–volume loop changes shape and ESP becomes closer to systolic RV pressure (sRVP), so that mPAP underestimates ESP in proportion to PH severity. We previously quantified this underestimation and proposed the

Supported by the German Research Foundation, Bonn, Germany (Collaborative Research Center 1213 "Pulmonary Hypertension and Cor Pulmonale" and Excellence Cluster "Cardio-Pulmonary System").

Author Contributions: M.J.R., H.A.G., N.S., H.G., F.G., W.S., and K.T. provided study design; M.J.R., D.P., H.A.G., F.R., H.G., W.S., and K.T. provided patient recruitment; M.J.R., D.P., H.A.G., R.N., F.R., N.S., H.G., F.G., W.S., and K.T. provided data collection and analysis; M.J.R., H.G., and K.T. provided statistical analyses; M.J.R., H.A.G., R.N., N.S., H.G., W.S., and K.T. provided drafting of the manuscript; M.J.R., D.P., H.A.G., R.N., F.R., N.S., H.G., F.G., W.S., and K.T. critically revised the manuscript for important intellectual content; and K.T. was the principal investigator, had access to all the data in the study, and takes full responsibility for the integrity and accuracy of the data analysis.

Originally Published in Press as DOI: 10.1164/rccm.201906-1195LE on September 20, 2019

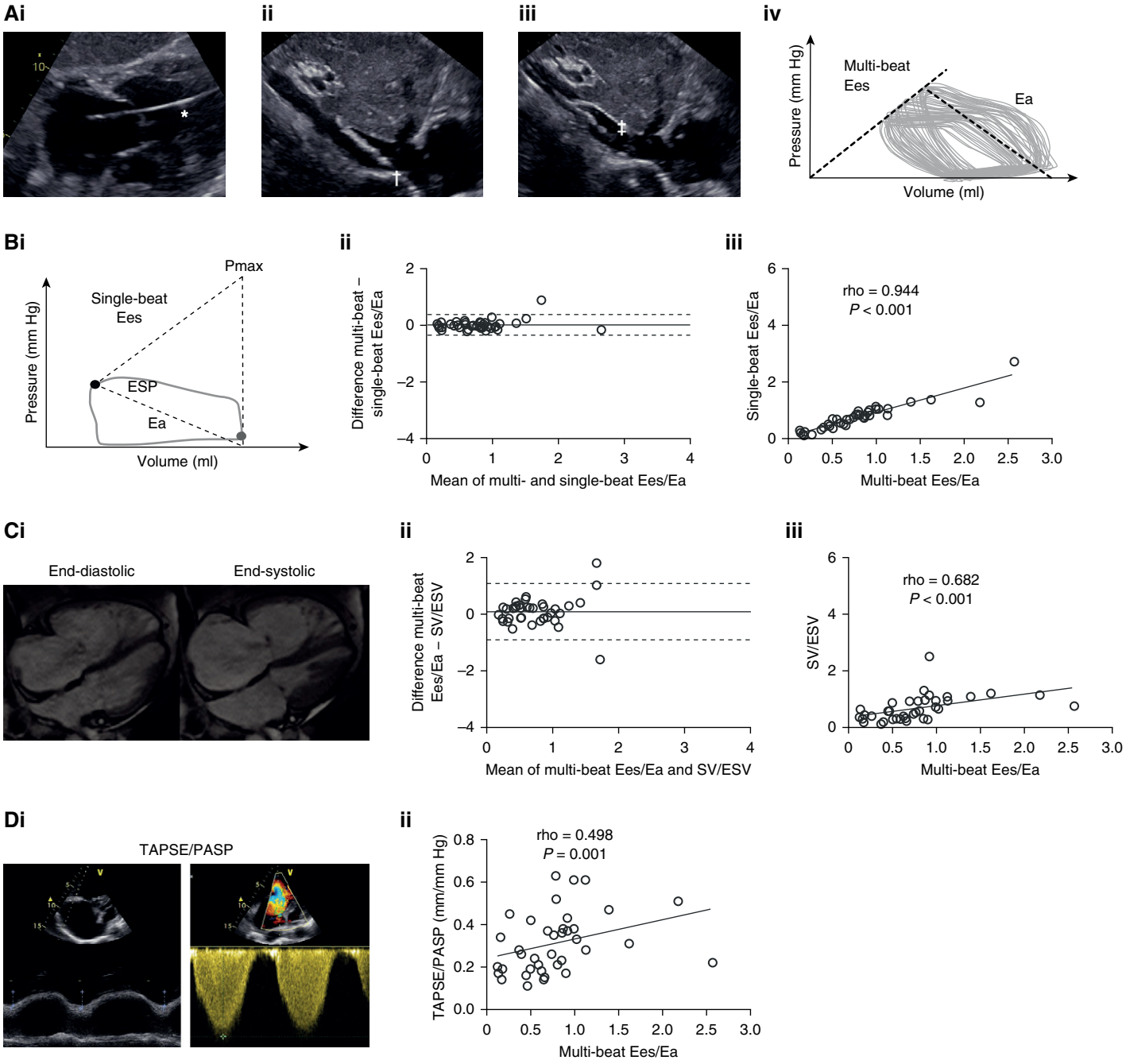

Figure 1. Comparison of methods for assessment of right ventricular (RV)–arterial coupling in patients with pulmonary hypertension. (*Ai*) In the gold standard multibeat method, RV pressure and volume were measured by a conductance catheter (indicated by an asterisk; CD Leycom, the Netherlands) during decreasing venous return resulting from balloon occlusion of the inferior vena cava ([*Aii*] deflated and [*Aiii*] inflated balloon, indicated by the dagger and double dagger, respectively; Amplatzer 24 mm Sizing Balloon II, St. Jude Medical [now Abbott], Belgium). (*Aiv*) End-systolic elastance (Ees) was acquired from a tangent fitted to the end-systolic portions of the pressure–volume loops; arterial elastance (Ea) was calculated as end-systolic pressure (ESP)/stroke volume (SV). (*Bi*) The single-beat method (with calculation of Ees from the theoretical isovolumetric maximum pressure [Pmax] and ESP) (3) was compared with the multibeat method by (*Bii*) Bland–Altman plot (bias: 0.009 [limits of agreement (LOA), −0.353 to 0.371]) and (*Biii*) scatter plot. (*Ci*) The volume method based on cardiac magnetic resonance imaging data (Ees/Ea = SV/end-systolic volume [ESV]) (6) was compared with the multibeat method by (*Cii*) Bland–Altman plot (bias: 0.085 [LOA, −0.905 to 1.075]) and (*Ciii*) scatter plot. (*Di*) The echocardiographic method (Ees/Ea = tricuspid annular plane systolic excursion [TAPSE]/systolic pulmonary arterial pressure [PASP]) (7) was compared with the multibeat method by (*Dii*) scatter plot. Three pressure methods were also evaluated (not shown), with ESP estimated using the following assumptions: ESP = mean pulmonary arterial pressure (mPAP) (5) (bias: −0.858 [LOA, −2.190 to 0.475]; rho = 0.676 [$P < 0.001$]); ESP = 1.65 × mPAP − 7.79 (9) (bias: −0.023 [LOA, −0.874 to 0.828]; rho = 0.730 [$P < 0.001$]); and ESP = systolic RV pressure (10) (bias: 0.207 [LOA, −0.232 to 0.579]; rho = 0.781 [$P < 0.001$]). The solid line of the Bland–Altman plot represents the bias, and the dashed lines represent the LOA. Correlations were assessed using the Spearman rho coefficient.

correction equation ESP = 1.65 × mPAP − 7.79 (9). The present study shows that calculation of Ees/Ea exclusively from RV pressure waveform analysis with a correction equation to estimate ESP from mPAP is accurate (no bias in Bland–Altman analysis) but with a deterioration of precision (increased limits of agreement) compared with single-beat assessment of Ees/Ea. Although ESP values come close to sRVP values in severe PH, replacing ESP with sRVP in the pressure-based calculation (10) results in a somewhat biased estimate of Ees/Ea.

The stroke volume (SV)/ESV ratio has shown prognostic relevance in patients with PAH, with a cut-off value of 0.5 (6). A decrease of the SV/ESV ratio below 0.5 is necessarily associated with an increase in RV volume to maintain SV. The implicit assumptions of linearity and zero-crossing of ESP–volume relationships for the estimation of Ees/Ea by SV/ESV are not met, which explains the moderately increased bias and wide limits of agreement compared with multibeat Ees/Ea in the present study.

The echocardiographic tricuspid annular plane systolic excursion/systolic pulmonary arterial pressure ratio has been proposed as a straightforward and prognostically relevant method for noninvasive evaluation of RV–arterial coupling (7). We show that tricuspid annular plane systolic excursion/systolic pulmonary arterial pressure is significantly correlated to multibeat Ees/Ea in PH, supporting its role as a bedside-ready simplified surrogate of RV–arterial coupling.

Although the prognostic importance of RV function in severe PH is well established (1), this has never been directly assessed using Ees/Ea measurements of RV–arterial coupling. In the present study, multibeat Ees/Ea was an independent predictor of outcome, with a cutoff of 0.7 to discriminate clinical worsening (defined as any of the following: reduction in exercise capacity [−15% compared with the baseline 6-minute-walk test], worsening in World Health Organization functional class, or clinical deterioration requiring hospital admission [need for new PAH therapies, lung transplantation, or death]; Figure 2). This is consistent with our previous finding that RV dilatation with a prognostically relevant decrease of ejection fraction below 35% occurs when the single-beat Ees/Ea ratio has decreased from normal values of 1.5–2.0 to below 0.8 (4).

The present study is limited by its small sample of only 38 patients. However, PAH is a rare disease, and the investigated methods of evaluation are invasive.

In conclusion, the present results validate the "classical" single-beat method and exclusive RV pressure waveform analysis for the measurement of Ees/Ea. Moreover, our study offers insight regarding the prognostic relevance of multi-beat Ees/Ea. ■

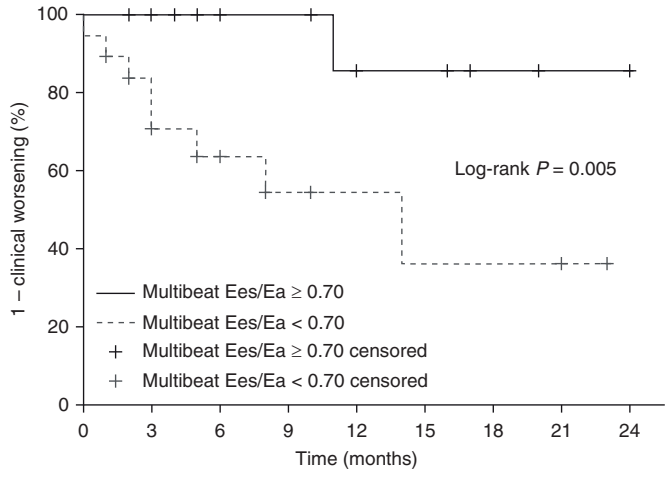

Number at risk			
	3 months	6 months	12 months
Multibeat Ees/Ea ≥ 0.70	14	9	5
Multibeat Ees/Ea < 0.70	10	7	3

Figure 2. Kaplan–Meier analysis of time to clinical worsening in patients with pulmonary hypertension who were dichotomized at a multibeat end-systolic/arterial elastance (Ees/Ea) ratio of 0.70. The cutoff was derived from receiver operating characteristic analyses and the Youden Index (area under the receiver operating characteristic curve, 0.736; $P = 0.035$; sensitivity, 62.1%; specificity, 89.9%).

Author disclosures are available with the text of this letter at www.atsjournals.org.

Acknowledgment: Editorial assistance was provided by Claire Mulligan, Ph.D. (Beacon Medical Communications Ltd., Brighton, UK), funded by the University of Giessen. Data from a subset of the patient population were analyzed in the Department of Pediatric Cardiology in the University Hospital in Bonn (Germany) with the support of Dr. Ulrike Herberg.

Manuel J. Richter, M.D.
Dana Peters
Justus-Liebig-University Giessen
Giessen, Germany

Hossein A. Ghofrani, M.D.
Justus-Liebig-University Giessen
Giessen, Germany
Rheuma and Thoracic Center
Bad Nauheim, Germany
and
Imperial College London
London, United Kingdom

Robert Naeije, Ph.D.
Erasme University Hospital
Brussels, Belgium

Fritz Roller, M.D.
Natascha Sommer, M.D., Ph.D.
Henning Gall, M.D., Ph.D.
Friedrich Grimminger, M.D.
Werner Seeger, M.D.
Khodr Tello, M.D.*
Justus-Liebig-University Giessen
Giessen, Germany

*Corresponding author (e-mail: khodr.tello@innere.med.uni-giessen.de).

References

1. Lahm T, Douglas IS, Archer SL, Bogaard HJ, Chesler NC, Haddad F, *et al*.; American Thoracic Society Assembly on Pulmonary Circulation.

Assessment of right ventricular function in the Research setting: knowledge gaps and pathways forward. An official American Thoracic Society Research Statement. *Am J Respir Crit Care Med* 2018;198:e15–e43.
2. Tedford RJ, Mudd JO, Girgis RE, Mathai SC, Zaiman AL, Housten-Harris T, *et al*. Right ventricular dysfunction in systemic sclerosis-associated pulmonary arterial hypertension. *Circ Heart Fail* 2013;6: 953–963.
3. Brimioulle S, Wauthy P, Ewalenko P, Rondelet B, Vermeulen F, Kerbaul F, *et al*. Single-beat estimation of right ventricular end-systolic pressure-volume relationship. *Am J Physiol Heart Circ Physiol* 2003; 284:H1625–H1630.
4. Tello K, Dalmer A, Axmann J, Vanderpool R, Ghofrani HA, Naeije R, *et al*. Reserve of right ventricular-arterial coupling in the setting of chronic overload. *Circ Heart Fail* 2019;12:e005512.
5. Trip P, Kind T, van de Veerdonk MC, Marcus JT, de Man FS, Westerhof N, *et al*. Accurate assessment of load-independent right ventricular systolic function in patients with pulmonary hypertension. *J Heart Lung Transplant* 2013;32:50–55.
6. Brewis MJ, Bellofiore A, Vanderpool RR, Chesler NC, Johnson MK, Naeije R, *et al*. Imaging right ventricular function to predict outcome in pulmonary arterial hypertension. *Int J Cardiol* 2016;218:206–211.
7. Tello K, Axmann J, Ghofrani HA, Naeije R, Narcin N, Rieth A, *et al*. Relevance of the TAPSE/PASP ratio in pulmonary arterial hypertension. *Int J Cardiol* 2018;266:229–235.
8. Bellofiore A, Vanderpool R, Brewis MJ, Peacock AJ, Chesler NC. A novel single-beat approach to assess right ventricular systolic function. *J Appl Physiol (1985)* 2018;124:283–290.
9. Tello K, Richter MJ, Axmann J, Buhmann M, Seeger W, Naeije R, *et al*. More on single-beat estimation of right ventriculoarterial coupling in pulmonary arterial hypertension. *Am J Respir Crit Care Med* 2018;198: 816–818.
10. Vanderpool RR, Pinsky MR, Naeije R, Deible C, Kosaraju V, Bunner C, *et al*. RV-pulmonary arterial coupling predicts outcome in patients referred for pulmonary hypertension. *Heart* 2015;101:37–43.

Video Teleheath and Pulmonary Rehabilitation: Need for a Better Understanding

To the Editor:

We read with great interest the recent article by Bhatt and colleagues (1). As mentioned by the authors, there is clearly a pressing need for a solution to the high rate of 30-day readmissions after hospitalization for an acute exacerbation of chronic obstructive pulmonary disease (AECOPD). Despite the effectiveness demonstrated by early pulmonary rehabilitation (PR) after AECOPD, there have been poor uptake, adherence, and completion rates for various reasons (2–4).

In this context, telehealth medicine has been proposed as an interesting solution, with the potential to broaden and facilitate access to PR, thereby possibly resulting in lower overall rates of hospital readmission after AECOPD. To address this question, Bhatt and colleagues compared a prospective group of patients participating in a video telehealth PR program (administered via smartphone) with a retrospective contemporaneous cohort who received comprehensive bundled care after hospital discharge. The primary outcome was the 30-day all-cause readmission rate. The results are impressive, with a 30-day absolute reduction in all-cause and AECOPD readmissions of 11.9% and 8.1%, respectively. These results are very appealing, but they should be interpreted with caution. First, the authors do not include patient acceptance or refusal data or overall patient participation rates. Another limitation of this study is related to the design, as this was not a randomized clinical trial. Despite efforts made to match the two groups, the significantly higher proportion of patients on domiciliary oxygen in the intervention group is concerning. This difference may have contributed to the observed improvement in the treatment group if, for example, more attention and closer follow-up was provided to these patients.

Furthermore, the methodological description of the video telehealth PR intervention was insufficient. Information on supervising roles and personnel during the telehealth sessions, or in personalizing exercise prescriptions during individual sessions, is critical to understanding this intervention. From a knowledge translation perspective, replication and wider dissemination of this intervention will require a more detailed description of its content and how it was administered.

Another aspect to question is the speed at which PR could realistically impact the 30-day hospital admission rate. Patients who received the intervention only started the telehealth PR program at the follow-up visit, which was 10 ± 2 days after discharge. Consequently, the effect of the intervention, evaluated at 30 days after discharge, would be measured after a maximal period of 22 days of active intervention.

Beyond the physical training component, support by healthcare professionals and behavioral change could have also had a significant impact on patient outcomes. To better understand the intervention, it would be important to know about the content and the delivery of the educational sessions and if patients had integrated specific behaviors or coping strategies into their daily life. The production of an effective new behavioral change intervention involves a progressive and meticulous process, such as that suggested by the ORBIT (Obesity-Related Behavioral Intervention Trials) model (5). This model was created after the negative results of a large-scale trial evaluating behavioral intervention, the Look AHEAD (Action for Health in Diabetes) trial (6). Just like in pharmaceutical development, behavioral change intervention development should evolve through a phase process that includes, among others, design, defining and refining the intervention, proof-of-concept, and pilot study. This process encourages a rigorous translation from idea to practice and avoids large expenses in inefficient interventions.

The results reported by Bhatt and colleagues (1) are surely interesting, and video telehealth could well be an acceptable, efficient, and effective way of delivering PR in the future. However, until we are better able to define the specific components and delivery of this intervention and its effect on patient coping strategies, the role of PR via video telehealth remains to be answered. ■

Originally Published in Press as DOI: 10.1164/rccm.201907-1394LE on August 6, 2019

Author disclosures are available with the text of this letter at www.atsjournals.org.

Sébastien Gagnon, M.D.*
Bryan Ross, M.D., M.Sc.
McGill University Health Centre
Montreal, Quebec, Canada

Anlage E

Cardiac Magnetic Resonance Imaging-Based Right Ventricular Strain Analysis for Assessment of Coupling and Diastolic Function in Pulmonary Hypertension.

Tello K, Dalmer A, Vanderpool R, Ghofrani HA, Naeije R, Roller F, Seeger W, Wilhelm J, Gall H, Richter MJ. JACC Cardiovasc Imaging. 2019 Nov;12(11 Pt 1):2155-2164

JACC: CARDIOVASCULAR IMAGING VOL. ■, NO. ■, 2019

PUBLISHED BY ELSEVIER

ORIGINAL RESEARCH

Cardiac Magnetic Resonance Imaging-Based Right Ventricular Strain Analysis for Assessment of Coupling and Diastolic Function in Pulmonary Hypertension

Khodr Tello, MD,[a] Antonia Dalmer,[a] Rebecca Vanderpool, PhD,[b] Hossein A. Ghofrani, MD,[a,c,d] Robert Naeije, MD, PhD,[e] Fritz Roller, MD,[f] Werner Seeger, MD,[a] Jochen Wilhelm, PhD,[a] Henning Gall, MD, PhD,[a] Manuel J. Richter, MD[a]

ABSTRACT

OBJECTIVES This study sought to compare cardiac magnetic resonance (CMR) imaging-derived right ventricular (RV) strain and invasively measured pressure-volume loop-derived RV contractility, stiffness, and afterload and RV-arterial coupling in pulmonary hypertension (PH).

BACKGROUND In chronic RV pressure overload, RV-arterial uncoupling is considered the driving cause of RV maladaptation and eventual RV failure. The pathophysiological and clinical value of CMR-derived RV strain relative to that of invasive pressure-volume loop-derived measurements in PH remains incompletely understood.

METHODS In 38 patients with PH, global RV CMR strain was measured within 24 h of diagnostic right heart catheterization and conductance (pressure-volume) catheterization. Associations were evaluated by correlation, multivariate logistic binary regression, and receiver operating characteristic analyses.

RESULTS Long-axis RV longitudinal and radial strain and short-axis RV radial and circumferential strain (mean ± SD or median [interquartile range]) were −18.0 ± 7.0%, 28.9% [IQR: 17.4% to 46.6%]; 15.6 ± 6.2%; and −9.8 ± 3.5%, respectively. RV-arterial coupling (end-systolic [Eds]/arterial elastance [Ea]) was 0.76 (IQR: 0.47 to 1.07). Peak RV strain correlated with Ees/Ea, afterload (Ea), RV diastolic dysfunction (Tau), and stiffness (end-diastolic elastance [Eed]) but not with contractility (Ees). In multivariate analysis, long-axis RV radial strain was associated with RV-arterial uncoupling (Ees/Ea: <0.805; odds ratio [OR]: 5.50; 95% confidence interval [CI]: 1.50 to 20.18), whereas long-axis RV longitudinal strain was associated with increased RV diastolic stiffness (Eed: ≥0.124 mm Hg/ml; OR: 1.23; 95% CI: 1.10 to 1.51). The long-axis RV longitudinal strain-to-RV end-diastolic volume/body surface area ratio strongly predicted RV diastolic stiffness (area under receiver operating characteristic curve: 0.908).

CONCLUSIONS In chronic RV overload, CMR-determined RV strain is associated with RV-arterial uncoupling and RV end-diastolic stiffness and represents a promising noninvasive alternative to current invasive methods for assessment of RV-arterial coupling and end-diastolic stiffness in patients with PH. (Right Ventricular Haemodynamic Evaluation and Response to Treatment [Rightheart I]; NCT03403868) (J Am Coll Cardiol Img 2019;■:■-■)
© 2019 by the American College of Cardiology Foundation.

From the [a]Department of Internal Medicine, Justus-Liebig-University Giessen, Universities of Giessen and Marburg Lung Center, Giessen, Germany; [b]Division of Translational and Regenerative Medicine, University of Arizona, Tucson, Arizona; [c]Department of Pneumology, Kerckhoff Heart, Rheuma, and Thoracic Center, Bad Nauheim, Germany; [d]Department of Medicine, Imperial College London, London, United Kingdom; [e]Department of Cardiology, Erasme University Hospital, Brussels, Belgium; and the [f]Department of Radiology, Justus-Liebig-University Giessen, Universities of Giessen and Marburg Lung Center, Giessen, Germany. Supported by the Excellence Cluster Cardio-Pulmonary System and Collaborative Research Center 1213 Pulmonary Hypertension and Cor Pulmonale grant SFB1213/1, and German Research Foundation project B08. Dr. Tello has received speaker

ISSN 1936-878X/$36.00 https://doi.org/10.1016/j.jcmg.2018.12.032

ABBREVIATIONS AND ACRONYMS

AUC = area under the curve

BSA = body surface area

CMR = cardiac magnetic resonance

Ea = arterial elastance

EDV = end-diastolic volume

Eed = end-diastolic elastance

Ees = end-systolic elastance

GCS = global circumferential strain

GLS = global longitudinal strain

GRS = global radial strain

PH = pulmonary hypertension

RV = right ventricular

Pulmonary hypertension (PH) is associated with progressive afterload-induced right ventricular (RV) remodeling with an increase in contractility (to preserve RV-pulmonary arterial coupling), diastolic stiffening, and eventual evolution to RV dilation and clinical right heart failure (1). In this regard, evaluation of RV function plays an essential role in managing patients with PH. Cardiac magnetic resonance (CMR) imaging was recently described by the American Thoracic Society as the standard imaging technique for measurement of RV function (2). Surrogates of RV contractility derived from CMR imaging, such as RV ejection fraction and stroke volume divided by end-systolic volume, help to predict the onset of RV dilation and have shown prognostic relevance (3–5). In addition, CMR feature tracking is a novel method for quantification of myocardial strain that has been associated with RV ejection fraction in PH (6) and has shown a stronger association with mortality than left ventricular ejection fraction in dilated cardiomyopathy (7). Nevertheless, the physiological correlate of RV strain remains to be defined, as it is still unclear whether RV strain in the setting of chronic overload is associated with direct measurements of RV diastolic stiffness (Eed), end-systolic elastance (Ees), arterial elastance (Ea), and the Ees/Ea ratio, which represents RV-arterial coupling. Assessing Eed and Ees/Ea requires the generation of pressure-volume loops measured with high-fidelity catheters, which is invasive, technically demanding, and expensive (8). CMR imaging-based surrogates of these variables would thus be of major clinical benefit.

Therefore, this study sought to assess the association between CMR-derived RV strain and that of invasively measured pressure-volume loop-derived RV contractility, stiffness, and afterload parameters and to define the pathophysiological and clinical value of CMR strain analysis in PH.

METHODS

STUDY DESIGN AND PATIENTS. This study examined consecutive patients with pulmonary arterial hypertension and chronic thromboembolic PH (diagnosed according to current guidelines [9]) who were prospectively enrolled in the Rightheart I (Right Ventricular Haemodynamic Evaluation and Response to Treatment study; NCT03403868) study and the Giessen PH Registry (10) between January 2016 and April 2018. A multidisciplinary board including pulmonary physicians and radiologists assessed each diagnosis before the patient was enrolled. All patients underwent CMR imaging on day 1 and pressure-volume/Swan-Ganz catheterization on day 2. All patients received targeted pulmonary arterial hypertension therapies based on clinical grounds and best standard of care. All participating patients gave written informed consent. The investigation conforms to Declaration of Helsinki tenets and was approved by the ethics committee of the Faculty of Medicine at the University of Giessen (approval 108/15).

CMR IMAGING. Imaging was performed using a 1.5-T scanner (Avanto, Siemens Healthineers, Erlangen, Germany) with a gradient strength and slew rate (SQ-engine, 45 mT/m at 200 T/m per s) using a 6-element phased array cardiac coil and a dedicated CMR protocol including axial, coronal, and sagittal thoracic survey images, steady-state free precession cine sequences in 2-, 3-, and 4-chamber views, and transaxial and short-axis stacks from base to apex (black-blood T2 turbo spin echo). Gadoteridol (Bracco Imaging, Milan, Italy) was injected at a dose of 0.15 mmol/kg. Late gadolinium enhancement imaging was performed 12 min after contrast medium was injected. Steady-state free precession imaging parameters were: 8-mm slice thickness; 300 × 400-mm field of view; 256 × 154 matrix; 59.62-ms temporal resolution; and 1.15-ms echo time. Late gadolinium enhancement imaging parameters were: 8-mm slice thickness; 293 × 360-mm field of view; 256 × 156

fees from Actelion and Bayer. Dr. Ghofrani is a consultant for Bayer, Actelion, Pfizer, Merck, GlaxoSmithKline, and Novartis; and is a compensated advisory board member for Bayer, Pfizer, GlaxoSmithKline, Actelion, and Takeda; has received lecture fees from Bayer HealthCare, GlaxoSmithKline, Actelion, and Encysive/Pfizer; and has received grants from Bayer HealthCare, Aires, Encysive/Pfizer, Novartis, the German Research Foundation, Excellence Cluster Cardiopulmonary Research, and the German Ministry for Education and Research. Dr. Naeije has received research support from, is a consultant for, and sits on scientific advisory boards of AOPOrphan Pharmaceuticals, Actelion, Bayer, Reata, Lung Biotechnology Corporation, and United Therapeutics. Dr. Seeger is a compensated speaker and consultant for Pfizer, Bayer Pharma AG, United Therapeutics, and Liquidia. Dr. Gall has received fees from Actelion, AstraZeneca, Bayer, Bristol-Myers Squibb, GlaxoSmithKline, Janssen-Cilag, Lilly, MSD SHARP & DOHME, Novartis, Optimal Medical Therapies, Pfizer, and United Therapeutics. Dr. Richter has received support from United Therapeutics and Bayer; has received speaker fees from Actelion, Mundipharma, Roche, and OMT; and has received consultant fees from Bayer. All other authors have reported that they have no relationships relevant to the contents of this paper to disclose.

Manuscript received July 31, 2018; revised manuscript received November 16, 2018, accepted December 20, 2018.

matrix; 843.2-ms temporal resolution; and 3.19-ms echo time. The steady-state free precession images were obtained during breath holds, and RV systolic and diastolic volumes (absolute values) were calculated from short-axis and transaxial cine images. Measurements were taken on end-diastolic images (first phase after the R-wave trigger) and end-systolic images (based on cine images with the visually smallest cavity area). RV endocardial contours were obtained semi-automatically with exclusion of papillary muscles and trabeculae from the cavity and with subsequent manual correction by the agreement of 2 investigators. Ventricular volumes were estimated using the Simpson rule. Ejection fraction was calculated as: [(end-diastolic volume [EDV] – end-systolic volume)/EDV]. End-systolic and end-diastolic diameters were measured using basal short-axis images. Post-processing was performed by using the cardiovascular imaging version 42 (cvi^{42}) software including feature/tissue tracking (Circle Cardiovascular Imaging, Calgary, Alberta, Canada). RV strain was quantified on contiguous short-axis cine images (8 to 10 slices on average, depending on patient and cardiac size) and long-axis cine images (2-, 3-, and 4-chamber views), using the feature/tissue tracking software tool. Global RV longitudinal, radial, and circumferential peak strains were analyzed (**Figure 1A**) (for further details see Supplemental Appendix).

Pulmonary arterial stiffness, capacitance, and distensibility were measured using CMR data as described previously (11) (see Supplemental Appendix).

RIGHT HEART CATHETERIZATION. An 8-F introducer sheath was used to insert a Swan-Ganz catheter through the internal jugular vein. Pressures were assessed continuously. Cardiac index was recorded as the average of 3 to 5 measurements, using the direct or indirect Fick method as available. Pulmonary vascular resistance was calculated as: [(mean pulmonary arterial pressure – pulmonary arterial wedge pressure)/cardiac output] (9).

PRESSURE-VOLUME CATHETERIZATION. A 4-F pressure-volume catheter (model CA-Nr 41063, CD Leycom, Zoetermeer, the Netherlands) was inserted through the same 8-F introducer sheath as indicated above and positioned in the RV apex, guided by transthoracic echocardiography and analysis of online pressure-volume loops (12). Pressure-volume loops were displayed beat-to-beat in real time by connection to an intracardiac analyzer (Inca, CD Leycom). Ees was calculated using the RV single-beat method (13), and Ea was calculated as end-systolic pressure/stroke volume (13). RV-arterial coupling was defined as the Ees/Ea ratio (Supplemental Methods, Supplemental Figure 1).

Diastolic stiffness β was calculated by fitting a nonlinear exponential curve $P = \alpha(e\beta V - 1)$ through the diastolic portion of the pressure-volume loops, using a customized MATLAB (MathWorks, Natick, Massachusetts) program (4). Three points were used for the exponential fit: origin (0,0), beginning diastolic point, and end-diastolic point. Eed was obtained from the relationship [$dP/dV = \alpha\beta \times e\beta \times EDV$] at calculated end-diastolic volumes (EDV) (14,15). When the pressure-volume loops showed a clear overlap, a single beat was chosen for extrapolation to a sinusoidal curve and for analysis of Eed. Volume measurements were calibrated with CMR imaging data.

STATISTICAL ANALYSES. Adherence to a Gaussian distribution was determined using the Kolmogorov-Smirnov test and visual assessment of histograms. Associations between variables were measured with Spearman's rank correlation, and trend lines were least square fittings of straight-line models and second-order polynomial models.

To determine which strain parameters were most strongly related to Ees/Ea, Ea, and Eed, all RV strain parameters were included in a multivariate logistic binary regression analysis. Receiver operating characteristic curve analysis was used to identify the RV strain parameter with the highest sensitivity and specificity for discriminating RV uncoupling (based on the Ees/Ea ratio), increased afterload (based on Ea), and diastolic stiffness (based on Eed). Reference values for Ees/Ea, Ea, and Eed that would indicate RV uncoupling, increased afterload, and diastolic stiffness are not yet available; therefore, receiver operating characteristic curve analysis and the Youden index to identify cutoff values that would discriminate RV maladaptation (defined as RV ejection fraction <35% [3,5]) and stroke volume/end-systolic volume of <0.534) were used (16,17). The cutoff values identified were 0.805 for Ees/Ea, 0.066 for Ea, and 0.124 for Eed (Supplemental Figure 2); these cutoff values were used to indicate RV uncoupling, increased afterload, and diastolic stiffness, respectively.

To determine which RV strain parameter was most impaired during RV dilation, RV EDV normalized to body surface area (BSA) was split into tertiles, classifying patients in the lowest tertile as the reference (nondilated) group. RV strain in patients with dilation (RV EDV/BSA tertiles 2 and 3) was expressed as a percentage of the median strain in the reference

FIGURE 1 Associations Among RV Global Strain and CMR RV Maladaptation, Invasive Pulmonary Hemodynamics, and Pressure-Volume Loop Measurements

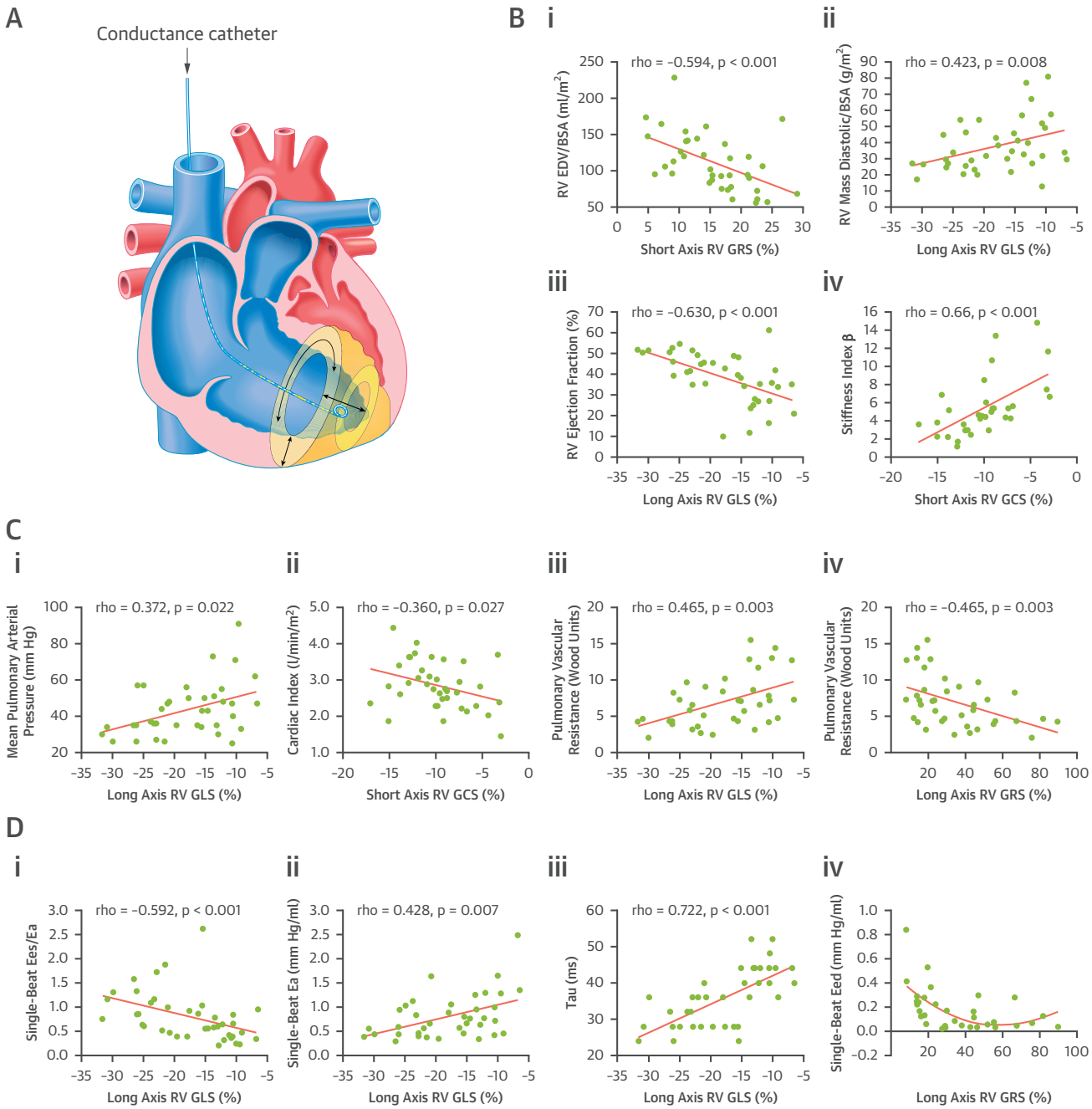

(A) RV longitudinal, radial, and circumferential peak strains were measured as shown. **(B[i], [B]ii, [B]iii)** RV maladaptation and **([B]iv)** pulmonary arterial stiffness were related to RV strain. **(C)** Key invasive pulmonary hemodynamic parameters and **(D)** pressure-volume loop parameters were associated with RV strain. BSA = body surface area; Ea = arterial elastance; EDV = end-diastolic volume; Eed = end-diastolic elastance; GCS = global circumferential strain; GLS = global longitudinal strain; GRS = global radial strain; RV = right ventricular.

group. Differences between multiple groups were analyzed with the independent samples Kruskal-Wallis test or 1-way analysis of variance as appropriate.

For all analyses, a p value of <0.05 was considered statistically significant. SPSS version 23.0 software (IBM, Armonk, New York) was used for statistical analyses.

RESULTS

PATIENTS. Characteristics of the 38 patients with PH, which included CMR and pressure-volume loop measurements, are presented in **Table 1**. Exemplary CMR images, strain curves, and pressure-volume loops are shown in Supplemental Figure 3. Idiopathic pulmonary arterial hypertension was diagnosed in most patients. The patients presented with severe PH and had high EDV (indicating RV dilation) and decreased RV ejection fraction and stroke volume/end-systolic volume ratio compared with values reported in healthy individuals (18).

ASSOCIATION BETWEEN CMR RV STRAIN AND RV MALADAPTATION. RV short-axis radial strain was correlated with RV dilation (RV EDV/BSA) (**Figure 1B**), and RV longitudinal, radial, and circumferential strain showed significant decreases in patients with severely dilated versus nondilated right ventricles (stratified by tertiles of RV EDV/BSA). Short-axis radial strain showed the most pronounced decrease, whereas only a trend was observed for long-axis radial strain (Supplemental Figure 4). Long-axis longitudinal strain was also correlated with hypertrophy (RV mass diastolic/BSA) and RV ejection fraction (**Figure 1B**). Short-axis circumferential strain (**Figure 1B**) and long-axis longitudinal strain (rho: 0.398; $p = 0.024$ [figure not shown]) were associated with pulmonary arterial stiffness. Moreover, long-axis longitudinal strain showed a significant correlation with distensibility (rho: −0.406; $p = 0.019$ [figure not shown]).

ASSOCIATION BETWEEN CMR RV STRAIN AND PULMONARY HEMODYNAMICS. Long-axis RV longitudinal strain was correlated with mean pulmonary arterial pressure and pulmonary vascular resistance (**Figure 1C**). Short-axis RV circumferential strain and long-axis RV radial strain were correlated with cardiac index and pulmonary vascular resistance, respectively (**Figure 1C**).

ASSOCIATION BETWEEN CMR RV STRAIN AND PRESSURE-VOLUME LOOP PARAMETERS. Ees/Ea (which showed a nonlinear relationship with RV ejection fraction) (Supplemental Figure 5) was related to long-axis RV radial strain (rho: 0.579; $p < 0.001$ [figure not shown]) and longitudinal strain (**Figure 1D**). Ea and Tau showed correlations with long-axis RV longitudinal strain (**Figure 1D**) and radial strain (Ea: rho: −0.426; $p = 0.008$; Tau rho: −0.721; $p < 0.001$ [figures not shown]). Eed showed a nonlinear

TABLE 1 Patient Characteristics, Pulmonary Hemodynamics, and Pressure-Volume Loop and CMR Measurements (N = 38)

Males/females	17/21
Age, yrs	55.5 (44.8-65.3)
PH subtype	
Idiopathic pulmonary arterial hypertension	25 (66)
Pulmonary arterial hypertension associated with	7 (18)
Human immunodeficiency virus infection	1
Portal hypertension	2
Connective tissue disease	3
Congenital heart disease	1
Chronic thromboembolic PH	6 (16)
Right heart catheterization	
Mean pulmonary arterial pressure, mm Hg	41.5 (34.0-50.3)
Right atrial pressure, mm Hg	7.0 (5.0-9.0)
Pulmonary vascular resistance, Wood units	6.6 (4.3-8.8)
Mean cardiac index, l/min per m^2	2.8 ± 0.7
Pulmonary arterial wedge pressure, mm Hg	8.5 ± 3.3
Treatment	
Phosphodiesterase type 5 inhibitor	17 (45)
Endothelin receptor antagonist	22 (58)
Soluble guanylate cyclase stimulator	16 (42)
Prostanoid	6 (16)
Combination therapy	
Dual therapy	12 (32)
Triple therapy	9 (24)
Pressure-volume loop measurements	
Ea, mm Hg/ml	0.70 (0.45-1.04)
Ees, mm Hg/ml	0.49 (0.35-0.74)
Ees/Ea ratio	0.76 (0.47-1.07)
End-systolic pressure, mm Hg	58.0 (42.8-78.3)
End-diastolic pressure, mm Hg	6.5 (3.0-11.0)
Tau, ms	36.0 (28.0-44.0)
Eed, mm Hg/ml*	0.124 (0.047-0.262)
CMR measurements	
RV EDV/BSA, ml/m^2	104.3 (83.1-140.9)
RV end-systolic volume/BSA, ml/m^2	61.4 (44.7-94.8)
RV mass diastolic/BSA, g/m^2	33.8 (27.1-47.5)
RV mass systolic/BSA, g/m^2	35.2 ± 13.3
RV mass/volume ratio, g/ml	0.33 (0.25-0.44)
RV ejection fraction, %	38.7 ± 12.3
RV stroke volume/end-systolic volume	0.69 (0.40-1.01)
Stiffness index β†	4.6 (3.1-6.5)
Capacitance, mm^3/mm Hg*	1.8 (1.4-2.7)
Distensibility, %/mm Hg*	0.44 (0.25-0.73)
Short-axis	
RV global radial strain, %	15.6 ± 6.2
RV global circumferential strain, %	−9.8 ± 3.5
Long-axis	
RV global radial strain, %	28.9 (17.4-46.6)
RV global longitudinal strain, %	−18.0 ± 7.0

Values are mean ± SD, n (%), or median (IQR), unless otherwise specified. *n = 33. †n = 32.

BSA = body surface area; CMR = cardiac magnetic resonance; Ea = arterial elastance; EDV = end-diastolic volume; Eed = end-diastolic elastance; Ees = end-systolic elastance; IQR = interquartile range; PH = pulmonary hypertension; RV = right ventricular.

FIGURE 2 Receiver Operating Characteristic Curve Analysis and Corresponding Cutoff Values

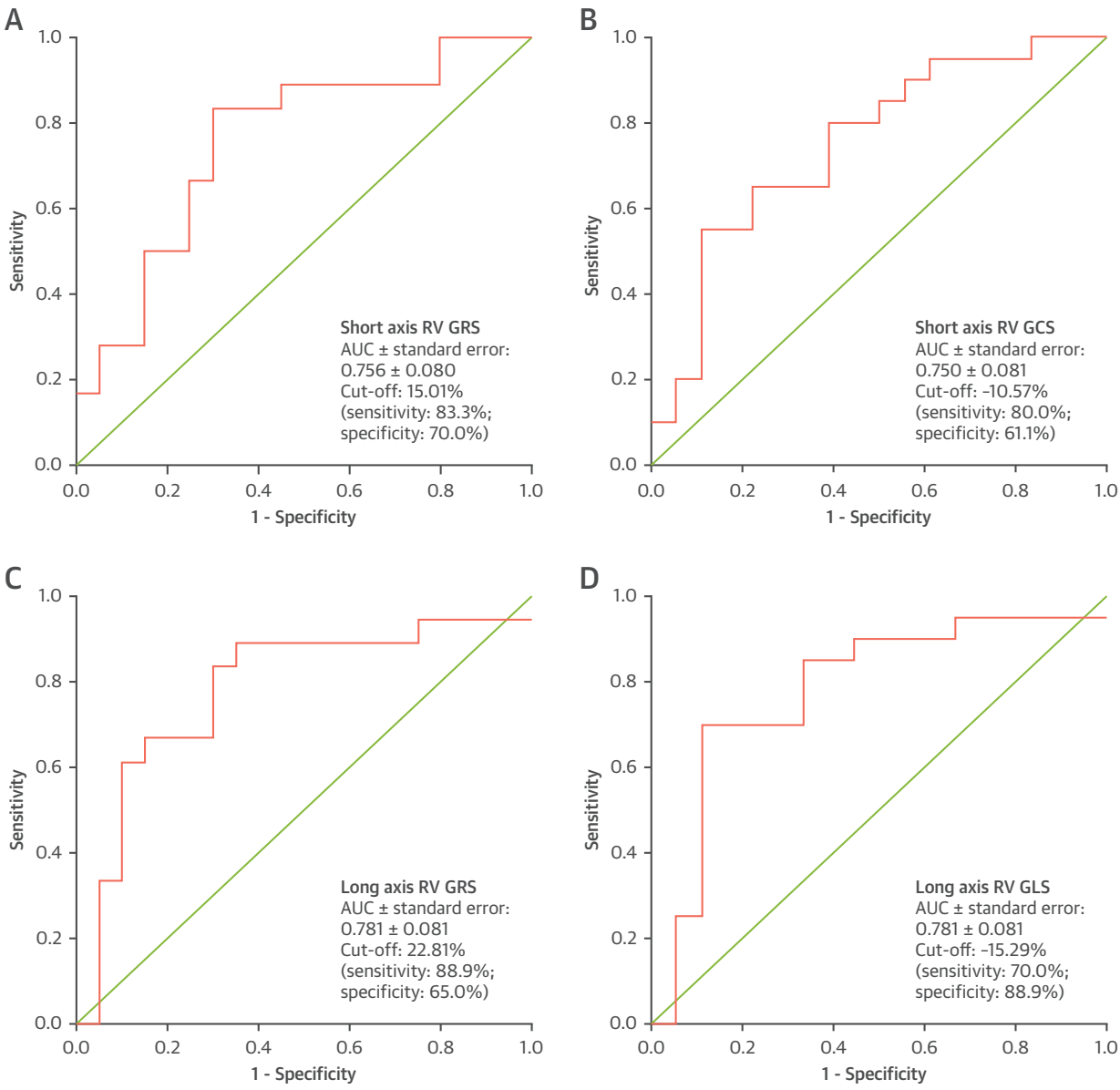

(A) Short-axis RV GRS; **(B)** Short-axis RV GCS; **(C)** Long-axis RV GRS, and **(D)** Long-axis RV GLS for discriminating RV-pulmonary arterial coupling. RV-pulmonary arterial coupling was defined as a single-beat Ees/Ea value ≥0.805 mm Hg/ml. AUC = area under the curve; Ees = end-systolic elastance; other abbreviations as in Figure 1.

association with long-axis RV radial strain (Figure 1D). No correlation between Ees and RV strain was observed (Supplemental Figure 6).

PREDICTIVE RELEVANCE OF RV STRAIN FOR RV-ARTERIAL COUPLING. In multivariate logistic regression analysis, long-axis RV radial strain remained independently associated with Ees/Ea dichotomized at 0.805 mm Hg/ml (multivariate odds ratio [OR]: 5.50; 95% confidence interval [CI]: 1.50 to 20.18; p = 0.010) and Ea dichotomized at 0.66 mm Hg/ml (multivariate OR: 0.96; 95% CI: 0.92 to 0.995; p = 0.026). Long-axis RV longitudinal strain remained independently associated with Eed dichotomized at 0.124 mm Hg/ml (multivariate OR: 1.23; 95% CI: 1.10 to 1.51; p = 0.002). Using receiver operating characteristic curve analyses and the Youden index, cutoff values of 22.81% for long-axis RV radial strain

and −15.29% for long-axis RV longitudinal strain for discriminating RV-arterial coupling (area under the curve [AUC]) were identified in each case (AUC: 0.781; p = 0.003) (Figure 2). Compared with the long-axis RV strain parameters, short-axis RV radial and circumferential strain showed somewhat lower AUC values (0.756 and 0.750, respectively) (Figure 2).

ASSOCIATIONS AMONG CMR RV VOLUME AND STRAIN/VOLUME RATIO AND DIASTOLIC RV DYSFUNCTION. RV EDV/BSA (dilation) showed linear correlations with Tau (diastolic dysfunction) and Eed (diastolic stiffness) in chronic pressure overload (Supplemental Figures 7A and 7B). RV EDV/BSA stratified by Eed (dichotomized at 0.124 mm Hg/ml) was also a strong discriminator of preserved or reduced long-axis RV longitudinal strain (Supplemental Figure 7C). The Eed/RV EDV/BSA ratio showed a nonlinear association with long-axis RV longitudinal strain (Supplemental Figure 7D). Moreover, the long-axis RV longitudinal strain-to-RV EDV/BSA ratio was related to Eed (Figure 3A), Tau, Ea, and pulmonary arterial stiffness (Supplemental Figure 8) and strongly predicted RV diastolic stiffness in receiver operating characteristic analysis (AUC = 0.908; p < 0.001) (Figure 3B).

FIGURE 3 Associations Between Cardiac Magnetic Resonance RV Strain/Volume Ratio and RV Diastolic Stiffness

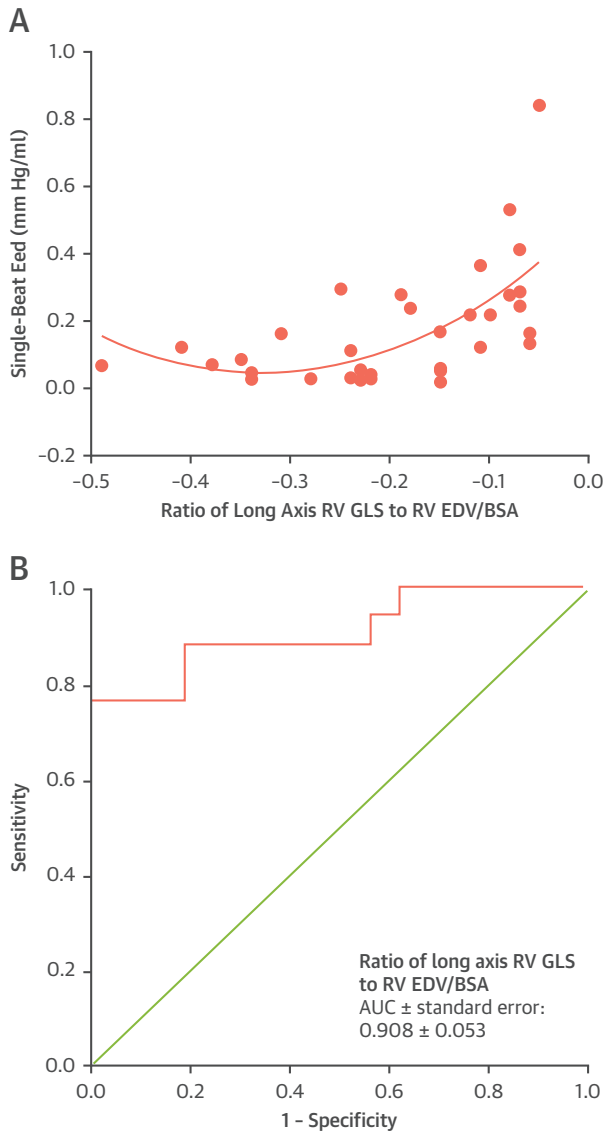

(A) The long-axis RV GLS-to-RV EDV/BSA ratio was associated with Eed, and **(B)** discriminated RV diastolic stiffness (Eed dichotomized at 0.124 mm Hg/ml) in receiver operating characteristic analysis. Abbreviations as in Figure 1.

DISCUSSION

The present data show for the first time a significant association between CMR imaging-derived RV strain parameters and the pressure-volume loop-derived parameters Ees/Ea, Ea, and Eed. RV strain assessed by CMR feature tracking was significantly associated with RV diastolic function (Tau), diastolic stiffness (Eed), and afterload (pulmonary arterial stiffness and Ea). Moreover, CMR RV strain mirrored RV-arterial coupling and was associated with RV dilation and hypertrophy as well as with conventional invasive hemodynamic parameters. Data show that CMR RV strain is a promising indicator of RV-arterial uncoupling and diastolic RV stiffness, broadening the already substantial range of potential applications for CMR in the assessment of RV function during follow-up of patients with PH. Furthermore, the present findings help to close the knowledge gap regarding the physiology of RV strain in chronic pressure overload, which was recently set as a research target by the American Thoracic Society (2).

The ability of the right ventricle to adapt to an increase in afterload (Ea) is related to its potential to increase contractility (Ees) (19). The optimal ratio between Ees and Ea ranges between 1.5 and 2.0, based on research of the left ventricle (20). However, several studies have shown that, as PH progresses, the increase in ventricular contractility becomes insufficient to compensate for the increase in afterload, leading to altered RV-arterial coupling (16,21-23). When the Ees/Ea ratio falls below a certain threshold (not yet precisely defined for the right ventricle but estimated to be 0.805 in the current study), RV dysfunction and failure may occur. Present data demonstrate a nonlinear association between

RV-arterial coupling and RV ejection fraction (Supplemental Figure 5), confirming this assumption.

Our findings may therefore have two pathophysiological explanations. First, in the present cohort with chronic pressure overload, the maximum increase in Ees may already have been reached. This possibility is supported by previous studies of Ees in settings of chronic pressure overload (24,25). Second, the present patients may have been in a state of relative RV-arterial uncoupling, in which Eed and Ea continue to increase without any further increase in Ees (1). Increased afterload has been reported to lead to elevated RV stiffness and fibrosis (26). Notably, our pressure-volume curve analysis shows not only that RV maladaptation is linked with RV dilation and thus "overexpansion" of the RV scaffold but also that the Eed/EDV ratio increases in the maladapted right ventricle and that this loss in lusitropic function is reflected by a decrease in CMR strain variables. Increases in Ea and Eed combined with an unchanging Ees explain why strain correlates with the Ees/Ea ratio but not with Ees. These findings are supported by results obtained previously by Guihaire et al. (27) in a porcine model of chronic pressure overload in which the usual indices of RV function were associated with RV-arterial coupling rather than with ventricular contractility. In addition, Vanderpool et al. (28) demonstrated that, because of the curvilinearity of both Ees and Eed curves, V0 increases with increasing Ea and that increased Ees and Eed are then mechanically associated, along with eventual increases in end-systolic volume and EDV.

This could lead to the conclusion, as shown in the present study, that Eed and Tau of the right ventricle play a crucial role in the setting of chronic pressure overload in PH. The present data are consistent with those from the study by Okumura et al. (29), who showed a significant correlation between RV diastolic function and strain assessed by echocardiography. Single beat-derived Eed has been shown to be increased in patients with pulmonary arterial hypertension and closely associated with markers of disease severity (15). In addition, the long-axis RV longitudinal strain-to-RV EDV/BSA ratio was identified as a novel parameter mirroring afterload (Ea) and RV diastolic dysfunction (Tau) and stiffness (Eed). Reduced RV longitudinal strain was in itself associated with elevated Eed and RV dilation, and the longitudinal strain-to-RV EDV/BSA ratio emerged as a robust noninvasive parameter for the prediction of RV diastolic stiffness. The association between strain and the load-independent measurement of Eed in the present study indicates that CMR strain analysis is a promising tool for the follow-up examination of patients with PH and has the potential to make invasive measurements of Eed and RV-arterial coupling superfluous.

Additionally, with increasing RV EDV/BSA, a significant reduction in each plane of strain is seen, indicating a change of the shape of the right ventricle leading to a reduction in its ability to deform during the cardiac cycle. This reduction is strongest for radial strain, with >50% loss of radial deformation in RV EDV/BSA tertile 3 compared with that in tertile 1. This finding is of interest because it was proposed previously that RV contractility occurs predominantly in the longitudinal plane due to the principal orientation of myocardial fibers (30,31). Previous studies have predominantly focused on RV longitudinal strain and have demonstrated impaired RV longitudinal strain in patients with PH, with subsequent associations between disease severity and mortality (32-34). However, the present data suggest a stronger decrease in radial strain than longitudinal strain in the maladaptive right ventricle. Nevertheless, the degree of longitudinal strain in this cohort of patients with PH ($-18.0 \pm 7.0\%$) was consistent with the impaired longitudinal strain reported previously by Puwanant et al. (32) ($-15.9 \pm 7.6\%$ in patients with PH compared with $-25.5 \pm 6.1\%$ in control subjects) (32). However, the present data lead to the conclusion that the predominant loss of RV radial strain in the setting of chronic pressure overload may mirror maladaptive processes in RV failure.

STUDY LIMITATIONS. The single-beat method was used to estimate Eed, Ees, and Ea parameters. It is not yet known if the multiple-beat approach would generate the same results. However, Inuzuka et al. (35) recently showed a good correlation between single-beat and multi-beat approaches. Reference values for Ees, Ea, and Eed and the Ees/Ea cutoff value at which RV maladaptation begins have not yet been precisely determined and were estimated for the current study. The temporal resolution of nearly 60 ms combined with the smoothing out of minor beat-to-beat differences across several beats may lead to underestimation of strain. The receiver operating characteristic curve and logistic regression analyses are biased by the moderate sample size. The sample size also prevents meaningful analysis of the effects of race and sex on the results but is reasonable given the comprehensive and demanding approach.

CONCLUSIONS

Our study reveals that diastolic stiffness significantly correlates with strain in the chronic pressure-overloaded right ventricle in PH. RV strain mirrors RV-arterial uncoupling, and its assessment also provides information on the adaptation of RV inotropic function to afterload, the associated alteration in lusitropic function, and adaptive versus maladaptive remodeling.

ACKNOWLEDGMENT The authors thank Claire Mulligan, PhD (Beacon Medical Communications Ltd., Brighton, United Kingdom), for manuscript and editorial assistance.

ADDRESS FOR CORRESPONDENCE: Dr. Khodr Tello, Department of Internal Medicine, Justus-Liebig-University Giessen, Klinikstrasse 32, 35392 Giessen, Germany. E-mail: Khodr.Tello@innere.med.uni-giessen.de.

PERSPECTIVES

COMPETENCY IN MEDICAL KNOWLEDGE: In the setting of chronic pressure overload in PH, RV strain parameters indicate that RV diastolic stiffness and RV-arterial uncoupling expand the scope of CMR in the follow-up examination of patients with PH. Furthermore, the present data provide new insights into RV maladaptation, suggesting that radial strain may decrease to a greater extent than longitudinal strain in the maladaptive right ventricle in PH.

TRANSLATIONAL OUTLOOK: Additional catheterization studies of conductance (using multiple-beat as well as single-beat approaches) will be needed to confirm the relationship between RV strain and RV maladaptation in larger populations of patients with PH and to further evaluate the effect of RV maladaptation on radial versus longitudinal strain.

REFERENCES

1. Vonk Noordegraaf A, Westerhof BE, Westerhof N. The relationship between the right ventricle and its load in pulmonary hypertension. J Am Coll Cardiol 2017;69:236–43.

2. Lahm T, Douglas IS, Archer SL, et al. Assessment of right ventricular function in the research setting: knowledge gaps and pathways forward. an Official American Thoracic Society research statement. Am J Respir Crit Care Med 2018;198:e15–43.

3. van de Veerdonk MC, Kind T, Marcus JT, et al. Progressive right ventricular dysfunction in patients with pulmonary arterial hypertension responding to therapy. J Am Coll Cardiol 2011;58:2511–9.

4. Vanderpool RR, Pinsky MR, Naeije R, et al. RV-pulmonary arterial coupling predicts outcome in patients referred for pulmonary hypertension. Heart 2015;101:37–43.

5. Vanderpool RR, Rischard F, Naeije R, Hunter K, Simon MA. Simple functional imaging of the right ventricle in pulmonary hypertension: can right ventricular ejection fraction be improved? Int J Cardiol 2016;223:93–4.

6. Oyama-Manabe N, Sato T, Tsujino I, et al. The strain-encoded (SENC) MR imaging for detection of global right ventricular dysfunction in pulmonary hypertension. Int J Cardiovasc Imaging 2013;29:371–8.

7. Romano S, Judd RM, Kim RJ, et al. Feature-tracking global longitudinal strain predicts death in a multicenter population of patients with ischemic and nonischemic dilated cardiomyopathy incremental to ejection fraction and late gadolinium enhancement. J Am Coll Cardiol Img 2018;11:1419–29.

8. Trip P, Kind T, van de Veerdonk MC, et al. Accurate assessment of load-independent right ventricular systolic function in patients with pulmonary hypertension. J Heart Lung Transplant 2013;32:50–5.

9. Galie N, Humbert M, Vachiery JL, et al. 2015 ESC/ERS Guidelines for the diagnosis and treatment of pulmonary hypertension: the Joint Task Force for the Diagnosis and Treatment of Pulmonary Hypertension of the European Society of Cardiology (ESC) and the European Respiratory Society (ERS): endorsed by: Association for European Paediatric and Congenital Cardiology (AEPC), International Society for Heart and Lung Transplantation (ISHLT). Eur Heart J 2016;37:67–119.

10. Gall H, Felix JF, Schneck FK, et al. The Giessen Pulmonary Hypertension Registry: survival in pulmonary hypertension subgroups. J Heart Lung Transplant 2017;36:957–67.

11. Sanz J, Kariisa M, Dellegrottaglie S, et al. Evaluation of pulmonary artery stiffness in pulmonary hypertension with cardiac magnetic resonance. J Am Coll Cardiol Img 2009;2:286–95.

12. Tello K, Richter MJ, Axmann J, et al. More on single-beat estimation of right ventriculoarterial coupling in pulmonary arterial hypertension. Am J Respir Crit Care Med 2018;198:816–8.

13. Brimioulle S, Wauthy P, Ewalenko P, et al. Single-beat estimation of right ventricular end-systolic pressure-volume relationship. Am J Physiol Heart Circ Physiol 2003;284:H1625–30.

14. Trip P, Rain S, Handoko ML, et al. Clinical relevance of right ventricular diastolic stiffness in pulmonary hypertension. Eur Respir J 2015;45:1603–12.

15. Rain S, Handoko ML, Trip P, et al. Right ventricular diastolic impairment in patients with pulmonary arterial hypertension. Circulation 2013;128:2016–25, 2011–2010.

16. Sanz J, Garcia-Alvarez A, Fernandez-Friera L, et al. Right ventriculo-arterial coupling in pulmonary hypertension: a magnetic resonance study. Heart 2012;98:238–43.

17. Brewis MJ, Bellofiore A, Vanderpool RR, et al. Imaging right ventricular function to predict outcome in pulmonary arterial hypertension. Int J Cardiol 2016;218:206–11.

18. Petersen SE, Aung N, Sanghvi MM, et al. Reference ranges for cardiac structure and function using cardiovascular magnetic resonance (CMR) in Caucasians from the UK Biobank population cohort. J Cardiovasc Magn Reson 2017;19:18.

19. Naeije R, Brimioulle S, Dewachter L. Biomechanics of the right ventricle in health and disease (2013 Grover Conference series). Pulm Circ 2014;4:395–406.

20. Suga H, Sagawa K, Shoukas AA. Load independence of the instantaneous pressure-volume ratio of the canine left ventricle and effects of epinephrine and heart rate on the ratio. Circ Res 1973;32:314–22.

21. Sagawa K. The end-systolic pressure-volume relation of the ventricle: definition, modifications and clinical use. Circulation 1981;63:1223–7.

22. Maughan WL, Shoukas AA, Sagawa K, Weisfeldt ML. Instantaneous pressure-volume relationship of the canine right ventricle. Circ Res 1979;44:309–15.

23. Chantler PD, Lakatta EG, Najjar SS. Arterial-ventricular coupling: mechanistic insights into cardiovascular performance at rest and during exercise. J Appl Physiol (1985) 2008;105:1342–51.

24. Guihaire J, Haddad F, Noly PE, et al. Right ventricular reserve in a piglet model of chronic pulmonary hypertension. Eur Respir J 2015;45:709–17.

25. Spruijt OA, de Man FS, Groepenhoff H, et al. The effects of exercise on right ventricular

contractility and right ventricular-arterial coupling in pulmonary hypertension. Am J Respir Crit Care Med 2015;191:1050–7.

26. Cheng TC, Philip JL, Tabima DM, Hacker TA, Chesler NC. Multiscale structure-function relationships in right ventricular failure due to pressure overload. Am J Physiol Heart Circ Physiol 2018;315:H699–708.

27. Guihaire J, Haddad F, Boulate D, et al. Non-invasive indices of right ventricular function are markers of ventricular-arterial coupling rather than ventricular contractility: insights from a porcine model of chronic pressure overload. Eur Heart J Cardiovasc Imaging 2013;14:1140–9.

28. Vanderpool RR, Desai AA, Knapp SM, et al. How prostacyclin therapy improves right ventricular function in pulmonary arterial hypertension. Eur Respir J 2017;50:1700764.

29. Okumura K, Slorach C, Mroczek D, et al. Right ventricular diastolic performance in children with pulmonary arterial hypertension associated with congenital heart disease: correlation of echocardiographic parameters with invasive reference standards by high-fidelity micromanometer catheter. Circ Cardiovasc Imaging 2014;7:491–501.

30. Rushmer RF, Crystal DK, Wagner C. The functional anatomy of ventricular contraction. Circ Res 1953;1:162–70.

31. Leather HA, Ama R, Missant C, Rex S, Rademakers FE, Wouters PF. Longitudinal but not circumferential deformation reflects global contractile function in the right ventricle with open pericardium. Am J Physiol Heart Circ Physiol 2006;290:H2369–75.

32. Puwanant S, Park M, Popovic ZB, et al. Ventricular geometry, strain, and rotational mechanics in pulmonary hypertension. Circulation 2010;121:259–66.

33. Marwick TH. Measurement of strain and strain rate by echocardiography: ready for prime time? J Am Coll Cardiol 2006;47:1313–27.

34. Sachdev A, Villarraga HR, Frantz RP, et al. Right ventricular strain for prediction of survival in patients with pulmonary arterial hypertension. Chest 2011;139:1299–309.

35. Inuzuka R, Hsu S, Tedford RJ, Senzaki H. Single-beat estimation of right ventricular contractility and its coupling to pulmonary arterial load in patients with pulmonary hypertension. J Am Heart Assoc 2018;7:e007929.

KEY WORDS contractility, coupling, lusitropic function, morphology, pulmonary hypertension, right ventricular contractile function, speckle tracking, strain

APPENDIX For an expanded Methods section and supplemental figures, please see the online version of this paper.

Anlage F

Reserve of Right Ventricular-Arterial Coupling in the Setting of Chronic Overload.

Tello K, Dalmer A, Axmann J, Vanderpool R, Ghofrani HA, Naeije R, Roller F, Seeger W, Sommer N, Wilhelm J, Gall H, Richter MJ. Circ Heart Fail. 2019 Jan;12(1)

Circulation: Heart Failure

ORIGINAL ARTICLE

Reserve of Right Ventricular-Arterial Coupling in the Setting of Chronic Overload

See Editorial by Hsu

BACKGROUND: Right ventricular (RV) maladaptation and failure determine outcome in pulmonary hypertension. The adaptation of RV function to loading (RV-pulmonary arterial coupling) is defined by a ratio of end-systolic to arterial elastances (Ees/Ea). How RV-pulmonary arterial coupling relates to pulmonary hypertension severity and onset of RV failure (defined by excessive volume increase and ejection fraction [EF] decrease) is not exactly known.

METHODS AND RESULTS: We performed cardiac magnetic resonance (CMR) imaging within 24 hours of a diagnostic right heart catheterization and invasive measurement of RV pressure-volume loops in 42 patients with pulmonary hypertension. Median (interquartile range) Ees and Ea were 0.49 (0.35–0.74) and 0.74 (0.45–1.04) mm Hg/mL, respectively; Ees/Ea was 0.73 (0.47–1.07). End-diastolic elastance (Eed) was 0.14 (0.06–0.24) mm Hg/mL. RV EF was 39±13%. End-systolic volume and end-diastolic volume/body surface area (BSA) were 62 (45–101) and 104 (83–143) mL/m^2, respectively. Ees/Ea decreased with increasing RV end-diastolic volume/BSA, mass/BSA, and pulmonary arterial stiffness, and with decreasing EF, from 0.89 to 1.09 in the least impaired tertiles to 0.55 to 0.61 in the most impaired tertiles. Eed increased with increasing RV mass/BSA, end-diastolic volume/BSA, and T1 mapping and with decreasing EF. Receiver operating characteristic analysis identified an Ees/Ea cutoff of 0.805 associated with onset of RV failure defined by increased RV volumes with EF <35%.

CONCLUSIONS: RV-pulmonary arterial coupling (Ees/Ea) has considerable reserve, from normal values of 1.5–2 to <0.8, and has the ability to detect pending RV failure in patients with pulmonary hypertension.

CLINICAL TRIAL REGISTRATION: URL: https://www.clinicaltrials.gov. Unique identifier: NCT03403868.

Khodr Tello, MD
Antonia Dalmer
Jens Axmann
Rebecca Vanderpool, PhD
Hossein A. Ghofrani, MD
Robert Naeije, MD, PhD
Fritz Roller, MD
Werner Seeger, MD
Natascha Sommer, MD, PhD
Jochen Wilhelm, PhD
Henning Gall, MD, PhD*
Manuel J. Richter, MD*

*Drs Gall and Richter contributed equally to this work.

Key Words: anatomy and histology ■ humans ■ hypertension, pulmonary ■ ROC curve ■ stroke volume

https://www.ahajournals.org/journal/circheartfailure

WHAT IS NEW?

- Right ventricular (RV)–pulmonary arterial coupling (end-systolic/arterial elastances derived from single-beat pressure-volume loops) has considerable reserve in patients with pulmonary hypertension, falling below 0.8 before RV failure occurs.
- RV-pulmonary arterial coupling is associated with RV ejection fraction and decreases with increasing RV volume, mass, and distensibility and capacitance of the pulmonary arteries (measured by cardiac magnetic resonance imaging).
- RV diastolic stiffness increases with increasing fibrosis (T1 mapping).
- The stroke volume/end-systolic volume ratio is at least as good as end-systolic/arterial elastances in discriminating RV failure (ejection fraction, <35%); neither stroke volume/end-systolic volume nor end-systolic/arterial elastance shows collinearity with ejection fraction as the dependent variable.

WHAT ARE THE CLINICAL IMPLICATIONS?

- The study contributes to an increased understanding of cardiac magnetic resonance results and their links to RV pathophysiology in the setting of chronic RV overload.
- The noninvasive cardiac magnetic resonance parameter stroke volume/end-systolic volume may be at least as useful as invasively measured end-systolic/arterial elastance in identifying pending RV failure, assuming noncollinearity.

Pulmonary hypertension (PH) is a disease of the pulmonary resistive vessels but with symptomatology and outcome predominantly determined by right ventricular (RV) failure induced by the increase in pulmonary vascular resistance.[1,2] Despite this, there is no consensus recommendation on how best to measure RV function in patients with PH.

RV failure can be defined as a dyspnea/fatigue syndrome with limitation of exercise capacity and eventual systemic congestion caused by the inability of the RV to adapt to the peripheral demand for increased flow output without increased dimensions.[2,3] As recently reviewed,[4] RV contractility is measured as end-systolic elastance (Ees; usually considered equal to maximum elastance), which is defined by an end-systolic pressure to end-systolic volume (ESV) relationship. The ratio of Ees to pulmonary arterial (PA) elastance (Ea; defined by an end-systolic pressure–stroke volume [SV] relationship) is used to assess how well RV contractility is adapted to afterload. Optimal RV-PA coupling allowing for ejection of flow at a minimal amount of energy occurs at an Ees/Ea ratio between 1.5 and 2.[2–4] However, the level of RV-PA uncoupling at which RV failure occurs is not exactly known.

We, therefore, combined cardiac magnetic resonance (CMR) imaging of the RV with invasive pressure-volume loop measurement of RV-PA coupling to determine the level of Ees/Ea below which substantial RV maladaptive processes begin. We also evaluated the association of excessive RV-PA uncoupling and RV diastolic stiffness (measured as end-diastolic elastance [Eed][5]) with CMR indices of RV maladaptation, such as RV mass,[6] RV mass/volume ratio,[7] RV ejection fraction (EF),[8] and T1 and T2 mapping,[9] and the association of RV-PA coupling with CMR-derived measures of PA stiffness as a possible major determinant of afterload,[10] to shed light on the pathophysiology of RV failure.

METHODS

The data that support the findings of this study are available from the corresponding author on reasonable request.

Study Design and Patients

We analyzed consecutive patients with PA hypertension (PAH) or chronic thromboembolic PH (diagnosed according to current guidelines[11]) who were prospectively enrolled into the Right Heart I study (NCT03403868) between January 2016 and July 2018. A multidisciplinary board, including pulmonary physicians and radiologists, assessed each diagnosis before enrollment. Patients with PH underwent CMR imaging on day 1 and pressure-volume/Swan-Ganz catheterization on day 2. Patients received targeted PAH therapies based on clinical grounds and best standard of care. All participating patients gave written informed consent to be enrolled into the Right Heart I study and the Giessen PH Registry.[12] The investigation conforms with the principles outlined in the Declaration of Helsinki and was approved by the ethics committee of the Faculty of Medicine at the University of Giessen (approval No. 108/15). All authors had full access to all the data in the study and take responsibility for its integrity and the data analysis.

CMR Imaging

CMR imaging and T1 mapping were performed as described previously.[13] T1 and T2 measurements were performed in the short axis at upper and lower RV insertion points and RV lateral and septum regions. T1 and T2 global parameters were defined as the arithmetic mean of all T1 and T2 individual parameters, respectively. Each patient was analyzed by 2 experienced examiners, and the results were averaged.

PA stiffness, capacitance, and distensibility were measured using CMR data as described previously.[10]

Right Heart Catheterization

A Swan-Ganz catheter was inserted via the internal jugular vein using an 8F introducer sheath. Pressure values were continuously assessed and the cardiac index was measured using the direct or indirect Fick method as available. Pulmonary vascular resistance was calculated as follows: (mean PA pressure–PA wedge pressure)/cardiac output.[11]

Pressure-Volume Catheterization

A 4F pressure-volume catheter (CA-Nr 41063; CD Leycom, Zoetermeer, the Netherlands) was positioned in the RV apex (using the same 8F introducer sheath as above), guided by transthoracic echocardiography and analysis of online pressure-volume loops. Real-time beat-to-beat display of pressure-volume loops was achieved by connection to an intracardiac analyzer (Inca; CD Leycom). Single-beat measurements were each evaluated separately by 2 experienced examiners who were blinded to the other data and supervised by the first author. Ees was calculated using the single-beat method for the RV.[14] Ea was calculated as end-systolic pressure/SV.[14] RV-arterial coupling was defined as Ees/Ea. Eed was calculated as an end-diastolic pressure/volume ratio,[5] which has been shown to agree with the more rigorous diastolic elastance coefficient β calculated from a curvilinear adjustment of end-systolic and end-diastolic pressure/volume ratios.[5,15] Volume measurements were calibrated with CMR.[16]

Statistical Analyses

SPSS, version 23.0 (IBM, Armonk, NY), and R, version 3.4.3 (The R Foundation for Statistical Computing, Vienna, Austria; https://www.R-project.org/), were used for statistical analyses. Adherence to a gaussian distribution was determined using the Kolmogorov-Smirnov test and visual assessment of histograms.

For further analysis, all variables with a nonnormal distribution were transformed (rechecked with the Kolmogorov-Smirnov test), and associations of these variables with other parameters were analyzed by linear regression models of the form log(y)=log(a)+b×log(x) (y=a×b) as indicated in the respective Figure legends. The coefficient b represents the size and direction of the change in y depending on x. The *P* refers to the *t* test of the null hypothesis: b=0. Residual diagnostic plots showed a good agreement of the data with the model assumptions (normal distribution and variance homogeneity of log[y]).

A cutoff value for Ees/Ea that would indicate RV-PA uncoupling is not yet available. Therefore, to analyze the reserve of Ees/Ea in relation to RV maladaptation, tertiles of RV end-diastolic volume (EDV), RV mass, RV mass/volume ratio, RV EF, and PA stiffness, capacitance, and distensibility were defined to mirror RV maladaptive processes (Table I in the Data Supplement). Analysis by tertiles and quartiles has been used previously to show the prognostic relevance of T1 mapping and Ea, respectively.[17,18] Differences between multiple groups were analyzed with the independent-samples Kruskal-Wallis test, or a pairwise comparison was performed using the Mann-Whitney *U* test.[19]

To derive a precise cutoff of Ees/Ea that would best discriminate maladaptive RV changes, receiver operating characteristic (ROC) curve analysis was used with the Youden index.[20] For the purpose of this ROC analysis, RV maladaptation was defined as RV EF <35%, because this value is modeled to be necessarily associated with an increase in EDV and ESV at preserved SV[21] and has been associated with increased mortality in patients with PH[8,22–24] and because RV EF is the least collineated CMR parameter. For direct comparison, SV/ESV and Ees/Ea were added into one ROC model, and a logistic binary regression model was build. Multicollinearity was assessed using the variance inflation factor. For all analyses, $P<0.05$ was considered statistically significant.

RESULTS

Characteristics of the 42 included patients with PH are presented in Table 1. The majority of patients had PAH (PH group 1) and presented with an advanced World Health Organization functional class. A high proportion of the patients were receiving combination therapy, and the 6-minute walking distance was impaired. End-diastolic pressure, Ees, Eed, and the Ees/Ea ratio are shown in Table 2, and CMR measurements of RV volumes and mass, PA stiffness, and T1 and T2 mapping are shown in Table 3. Compared with values reported in healthy individuals,[25] ESV and EDV were increased and EF decreased.

To explore the reserve of Ees/Ea according to maladaptive RV changes, we compared pressure-volume loop data in different tertiles of CMR parameters reflecting RV dilatation, hypertrophy, and function (Figure 1; Table II in the Data Supplement). Exemplative CMR images and diagrams of pressure-volume loops are shown for a patient with an early stage of RV maladaptation and preserved Ees/Ea and a patient with substantial impairment of Ees/Ea and RV maladaptation (Figure 1A). Our data show that Ees/Ea is substantially impaired in RV EDV/body surface area tertile 3 versus 1 and deteriorates in different tertiles reflecting worsening RV hypertrophy (RV mass diastolic/body surface area) and EF to a median of 0.56 (Figure 1B). In addition, our data show a similar pattern for Eed, with substantial impairment in advanced RV maladaptation (Figure 1C). Our findings are visualized in the context of the currently proposed stages[4] of the course of PH in Figure 1D, showing that Ees/Ea and Eed have a reserve during the initial course of the disease and are associated with extensive maladaptive RV dilatation, hypertrophy, and reduced RV EF at the point of RV-PA uncoupling.

Ees/Ea also showed significant reserve when compared between tertiles 1 and 3 of PA stiffness and capacitance and in different tertiles of PA distensibility (Figure 2; Table III in the Data Supplement). Median (interquartile range) Ees/Ea was significantly decreased in PA stiffness tertile 3 versus 1 and in PA capacitance tertile 1 versus 3 (Figure 2Ai and 2Aii). Ees/Ea also showed a significant decrease in different tertiles reflecting worsening PA distensibility (Figure 2Aiii). Moreover, Ees/Ea showed significant associations with PA capacitance and distensibility (Figure 2B), while a trend toward an association with stiffness index β was observed (Figure I in the Data Supplement). In addition, Ea showed a significant association with stiffness index β (Figure 2C).

Table 1. Patient Characteristics and Pulmonary Hemodynamics

	Patients With PH (n=42)
Men/women, n	20/22
Age, y	55 (48–65)
PH subtype, n (%)	
Idiopathic PAH	28 (67)
Heritable PAH	1 (2)
PAH associated with the following	7 (17)
HIV infection	1
Portal hypertension	2
Connective tissue disease	3
Congenital heart disease	1
Chronic thromboembolic PH	6 (14)
Treatment, n (%)	
Phosphodiesterase type 5 inhibitor	19 (45)
Endothelin receptor antagonist	23 (55)
Soluble guanylate cyclase stimulator	16 (38)
Prostanoid	8 (19)
Combination therapy, n (%)	
Dual therapy	13 (31)
Triple therapy	10 (24)
WHO functional class, n (%)*	
I	2 (5.0)
II	13 (32.5)
III	25 (62.5)
6-min walking distance, m*	425 (314–490)
Tricuspid regurgitation, n (%)†	
None/mild	16 (41)
Moderate	15 (39)
Severe	8 (20)
Right heart catheterization	
mPAP, mm Hg	43 (34–52)
RAP, mm Hg	7±4
PVR, WU	6.9 (4.3–9.8)
Cardiac index, L/min per m^2	2.82±0.65
PAWP, mm Hg	9±3

Values represent mean±SD, for normally distributed data, or median (interquartile range), for non-normally distributed data, unless otherwise specified. mPAP indicates mean pulmonary arterial pressure; PAH, pulmonary arterial hypertension; PAWP, pulmonary arterial wedge pressure; PH, pulmonary hypertension; PVR, pulmonary vascular resistance; RAP, right atrial pressure; and WHO, World Health Organization.

*n=40, †n=39.

We also assessed the relationship of pressure-volume loop parameters with myocardial tissue characteristics (evaluated using T1 and T2 mapping; Figure 3). Example images of T1 and T2 mapping are shown in Figure 3A. Ees/Ea showed a trend toward an association with T1 global mapping values (Figure 3B), whereas EDV/body surface area showed a significant association (Figure II in the Data Supplement). Moreover, Eed showed an increase in higher tertiles of T1 global mapping values, indicating a higher degree of RV diastolic stiffness in patients with more advanced myocardial fibrosis (Figure 3Ci; Table IV in the Data Supplement). In addition, Eed showed significant associations with T1 global and T1 lower RV insertion point mapping values (Figure 3Cii and 3Ciii), while a trend toward an association with T2 lower RV insertion point mapping values was observed (Figure 3Civ).

Table 2. Pressure-Volume Loop Measurements

	Patients With PH (n=42)
Ea, mm Hg/mL	0.74 (0.45–1.04)
Ees, mm Hg/mL	0.49 (0.35–0.74)
Ees/Ea ratio	0.73 (0.47–1.07)
Eed, mm Hg/mL	0.14 (0.06–0.24)
RV EDP, mm Hg	7 (3–11)

Values represent median (interquartile range), for non-normally distributed data.

Ea indicates arterial elastance; EDP, end-diastolic pressure; Eed, end-diastolic elastance; Ees, end-systolic elastance; PH, pulmonary hypertension; and RV, right ventricle.

Table 3. Cardiac Magnetic Resonance Imaging Measurements

	Patients With PH (n=42)
RV EDV/BSA, mL/m^2	104 (83–143)
RV ESV/BSA, mL/m^2	62 (45–101)
RV mass diastolic/BSA, g/m^2	35 (27–50)
RV mass systolic/BSA, g/m^2	36±14
RV mass/volume ratio, g/mL	0.33 (0.25–0.44)
RV EF, %	38±13
RV SV/ESV	0.66 (0.33–1.01)
Stiffness index β*	4.6 (3.0–6.0)
Capacitance, mm^3/mm Hg	1.9 (1.4–3.2)
Distensibility, %/mm Hg†	0.46 (0.27–0.72)
T1 mapping	
RV global, ms	1016±46
Upper RVIP, ms‡	1045 (986–1092)
Lower RVIP, ms	1063±99
RV septum, ms	994±63
RV lateral, ms§	971±70
T2 mapping	
RV global, ms	59 (54–62)
Upper RVIP, ms	62 (57–67)
Lower RVIP, ms	62±7
RV septum, ms	52 (49–57)
RV lateral, ms	57±6

Values represent mean±SD, for normally distributed data, or median (interquartile range), for non-normally distributed data. BSA indicates body surface area; EDV, end-diastolic volume; EF, ejection fraction; ESV, end-systolic volume; PH, pulmonary hypertension; RV, right ventricle; RVIP, right ventricular insertion point; and SV, stroke volume.

*n=39, †n=38, ‡n=37, §n=41.

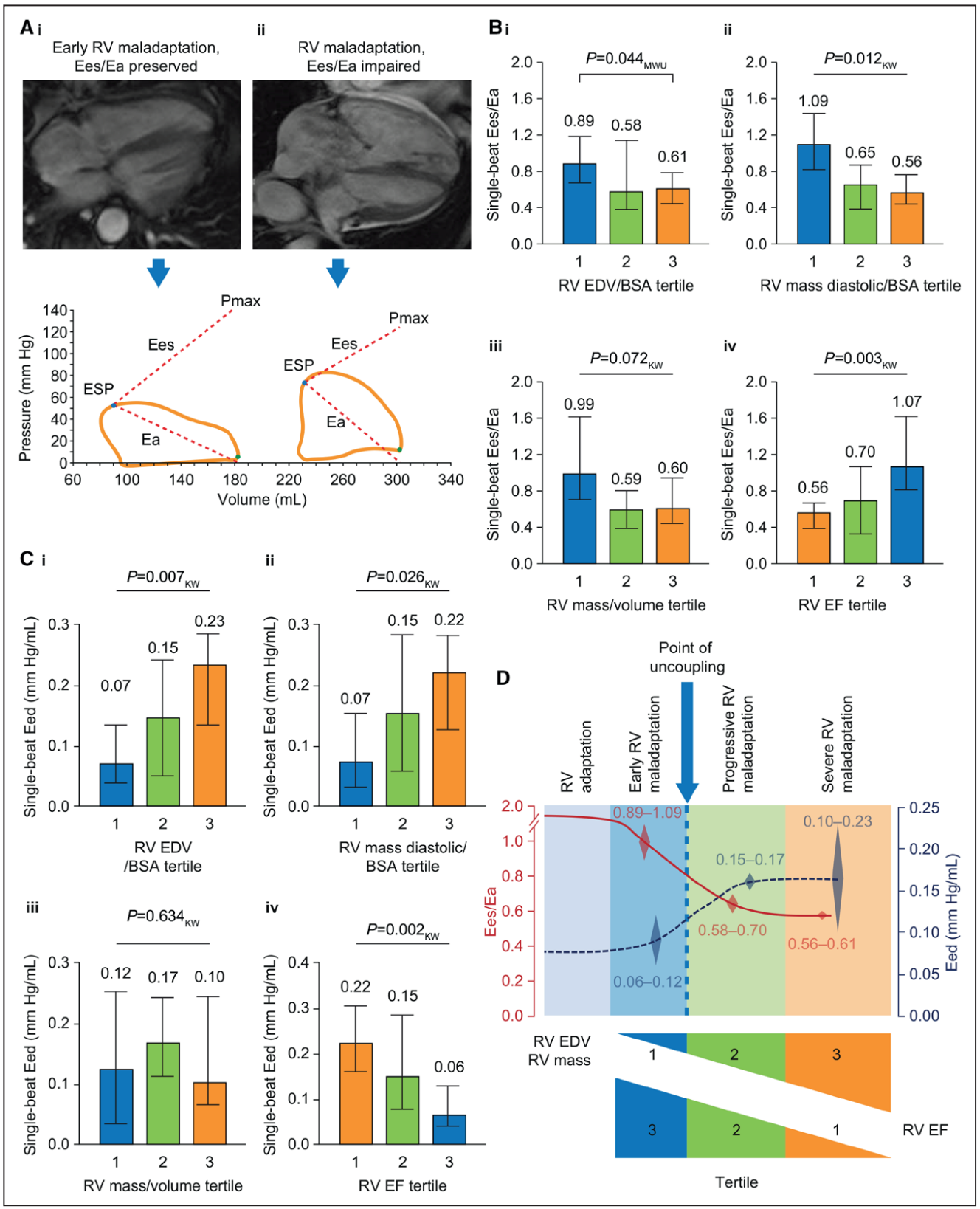

Figure 1. Reserve of right ventricular (RV)-arterial coupling (end-systolic elastance [Ees]/arterial elastance [Ea]) stratified by RV maladaptive changes in patients with pulmonary hypertension.

A, Representative 4-chamber cardiac magnetic resonance imaging and diagrams of pressure-volume loop analysis for patients with (**Ai**) preserved Ees/Ea and early signs of maladaptive RV changes, and (**Aii**) impaired Ees/Ea and severe RV maladaptation. **B**, Ees/Ea and (**C**) end-diastolic elastance (Eed) stratified by tertiles of (**Bi** and **Ci**) RV end-diastolic volume (EDV)/body surface area (BSA), (**Bii** and **Cii**) RV mass/BSA, (**Biii** and **Ciii**) RV mass/volume ratio, and (**Biv** and **Civ**) RV ejection fraction (EF), showing significant impairment of Ees/Ea in RV EDV/BSA tertile 3 vs 1 and in different tertiles reflecting worsening hypertrophy (RV mass/BSA) and RV EF, and significant impairment of Eed in different tertiles reflecting worsening of all RV maladaptation parameters except RV mass/volume ratio. (*Continued*)

Figure 1 Continued. Data are shown as median [interquartile range] (values are listed in Table II in the Data Supplement), and differences between tertiles were analyzed using the independent-samples Kruskal-Wallis (KW) test or Mann-Whitney *U* (MWU) test. **D**, During the course of pulmonary hypertension, the RV initially adapts to the increased afterload; as the disease progresses, RV-arterial uncoupling ensues with severe RV maladaptation as illustrated previously.[4] Our data indicate that Ees/Ea has a considerable reserve, falling from median values of 0.89 to 1.09 in early RV maladaptation to 0.56 to 0.61 in severe RV maladaptation. ESP indicates end-systolic pressure; and Pmax, theoretical maximum isovolumic pressure calculated from a nonlinear extrapolation of the early and late portions of the RV pressure curve.

We next evaluated the ability of Ees/Ea and SV/ESV to discriminate maladaptive RV function using ROC analysis (Figure 4). The area under the ROC curve was 0.738 (*P*=0.010) for Ees/Ea and 0.865 (*P*<0.001) for SV/ESV. We identified a cutoff of 0.805 for Ees/Ea, which had a sensitivity of 65.4% and a specificity of 87.5% for discriminating RV EF <35% (positive predictive value of 87.5% and negative predictive value of 65.8%; Youden index, 0.529). The ROC analyses were supported by univariate logistic regression analysis, which showed significant relationships with RV function (RV EF dichotomized at 35%) for both Ees/Ea (odds ratio, 4.35; 95% CI, 1.22–15.49; *P*=0.023) and SV/ESV (odds ratio, 25.29; 95% CI, 3.77–170.31; *P*=0.001). However, a bivariate model indicated superiority of SV/ESV over Ees/Ea (Wald values: 8.923 and 0.234, respectively), despite absence of collinearity for both variables (variance inflation factor, 1.374 for both SV/ESV and Ees/Ea with RV EF as the dependent variable).

DISCUSSION

The present results show that the coupling of RV contractility to increased afterload in PH has considerable reserve, as Ees/Ea has to decrease from normal values of 1.5 to 2 to <0.8 before substantial RV maladaptation occurs as characterized by an increase in volumes and decrease in EF below the critical value of 35%. The relevance of Ees/Ea as a measure of RV-PA coupling was supported by its association with RV dilatation, function, mass, EF and distensibility, and capacitance of the PAs. Interestingly, SV/ESV (a noninvasive surrogate for Ees/Ea[18,24]) was at least as useful as Ees/Ea in identifying pending RV failure.

It has been recently demonstrated that patients with PAH receiving targeted therapies may remain stable for several years but eventually present with increased RV dimensions and decreased EF heralding clinical deterioration and decreased survival.[4,23,26] As increased RV dimensions and decreased EF can only be the consequence of RV-PA uncoupling, our study aimed to define the Ees/Ea ratio—the gold standard measure of RV-PA coupling—at which relevant RV maladaptation begins. Because the transition from adaptation to maladaptation and failure is progressive and cutoff values on volumes are difficult to define, we decided to define maladaptation or failure as RV EF <35%. RV EF

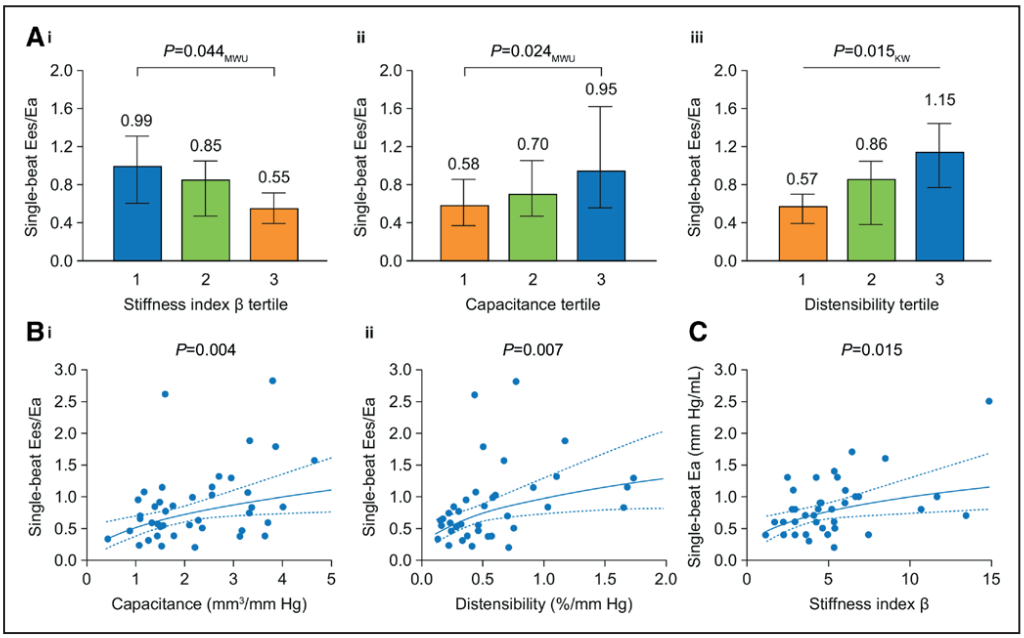

Figure 2. Reserve of right ventricular (RV)-arterial coupling (end-systolic elastance [Ees]/arterial elastance [Ea]) stratified by pulmonary arterial stiffness, capacitance, and distensibility.
A, Ees/Ea stratified by tertiles of (**Ai**) pulmonary arterial stiffness, (**Aii**) capacitance, and (**Aiii**) distensibility, showing a significant difference in Ees/Ea between tertiles 1 and 3 of pulmonary arterial stiffness and capacitance and in different tertiles of pulmonary arterial distensibility. Data are shown as median [interquartile range] (values are listed in Table III in the Data Supplement), and differences between tertiles were analyzed using independent-samples Kruskal-Wallis (KW) test or Mann-Whitney *U* (MWU) test. **B**, Associations of Ees/Ea with (**Bi**) capacitance and (**Bii**) distensibility. **C**, Association of Ea with pulmonary arterial stiffness. Associations between parameters were analyzed by linear regression models of the form log(y)=log(a)+b×log(x) (y=a×b); the coefficient b represents the size and direction of the change in y depending on x, and significance was assessed by *t* test (null hypothesis: b=0).

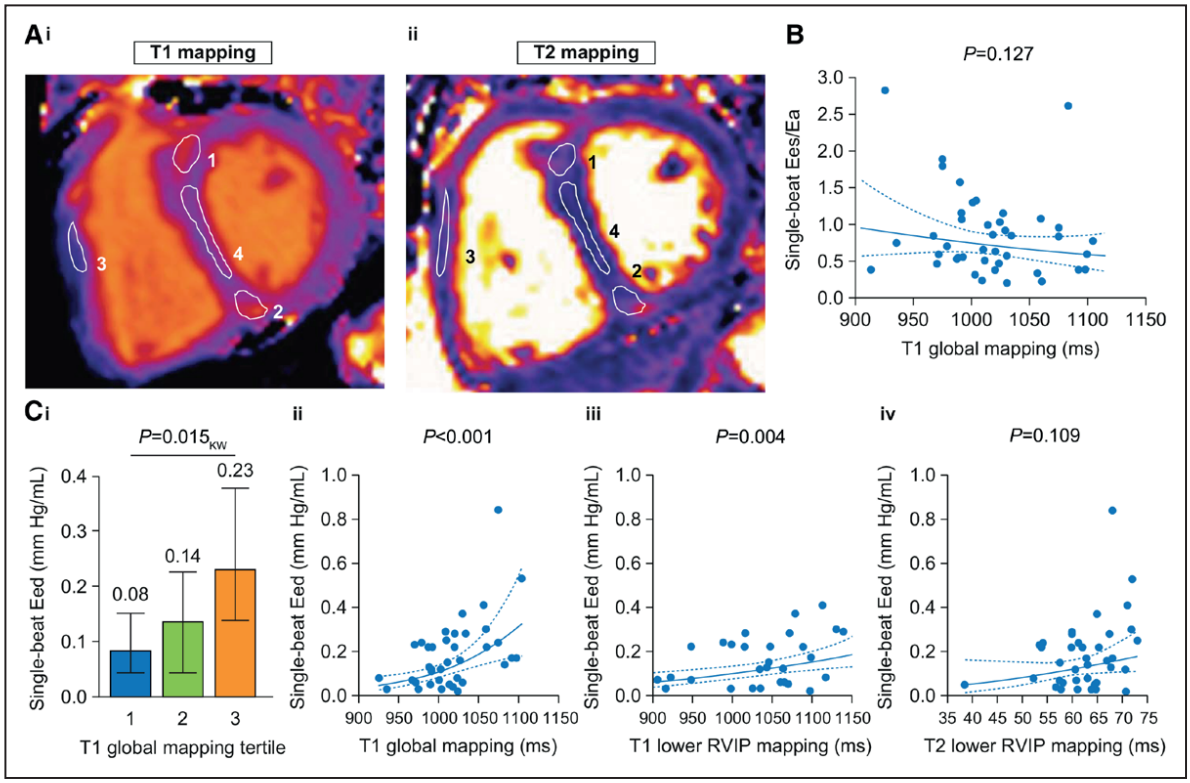

Figure 3. Association of T1 and T2 mapping values with right ventricular (RV)-arterial coupling and RV diastolic stiffness.
A, T1 (**Ai**) and T2 (**Aii**) mapping of the RV in regions of interest (upper and lower RV insertion points [RVIPs; labeled as regions 1 and 2, respectively], RV lateral [region 3], and septum [region 4], with RV global being defined as the arithmetic mean of these parameters). Example images from a patient with impaired end-systolic elastance (Ees)/arterial elastance (Ea) and RV maladaptive changes are shown. **B**, Trend toward an association between RV-arterial coupling (Ees/Ea) and T1 global mapping. **C**, RV diastolic stiffness (end-diastolic elastance [Eed]) showed (**Ci**) a significant increase in higher T1 global mapping tertiles, associations with (**Cii**) T1 global mapping and (**Ciii**) T1 lower RVIP mapping, and (**Civ**) a trend toward an association with T2 lower RVIP mapping values. Data in **Ci** are shown as median [interquartile range] (values are listed in Table IV in the Data Supplement), and the difference between tertiles was analyzed using the independent-samples Kruskal-Wallis (KW) test. Associations between parameters were analyzed by linear regression models of the form log(y)=log(a)+b×log(x) (y=a×b); the coefficient b represents the size and direction of the change in y depending on x, and significance was assessed by *t* test (null hypothesis: b=0).

<35% has consistently been shown to be associated with decreased survival in severe PH[8,22–24] and is easily modeled to be associated with rapid increases in EDV and ESV when SV is to be preserved.[21] Furthermore, RV EF was the least collineated CMR parameter in the present study.

Reports of Ees and Ea measured with gold standard high-fidelity technology in patients with PH are scarce. The first was by Kuehne et al[27] in 2004. The authors validated the use of fluid-filled catheters against high-fidelity micromanometer-tipped catheters for the measurement of RV pressures in experimental animals and reported an ≈3-fold increase in Ees in the presence of a 6-fold increase in Ea, resulting in a substantially decreased Ees/Ea ratio (on average from 2 to 1) but still without an increase in RV dimensions. Subsequent studies showed similarly increased Ees but decreased Ees/Ea in idiopathic PAH,[28,29] PAH associated with systemic sclerosis,[28,30] chronic thromboembolic PH,[29,31] and even in a patient with a systemic RV.[32] Two of the studies also reported measurements during exercise, showing decreased Ees/Ea even in patients with PAH who had persistently normal values at rest,[29,30] in contrast with controls who maintained their Ees/Ea ratio during exercise. Decreased Ees/Ea during exercise in PAH was, as expected, associated with increased RV ESV and EDV[30] because exhaustion of homeometric adaptation (increased contractility) leads to the use of heterometric adaptation (increased dimensions) to maintain RV flow output at the level required to meet peripheral demand. There has been no previous report of substantial RV maladaptive changes along with decreased Ees/Ea at rest in patients with PH. Our results show for the first time that the Ees/Ea ratio must be considerably decreased before RV failure occurs at rest.

The reasons why the onset of RV dilatation and eventual RV failure require such a considerable amount of RV-PA uncoupling are not entirely clear. It appears that the homeometric (contractile) adaptation of the RV to afterload buffers the Ees/Ea ratio in the presence of significant worsening of PH[4] and makes it insensitive to efficacious therapeutic interventions.[33] In animal models of embolic PH, the RV dilated when the Ees/Ea ratio decreased to 0.7 to 1.0,[34,35] and the Ees/Ea ratio was not sensitive to interventions that effectively decreased Ea because Ees decreased proportionally to Ea.[36] Experimental work on isolated canine hearts showed that on average, maximal stroke work occurs at Ea/Ees of

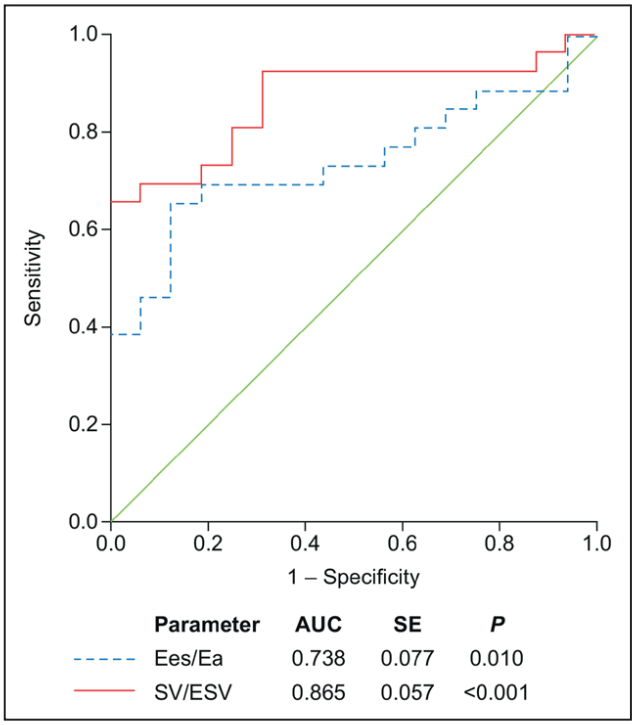

Figure 4. Receiver operating characteristic (ROC) curve analysis of end-systolic elastance (Ees)/arterial elastance (Ea) and stroke volume (SV)/end-systolic volume (ESV) for discriminating maladaptive right ventricular (RV) function (defined as RV ejection fraction <35%).
Ees/Ea and SV/ESV were evaluated together in 1 ROC model. AUC indicates area under the curve.

0.80±0.16, whereas ventricular efficiency (stroke work/myocardial oxygen consumption) is maximal at Ea/Ees of 0.70±0. 15, suggesting that optimal RV-PA coupling might occur at values lower than the range of 1.5 to 2 predicted by mathematical models.[37] However, the results of this study have not been confirmed. More recently, Axell et al[38] defined the Ees/Ea threshold below which SV or cardiac output decreased in either animal models or patients with chronic thromboembolic PH as around 0.7, which is slightly lower than the cutoff we identified for RV EF <35%.

Both Ees and Ea are small numbers and expressions of quotients, which makes the assessment of RV-PA coupling based on the Ees/Ea ratio sensitive to measurement errors. Because both Ees and Ea have a common pressure term, it has been proposed to simplify the Ees/Ea ratio to a ratio of volumes or SV/ESV.[18] In a clinical study of patients referred for PH of various severities, the SV/ESV ratio was superior to EF for the prediction of outcome.[24] However, both EF and SV/ESV were independent predictors of outcome in a study of patients with advanced PAH.[22]

Even with gold standard high-fidelity pressure-volume technology for the measurement of RV volumes, Ees and Ea measurements have relied either on a multiple-beat method allowing for elastance calculations on a family of pressure-volume loops generated during a decrease of venous return, for example during a Valsalva maneuver,[28,30] or a single-beat method with Pmax calculations and measurement of relative change in volume on just 1 pressure-volume loop.[27,29] The single-beat method has been validated in healthy dogs with or without acute hypoxia-induced PH,[14] but it has not been systematically compared with the multiple-beat method considered as a gold standard reference in patients with severe PH.[28,30] Most recently, the single-beat method was shown to be tightly correlated with the multiple-beat method for assessment of RV-PA coupling in patients with and without PH but only after some additional adjustment for the nonlinearity of the Ees curve.[39] In that study, the standard single-beat method assuming linearity of the Ees curve was less well correlated with the multiple-beat method for assessment of RV-PA coupling. This may need further clarification and clinical evaluation.

Myocardial T1 mapping is a method of myocardial tissue characterization with the potential to identify focal and diffuse myocardial fibrosis.[40] In patients with PH, native T1 values at the insertion regions were significantly related to disease severity.[41] Garcia-Alvarez et al[9] showed significant correlations of hemodynamics and RV-PA coupling with native T1 values at RV insertion points in an experimental porcine model of PH. Interestingly, we show a significant relationship between end-diastolic stiffness and RV T1 mapping, which might be explained by increased fibrosis.[15,42] Myocardial T2 mapping is associated with myocardial inflammation and edema,[43] and elevated T2 mapping values were recently reported in patients with PAH.[44] The present study was only able to show a trend toward an association between T2 mapping and Eed, which nevertheless merits further investigation because it may suggest an important role for inflammation and edema in altering RV diastolic stiffness.

Invasive measurement of pressure-volume loops is a demanding and complex procedure; CMR measures that provide information on RV maladaptation would, therefore, be valuable in daily clinical practice. The association of T1 mapping (as an indicator of fibrosis) with Eed may be relevant to daily clinical practice, because diastolic RV stiffness was previously found to be associated with clinical progression.[5] The association of RV volume, mass, and EF with invasively measured RV-PA coupling may help clinicians to derive additional information from CMR data and link the results to pathophysiology.

Our study has several limitations. The statistical analysis is limited by the sample size. However, given the rareness of invasive pressure-volume catheter characterization of patients with PH, the size of the included cohort is comparable with and to some extent exceeds that of previously published cohorts.[27–30,32,39] Only the single-beat method was used to estimate Ees and Ea in patients with RV failure, without validation against

multiple-beat methodology. The relationship of Ees/Ea with RV EF, PA capacitance, or proximal PA stiffness as estimations of afterload might be limited by the individual variability in RV-PA preservation in severe PH. Finally, despite the lack of statistically significant collinearity for Ees/Ea and SV/ESV, the physiological link between these parameters may have influenced our results.

In conclusion, our analysis of CMR, hemodynamic, and single-beat pressure-volume loop data in 42 consecutive patients with PH shows that RV-PA coupling defined by Ees/Ea has considerable reserve and is associated with parameters reflecting RV maladaptation. SV/ESV might be at least as useful as Ees/Ea in detecting pending RV failure in PH.

ARTICLE INFORMATION

Received August 14, 2018; accepted December 10, 2018.

Guest Editor for this article was Ryan J. Tedford, MD.

The Data Supplement is available at https://www.ahajournals.org/doi/suppl/10.1161/CIRCHEARTFAILURE.118.005512.

Correspondence

Khodr Tello, MD, Department of Internal Medicine, Justus-Liebig-University Giessen, Klinikstrasse 32, 35392 Giessen, Germany. Email khodr.tello@innere.med.uni-giessen.de.

Affiliations

Department of Internal Medicine (K.T., A.D., J.A., H.A.G., W.S., N.S., J.W., H.G., M.J.R.) and Department of Radiology (F.R.), Justus-Liebig-University Giessen, Universities of Giessen and Marburg Lung Center, Member of the German Center for Lung Research. Division of Translational and Regenerative Medicine, University of Arizona, Tucson (R.V.). Department of Pneumology, Kerckhoff Heart, Rheuma, and Thoracic Center, Bad Nauheim, Germany (H.A.G.). Department of Medicine, Imperial College London, United Kingdom (H.A.G.). Department of Cardiology, Erasme University Hospital, Brussels, Belgium (R.N.).

Acknowledgments

We acknowledge the editorial assistance provided by Dr Claire Mulligan (Beacon Medical Communications, Ltd, Brighton, United Kingdom).

Sources of Funding

This work was funded by the Excellence Cluster Cardio-Pulmonary System and the Collaborative Research Center (SFB) 1213–Pulmonary Hypertension and Cor Pulmonale, grant number SFB1213/1, project B08 (German Research Foundation, Bonn, Germany). For the manuscript, editorial assistance was provided by Dr Claire Mulligan (Beacon Medical Communications, Ltd, Brighton, United Kingdom), funded by the University of Giessen.

Disclosures

Dr Tello has received speaking fees from Actelion and Bayer. Dr Ghofrani has received consultancy fees from Bayer, Actelion, Pfizer, Merck, GSK, and Novartis; fees for participation in advisory boards from Bayer, Pfizer, GSK, Actelion, and Takeda; lecture fees from Bayer HealthCare, GSK, Actelion, and Encysive/Pfizer; industry-sponsored grants from Bayer HealthCare, Aires, Encysive/Pfizer, and Novartis; and sponsored grants from the German Research Foundation, Excellence Cluster Cardiopulmonary Research, and the German Ministry for Education and Research. Dr Naeije has relationships with drug companies, including AOPOrphan Pharmaceuticals, Actelion, Bayer, Reata, Lung Biotechnology Corporation, and United Therapeutics. In addition to being an investigator in trials involving these companies, relationships include consultancy service, research grants, and membership of scientific advisory boards. Dr Seeger has received speaker/consultancy fees from Pfizer and Bayer Pharma AG. Dr Sommer has received travel grants and speaking fees from Actelion and Bayer. Dr Wilhelm has nothing to disclose. Dr Gall has received fees from Actelion, AstraZeneca, Bayer, BMS, GSK, Janssen-Cilag, Lilly, MSD, Novartis, OMT, Pfizer, and United Therapeutics. Dr Richter has received support from United Therapeutics and Bayer; speaker fees from Actelion, Mundipharma, Roche, and OMT; and consultancy fees from Bayer. The other authors report no conflicts.

REFERENCES

1. Galiè N, Palazzini M, Manes A. Pulmonary arterial hypertension: from the kingdom of the near-dead to multiple clinical trial meta-analyses. *Eur Heart J*. 2010;31:2080–2086. doi: 10.1093/eurheartj/ehq152
2. Vonk-Noordegraaf A, Haddad F, Chin KM, Forfia PR, Kawut SM, Lumens J, Naeije R, Newman J, Oudiz RJ, Provencher S, Torbicki A, Voelkel NF, Hassoun PM. Right heart adaptation to pulmonary arterial hypertension: physiology and pathobiology. *J Am Coll Cardiol*. 2013;62(suppl 25):D22–D33. doi: 10.1016/j.jacc.2013.10.027
3. Naeije R, Manes A. The right ventricle in pulmonary arterial hypertension. *Eur Respir Rev*. 2014;23:476–487. doi: 10.1183/09059180.00007414
4. Vonk Noordegraaf A, Westerhof BE, Westerhof N. The relationship between the right ventricle and its load in pulmonary hypertension. *J Am Coll Cardiol*. 2017;69:236–243. doi: 10.1016/j.jacc.2016.10.047
5. Trip P, Rain S, Handoko ML, van der Bruggen C, Bogaard HJ, Marcus JT, Boonstra A, Westerhof N, Vonk-Noordegraaf A, de Man FS. Clinical relevance of right ventricular diastolic stiffness in pulmonary hypertension. *Eur Respir J*. 2015;45:1603–1612. doi: 10.1183/09031936.00156714
6. van Wolferen SA, Marcus JT, Boonstra A, Marques KM, Bronzwaer JG, Spreeuwenberg MD, Postmus PE, Vonk-Noordegraaf A. Prognostic value of right ventricular mass, volume, and function in idiopathic pulmonary arterial hypertension. *Eur Heart J*. 2007;28:1250–1257. doi: 10.1093/eurheartj/ehl477
7. Badagliacca R, Poscia R, Pezzuto B, Papa S, Pesce F, Manzi G, Giannetta E, Raineri C, Schina M, Sciomer S, Parola D, Francone M, Carbone I, Fedele F, Vizza CD. Right ventricular concentric hypertrophy and clinical worsening in idiopathic pulmonary arterial hypertension. *J Heart Lung Transplant*. 2016;35:1321–1329. doi: 10.1016/j.healun.2016.04.006
8. Baggen VJ, Leiner T, Post MC, van Dijk AP, Roos-Hesselink JW, Boersma E, Habets J, Sieswerda GT. Cardiac magnetic resonance findings predicting mortality in patients with pulmonary arterial hypertension: a systematic review and meta-analysis. *Eur Radiol*. 2016;26:3771–3780. doi: 10.1007/s00330-016-4217-6
9. García-Álvarez A, García-Lunar I, Pereda D, Fernández-Jimenez R, Sánchez-González J, Mirelis JG, Nuño-Ayala M, Sánchez-Quintana D, Fernández-Friera L, García-Ruiz JM, Pizarro G, Agüero J, Campelos P, Castellá M, Sabaté M, Fuster V, Sanz J, Ibañez B. Association of myocardial T1-mapping CMR with hemodynamics and RV performance in pulmonary hypertension. *JACC Cardiovasc Imaging*. 2015;8:76–82. doi: 10.1016/j.jcmg.2014.08.012
10. Sanz J, Kariisa M, Dellegrottaglie S, Prat-González S, Garcia MJ, Fuster V, Rajagopalan S. Evaluation of pulmonary artery stiffness in pulmonary hypertension with cardiac magnetic resonance. *JACC Cardiovasc Imaging*. 2009;2:286–295. doi: 10.1016/j.jcmg.2008.08.007
11. Galiè N, Humbert M, Vachiery JL, Gibbs S, Lang I, Torbicki A, Simonneau G, Peacock A, Vonk Noordegraaf A, Beghetti M, Ghofrani A, Gomez Sanchez MA, Hansmann G, Klepetko W, Lancellotti P, Matucci M, McDonagh T, Pierard LA, Trindade PT, Zompatori M, Hoeper M. 2015 ESC/ERS Guidelines for the diagnosis and treatment of pulmonary hypertension: The joint task force for the diagnosis and treatment of pulmonary hypertension of the European Society of Cardiology (ESC) and the European Respiratory Society (ERS): endorsed by: Association for European Paediatric and Congenital Cardiology (AEPC), International Society for Heart and Lung Transplantation (ISHLT). *Eur Respir J*. 2015;46:903–975. doi: 10.1183/13993003.01032-2015
12. Gall H, Felix JF, Schneck FK, Milger K, Sommer N, Voswinckel R, Franco OH, Hofman A, Schermuly RT, Weissmann N, Grimminger F, Seeger W, Ghofrani HA. The Giessen Pulmonary Hypertension Registry: survival in pulmonary hypertension subgroups. *J Heart Lung Transplant*. 2017;36:957–967. doi: 10.1016/j.healun.2017.02.016
13. Roller FC, Wiedenroth C, Breithecker A, Liebetrau C, Mayer E, Schneider C, Rolf A, Hamm C, Krombach GA. Native T1 mapping and extracellular volume fraction measurement for assessment of right ventricular insertion point and septal fibrosis in chronic thromboembolic pulmonary hypertension. *Eur Radiol*. 2017;27:1980–1991. doi: 10.1007/s00330-016-4585-y

14. Brimioulle S, Wauthy P, Ewalenko P, Rondelet B, Vermeulen F, Kerbaul F, Naeije R. Single-beat estimation of right ventricular end-systolic pressure-volume relationship. *Am J Physiol Heart Circ Physiol*. 2003;284:H1625–H1630. doi: 10.1152/ajpheart.01023.2002
15. Rain S, Handoko ML, Trip P, Gan CT, Westerhof N, Stienen GJ, Paulus WJ, Ottenheijm CA, Marcus JT, Dorfmüller P, Guignabert C, Humbert M, Macdonald P, Dos Remedios C, Postmus PE, Saripalli C, Hidalgo CG, Granzier HL, Vonk-Noordegraaf A, van der Velden J, de Man FS. Right ventricular diastolic impairment in patients with pulmonary arterial hypertension. *Circulation*. 2013;128:2016–25, 1. doi: 10.1161/CIRCULATIONAHA.113.001873
16. Tello K, Richter MJ, Axmann J, Buhmann M, Seeger W, Naeije R, Ghofrani HA, Gall H. More on single-beat estimation of right ventriculoarterial coupling in pulmonary arterial hypertension. *Am J Respir Crit Care Med*. 2018;198:816–818. doi: 10.1164/rccm.201802-0283LE
17. Lee H, Park JB, Yoon YE, Park EA, Kim HK, Lee W, Kim YJ, Cho GY, Sohn DW, Greiser A, Lee SP. Noncontrast myocardial T1 mapping by cardiac magnetic resonance predicts outcome in patients with aortic stenosis. *JACC Cardiovasc Imaging*. 2018;11:974–983. doi: 10.1016/j.jcmg.2017.09.005
18. Sanz J, García-Alvarez A, Fernández-Friera L, Nair A, Mirelis JG, Sawit ST, Pinney S, Fuster V. Right ventriculo-arterial coupling in pulmonary hypertension: a magnetic resonance study. *Heart*. 2012;98:238–243. doi: 10.1136/heartjnl-2011-300462
19. Bewick V, Cheek L, Ball J. Statistics review 10: further nonparametric methods. *Crit Care*. 2004;8:196–199. doi: 10.1186/cc2857
20. Ruopp MD, Perkins NJ, Whitcomb BW, Schisterman EF. Youden Index and optimal cut-point estimated from observations affected by a lower limit of detection. *Biom J*. 2008;50:419–430. doi: 10.1002/bimj.200710415
21. Vanderpool RR, Rischard F, Naeije R, Hunter K, Simon MA. Simple functional imaging of the right ventricle in pulmonary hypertension: can right ventricular ejection fraction be improved? *Int J Cardiol*. 2016;223:93–94. doi: 10.1016/j.ijcard.2016.08.138
22. Brewis MJ, Bellofiore A, Vanderpool RR, Chesler NC, Johnson MK, Naeije R, Peacock AJ. Imaging right ventricular function to predict outcome in pulmonary arterial hypertension. *Int J Cardiol*. 2016;218:206–211. doi: 10.1016/j.ijcard.2016.05.015
23. van de Veerdonk MC, Kind T, Marcus JT, Mauritz GJ, Heymans MW, Bogaard HJ, Boonstra A, Marques KM, Westerhof N, Vonk-Noordegraaf A. Progressive right ventricular dysfunction in patients with pulmonary arterial hypertension responding to therapy. *J Am Coll Cardiol*. 2011;58:2511–9.
24. Vanderpool RR, Pinsky MR, Naeije R, Deible C, Kosaraju V, Bunner C, Mathier MA, Lacomis J, Champion HC, Simon MA. RV-pulmonary arterial coupling predicts outcome in patients referred for pulmonary hypertension. *Heart*. 2015;101:37–43. doi: 10.1136/heartjnl-2014-306142
25. Petersen SE, Aung N, Sanghvi MM, Zemrak F, Fung K, Paiva JM, Francis JM, Khanji MY, Lukaschuk E, Lee AM, Carapella V, Kim YJ, Leeson P, Piechnik SK, Neubauer S. Reference ranges for cardiac structure and function using cardiovascular magnetic resonance (CMR) in Caucasians from the UK Biobank population cohort. *J Cardiovasc Magn Reson*. 2017;19:18. doi: 10.1186/s12968-017-0327-9
26. van de Veerdonk MC, Marcus JT, Westerhof N, de Man FS, Boonstra A, Heymans MW, Bogaard HJ, Vonk Noordegraaf A. Signs of right ventricular deterioration in clinically stable patients with pulmonary arterial hypertension. *Chest*. 2015;147:1063–1071.
27. Kuehne T, Yilmaz S, Steendijk P, Moore P, Groenink M, Saaed M, Weber O, Higgins CB, Ewert P, Fleck E, Nagel E, Schulze-Neick I, Lange P. Magnetic resonance imaging analysis of right ventricular pressure-volume loops: *in vivo* validation and clinical application in patients with pulmonary hypertension. *Circulation*. 2004;110:2010–2016. doi: 10.1161/01.CIR.0000143138.02493.DD
28. Tedford RJ, Mudd JO, Girgis RE, Mathai SC, Zaiman AL, Housten-Harris T, Boyce D, Kelemen BW, Bacher AC, Shah AA, Hummers LK, Wigley FM, Russell SD, Saggar R, Saggar R, Maughan WL, Hassoun PM, Kass DA. Right ventricular dysfunction in systemic sclerosis-associated pulmonary arterial hypertension. *Circ Heart Fail*. 2013;6:953–963. doi: 10.1161/CIRCHEARTFAILURE.112.000008
29. Spruijt OA, de Man FS, Groepenhoff H, Oosterveer F, Westerhof N, Vonk-Noordegraaf A, Bogaard HJ. The effects of exercise on right ventricular contractility and right ventricular-arterial coupling in pulmonary hypertension. *Am J Respir Crit Care Med*. 2015;191:1050–1057. doi: 10.1164/rccm.201412-2271OC
30. Hsu S, Houston BA, Tampakakis E, Bacher AC, Rhodes PS, Mathai SC, Damico RL, Kolb TM, Hummers LK, Shah AA, McMahan Z, Corona-Villalobos CP, Zimmerman SL, Wigley FM, Hassoun PM, Kass DA, Tedford RJ. Right ventricular functional reserve in pulmonary arterial hypertension. *Circulation*. 2016;133:2413–2422. doi: 10.1161/CIRCULATIONAHA.116.022082
31. McCabe C, White PA, Rana BS, Gopalan D, Agrawal B, Pepke-Zaba J, Hoole SP. Right ventricle functional assessment: have new techniques supplanted the old faithful conductance catheter? *Cardiol Rev*. 2014;22:233–240. doi: 10.1097/CRD.0000000000000020
32. Wauthy P, Naeije R, Brimioulle S. Left and right ventriculo-arterial coupling in a patient with congenitally corrected transposition. *Cardiol Young*. 2005;15:647–649. doi: 10.1017/S1047951105001848
33. Vanderpool RR, Desai AA, Knapp SM, Simon MA, Abidov A, Yuan JX, Garcia JGN, Hansen LM, Knoper SR, Naeije R, Rischard FP. How prostacyclin therapy improves right ventricular function in pulmonary arterial hypertension. *Eur Respir J*. 2017;50:1700764.
34. Ghuysen A, Lambermont B, Kolh P, Tchana-Sato V, Magis D, Gerard P, Mommens V, Janssen N, Desaive T, D'Orio V. Alteration of right ventricular-pulmonary vascular coupling in a porcine model of progressive pressure overloading. *Shock*. 2008;29:197–204. doi: 10.1097/SHK.0b013e318070c790
35. Fourie PR, Coetzee AR, Bolliger CT. Pulmonary artery compliance: its role in right ventricular-arterial coupling. *Cardiovasc Res*. 1992;26:839–844.
36. Rex S, Missant C, Claus P, Buhre W, Wouters PF. Effects of inhaled iloprost on right ventricular contractility, right ventriculo-vascular coupling and ventricular interdependence: a randomized placebo-controlled trial in an experimental model of acute pulmonary hypertension. *Crit Care*. 2008;12:R113. doi: 10.1186/cc7005
37. De Tombe PP, Jones S, Burkhoff D, Hunter WC, Kass DA. Ventricular stroke work and efficiency both remain nearly optimal despite altered vascular loading. *Am J Physiol*. 1993;264(6 pt 2):H1817–H1824. doi: 10.1152/ajpheart.1993.264.6.H1817
38. Axell RG, Messer SJ, White PA, McCabe C, Priest A, Statopoulou T, Drozdzynska M, Viscasillas J, Hinchy EC, Hampton-Till J, Alibhai HI, Morrell N, Pepke-Zaba J, Large SR, Hoole SP. Ventriculo-arterial coupling detects occult RV dysfunction in chronic thromboembolic pulmonary vascular disease. *Physiol Rep*. 2017;5:e13227.
39. Inuzuka R, Hsu S, Tedford RJ, Senzaki H. Single-beat estimation of right ventricular contractility and its coupling to pulmonary arterial load in patients with pulmonary hypertension. *J Am Heart Assoc*. 2018;7:e007929.
40. Crowe T, Jayasekera G, Peacock AJ. Non-invasive imaging of global and regional cardiac function in pulmonary hypertension. *Pulm Circ*. 2018;8:2045893217742000. doi: 10.1177/2045893217742000
41. Spruijt OA, Vissers L, Bogaard HJ, Hofman MB, Vonk-Noordegraaf A, Marcus JT. Increased native T1-values at the interventricular insertion regions in precapillary pulmonary hypertension. *Int J Cardiovasc Imaging*. 2016;32:451–459. doi: 10.1007/s10554-015-0787-7
42. Rain S, Andersen S, Najafi A, Gammelgaard Schultz J, da Silva Goncalves Bos D, Handoko ML, Bogaard HJ, Vonk-Noordegraaf A, Andersen A, van der Velden J, Ottenheijm CA, de Man FS. Right ventricular myocardial stiffness in experimental pulmonary arterial hypertension: relative contribution of fibrosis and myofibril stiffness. *Circ Heart Fail*. 2016;9:e002636. doi: 10.1161/CIRCHEARTFAILURE.115.002636
43. Messroghli DR, Moon JC, Ferreira VM, Grosse-Wortmann L, He T, Kellman P, Mascherbauer J, Nezafat R, Salerno M, Schelbert EB, Taylor AJ, Thompson R, Ugander M, van Heeswijk RB, Friedrich MG. Clinical recommendations for cardiovascular magnetic resonance mapping of T1, T2, T2* and extracellular volume: a consensus statement by the Society for Cardiovascular Magnetic Resonance (SCMR) endorsed by the European Association for Cardiovascular Imaging (EACVI). *J Cardiovasc Magn Reson*. 2017;19:75. doi: 10.1186/s12968-017-0389-8
44. Wang J, Zhao H, Wang Y, Herrmann HC, Witschey WRT, Han Y. Native T1 and T2 mapping by cardiovascular magnetic resonance imaging in pressure overloaded left and right heart diseases. *J Thorac Dis*. 2018;10:2968–2975. doi: 10.21037/jtd.2018.04.141

Anlage G

Impaired right ventricular lusitropy is associated with ventilatory inefficiency in pulmonary arterial hypertension.

Tello K, Dalmer A, Vanderpool R, Ghofrani HA, Naeije R, Roller F, Seeger W, Dumitrescu D, Sommer N, Brunst A, Gall H, Richter MJ. Eur Respir J. 2019 Nov 21;54(5)

Impaired right ventricular lusitropy is associated with ventilatory inefficiency in pulmonary arterial hypertension

Khodr Tello[1], Antonia Dalmer[1], Rebecca Vanderpool[2], Hossein A. Ghofrani[1,3,4], Robert Naeije[5], Fritz Roller[6], Werner Seeger[1], Daniel Dumitrescu[7], Natascha Sommer[1], Anne Brunst[1], Henning Gall[1] and Manuel J. Richter[1]

Affiliations: [1]Dept of Internal Medicine, Justus-Liebig-University Giessen, Universities of Giessen and Marburg Lung Center (UGMLC), Member of the German Center for Lung Research (DZL), Giessen, Germany. [2]University of Arizona, Tucson, AZ, USA. [3]Dept of Pneumology, Kerckhoff Heart, Rheuma and Thoracic Center, Bad Nauheim, Germany. [4]Dept of Medicine, Imperial College London, London, UK. [5]Erasme University Hospital, Brussels, Belgium. [6]Dept of Radiology, Justus-Liebig-University Giessen, Universities of Giessen and Marburg Lung Center (UGMLC), Member of the German Center for Lung Research (DZL), Giessen, Germany. [7]Dept of Cardiology, Heart and Diabetes Center NRW, Ruhr University Bochum, Bad Oeynhausen, Germany.

Correspondence: Khodr Tello, Dept of Internal Medicine, Justus-Liebig-University Giessen, Klinikstrasse 32, 35392 Giessen, Germany. E-mail: Khodr.Tello@innere.med.uni-giessen.de

@ERSpublications
Right ventricular diastolic stiffness and afterload (pressure–volume loop measurement) are associated with ventilatory inefficiency during exercise and may contribute to dyspnoea *via* increased chemosensitivity in pulmonary arterial hypertension http://bit.ly/30lLy9t

Cite this article as: Tello K, Dalmer A, Vanderpool R, *et al*. Impaired right ventricular lusitropy is associated with ventilatory inefficiency in pulmonary arterial hypertension. *Eur Respir J* 2019; 54: 1900342 [https://doi.org/10.1183/13993003.00342-2019].

ABSTRACT Cardiopulmonary exercise testing (CPET) is an important tool for assessing functional capacity and prognosis in pulmonary arterial hypertension (PAH). However, the associations of CPET parameters with the adaptation of right ventricular (RV) function to afterload remain incompletely understood.

In this study, 37 patients with PAH (idiopathic in 31 cases) underwent single-beat pressure–volume loop measurements of RV end-systolic elastance (Ees), arterial elastance (Ea) and diastolic elastance (Eed). Pulmonary arterial stiffness was assessed by magnetic resonance imaging. The results were correlated to CPET variables. The predictive relevance of RV function parameters for clinically relevant ventilatory inefficiency, defined as minute ventilation/carbon dioxide production (V'_E/V'_{CO_2}) slope >48, was evaluated using logistic regression analysis.

The median (interquartile range) of the V'_E/V'_{CO_2} slope was 42 (32–52) and the V'_E/V'_{CO_2} nadir was 40 (31–44). The mean±SD of peak end-tidal carbon dioxide tension (P_{ETCO_2}) was 23±8 mmHg. Ea, Eed and parameters reflecting pulmonary arterial stiffness (capacitance and distensibility) correlated with the V'_E/V'_{CO_2} slope, V'_E/V'_{CO_2} nadir, P_{ETCO_2} and peak oxygen pulse. RV Ees and RV–arterial coupling as assessed by the Ees/Ea ratio showed no correlations with CPET parameters. Ea (univariate OR 7.28, 95% CI 1.20–44.04) and Eed (univariate OR 2.21, 95% CI 0.93–5.26) were significantly associated with ventilatory inefficiency ($p<0.10$).

Our data suggest that impaired RV lusitropy and increased afterload are associated with ventilatory inefficiency in PAH.

This article has supplementary material available from erj.ersjournals.com

Individual participant data that underlie the results reported in this article, after de-identification, may be shared upon reasonable request, subject to approval from the Right Heart I study committee.

Received: 18 Feb 2019 | Accepted after revision: 15 Aug 2019

Introduction

Shortness of breath dominates the symptomatology of pulmonary arterial hypertension (PAH). Much of it is related to an excess of ventilation (V'_E) at any level of metabolic rate, as defined by an elevated V'_E/carbon dioxide output (V'_{CO_2}) slope during a cardiopulmonary exercise test (CPET) [1, 2]. An increase in V'_E/V'_{CO_2} slope is an important predictor of outcome in patients with PAH [3, 4] and evaluating the V'_E/V'_{CO_2} slope has therefore been recommended as part of the risk assessment in these patients [5]. However, the pathophysiology of PAH is currently understood to depend on the adaptation of right ventricular (RV) function to afterload [6–8]. Thus, symptomatology and survival in these patients is critically dependent on the adequacy of RV–pulmonary arterial (PA) coupling, as defined by a preserved ratio of end-systolic elastance (Ees) to arterial elastance (Ea) at a normally low end-diastolic elastance (Eed) [6–8]. Although the V'_E/V'_{CO_2} slope has previously shown associations with other parameters reflecting RV afterload and function in heart failure [9, 10], the relationship of wasted ventilation to Ees/Ea and Eed in PAH remains incompletely understood.

We therefore investigated RV function by invasive determination of RV pressure–volume loops to calculate Ees, Ea and Eed and related the results to V'_E/V'_{CO_2} slope or nadir and other CPET parameters previously reported to be of relevance, such as peak oxygen uptake (V'_{O_2}) and O_2 pulse [11]. We also measured PA compliance as an important determinant of RV afterload by magnetic resonance imaging (MRI) [12].

Methods

Study design and patients

For the current analysis, we included consecutive patients with PAH who were prospectively enrolled into the Right Heart I study (NCT03403868) and the Giessen Pulmonary Hypertension Registry [13] between January 2016 and April 2019. A subset of the patients had also been included in previously published analyses from the Right Heart I study [14–17]. The patients were diagnosed according to current recommendations [5], and each diagnosis was assessed by a multidisciplinary board (including pulmonary physicians and radiologists) before enrolment. All patients underwent CPET, MRI and pressure–volume/Swan-Ganz catheterisation. PAH therapies were administered based on clinical grounds and best standard of care. B-type natriuretic peptide (BNP) was measured with a fully automated, two-site sandwich immunoassay (ADVIA Centaur BNP Test; Siemens Healthineers, Erlangen, Germany). Diffusion capacity of the lung for carbon monoxide (D_{LCO}) was measured by the single-breath technique [18]. All participating patients gave written informed consent for enrolment into the Right Heart I study. The investigation conformed to the principles of the Declaration of Helsinki and was approved by the ethics committee of the Faculty of Medicine at the University of Giessen (approval no. 108/15).

Cardiopulmonary exercise testing

All patients underwent symptom-limited incremental CPET (Vmax 229® system; Carefusion®, now part of Vyaire™ Medical, Yorba Linda, CA, USA) using a cycle ergometer in a semi-supine position and wearing a face mask. After an initial baseline measurement without exercise for 2 min, exercise was initiated at a work rate of 10–30 W, which was increased by 10–30 W every 1–2 min using a stepwise protocol as published previously [19]. Blood gases were analysed at rest and maximal exercise (from the hyperaemic ear lobe); heart rate was continuously monitored and a noninvasive blood pressure measurement was performed every 2 min. Peak oxygen uptake (V'_{O_2}) was defined as the V'_{O_2} measured during the last 30 s of peak exercise. The respiratory exchange ratio (RER) was calculated as V'_{CO_2}/V'_{O_2}, and O_2 pulse as V'_{O_2}/heart rate. The ventilatory equivalents for carbon dioxide were calculated by dividing V'_E (corrected for equipment external dead space) by V'_{CO_2}. V'_E/V'_{CO_2} slopes were measured between warm up and anaerobic threshold. The nadir of V'_E/V'_{CO_2} was assessed as described previously [20]. Arterial carbon dioxide tension (P_{aCO_2}) to end-tidal carbon dioxide tension (P_{ETCO_2}) carbon dioxide gradient ($P_{(a-ET)CO_2}$) was measured at rest and during exercise [19].

Magnetic resonance imaging

Imaging was performed with the Avanto 1.5 Tesla scanner system (Siemens Healthineers; gradient strength and slew rate: SQ-Engine (45 $mT \cdot m^{-1}$ at 200 $T \cdot m^{-1} \cdot s^{-1}$)). Stiffness, distensibility and capacitance of the pulmonary arteries were measured as described in detail previously [12].

Right heart catheterisation

Resting right heart catheterisation was performed as described previously [21]. Pressure values were continuously assessed. Cardiac index was measured using the direct or indirect Fick method as available. Pulmonary vascular resistance (PVR) was calculated as (mean pulmonary arterial pressure (mPAP)–pulmonary arterial wedge pressure)/cardiac output [5].

Pressure–volume catheterisation

Pressure–volume catheterisation was performed and pressure–volume loops were generated as described previously [14]. Ees was calculated using the single-beat method for the right ventricle, and Ea was calculated as end-systolic pressure/stroke volume [22]. RV–PA coupling was calculated as Ees/Ea. A diastolic stiffness factor β was calculated as described previously by a nonlinear fit of diastolic pressure–volume coordinates as $p=\alpha(e^{\beta V}-1)$ (where p is pressure, V is volume and α is a curve-fitting parameter) through the diastolic portion of the pressure–volume loops using a custom MATLAB program [23–25]. Three points (origin (0,0), beginning diastolic point and end-diastolic point) were used for the exponential fit. Eed was obtained from the relationship $dP/dV=\alpha\beta\times e^{\beta\times\text{end-diastolic volume}}$ at calculated end-diastolic volumes [23, 25, 26]. Volume measurements were calibrated with MRI data.

Statistical analyses

Histograms were visually assessed and the Kolmogorov–Smirnov test was used to determine adherence to a Gaussian distribution. Associations of functional parameters (derived from CPET) with pressure–volume variables and PA parameters were measured with Spearman's rank correlation coefficient; lines show least-squares fits of straight-line models. In addition, Ea and Eed were stratified according to the categories of V'_E/V'_{CO_2} slope proposed for risk assessment of patients with PAH in current guidelines [5]. Between-group differences were analysed with the Kruskal–Wallis test or unpaired t-tests as appropriate. For these analyses, $p<0.05$ was considered statistically significant.

TABLE 1 Clinical characteristics

	Patients with PAH
Subjects n	37
Sex	
Male	17
Female	20
Age years	50±14
PAH subtype	
Idiopathic PAH	31 (84)
Heritable PAH	2 (5)
PAH associated with	4 (11)
HIV infection	1
Connective tissue disease	3
Treatment	
PDE5i	16 (43)
ERA	22 (59)
sGC stimulator	14 (38)
Prostanoid	8 (22)
Selexipag	3 (8)
Combination therapy	
Dual therapy	10 (27)
Triple therapy	9 (24)
WHO functional class[#]	
I	2 (6)
II	17 (47)
III	17 (47)
BNP[¶] **pg·mL^{-1}**	66 (26–177)
D_{LCO}[#] **% predicted**	61 (48–71)
Right heart catheterisation	
mPAP mmHg	38 (34–54)
RAP mmHg	6±3
PVR Wood units	6.6 (4.3–10.4)
Cardiac index L·min^{-1}·m^{-2}	2.8±0.7
PAWP mmHg	9±3

Data are presented as n (%), mean±SD and median (interquartile range), unless otherwise indicated. PAH: pulmonary arterial hypertension; PDE5i: phosphodiesterase type 5 inhibitor; ERA: endothelin receptor antagonist; sGC: soluble guanylate cyclase; WHO: World Health Organization; BNP: B-type natriuretic peptide; D_{LCO}: diffusion capacity of the lung for carbon monoxide; mPAP: mean pulmonary artery pressure; RAP: right atrial pressure; PVR: pulmonary vascular resistance; PAWP: pulmonary artery wedge pressure. [#]: n=36; [¶]: n=35.

To determine which pressure–volume loop parameter is most strongly related to ventilatory inefficiency based on the previously recommended prognostically relevant cut-off value of >48 for V'_E/V'_{CO_2} slope [4, 27], Ea, Ees, Ees/Ea and Eed were included in a univariate logistic binary regression analysis as continuous variables. We then built a multivariate model including BNP, sex, Ea and Eed; multicollinearity was assessed using the variance inflation factor. For the regression analysis, p<0.10 was considered statistically significant.

SPSS version 23.0 (IBM, Armonk, NY, USA) was used for statistical analyses.

Results

Patients

In total, 37 patients with PAH were included in the analysis; the majority of the patients (84%) presented with idiopathic PAH (table 1). A substantial proportion of the patients were already receiving double or

TABLE 2 Right ventricular pressure–volume loop measurements and CPET and MRI-derived parameters

	Patients with PAH
Subjects n	37
Pressure–volume loop measurements	
Ea mmHg·mL^{-1}	0.69 (0.46–1.04)
Ees mmHg·mL^{-1}	0.61 (0.45–0.78)
Ees/Ea ratio	0.88 (0.50–1.24)
Eed mmHg·mL^{-1}	0.12 (0.05–0.22)
Tau ms	32 (28–40)
EDP mmHg	6 (4–11)
ESP mmHg	54 (44–81)
MRI measurements	
Stiffness index β[#]	4.2 (3.0–6.0)
Capacitance[¶] mL·mmHg^{-1}	2.2 (1.5–3.1)
Distensibility[+] %·mmHg^{-1}	0.5 (0.3–0.7)
CPET	
V'_{O_2} rest L·min^{-1}	0.3±0.1
V'_{O_2} peak L·min^{-1}	1.1±0.4
V'_{O_2} peak mL·kg^{-1}·min^{-1}	13 (11–17)
V'_{O_2} peak % pred	56 (39–87)
V'_E rest L·min^{-1}	13 (10–16)
V'_E peak L·min^{-1}	46 (38–56)
O_2 pulse rest mL·beat^{-1}	4 (3–5)
O_2 pulse peak mL·beat^{-1}	8 (6–10)
V'_E/V'_{CO_2} rest[§]	42 (38–50)
V'_E/V'_{CO_2} peak[§]	41 (34–54)
V'_E/V'_{CO_2} nadir[§]	40 (31–44)
V'_E/V'_{CO_2} slope	42 (32–52)
P_{ETCO_2} rest mmHg	25±6
P_{ETCO_2} peak mmHg	23±8
P_{aCO_2} rest mmHg	32±6
P_{aCO_2} peak mmHg	33±6
P_{O_2} rest mmHg	67±13
P_{O_2} peak mmHg	69±18
$P_{(a-ET)CO_2}$ rest mmHg	7.7±5.1
$P_{(a-ET)CO_2}$ peak mmHg	9.8±4.5
RER rest	0.84 (0.74–0.93)
RER peak	1.01 (0.89–1.13)
Endurance time s	623±165
Work rate watts	60 (45–85)

Values represent mean±SD or median (interquartile range). PAH: pulmonary arterial hypertension; Ea: arterial elastance; Ees: end-systolic elastance; Eed: end-diastolic elastance; EDP: end-diastolic pressure; ESP: end-systolic pressure; MRI: magnetic resonance imaging; CPET: cardiopulmonary exercise testing; V'_{O_2}: oxygen uptake; V'_E: minute ventilation; V'_E/V'_{CO_2}: minute ventilation/carbon dioxide production (ventilatory equivalent for carbon dioxide); P_{ETCO_2}: end-tidal carbon dioxide tension; P_{aCO_2}: arterial carbon dioxide tension; P_{O_2}: oxygen tension; $P_{(a-ET)CO_2}$: arterial to end-tidal carbon dioxide tension gradient; RER: respiratory exchange ratio. [#]: n=33; [¶]: n=36; [+]: n=32; [§]: n=35.

triple combinations of drugs targeting the pulmonary circulation, and the majority presented in World Health Organization (WHO) functional classes II or III. Right heart catheterisation measurements showed that the patients had severe, chronic pressure overload. Mean D_{LCO} was 61% of predicted. Pressure–volume loop measurements (table 2) showed that the Ees/Ea ratio was lower than the optimal value for RV–PA coupling (1.5–2.0) [15]. MRI measurements revealed a high stiffness index β and low capacitance and distensibility in the pulmonary artery. CPET measurements showed an impaired peak work rate with low peak V'_{O_2} (in mL·min^{-1}·kg^{-1} and % predicted) and peak O_2 pulse, a high V'_E/V'_{CO_2} slope and a low P_{ETCO_2} at peak exercise. The $P_{(a-ET)CO_2}$ gradient was moderately elevated. Maximum RER slightly exceeded 1.

Association of CPET parameters with pressure–volume loop-derived measurements of RV function and afterload and MRI-derived measurements of PA stiffness

The pressure–volume loop-derived parameters Ea and Eed correlated with V'_E/V'_{CO_2} slope and peak P_{ETCO_2} (figure 1). In addition, Ea correlated with peak O_2 pulse. V'_E/V'_{CO_2} slope and peak P_{ETCO_2} also correlated with PVR (supplementary figure E1). Of note, Eed strongly correlated with resting cardiac index (supplementary figure E2). BNP levels correlated with Ea and Eed as well as V'_E/V'_{CO_2} slope and peak P_{ETCO_2} (supplementary figure E3). There were no correlations between Ees/Ea or Ees and CPET parameters (data not shown). There was no correlation between pressure–volume loop-derived measurements and peak V'_{O_2}. MRI-derived measurements of the stiffness of the pulmonary arteries correlated with V'_E/V'_{CO_2} slope, peak P_{ETCO_2} and peak O_2 pulse (figure 2). V'_E/V'_{CO_2} nadir showed even more significant correlations with Ea, Eed, stiffness of the pulmonary arteries, PVR and BNP than V'_E/V'_{CO_2} slope (figure 3).

Eed and Ea were related to V'_E/V'_{CO_2} slope cut-offs proposed for risk assessment of patients with PAH in current guidelines (figure 4) [5].

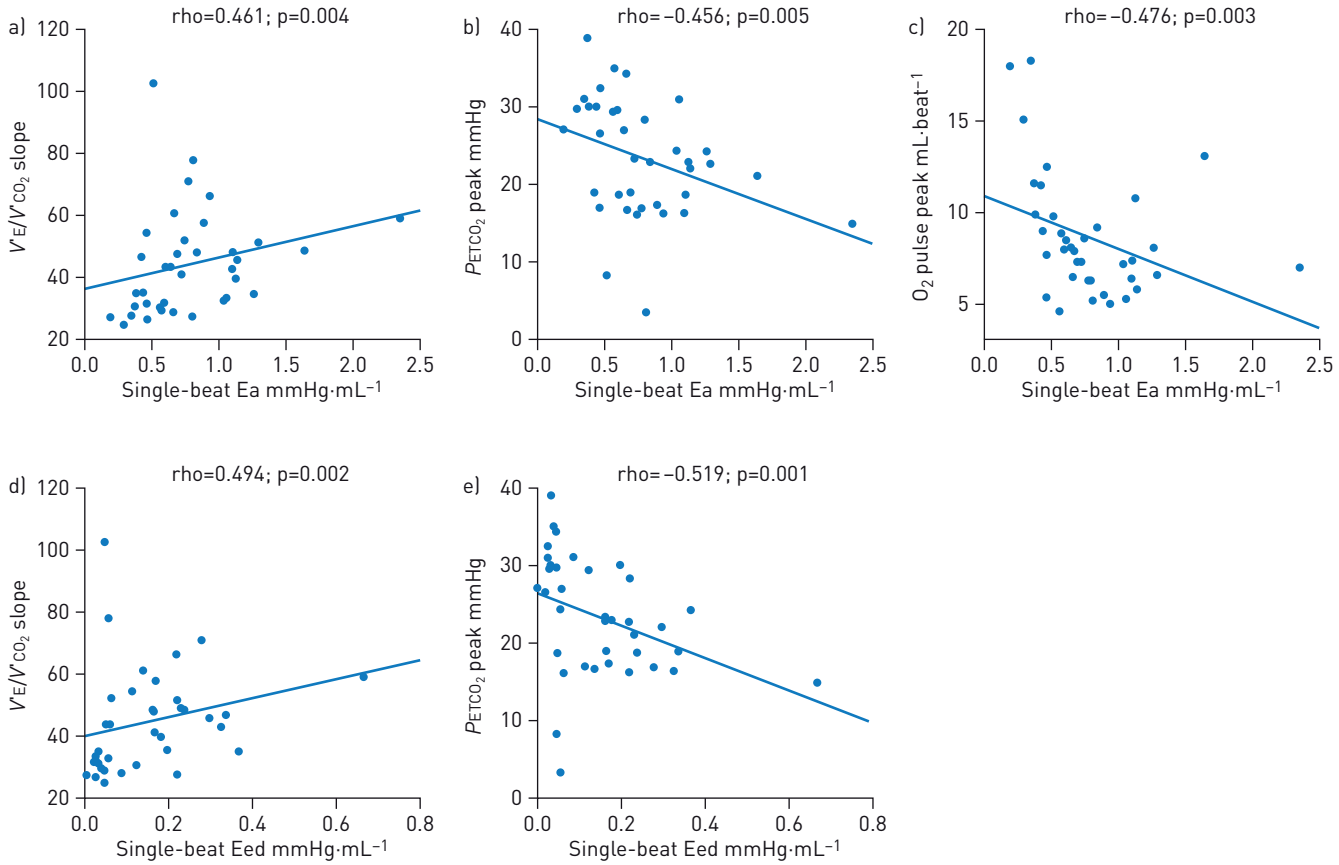

FIGURE 1 Association of cardiopulmonary exercise test parameters with single-beat pressure–volume loop-derived measurements of right ventricular a–c) afterload and d, e) diastolic stiffness. V'_E/V'_{CO_2}: minute ventilation/carbon dioxide production (ventilatory equivalent for carbon dioxide); Ea: arterial elastance; P_{ETCO_2}: end-tidal carbon dioxide tension; Eed: end-diastolic elastance.

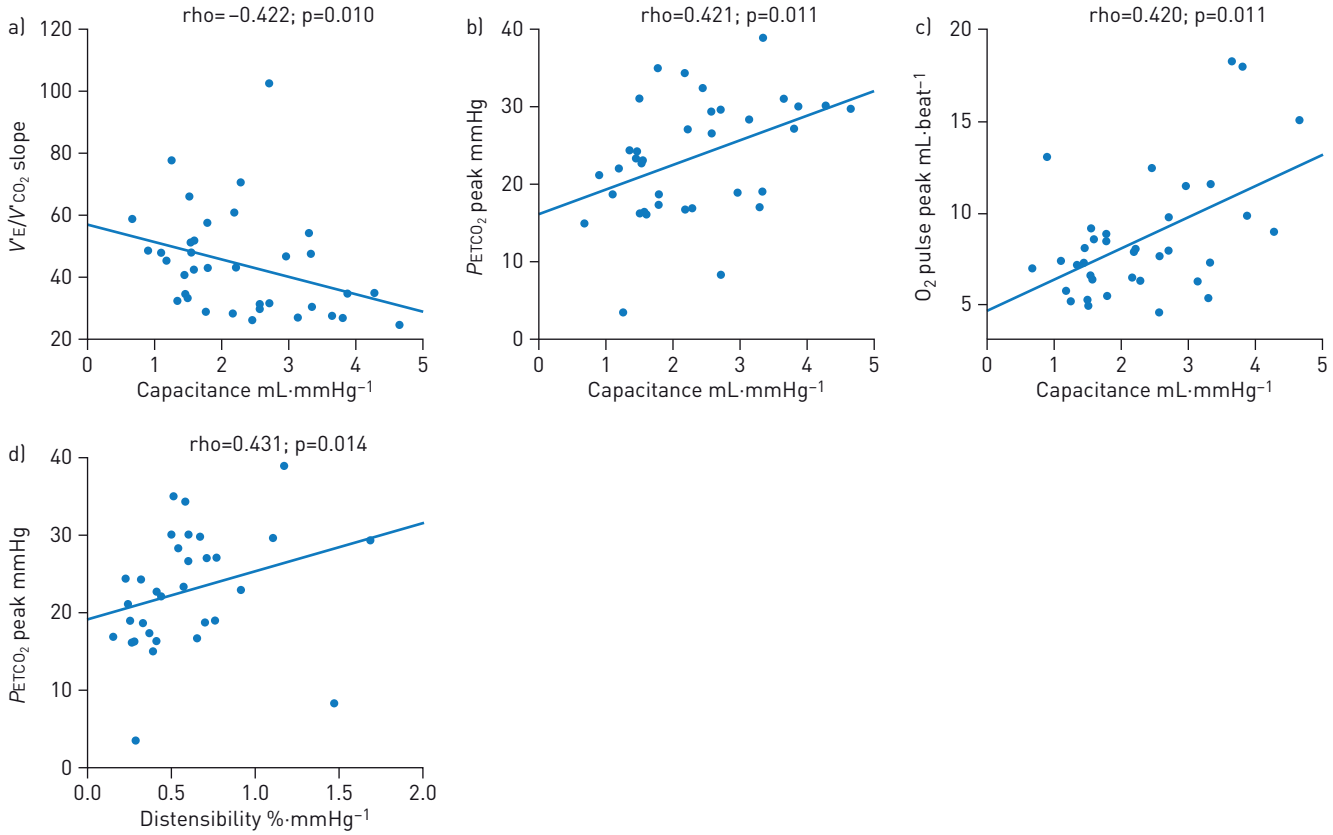

FIGURE 2 Association of cardiopulmonary exercise test parameters with magnetic resonance imaging-derived pulmonary arterial a–c) capacitance and d) distensibility. V'_E/V'_{CO_2}: minute ventilation/carbon dioxide production (ventilatory equivalent for carbon dioxide); P_{ETCO_2}: end-tidal carbon dioxide tension.

Predictive relevance of Ea and Eed for ventilatory inefficiency

In univariate logistic regression analysis, Ea (univariate OR 7.28, 95% CI 1.20–44.04, p=0.031) and Eed (univariate OR 2.21, 95% CI 0.93–5.26, p=0.073), but not Ees (univariate OR 1.04, p=0.955) or Ees/Ea (univariate OR 2.30, p=0.129), were significantly associated with ventilatory inefficiency (V'_E/V'_{CO_2} slope >48). A model including BNP, sex, Eed and Ea as predictor variables indicated superiority of Ea over Eed (Wald values 3.111 and 0.468, respectively). Multivariate odds ratios for the association of Ea and Eed with ventilatory inefficiency were 13.16 (95% CI 0.75–230.53, p=0.078) and 1.71 (95% CI 0.37–7.87, p=0.494), respectively.

Discussion

In the present study, both diastolic stiffness and increased afterload of the right ventricle were associated with exercise hyperventilation in patients with PAH, while RV contractility (Ees) in isolation or coupled to afterload (Ees/Ea) was not.

Hyperventilation in PAH is caused by a combination of increased dead space ventilation and increased chemosensitivity [1, 2]. In the present study, the $P_{(a-ET)CO_2}$ gradients were only moderately elevated, on average by 2–3 mmHg above the upper limit of normal of 5 mmHg [28], and both P_{ETCO_2} and P_{aCO_2} were low, arguing in favour of a dominant role of increased chemosensitivity [29]. Increased ventilatory responses to both hypercapnia and hypoxia have been reported in patients with severe pulmonary hypertension [30]. Consistent with those observations, increased sympathetic nervous system activity has been demonstrated by microneurography in patients with PAH [31]. Increased sympathetic nervous system activity predicts a poor prognosis in PAH [32], and an increased V'_E/V'_{CO_2} slope has also been identified as a predictor of poor prognosis in PAH, albeit with some variability between PAH subtypes [3, 4]. The mechanisms of increased chemosensitivity in PAH remain incompletely understood. Atrial septostomy has been reported to decrease sympathetic nervous system tone in PAH, in spite of right-to-left atrial shunt-induced hypoxaemia, which the authors explained by a reverse Bainbridge reflex [33]. Thus, right atrial (and RV) stretch or stiffness could be an important trigger of chemosensitivity and sympathetic nervous system tone in PAH. The increased BNP levels correlating with

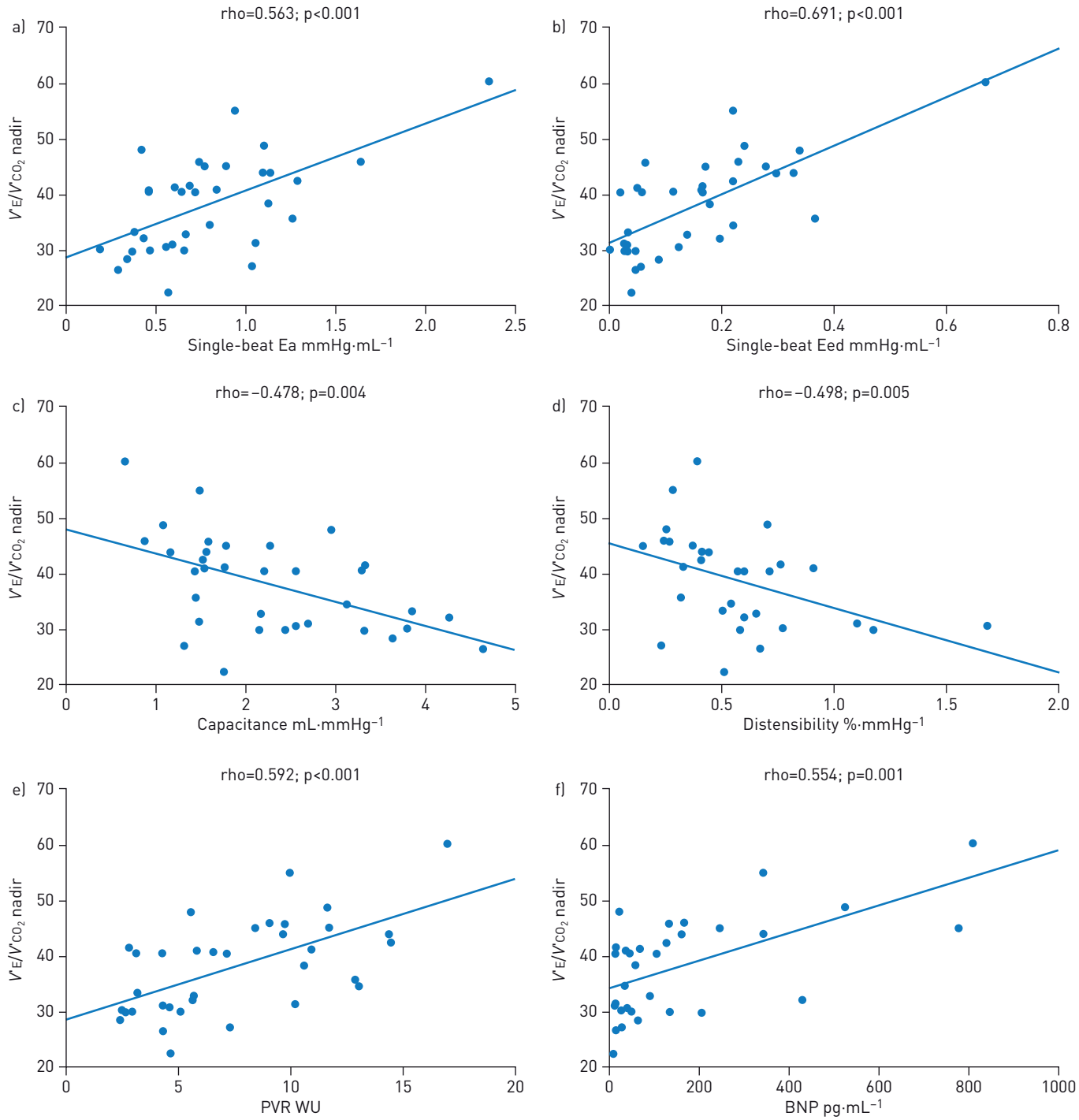

FIGURE 3 Association of V'_E/V'_{CO_2} nadir with a) single-beat arterial elastance (Ea), b) single-beat end-diastolic elastance (Eed), c) capacitance, d) distensibility, e) pulmonary vascular resistance (PVR) and f) B-type natriuretic peptide (BNP). V'_E/V'_{CO_2}: minute ventilation/carbon dioxide production (ventilatory equivalent for carbon dioxide); WU: Wood units.

increased V'_E/V'_{CO_2} in the present study support this mechanism, as does the observed prediction of ventilatory inefficiency by increased RV diastolic stiffness (Eed) in the presence of increased afterload (Ea). As illustrated in figure 5, plotting of V'_E/V'_{CO_2} as a function of P_{aCO_2} revealed a characteristic leftward shift of the curve (indicative of increased chemosensitivity [34]) in the patients with PAH who also had maladaptive high Eed (based on a previously described cut-off [17]). In addition, V'_E/V'_{CO_2} was substantially increased at rest and during exercise in patients with high *versus* low Eed (figure 5b).

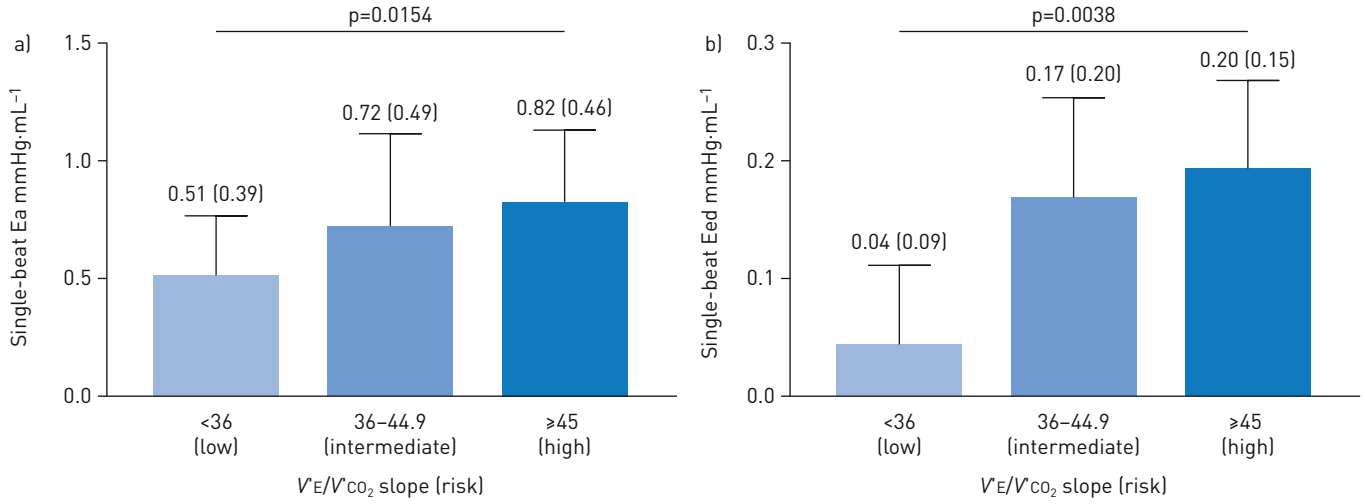

FIGURE 4 a) Afterload and b) right ventricular diastolic stiffness stratified according to the V'_E/V'_{CO_2} slope proposed for risk assessment of patients with pulmonary arterial hypertension in current guidelines [5]. Bar graphs show median and interquartile range. Statistical significance was assessed using the Kruskal–Wallis test. Ea: arterial elastance; V'_E/V'_{CO_2}: minute ventilation/carbon dioxide production (ventilatory equivalent for carbon dioxide); Eed: end-diastolic elastance.

Another possible reflex mechanism would be triggered by PA distension, but this is less convincingly supported by the available evidence. Nevertheless, we found a significant correlation between MRI-derived parameters of PA stiffness and exercise hyperventilation; this might be mediated *via* the association of these parameters with afterload [12] rather than a direct relationship.

The right ventricle in severe pulmonary hypertension initially adapts by increasing contractility to match the increased afterload [6, 7]. This "homeometric adaptation" is assessed by an Ees/Ea ratio determined from pressure–volume loops. When RV–PA coupling deteriorates, reflected by a progressive decrease in Ees/Ea, a "heterometric adaptation" (dimension-dependent) is turned on to preserve cardiac output responses to peripheral demand. This eventually occurs at the price of excessive RV dilatation and systemic congestion. We previously showed that RV–PA coupling in severe PAH has a lot of reserve, because the Ees/Ea ratio needs to decrease from normal values of 1.5–2 to <0.8 before excessive RV dilatation occurs [15]. While RV dilatation is an obvious cause of increased atrial and RV stretch and stiffness, diastolic elastance may also increase out of proportion to systolic elastance in the presence of increased afterload [23]. The present data indirectly support the occurrence of this dissociation because V'_E/V'_{CO_2} increased in association with Eed and Ea. Of note, a further differentiation of Ea and Eed according to the risk stratification cut-offs proposed for the V'_E/V'_{CO_2} slope in current guidelines [5] showed a distinctive pattern. This sub-differentiation revealed that even patients with an intermediate elevation of V'_E/V'_{CO_2} slope [5], and thus ventilatory inefficiency, had a substantial increase in Ea and Eed.

In the present study, RV Ees, Ea and Eed were determined using the single-beat method, which was experimentally validated in animals [22] and thereafter applied to patients with PAH [15, 35, 36]. The alternative would be to derive these measurements using a multiple-beat approach with families of RV pressure–volume loops obtained at decreasing venous return, as was initially reported in isolated heart preparations [37] and later applied to patients with PAH [38, 39]. A decrease in venous return can be obtained by inflating a balloon in the inferior vena cava [16] (although this additional invasive procedure may carry some risk and cause ethical concern) or by a Valsalva manoeuvre [38, 39]. However, it is not known how positive intrathoracic pressures affect RV–PA coupling. Furthermore, decreasing venous return may decrease Ees/Ea because of sympathetic nervous system activation leading to an increase in Ea [22]. On the other hand, the single-beat analysis depends on a maximum RV pressure calculation based on extrapolation of RV pressure curves, which may be technically challenging. Further studies are needed to validate single- and multiple-beat methods against each other. In the meantime, it is conceivable that Ees or Ees/Ea determined by different methods, while being consistent and tending to agree [40], may still differ in terms of correlation to V'_E/V'_{CO_2}. RV Ees and V'_E/V'_{CO_2} showed a borderline significant correlation (p=0.049) in a multiple-beat study of RV function in a mixed population of patients with systemic sclerosis-associated and idiopathic PAH [38], whereas this correlation did not achieve significance in the present single-beat study of patients with predominantly idiopathic PAH.

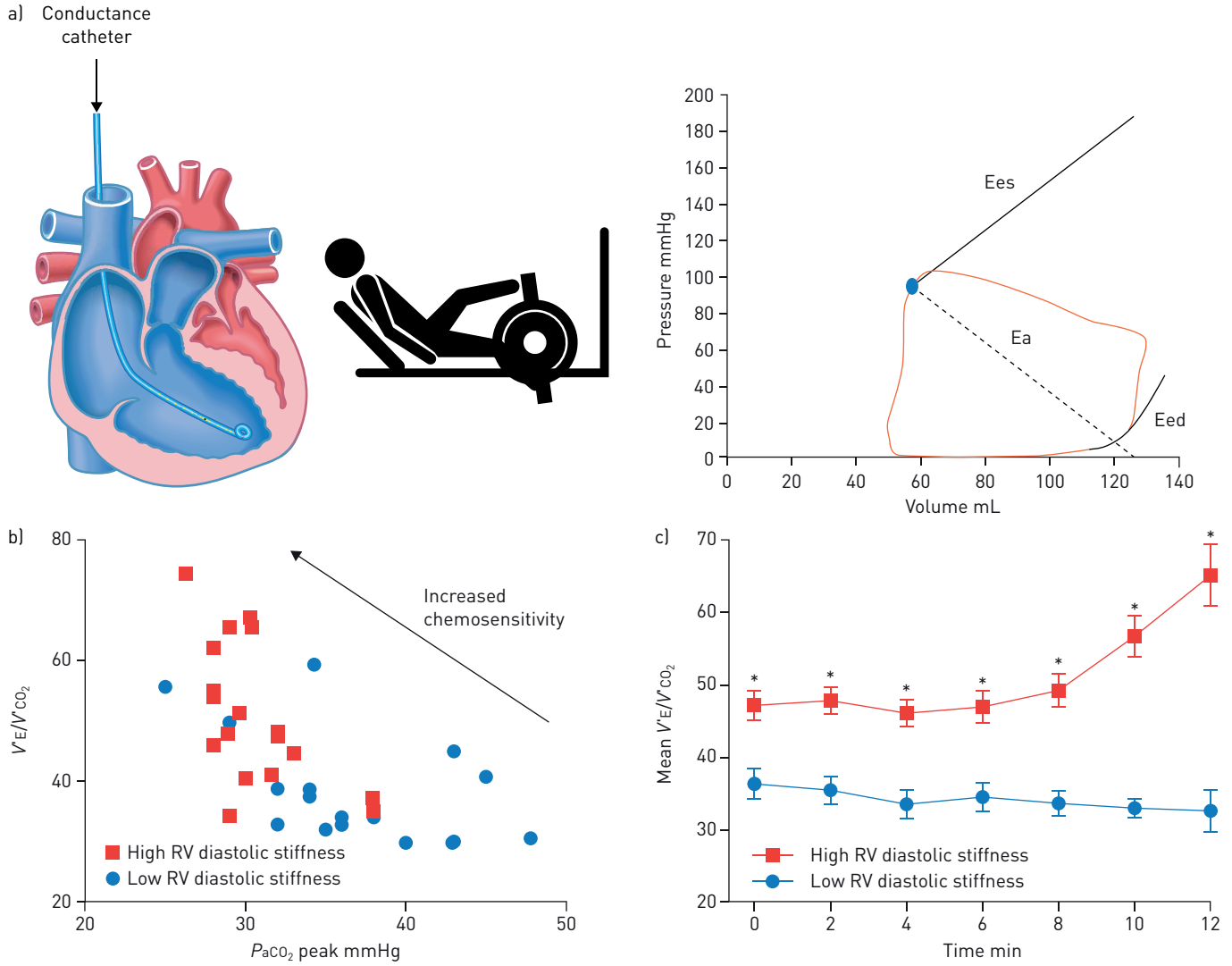

FIGURE 5 Pathophysiological concept of the association of increased diastolic stiffness with increased chemosensitivity in pulmonary arterial hypertension. a) Conductance catheterisation and cardiopulmonary exercise testing allow assessment of right ventricular (RV) diastolic stiffness (end-diastolic elastance (Eed)) and its relationship with chemosensitivity. b) A leftward shift of V'_E/V'_{CO_2} *versus* arterial carbon dioxide tension (P_{aCO_2}) plots to lower P_{aCO_2} and higher V'_E/V'_{CO_2} indicates increased chemosensitivity [34], which was found to be present in patients with high RV diastolic stiffness in the current study. c) V'_E/V'_{CO_2} at rest (0 min) and during symptom-limited incremental cycle exercise (2–12 min) was increased in patients with high *versus* low RV diastolic stiffness. High RV diastolic stiffness was defined as Eed>0.124 mmHg·mL^{-1} as previously described [17]. Error bars show standard error of the mean. *: p<0.01 (between-group differences analysed with unpaired t-test). Ea: arterial elastance; V'_E/V'_{CO_2}: minute ventilation/carbon dioxide production (ventilatory equivalent for carbon dioxide).

The ventilatory response to exercise is usually assessed by the slope of V'_E as a function of V'_{CO_2}. Although studies of the prognostic role of the V'_E/V'_{CO_2} slope have produced variable results in PAH [3, 4, 41, 42], the V'_E/V'_{CO_2} slope has been identified as an important and potent predictor of outcome in left-sided heart failure [43, 44] and PAH [3, 4, 27], and has been reported to be associated with afterload (assessed as PVR) in heart failure with preserved ejection fraction [9]. It has been argued that the slope of V'_E/V'_{CO_2} would be better replaced by its nadir as being a less effort-dependent and more stable measurement [20]. In the present study, the nadir of V'_E/V'_{CO_2} actually showed a better correlation with RV diastolic stiffness and afterload than did the slope of V'_E/V'_{CO_2}. However, V'_E/V'_{CO_2} to predict outcome in PAH or left-sided heart failure is usually reported as slope instead of nadir.

In addition, echocardiographic measurements of RV dimensions and systolic function have been shown to be related to ventilatory inefficiency in patients with severe left heart failure [10], in keeping with the notion of increased chemosensitivity secondary to increased RV stretch and stiffness. Whether a right heart phenotype might worsen wasted ventilation and associated dyspnoea in heart failure remains to be clarified.

There is more to shortness of breath in PAH than wasted ventilation. Recent studies have suggested a significant contribution of dynamic hyperinflation during exercise in these patients [45, 46]. Even though this mechanism is not a cause of ventilatory limitation to aerobic exercise and is not related to respiratory muscle weakness in PAH [47], it contributes to exercise intolerance by worsening dyspnoea at any level of workload. However, the extent to which hyperventilation, dead space ventilation, chemosensitivity and/or the abnormal response of the pulmonary circulation during exercise contribute to excessive dynamic hyperinflation is currently unknown.

The patients with PAH included in the present study were severely ill, with about half in WHO functional class III and most of the others in WHO functional class II (the remaining two patients were in WHO functional class I). However, they are representative of patients with PAH admitted and followed in pulmonary hypertension referral centres. In a review of 11 PAH registries, McGoon *et al.* [48] reported that 54%–80% of the patients were in WHO functional classes III/IV; previous PAH registry populations were thus even more severely ill than our cohort. The peak V'_{O_2} and workload values in the present study were typical for patients with PAH [4, 27, 42, 49], and similar to those reported in multiple-beat RV function studies [38]. It cannot be excluded that clustering of Ees at a very low range of values prevented the uncovering of significant correlations with V'_E/V'_{CO_2}.

Limitations

We compared pressure–volume parameters at rest with parameters assessed under exercise (CPET). The analysis is thus limited by the fact that pressure–volume loops were not generated during exercise. We performed a single-beat analysis of pressure–volume loops, and it is unclear if the multiple-beat approach would produce similar results. The prognostic V'_E/V'_{CO_2} cut-off value of 48 relied mainly on the study by Groepenhoff and co-workers [4, 27] and may thus not be sufficiently robust [3]. The small size, the relatively low RER and the advanced functional status of our study population may also have biased our results. Nevertheless, we believe the sample size is reasonable for a study of invasive pressure–volume catheterisation in patients with PAH, and submaximal exercise testing yielding a RER <0.9 in PAH did not affect key ventilatory parameters [50]. The small sample size limited the univariate and multivariate logistic regression analyses and prevented further in-depth or receiver operating characteristic analysis. In addition, data-driven cut-offs, especially in small sample sizes, should be interpreted with caution and need external validation. Finally, it has to be underscored that showing independent prediction of V'_E/V'_{CO_2} by RV Eed and Ea does not prove causation, which needs to be further investigated by dedicated studies.

Conclusion

Our data suggest that both impaired RV lusitropy and increased RV afterload are associated with ventilatory inefficiency in PAH. The potential implications of this finding for PAH treatment warrant further study.

Acknowledgements: We thank Claire Mulligan (Beacon Medical Communications Ltd, Brighton, UK) for editorial support, funded by the University of Giessen.

Support statement: Funded by the Deutsche Forschungsgemeinschaft (DFG, German Research Foundation) – Projektnummer 268555672 – SFB 1213, Project B08. Funding information for this article has been deposited with the Crossref Funder Registry.

Conflict of interest: K. Tello reports that this work was funded by the Excellence Cluster Cardio-Pulmonary System (ECCPS) and the Collaborative Research Center (SFB) 1213 - Pulmonary Hypertension and Cor Pulmonale, grant number SFB1213/1, project B08 (grant from German Research Foundation, Bonn, Germany) and editorial support was funded by University of Giessen, during the conduct of the study; and personal fees for lectures from Actelion and Bayer, outside the submitted work. A. Dalmer has nothing to disclose. R. Vanderpool has nothing to disclose. H.A. Ghofrani reports that this work was funded by the ECCPS and the Collaborative Research Center (SFB) 1213 - Pulmonary Hypertension and Cor Pulmonale, grant number SFB1213/1, project B08 (grant from German Research Foundation, Bonn, Germany) and editorial support was funded by University of Giessen, during the conduct of the study; and personal fees for consultancy and advisory board work from Bayer and Pfizer, personal fees for consultancy, lectures and advisory board work from Actelion and GSK, personal fees for consultancy from Merck, grants and personal fees for consultancy from Novartis, grants and personal fees for lectures from Bayer HealthCare and Encysive/Pfizer, grants from Aires, German Research Foundation, Excellence Cluster Cardiopulmonary Research and German Ministry for Education and Research, and personal fees for advisory board work from Takeda, outside the submitted work. R. Naeije reports grants and personal fees for consultancy and advisory board work from AOP Orphan Pharmaceuticals, Actelion, Bayer, Reata, Lung Biotechnology Corporation and United Therapeutics, outside the submitted work. F. Roller has nothing to disclose. W. Seeger reports that this work was funded by the ECCPS and the Collaborative Research Center (SFB) 1213 - Pulmonary Hypertension and Cor Pulmonale, grant number SFB1213/1, project B08 (grant from German Research Foundation, Bonn, Germany) and editorial support was funded by University of Giessen, during the conduct of the study; and personal fees for consultancy and lectures from Pfizer and Bayer Pharma AG, outside the submitted work. D. Dumitrescu reports personal fees and advisory board membership from

Actelion and Novartis, and personal fees from Bayer Healthcare, GSK, MSD and Servier, outside the submitted work. N. Sommer reports personal fees from Actelion, outside the submitted work. A. Brunst has nothing to disclose. H. Gall reports that this work was funded by the ECCPS and the Collaborative Research Center (SFB) 1213 - Pulmonary Hypertension and Cor Pulmonale, grant number SFB1213/1, project B08 (grant from German Research Foundation, Bonn, Germany) and editorial support was funded by University of Giessen, during the conduct of the study; and personal fees from Actelion, AstraZeneca, Bayer, BMS, GSK, Janssen-Cilag, Lilly, MSD, Novartis, OMT, Pfizer and United Therapeutics, outside the submitted work. M.J. Richter reports that this work was funded by the ECCPS and the Collaborative Research Center (SFB) 1213 - Pulmonary Hypertension and Cor Pulmonale, grant number SFB1213/1, project B08 (grant from German Research Foundation, Bonn, Germany) and editorial support was funded by University of Giessen, during the conduct of the study; and grants from United Therapeutics, grants and personal fees for consultancy and lectures from Bayer, and personal fees for lectures from Actelion, Mundipharma, Roche and OMT, outside the submitted work.

References

1 Weatherald J, Sattler C, Garcia G, *et al.* Ventilatory response to exercise in cardiopulmonary disease: the role of chemosensitivity and dead space. *Eur Respir J* 2018; 51: 1700860.
2 Dumitrescu D, Sitbon O, Weatherald J, *et al.* Exertional dyspnoea in pulmonary arterial hypertension. *Eur Respir Rev* 2017; 26: 170039.
3 Deboeck G, Scoditti C, Huez S, *et al.* Exercise testing to predict outcome in idiopathic versus associated pulmonary arterial hypertension. *Eur Respir J* 2012; 40: 1410–1419.
4 Groepenhoff H, Vonk-Noordegraaf A, Boonstra A, *et al.* Exercise testing to estimate survival in pulmonary hypertension. *Med Sci Sports Exerc* 2008; 40: 1725–1732.
5 Galie N, Humbert M, Vachiery JL, *et al.* 2015 ESC/ERS guidelines for the diagnosis and treatment of pulmonary hypertension. *Eur Respir J* 2015; 46: 903–975.
6 Vonk Noordegraaf A, Chin KM, Haddad F, *et al.* Pathophysiology of the right ventricle and of the pulmonary circulation in pulmonary hypertension: an update. *Eur Respir J* 2019; 53: 1801900.
7 Vonk Noordegraaf A, Westerhof BE, Westerhof N. The relationship between the right ventricle and its load in pulmonary hypertension. *J Am Coll Cardiol* 2017; 69: 236–243.
8 Naeije R, Manes A. The right ventricle in pulmonary arterial hypertension. *Eur Respir Rev* 2014; 23: 476–487.
9 Klaassen SHC, Liu LCY, Hummel YM, *et al.* Clinical and hemodynamic correlates and prognostic value of VE/VCO_2 slope in patients with heart failure with preserved ejection fraction and pulmonary hypertension. *J Card Fail* 2017; 23: 777–782.
10 Methvin AB, Owens AT, Emmi AG, *et al.* Ventilatory inefficiency reflects right ventricular dysfunction in systolic heart failure. *Chest* 2011; 139: 617–625.
11 Farina S, Correale M, Bruno N, *et al.* "Right and Left Heart Failure Study Group" of the Italian Society of Cardiology. The role of cardiopulmonary exercise tests in pulmonary arterial hypertension. *Eur Respir Rev* 2018; 27: 170134.
12 Sanz J, Kariisa M, Dellegrottaglie S, *et al.* Evaluation of pulmonary artery stiffness in pulmonary hypertension with cardiac magnetic resonance. *JACC Cardiovasc Imaging* 2009; 2: 286–295.
13 Gall H, Felix JF, Schneck FK, *et al.* The Giessen Pulmonary Hypertension Registry: survival in pulmonary hypertension subgroups. *J Heart Lung Transplant* 2017; 36: 957–967.
14 Tello K, Richter MJ, Axmann J, *et al.* More on single-beat estimation of right ventriculoarterial coupling in pulmonary arterial hypertension. *Am J Respir Crit Care Med* 2018; 198: 816–818.
15 Tello K, Dalmer A, Axmann J, *et al.* Reserve of right ventricular-arterial coupling in the setting of chronic overload. *Circ Heart Fail* 2019; 12: e005512.
16 Tello K, Dalmer A, Husain-Syed F, *et al.* Multi-beat right ventricular-arterial coupling during a positive acute vaso-reactivity test. *Am J Respir Crit Care Med* 2019; 199: e41–e42.
17 Tello K, Dalmer A, Vanderpool R, *et al.* Cardiac magnetic resonance imaging-based right ventricular strain analysis for assessment of coupling and diastolic function in pulmonary hypertension. *JACC Cardiovasc Imaging* 2019; 12: 2155–2164.
18 Macintyre N, Crapo RO, Viegi G, *et al.* Standardisation of the single-breath determination of carbon monoxide uptake in the lung. *Eur Respir J* 2005; 26: 720–735.
19 Scheidl SJ, Englisch C, Kovacs G, *et al.* Diagnosis of CTEPH versus IPAH using capillary to end-tidal carbon dioxide gradients. *Eur Respir J* 2012; 39: 119–124.
20 Wasserman K, Hansen JE, Sue DY, *et al.* Principles of Exercise Testing and Interpretation. 5th Edn. Philadelphia, Lippincott Williams & Wilkins, 2011.
21 Tello K, Axmann J, Ghofrani HA, *et al.* Relevance of the TAPSE/PASP ratio in pulmonary arterial hypertension. *Int J Cardiol* 2018; 266: 229–235.
22 Brimioulle S, Wauthy P, Ewalenko P, *et al.* Single-beat estimation of right ventricular end-systolic pressure-volume relationship. *Am J Physiol Heart Circ Physiol* 2003; 284: H1625–H1630.
23 Rain S, Handoko ML, Trip P, *et al.* Right ventricular diastolic impairment in patients with pulmonary arterial hypertension. *Circulation* 2013; 128: 2016–2025.
24 Vanderpool RR, Pinsky MR, Naeije R, *et al.* RV-pulmonary arterial coupling predicts outcome in patients referred for pulmonary hypertension. *Heart* 2015; 101: 37–43.
25 Vanderpool RR, Puri R, Osorio A, *et al.* EXPRESS: surfing the right ventricular pressure waveform: methods to assess global, systolic and diastolic RV function from a clinical right heart catheterization. *Pulm Circ* 2019; in press [https://doi.org/10.1177/2045894019850993].
26 Trip P, Rain S, Handoko ML, *et al.* Clinical relevance of right ventricular diastolic stiffness in pulmonary hypertension. *Eur Respir J* 2015; 45: 1603–1612.
27 Groepenhoff H, Vonk-Noordegraaf A, van de Veerdonk MC, *et al.* Prognostic relevance of changes in exercise test variables in pulmonary arterial hypertension. *PLoS One* 2013; 8: e72013.
28 Robin ED, Forkner CE Jr., Bromberg PA, *et al.* Alveolar gas exchange in clinical pulmonary embolism. *N Engl J Med* 1960; 262: 283–287.
29 Naeije R, Faoro V. The breathlessness of pulmonary hypertension. *Int J Cardiol* 2018; 259: 183–184.

30 Farina S, Bruno N, Agalbato C, *et al.* Physiological insights of exercise hyperventilation in arterial and chronic thromboembolic pulmonary hypertension. *Int J Cardiol* 2018; 259: 178–182.
31 Velez-Roa S, Ciarka A, Najem B, *et al.* Increased sympathetic nerve activity in pulmonary artery hypertension. *Circulation* 2004; 110: 1308–1312.
32 Ciarka A, Doan V, Velez-Roa S, *et al.* Prognostic significance of sympathetic nervous system activation in pulmonary arterial hypertension. *Am J Respir Crit Care Med* 2010; 181: 1269–1275.
33 Ciarka A, Vachiery JL, Houssiere A, *et al.* Atrial septostomy decreases sympathetic overactivity in pulmonary arterial hypertension. *Chest* 2007; 131: 1831–1837.
34 Naeije R, Faoro V. The great breathlessness of cardiopulmonary diseases. *Eur Respir J* 2018; 51: 1702517.
35 Kuehne T, Yilmaz S, Steendijk P, *et al.* Magnetic resonance imaging analysis of right ventricular pressure-volume loops: *in vivo* validation and clinical application in patients with pulmonary hypertension. *Circulation* 2004; 110: 2010–2016.
36 Spruijt OA, de Man FS, Groepenhoff H, *et al.* The effects of exercise on right ventricular contractility and right ventricular-arterial coupling in pulmonary hypertension. *Am J Respir Crit Care Med* 2015; 191: 1050–1057.
37 Maughan WL, Shoukas AA, Sagawa K, *et al.* Instantaneous pressure-volume relationship of the canine right ventricle. *Circ Res* 1979; 44: 309–315.
38 Hsu S, Houston BA, Tampakakis E, *et al.* Right ventricular functional reserve in pulmonary arterial hypertension. *Circulation* 2016; 133: 2413–2422.
39 Tedford RJ, Mudd JO, Girgis RE, *et al.* Right ventricular dysfunction in systemic sclerosis-associated pulmonary arterial hypertension. *Circ Heart Fail* 2013; 6: 953–963.
40 Inuzuka R, Hsu S, Tedford RJ, *et al.* Single-beat estimation of right ventricular contractility and its coupling to pulmonary arterial load in patients with pulmonary hypertension. *J Am Heart Assoc* 2018; 7: e007929.
41 Wensel R, Francis DP, Meyer FJ, *et al.* Incremental prognostic value of cardiopulmonary exercise testing and resting haemodynamics in pulmonary arterial hypertension. *Int J Cardiol* 2013; 167: 1193–1198.
42 Wensel R, Opitz CF, Anker SD, *et al.* Assessment of survival in patients with primary pulmonary hypertension: importance of cardiopulmonary exercise testing. *Circulation* 2002; 106: 319–324.
43 Francis DP, Shamim W, Davies LC, *et al.* Cardiopulmonary exercise testing for prognosis in chronic heart failure: continuous and independent prognostic value from VE/VCO_2 slope and peak VO_2. *Eur Heart J* 2000; 21: 154–161.
44 Sue DY. Excess ventilation during exercise and prognosis in chronic heart failure. *Am J Respir Crit Care Med* 2011; 183: 1302–1310.
45 Richter MJ, Voswinckel R, Tiede H, *et al.* Dynamic hyperinflation during exercise in patients with precapillary pulmonary hypertension. *Respir Med* 2012; 106: 308–313.
46 Laveneziana P, Garcia G, Joureau B, *et al.* Dynamic respiratory mechanics and exertional dyspnoea in pulmonary arterial hypertension. *Eur Respir J* 2013; 41: 578–587.
47 Laveneziana P, Humbert M, Godinas L, *et al.* Inspiratory muscle function, dynamic hyperinflation and exertional dyspnoea in pulmonary arterial hypertension. *Eur Respir J* 2015; 45: 1495–1498.
48 McGoon MD, Benza RL, Escribano-Subias P, *et al.* Pulmonary arterial hypertension: epidemiology and registries. *J Am Coll Cardiol* 2013; 62: D51–D59.
49 Deboeck G, Niset G, Lamotte M, *et al.* Exercise testing in pulmonary arterial hypertension and in chronic heart failure. *Eur Respir J* 2004; 23: 747–751.
50 Woods PR, Frantz RP, Taylor BJ, *et al.* The usefulness of submaximal exercise gas exchange to define pulmonary arterial hypertension. *J Heart Lung Transplant* 2011; 30: 1133–1142.

Anlage H

Relevance of the TAPSE/PASP ratio in pulmonary arterial hypertension.

Tello K, Axmann J, Ghofrani HA, Naeije R, Narcin N, Rieth A, Seeger W, Gall H, Richter MJ. Int J Cardiol. 2018 Sep 1;266:229-235

International Journal of Cardiology 266 (2018) 229–235

Contents lists available at ScienceDirect

International Journal of Cardiology

journal homepage: www.elsevier.com/locate/ijcard

Relevance of the TAPSE/PASP ratio in pulmonary arterial hypertension

Khodr Tello [a,1], Jens Axmann [a,1], Hossein A. Ghofrani [a,b,c,1], Robert Naeije [d,1], Newroz Narcin [a,1], Andreas Rieth [e,1], Werner Seeger [a,1], Henning Gall [a,1,2], Manuel J. Richter [a,*,1,2]

[a] Department of Internal Medicine, Justus-Liebig-University Giessen, Universities of Giessen and Marburg Lung Center (UGMLC), Member of the German Center for Lung Research (DZL), Giessen, Germany
[b] Department of Pneumology, Kerckhoff Heart, Rheuma and Thoracic Center, Bad Nauheim, Germany
[c] Department of Medicine, Imperial College London, London, UK
[d] Erasme University Hospital, Brussels, Belgium
[e] Department of Cardiology, Kerckhoff Heart, Rheuma and Thoracic Center, Bad Nauheim, Germany

ARTICLE INFO

Article history:
Received 4 December 2017
Received in revised form 3 January 2018
Accepted 10 January 2018

Keywords:
Right ventricular contractile function
Pulmonary hypertension
TAPSE
PASP
Survival

ABSTRACT

Background: The ratio of echocardiography-derived tricuspid annular plane systolic excursion (TAPSE) and pulmonary arterial systolic pressure (PASP) has recently been reported as an independent prognostic parameter in heart failure. The TAPSE/PASP ratio has not been evaluated in detail in patients with pulmonary arterial hypertension (PAH).

Methods: We analyzed TAPSE/PASP in 290 patients with PAH entered into the Giessen Pulmonary Hypertension Registry between November 2003 and July 2014. The prognostic relevance of TAPSE/PASP was assessed with multivariate Cox regression models, adjusting for clinical covariates, echocardiographic parameters, or hemodynamics, and was confirmed by Kaplan–Meier analyses.

Results: When stratified by tertile of TAPSE/PASP (low: <0.19 mm/mmHg; middle: 0.19–0.32 mm/mmHg; high: >0.32 mm/mmHg), patients in the low tertile showed significantly compromised hemodynamic, functional, and echocardiographic status compared with patients in the middle and high tertiles. In all multivariate models, TAPSE/PASP remained independently associated with overall mortality: the hazard ratio (95% confidence interval) was 1.87 (1.35–2.59) when adjusting for clinical covariates ($p < .001$), 5.21 (2.17–12.5) when adjusting for echocardiographic parameters ($p < .001$), 1.92 (1.30–2.83) when adjusting for hemodynamics ($p = .001$), and 4.13 (2.02–8.48) when adjusting for a selection of previously identified independent echocardiographic and hemodynamic prognostic indicators ($p < .001$). Kaplan–Meier analyses showed better overall survival in the middle and high tertiles versus the low tertile (log-rank $p < .001$).

Conclusions: The TAPSE/PASP ratio is a meaningful prognostic parameter in patients with PAH and is associated with hemodynamics and functional class.

1. Introduction

Pulmonary arterial hypertension (PAH) is characterized by an elevated mean pulmonary arterial pressure (mPAP) and an increased pulmonary vascular resistance (PVR) [1]. During the course of the disease, maladaptive right ventricular (RV) hypertrophy and/or dilatation occur, eventually resulting in RV failure [2, 3]. Several echocardiographic parameters of RV function including tricuspid annular plane systolic excursion (TAPSE) and pulmonary arterial systolic pressure (PASP) have been shown to be of prognostic relevance in patients with PAH [4, 5]. The ratio of TAPSE/PASP has been described as an index of in vivo RV shortening in the longitudinal axis versus developed force in patients with heart failure [6], and was introduced as a non-invasive, indirect measurement of RV contractile function and RV-pulmonary arterial (PA) coupling [6–8]. The TAPSE/PASP ratio has been validated as an important clinical and prognostic parameter in patients with heart failure with and without pulmonary hypertension (PH) [7–11], and was identified as an independent and strong predictor

Abbreviations: BMI, body mass index; CI, confidence interval; CO, cardiac output; dPAP, diastolic pulmonary arterial pressure; ERA, endothelin receptor antagonist; FAC, fractional area change; HIV, human immunodeficiency virus; HR, hazard ratio; IQR, interquartile range; LV, left ventricular; mPAP, mean pulmonary arterial pressure; PA, pulmonary arterial; PAC, pulmonary arterial capacitance; PAH, pulmonary arterial hypertension; PASP, pulmonary arterial systolic pressure; PAWP, pulmonary arterial wedge pressure; PDE5i, phosphodiesterase type 5 inhibitor; PH, pulmonary hypertension; PP, pulse pressure; PVOD, pulmonary veno-occlusive disease; PVR, pulmonary vascular resistance; RA, right atrial; RAP, right atrial pressure; RV, right ventricular; RV S′, systolic annular tissue velocity of the lateral tricuspid annulus; SD, standard deviation; sGC, soluble guanylate cyclase stimulator; sPAP, systolic pulmonary arterial pressure; SV, stroke volume; SvO_2, mixed venous oxygen saturation; TAPSE, tricuspid annular plane systolic excursion; Tei, myocardial performance; TR, tricuspid regurgitation; WHO, World Health Organization.

* Corresponding author at: Department of Internal Medicine, Justus-Liebig-University Giessen, Klinikstrasse 32, 35392 Giessen, Germany.
E-mail address: manuel.richter@innere.med.uni-giessen.de (M.J. Richter).

[1] This author takes responsibility for all aspects of the reliability and freedom from bias of the data presented and their discussed interpretation.

[2] These authors have contributed equally to this work.

https://doi.org/10.1016/j.ijcard.2018.01.053
0167-5273/

of outcome in patients with combined post- and pre-capillary PH [12]. Moreover, a close relationship of the TAPSE/PASP ratio with pulmonary arterial capacitance (PAC; a measure of the compliance of the pulmonary artery and RV afterload) and PVR has been shown [8, 12].

However, to the best of our knowledge, the TAPSE/PASP ratio has not been explored in detail in patients presenting with PAH. Our present study therefore had the following aims: 1) to assess the prognostic value of the TAPSE/PASP ratio in PAH and 2) to explore the relationship between TAPSE/PASP and hemodynamic parameters including PAC.

2. Methods

2.1. Study design and patients

We analyzed patients with PAH enrolled between November 2003 and July 2014 in the Giessen PH Registry, a prospectively recruiting single-center registry in Germany [13]. The analysis included consecutive patients with complete echocardiographic and invasive hemodynamic data at the time of enrollment and complete follow-up data. Follow-up data were retrieved from the Giessen PH Registry up to May 2017. A multidisciplinary board, including pulmonary physicians and radiologists, assessed the diagnosis in all patients with PAH before enrollment. All of the patients were receiving targeted PAH therapies based on clinical grounds and best standard of care, and changes in PAH medication were based on clinical decisions. The investigation conforms with the principles outlined in the Declaration of Helsinki and was approved by the ethics committee of the Faculty of Medicine at the University of Giessen (Approval No. 186/16, 266/11). All participating patients gave written informed consent to be enrolled in the Giessen PH Registry.

2.2. Right heart catheterization

All patients underwent right heart catheterization by insertion of a Swan-Ganz catheter under local anesthesia according to standard techniques in the left or right jugular vein. Pressure values were continuously assessed [mPAP, right atrial pressure (RAP), pulmonary arterial wedge pressure (PAWP), and systolic and diastolic pulmonary arterial pressure (sPAP and dPAP, respectively)] and the cardiac output (CO) was measured using the direct Fick method [1], as available. PVR and cardiac index were calculated as [PVR = (mPAP − PAWP)/CO; cardiac index = (CO/body surface area)] [1]. PAC was calculated as [PAC = stroke volume (SV)/pulse pressure (PP) = (CO/heart rate)/(sPAP − dPAP)] [14].

2.3. Right heart echocardiography

All echocardiographic measurements, including TAPSE, were obtained from the Giessen PH Registry and were entered into this registry at enrollment. The measurements were obtained using a Vivid E9 and a Vivid S5 (GE Healthcare, Wauwatosa, WI, USA), with supervision by experienced examiners at the time of the original assessments to ensure adherence to echocardiographic guidelines [15–17]. TAPSE was measured in the four-chamber apical view by placing the M-mode cursor through the lateral tricuspid annulus. The peak excursion of the lateral annulus represented the TAPSE (in mm). RV systolic pressure was assessed by estimating the pressure gradient across the tricuspid valve (based on the tricuspid regurgitation [TR] jet, applying the simplified Bernoulli equation) and adding the RAP (estimated based on the collapse and diameter of the inferior vena cava) [15, 18]. Right atrial (RA) size was quantified by measuring the RA area in end-systole, and the systolic annular tissue velocity of the lateral tricuspid annulus (RV S′) was also measured [15]. Tei index was measured as the ratio of isovolumic contraction time and isovolumic relaxation time divided by ejection time [15]. The degrees of RA and RV enlargement, obtained from the four-chamber apical view, were described as none, mild, moderate, or severe based on visual assessment by an experienced examiner at the time of enrollment [19]. TR severity was classified as none, mild, moderate, or severe at enrollment [15]. For further analyses, patients with no or mild enlargement were grouped together, as were patients with no or mild TR.

2.4. Outcome

The primary outcome was overall mortality, which was assessed using follow-up data from the Giessen PH Registry.

2.5. Statistical analyses

SPSS version 23.0 (IBM, Armonk, NY, USA) was used for statistical analyses. Normally distributed data are expressed as mean ± standard deviation (SD); non-normally distributed data are expressed as median [interquartile range (IQR)]. Patients were divided into subgroups based on TAPSE/PASP ratio tertiles. Between-group differences were analyzed with one-way ANOVA, the Kruskal–Wallis test, and (for categorical parameters) the Pearson Chi-square test as appropriate, with $p < .05$ considered statistically significant. For further analysis, variables were ln-transformed in cases of a non-normal distribution (see for example Fig. S1 online).

Multivariate Cox proportional-hazards regression models were used to assess prognostic relevance. The minimum number of events per adjustment variable in the multivariate Cox regression analysis was set at 10, based on previous recommendations [20]. We therefore built four different multivariate Cox models to avoid overfitting. For model 1, covariate selection was based on clinical relevance [8] and included the TAPSE/PASP ratio as a continuous variable, along with age, gender, body mass index, arterial hypertension, atrial fibrillation, diabetes mellitus, and World Health Organization (WHO) functional class. Model 2 included the TAPSE/PASP ratio as a continuous variable and the following echocardiographic parameters (also as continuous variables): TAPSE, PASP, RA size, RV S′, Tei index, and left ventricular ejection fraction. TAPSE and PASP were included in the model despite showing strong collinearity with the TAPSE/PASP ratio [$r = 0.695$ ($p < .001$) and $r = 0.756$ ($p < .001$), respectively], to allow direct comparison of their prognostic impact. Model 3 included the TAPSE/PASP ratio as a continuous variable and the following hemodynamic parameters (also as continuous variables): PVR, mPAP, CO, PAC, mixed venous oxygen saturation (SvO_2), PP, SV, RAP, and PAWP. Model 4 included the TAPSE/PASP ratio as a continuous variable and previously identified independent hemodynamic [21–23] and echocardiographic prognostic parameters [4, 24–26] (also as continuous variables): CO, SvO_2, RAP, TAPSE, PASP, RA size, and Tei index. The prognostic relevance of the TAPSE/PASP ratio was also evaluated by Kaplan–Meier analyses with log-rank tests. For the Cox regression and Kaplan–Meier analyses, $p < .01$ was considered statistically significant.

3. Results

3.1. Patients

In total, 290 patients with PAH were included in the analysis (Table 1) and were stratified into tertiles according to TAPSE/PASP ratio (low: <0.19 mm/mmHg; middle: 0.19–0.32 mm/mmHg; high: >0.32 mm/mmHg). The majority of the patients were diagnosed with idiopathic PAH and were in WHO functional class III, presenting with severe precapillary PH with substantially elevated PVR and mPAP. Patients in the low and middle TAPSE/PASP tertiles showed a significantly more compromised hemodynamic status than those in the high tertile, with substantially increased mPAP, RAP, and PVR and decreased cardiac index, SvO_2, and PAC. Moreover, patients in the low tertile presented with a larger RA size, higher PASP, lower TAPSE, more compromised Tei index, higher rate of severe RA/RV enlargement, higher rate of severe TR, and lower RV S′ than patients in the middle and high tertiles. The initiation of specific vasoactive treatment after enrollment did not differ significantly between the tertile groups, although a numerical trend towards a higher rate of prostanoid and triple combination treatment was observed in the low tertile.

3.2. Prognostic relevance of TAPSE/PASP in PAH

The mean ± SD follow-up period was 81.3 ± 55.7 months [median [IQR]: 72.5 [89.4] months], during which 145 (50.0%) of the patients died. The median [IQR] follow-up time in TAPSE/PASP tertiles 1, 2, and 3 was 64.0 [89.5] months, 85.0 [85.5] months, and 73.5 [106.3] months, respectively.

In multivariate analyses including TAPSE/PASP as a continuous variable, model 1 (adjusting for clinical covariates) showed a significant, independent association of the TAPSE/PASP ratio with overall mortality. Of note, age and body mass index also remained significantly associated with mortality in this model. In model 2 (adjusting for echocardiographic parameters), only the TAPSE/PASP ratio remained significantly associated with overall mortality. The TAPSE/PASP ratio was also independently associated with overall mortality in model 3, along with CO, mPAP, SvO_2, and PAC. In addition, after adjusting for previously identified independent hemodynamic and echocardiographic prognostic parameters (model 4), the TAPSE/PASP ratio remained significantly associated with overall mortality (Table 2).

The prognostic significance of the TAPSE/PASP ratio was confirmed by Kaplan–Meier analyses which showed significantly better overall survival in the middle and high TAPSE/PASP tertiles compared with the low tertile (log-rank $p < .001$; Fig. 1). Five-year overall survival was 58.1%, 73.0%, and 70.0% in the low, middle, and high TAPSE/PASP tertiles, respectively (Fig. 1).

Table 1
Baseline characteristics, pulmonary hemodynamics, and right heart echocardiography at the time of enrollment according to tertiles of the TAPSE/PASP ratio.

	Total	TAPSE/PASP tertile (mm/mmHg)			*p*
		Low (<0.19)	Middle (0.19–0.32)	High (>0.32)	
Patients, *n*	290	97	101	92	
Male/female, *n*/*n*	120/170	37/60	41/60	42/50	0.57
Age, years	50.9 ± 15.8	50.7 ± 16.5	49.4 ± 15.8	52.9 ± 15.2	0.31
PH subtype, *n* (%)					0.29
Idiopathic	193 (66.6)	69 (71.1)	66 (65.3)	58 (63.0)	
Heritable	1 (0.3)	1 (1.0)	none	none	
Associated with					
HIV infection	15 (5.2)	3 (3.1)	4 (4.0)	8 (8.7)	
Portal hypertension	27 (9.3)	5 (5.2)	9 (8.9)	13 (14.1)	
Congenital heart disease	41 (14.1)	14 (14.4)	16 (15.8)	11 (12.0)	
Pulmonary veno-occlusive disease	13 (4.5)	5 (5.2)	6 (5.9)	2 (2.2)	
WHO functional class, *n* (%)[a]					0.187
I	8 (2.8)	2 (2.1)	2 (2.0)	4 (4.3)	
II	57 (19.7)	13 (13.5)	19 (18.8)	25 (27.2)	
III	178 (61.6)	61 (63.5)	66 (65.3)	51 (55.4)	
IV	46 (15.9)	20 (20.8)	14 (13.9)	12 (13.0)	
Comorbidities, %					
BMI ≥ 30 kg/m^2	19.7	14.4	25.7	18.5	0.13
Hypertension	34.1	34.0	28.7	40.2	0.24
Atrial fibrillation	13.4	15.5	10.9	14.1	0.62
Diabetes mellitus	19.3	17.5	18.8	21.7	0.76
Coronary artery disease	17.2	13.4	15.8	22.8	0.21
Right heart catheterization					
mPAP, mmHg	51.3 ± 14.6	58.0 ± 15.0	51.3 ± 13.1	44.4 ± 12.4	<0.001
RAP, mmHg	7.6 ± 5.9	9.5 ± 6.6	7.3 ± 6.0	6.1 ± 4.5	<0.001
PVR, dyne·s/cm^5	837.9 [659.0]	1138.0 [702.0]	830.0 [579.0]	583.1 [473.0]	<0.001[b]
Cardiac index, L/min/m^2	2.3 ± 0.8	2.0 ± 0.6	2.4 ± 0.7	2.7 ± 0.8	<0.001
CO, L/min	4.3 ± 1.5	3.6 ± 1.1	4.4 ± 1.5	5.0 ± 1.6	<0.001
PAWP, mmHg	8.0 ± 3.3	8.4 ± 3.3	7.7 ± 3.6	7.8 ± 3.0	0.28
PAC, mL/mmHg	1.08 [0.80]	0.84 [0.41]	1.09 [0.76]	1.52 [1.05]	<0.001[b]
SV, mL	56.7 ± 21.5	45.6 ± 16.5	59.3 ± 21.4	65.6 ± 21.4	<0.001
PP, mmHg	48.6 ± 14.3	53.1 ± 16.0	49.2 ± 11.9	43.2 ± 13.1	<0.001
SvO_2, %	62.6 ± 9.8	57.6 ± 9.7	63.4 ± 9.3	66.9 ± 8.0	<0.001
Heart rate, beats/min	78.2 ± 13.7	81.7 ± 13.2	76.7 ± 14.4	76.0 ± 12.9	0.006
Echocardiography					
TAPSE/PASP, mm/mmHg	0.25 [0.20]	0.15 [0.04]	0.25 [0.07]	0.45 [0.20]	<0.001[b]
TAPSE, mm	18.1 ± 5.6	13.3 ± 3.5	18.1 ± 3.5	23.1 ± 4.8	<0.001
PASP, mmHg	72.4 ± 24.5	94.3 ± 20.3	72.3 ± 14.3	49.6 ± 14.6	<0.001
RA size, cm^2	22.8 ± 8.3	26.2 ± 8.3	23.4 ± 8.6	18.9 ± 6.0	<0.001
RV S′, cm/s	12.5 ± 3.3	11.3 ± 4.0	12.8 ± 2.9	13.2 ± 2.8	0.005
Tei index	0.63 ± 0.28	0.70 ± 0.25	0.65 ± 0.27	0.52 ± 0.29	<0.001
LV ejection fraction, %	71.5 ± 13.3	72.0 ± 14.0	72.3 ± 12.0	70.3 ± 14.1	0.57
TR, *n* (%)[a]					<0.001
None/mild	95 (32.9)	11 (11.3)	28 (28.0)	56 (60.9)	
Moderate	100 (34.6)	28 (28.9)	47 (47.0)	25 (27.2)	
Severe	94 (32.5)	58 (59.8)	25 (25.0)	11 (12.0)	
RA enlargement, *n* (%)[a]					<0.001
None/mild	77 (26.6)	13 (13.4)	20 (19.8)	44 (47.8)	
Moderate	105 (36.2)	25 (25.8)	44 (43.6)	36 (39.1)	
Severe	108 (37.2)	59 (60.8)	37 (36.6)	12 (13.0)	
RV enlargement, *n* (%)					<0.001
None/mild	75 (25.9)	13 (13.4)	19 (18.8)	43 (46.7)	
Moderate	109 (37.6)	26 (26.8)	46 (45.5)	37 (40.2)	
Severe	106 (36.6)	58 (59.8)	36 (35.6)	12 (13.0)	
Treatment, *n* (%)[c]					
PDE5i	215 (74.1)	80 (82.5)	73 (72.3)	62 (67.4)	0.05
ERA	171 (59.0)	62 (63.9)	62 (61.4)	47 (51.1)	0.17
sGC	10 (3.4)	1 (1.0)	4 (4.0)	5 (5.4)	0.24
Prostanoid	73 (25.2)	29 (29.9)	26 (25.7)	18 (19.6)	0.26
Combination therapy, *n* (%)[c]					
Dual therapy	96 (33.1)	38 (39.2)	34 (33.7)	24 (26.1)	0.16
Triple therapy	46 (15.9)	19 (19.6)	15 (14.9)	12 (13.0)	0.31

Values represent mean ± standard deviation or median [interquartile range], unless otherwise specified.
BMI, body mass index; CO, cardiac output; ERA, endothelin receptor antagonist; HIV, human immunodeficiency virus; LV, left ventricular; mPAP, mean pulmonary arterial pressure; PAC, pulmonary arterial capacitance; PASP, pulmonary arterial systolic pressure; PAWP, pulmonary arterial wedge pressure; PDE5i, phosphodiesterase type 5 inhibitor; PH, pulmonary hypertension; PP, pulse pressure; PVR, pulmonary vascular resistance; RA, right atrial; RAP, right atrial pressure; RV, right ventricular; RV S′, systolic annular tissue velocity of the lateral tricuspid annulus; sGC, soluble guanylate cyclase stimulator; SV, stroke volume; SvO_2, mixed venous oxygen saturation; TAPSE, tricuspid annular plane systolic excursion; Tei, myocardial performance; TR, tricuspid regurgitation; WHO, World Health Organization.
[a] $n = 289$.
[b] Kruskal–Wallis test.
[c] Treatment initiation at time of enrollment.

3.3. Relationship of the TAPSE/PASP ratio with hemodynamic parameters, RV echocardiography, and WHO functional class

PVR showed a logistic function-based relationship with TAPSE/PASP (Fig. 2A), with the distribution moving towards lower PVR values as the TAPSE/PASP tertile increased (Fig. 2B). SvO_2 and TAPSE/PASP showed a positive logistic function-based relationship, with SvO_2 values increasing as the TAPSE/PASP ratio increased (Fig. 2C). PAC and TAPSE/PASP were significantly linearly correlated with each other (Fig. 2D); consistent with this finding, PVR and PAC showed a logistic function-based relationship (Fig. 2E) similar to that observed for PVR and TAPSE/PASP (Fig. 2A).

The TAPSE/PASP ratio was significantly lower in patients with moderate and severe TR than in patients with no or mild TR (Fig. 2F). Patients with moderate and severe enlargement of the right chambers of the heart also had a significantly lower TAPSE/PASP ratio than patients with no or mild enlargement (Fig. 2G, H). In addition, the TAPSE/PASP ratio was able to differentiate between tertiles of TAPSE (Fig. 2I).

As shown in Fig. 2J, an inverse relationship was observed between TAPSE/PASP and WHO functional class, with TAPSE/PASP decreasing as the severity of WHO functional class increased.

We next assessed whether using invasively measured sPAP rather than the echocardiographic parameter PASP would alter our results. PVR and SvO_2 showed logistic function-based relationships with TAPSE/sPAP which were broadly similar to those observed with TAPSE/PASP (Fig. S2 online). In addition, the correlation between PAC and TAPSE/sPAP remained significant ($r = 0.77$, $p < .001$; Fig. S3A online), and the pattern of TAPSE/sPAP tertiles across the scatter plot of PVR versus PAC was broadly similar to that observed with TAPSE/PASP tertiles (Fig. S3B online). There was a significant correlation between TAPSE/PASP and TAPSE/sPAP ($r = 0.79$, $p < .001$; Fig. S4A online). Bland–Altman analysis [27] also indicated that the ratios obtained non-invasively and invasively were significantly related (Fig. S4B online), and the majority of the data points were within ±2 SDs of the mean difference (+0.05; limits of agreement: −0.19 and +0.30).

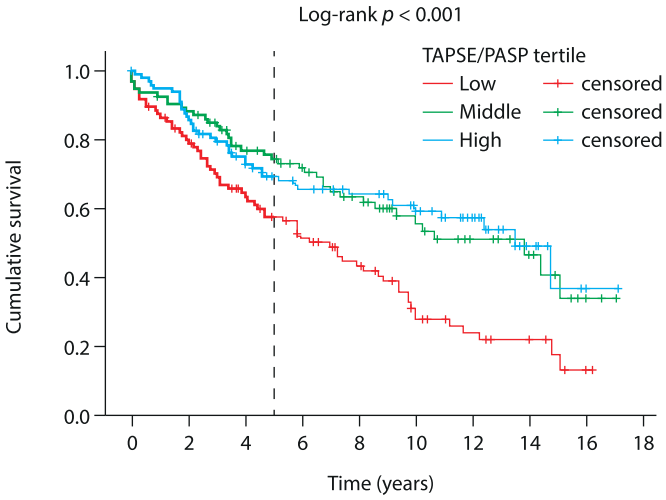

Number at risk	1 year	3 years	5 years
Low tertile	83	64	50
Middle tertile	93	81	63
High tertile	85	66	50

Fig. 1. Kaplan–Meier overall survival curves as a function of the TAPSE/PASP ratio tertile in patients with pulmonary arterial hypertension ($n = 290$; log-rank $p < .001$). PASP, pulmonary arterial systolic pressure; TAPSE, tricuspid annular plane systolic excursion.

Table 2
Hazard ratios and 95% confidence intervals for independent predictors of overall mortality identified by stepwise multivariate Cox regression analysis.

	Overall mortality	
Variables	HR [95% CI]	*p*
Model 1[a]		
TAPSE/PASP ratio, mm/mmHg	1.87 [1.35–2.59]	<0.001
BMI < 30 kg/m^2 vs ≥ 30 kg/m^2	1.97 [1.20–3.25]	0.008
Age, years	1.03 [1.02–1.04]	<0.001
Model 2[b]		
TAPSE/PASP ratio, mm/mmHg	5.21 [2.17–12.5]	<0.001
Model 3[c]		
TAPSE/PASP ratio, mm/mmHg	1.92 [1.30–2.83]	0.001
CO, L/min	1.43 [1.14–1.79]	0.002
mPAP, mmHg	1.03 [1.01–1.06]	0.003
SvO_2, %	1.04 [1.02–1.07]	0.001
PAC, mL/mmHg	2.98 [1.41–6.29]	0.004
Model 4[d]		
TAPSE/PASP ratio, mm/mmHg	4.13 [2.02–8.48]	<0.001

TAPSE/PASP ratio, PVR, and PAC were ln-transformed.
BMI, body mass index; CI, confidence interval; CO, cardiac output; HR, hazard ratio; mPAP, mean pulmonary arterial pressure; PAC, pulmonary arterial capacitance; PASP, pulmonary arterial systolic pressure; PVR, pulmonary vascular resistance; RA, right atrial; SvO_2, mixed venous oxygen saturation; TAPSE, tricuspid annular plane systolic excursion.
[a] Stepwise multivariate analysis was applied to TAPSE/PASP ratio as a continuous variable, age, sex, BMI, arterial hypertension, atrial fibrillation, diabetes mellitus, and World Health Organization functional class.
[b] Stepwise multivariate analysis was applied to TAPSE/PASP ratio as a continuous variable, TAPSE, PASP, RA size, systolic annular tissue velocity of the lateral tricuspid annulus, Tei (myocardial performance) index, and left ventricular ejection fraction.
[c] Stepwise multivariate analysis was applied to TAPSE/PASP ratio as a continuous variable, pulmonary vascular resistance, mPAP, CO, PAC, SvO_2, pulse pressure, stroke volume, RA pressure, and pulmonary arterial wedge pressure.
[d] Stepwise multivariate analysis was applied to TAPSE/PASP ratio as a continuous variable, CO, SvO_2, RAP, TAPSE, PASP, right atrial size, and Tei index.

4. Discussion

We have presented a comprehensive analysis of the TAPSE/PASP ratio in a large cohort of patients with PAH. Novel findings of our study include the following: 1) the TAPSE/PASP ratio is an important and meaningful prognostic parameter in patients with PAH; 2) TAPSE/PASP correlates with PAC and consistently has a logistic function-based association with PVR and SvO_2, while TAPSE/PASP tertiles show a clear pattern of distribution across the PAC versus PVR curve, with the lowest tertile towards the more severe end of the curve (with low PAC and high PVR); and 3) TAPSE/PASP values decrease as TR, RA/RV enlargement, and WHO functional class increase in patients with PAH.

Our study population consisted mostly of patients with idiopathic PAH, severely compromised pulmonary hemodynamics, and impaired functional status. The TAPSE/PASP ratio was low overall. In general, our patient population showed a more compromised hemodynamic status (lower cardiac index and higher mPAP) than patient populations of previous studies exploring RV dysfunction and contractility in PAH [28–30]. This might partly account for the relatively low TAPSE/PASP ratio in our cohort compared with patients with chronic left heart failure [8, 31, 32]. In this regard, Ghio and coworkers also described a very low TAPSE/PASP ratio in patients with PAH after the start or escalation of specific PH therapy [33].

Our data introduce the TASPE/PASP ratio as an independent prognostic echocardiographic parameter in patients with PAH. Although several echocardiographic parameters of RV function have been related to survival [5], our data indicate that in direct comparison the TAPSE/PASP ratio might be superior as it better reflects the load-dependent status of the pulmonary circulation. As a measure of afterload, the TAPSE/PASP ratio combines longitudinal shortening with the ability of the RV to generate pulmonary pressure, and shows

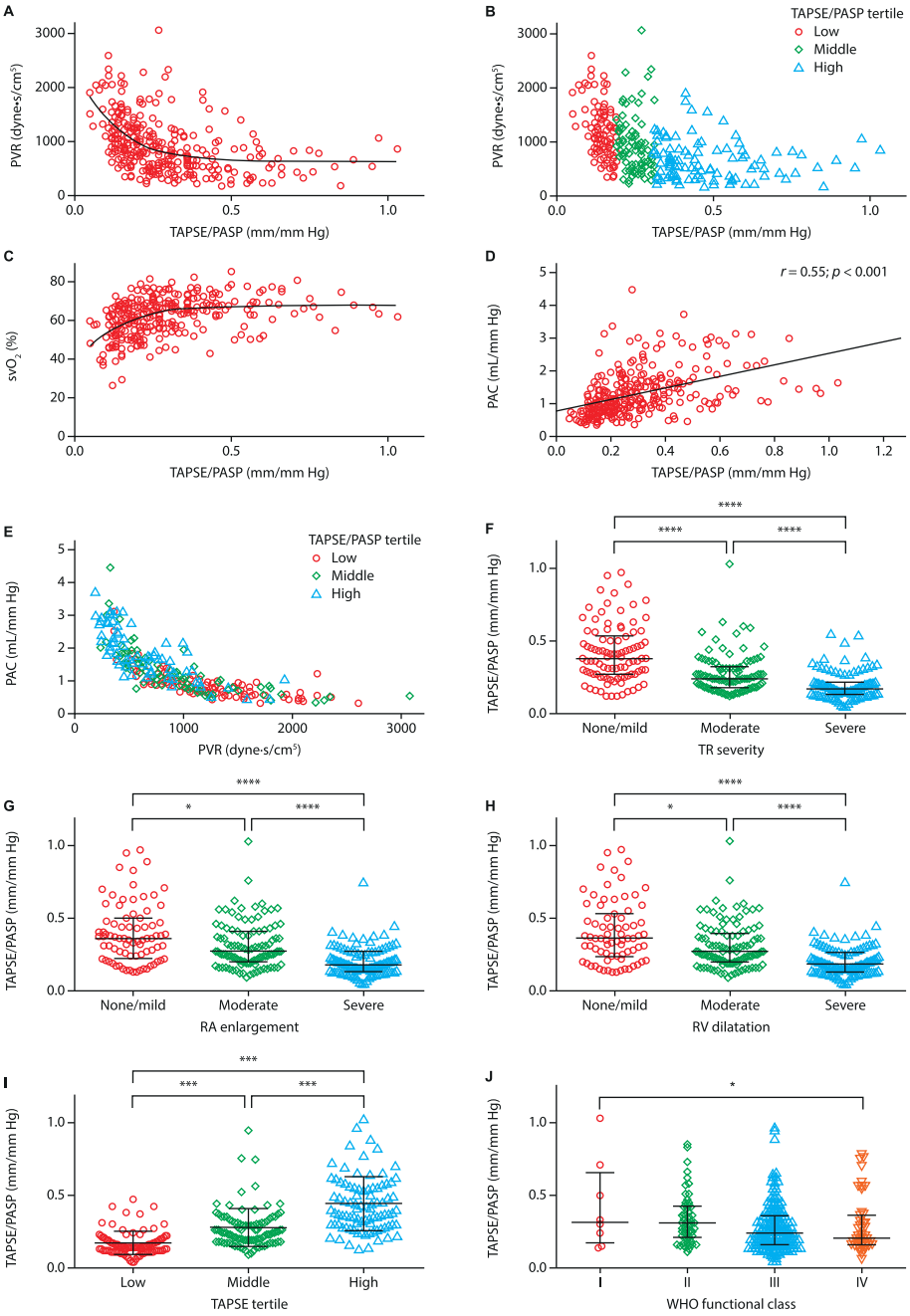

Fig. 2. Relationship of the TAPSE/PASP ratio with PVR, SvO_2, PAC, TR, RA/RV enlargement, TAPSE tertiles, and WHO functional class. Scatterplots show (A) PVR versus TAPSE/PASP, (B) PVR versus TAPSE/PASP stratified according to TAPSE/PASP tertile, (C) SvO_2 versus TAPSE/PASP, (D) Spearman correlation of PAC with TAPSE/PASP, (E) PAC versus PVR stratified by TAPSE/PASP tertile, and TAPSE/PASP ratio stratified by (F) TR severity ($n = 289$), (G) RA enlargement ($n = 289$), (H) RV dilatation ($n = 290$), (I) TAPSE tertiles ($n = 290$; tertile 1: <15 mm; tertile 2: ≥ 15–< 20 mm; tertile 3: ≥ 20 mm), and (J) WHO functional class ($n = 289$). Lines in panels F–J indicate median and interquartile range. $^{*}p < .05$, $^{***}p < .001$, and $^{****}p < .0001$ (Kruskal-Wallis test). PAC, pulmonary arterial capacitance; PASP, pulmonary arterial systolic pressure; PVR, pulmonary vascular resistance; RA, right atrial; RV, right ventricular; SvO_2, mixed venous oxygen saturation; TAPSE, tricuspid annular plane systolic excursion; TR, tricuspid regurgitation; WHO, World Health Organization.

relevant associations with overall survival, disease severity, and WHO functional class in PAH. Nevertheless, several echocardiographic indices of RV function in patients with idiopathic PAH have been investigated previously, and have undoubtedly proven their value in daily clinical practice [34]. Of note, Ghio and coworkers previously reported that the TAPSE/PASP ratio at follow-up (4–12 months after starting or escalating specific PH therapy) but not at baseline was significantly associated with mortality in patients with PAH. The different sample size (Ghio and coworkers included 81 patients) and the design of this study might be accountable for the different findings compared with our study [33].

Our data indicate that the TAPSE/PASP ratio is related to the severity of TR. This finding is of clinical value because severe TR per se has been identified as an independent prognostic feature in patients with PAH [35]. However, TAPSE might be overestimated in the presence of severe TR [34], and severe TR has also been reported to influence the relationship between TAPSE and RV ejection fraction [36]. Interestingly, our data indicate that the maladaptive morphological changes of RA/RV chamber enlargement, which cause annular dilation and leaflet tethering leading to TR in patients with PAH [37], are also related to the TAPSE/PASP ratio. The importance of RV morphology and function with respect to specific vasoactive therapy was recently demonstrated

in patients with idiopathic PAH, which might mirror the clinical importance of TAPSE/PASP observed in our data [38].

In our analysis, the TAPSE/PASP ratio was strongly correlated with the afterload-dependent parameters PVR and PAC, which have been separately related to outcome in patients with PAH [21, 39, 40]. It has been suggested that the observed relationship between PAC and PVR in heart failure might be reflective of early pathological changes within the pulmonary vasculature which contribute to both elevated PVR and reduced PAC [39, 40]. Reduced PAC is associated with greater stiffness of the pulmonary vasculature, which is associated with RV dysfunction [29]. The correlation of TAPSE/PASP with PAC as well as the logistic function-based relationship with PVR might support a role for the TAPSE/PASP ratio as a measure of afterload, similar to PAC, and explain its prognostic value both in our cohort and in the previously published cohort of patients with heart failure with preserved ejection fraction [8]. The observed association of the TAPSE/PASP ratio with SvO_2 in our cohort also mirrors the previously described inverse association between pulmonary vascular stiffness and RV ejection fraction [41]. Since PAC is associated with pulmonary vascular stiffness, the possibility of a correlation between TAPSE/PASP and pulmonary vascular stiffness should be researched, as it could further illuminate the physiological meaning of the TAPSE/PASP ratio.

Guazzi and coworkers introduced the TAPSE/PASP ratio as a non-invasive measurement of the RV contractile state [6] and ventriculo-arterial coupling in heart failure [8]. The TAPSE/PASP ratio showed a significant correlation with calculated RV Ees/Ea (RV Ees = PASP/RV end-systolic area; RV Ea = PASP/SV) [8], but has not yet been correlated with Ees/Ea measured directly by pressure–volume loops (the gold standard for measuring Ees when evaluating RV-PA coupling). Therefore, further studies should be conducted to correlate TAPSE/PASP with pressure–volume loop-derived Ees/Ea, in order to enhance current knowledge regarding contractility and ventriculo-arterial coupling in patients with PAH. Of note, the ability of echocardiography/pressure ratios to mirror relevant pathophysiological RV mechanisms was explored in PAH recently, and TAPSE/mPAP or fractional area change (FAC)/mPAP was found to be related to a relevant biomarker of RV function (interleukin-6) [42].

4.1. Limitations

Limitations of the analysis include its retrospective design (using data from a prospectively recruiting registry) and the fact that parameters other than TAPSE that represent RV function, such as FAC and especially global longitudinal strain, have not been assessed in our study but might also be indicative of contractility/coupling and associated with outcome. In addition, only a small proportion of our study population had measurements of the diastolic and systolic eccentricity index, which have shown prognostic and clinical value in patients with PAH previously [24]. However, the most clinically important parameters derived from right heart echocardiography were included in the multivariate model. Moreover, we found a certain level of disagreement between invasively derived TAPSE/sPAP and non-invasively derived TAPSE/PASP especially at higher ratios, as shown previously [8]. TAPSE reflects longitudinal shortening of the right ventricle. As RV dysfunction progresses, TAPSE reaches a minimum and shows no further decrease [43]. The reliability of TAPSE as a parameter of RV function (and therefore the utility of the TAPSE/PASP ratio) may thus be reduced in the later stages of RV failure. The utility of the TAPSE/PASP ratio within the failing heart or in acute decompensated status was beyond the scope of our study and merits further investigation. Moreover, in common with other echocardiographic parameters [44], the TAPSE/PASP ratio might be limited by intra- and inter-observer variability. Finally, the inclusion of patients with pulmonary veno-occlusive disease (PVOD) might have influenced the predictive capacity of the TAPSE/PASP ratio, as those patients per se present with a higher mortality than those with PAH [13]. However, relatively few patients in our study had PVOD (the majority had idiopathic PAH), and any bias resulting from their inclusion is likely to be small.

5. Conclusion

In conclusion, the TAPSE/PASP ratio is a non-invasive parameter that is straightforward to measure and is significantly associated with outcome, hemodynamics, and functional class in patients with PAH.

Funding

This work was funded by the Excellence Cluster Cardio-Pulmonary System (ECCPS) and the Collaborative Research Center (SFB) 1213 - Pulmonary Hypertension and Cor Pulmonale (grant number: SFB1213/1, project B08). For the manuscript, editorial assistance was provided by Dr. Claire Mulligan (Beacon Medical Communications Ltd., Brighton, UK), funded by the University of Giessen.

Conflicts of interest

Dr. Tello has received speaking fees from Actelion and Bayer. Mr. Axmann has nothing to disclose. Dr. Ghofrani has received consultancy fees from Bayer, Actelion, Pfizer, Merck, GSK, and Novartis; fees for participation in advisory boards from Bayer, Pfizer, GSK, Actelion, and Takeda; lecture fees from Bayer HealthCare, GSK, Actelion, and Encysive/Pfizer; industry-sponsored grants from Bayer HealthCare, Aires, Encysive/Pfizer, and Novartis; and sponsored grants from the German Research Foundation, Excellence Cluster Cardiopulmonary Research, and the German Ministry for Education and Research. Dr. Naeije has relationships with drug companies including AOPOrphan Pharmaceuticals, Actelion, Bayer, Reata, Lung Biotechnology Corporation, and United Therapeutics. In addition to being an investigator in trials involving these companies, relationships include consultancy service, research grants, and membership of scientific advisory boards. Dr. Rieth has received a research grant from Pfizer and speaker fees from Servier, St. Jude Medical, Cardiokinetix, and Actelion. Dr. Seeger has received speaker/consultancy fees from Pfizer and Bayer Pharma AG. Dr. Gall has received fees from Actelion, AstraZeneca, Bayer, BMS, GSK, Janssen-Cilag, Lilly, MSD, Novartis, OMT, Pfizer, and United Therapeutics. Dr. Richter has received support from United Therapeutics and Bayer; speaker fees from Actelion, Mundipharma, Roche, and OMT; and has received consultancy fees from Bayer.

Supplementary data to this article can be found online at https://doi.org/10.1016/j.ijcard.2018.01.053.

Acknowledgement

For the manuscript, editorial assistance was provided by Dr. Claire Mulligan (Beacon Medical Communications Ltd., Brighton, UK), funded by the University of Giessen.

The manuscript is part of the doctoral thesis of Newroz Narcin.

References

[1] N. Galie, M. Humbert, J.L. Vachiery, et al., 2015 ESC/ERS guidelines for the diagnosis and treatment of pulmonary hypertension: the joint task force for the diagnosis and treatment of pulmonary hypertension of the European Society of Cardiology (ESC) and the European Respiratory Society (ERS): endorsed by: Association for European Paediatric and Congenital Cardiology (AEPC), International Society for Heart and Lung Transplantation (ISHLT), Eur. Heart J. 37 (2016) 67–119.

[2] A. Harrison, N. Hatton, J.J. Ryan, The right ventricle under pressure: evaluating the adaptive and maladaptive changes in the right ventricle in pulmonary arterial hypertension using echocardiography (2013 Grover conference series), Pulm. Circ. 5 (2015) 29–47.

[3] A. Vonk Noordegraaf, B.E. Westerhof, N. Westerhof, The relationship between the right ventricle and its load in pulmonary hypertension, J. Am. Coll. Cardiol. 69 (2017) 236–243.

[4] P.R. Forfia, M.R. Fisher, S.C. Mathai, et al., Tricuspid annular displacement predicts survival in pulmonary hypertension, Am. J. Respir. Crit. Care Med. 174 (2006) 1034–1041.

[5] R. Naeije, Assessment of right ventricular function in pulmonary hypertension, Curr. Hypertens. Rep. 17 (2015) 35.
[6] M. Guazzi, F. Bandera, G. Pelissero, et al., Tricuspid annular plane systolic excursion and pulmonary arterial systolic pressure relationship in heart failure: an index of right ventricular contractile function and prognosis, Am. J. Physiol. Heart Circ. Physiol. 305 (2013) H1373–1381.
[7] I. Hussain, S.F. Mohammed, P.R. Forfia, et al., Impaired right ventricular-pulmonary arterial coupling and effect of sildenafil in heart failure with preserved ejection fraction: an ancillary analysis from the Phosphodiesterase-5 inhibition to improve clinical status and exercise capacity in diastolic heart failure (RELAX) trial, Circ. Heart Fail. 9 (2016), e002729.
[8] M. Guazzi, D. Dixon, V. Labate, et al., RV contractile function and its coupling to pulmonary circulation in heart failure with preserved ejection fraction: stratification of clinical phenotypes and outcomes, JACC Cardiovasc. Imaging 10 (2017) 1211–1221.
[9] T.M. Gorter, D.J. van Veldhuisen, A.A. Voors, et al., Right ventricular-vascular coupling in heart failure with preserved ejection fraction and pre- vs. post-capillary pulmonary hypertension, Eur. Heart J. Cardiovasc. Imaging 19 (4) (2018) 425–432.
[10] M. Guazzi, S. Villani, G. Generati, et al., Right ventricular contractile reserve and pulmonary circulation uncoupling during exercise challenge in heart failure: pathophysiology and clinical phenotypes, JACC Heart Fail. 4 (2016) 625–635.
[11] M. Guazzi, R. Naeije, R. Arena, et al., Echocardiography of right ventriculoarterial coupling combined with cardiopulmonary exercise testing to predict outcome in heart failure, Chest 148 (2015) 226–234.
[12] M. Gerges, C. Gerges, A.M. Pistritto, et al., Pulmonary hypertension in heart failure. Epidemiology, right ventricular function, and survival, Am. J. Respir. Crit. Care Med. 192 (2015) 1234–1246.
[13] H. Gall, J.F. Felix, F.K. Schneck, et al., The Giessen pulmonary hypertension registry: survival in pulmonary hypertension subgroups, J Heart Lung Transplant 36 (2017) 957–967.
[14] S.K. Medrek, C. Kloefkorn, D.T.M. Nguyen, E.A. Graviss, A.E. Frost, Z. Safdar, Longitudinal change in pulmonary arterial capacitance as an indicator of prognosis and response to therapy and in pulmonary arterial hypertension, Pulm. Circ. 7 (2017) 399–408.
[15] L.G. Rudski, W.W. Lai, J. Afilalo, et al., Guidelines for the echocardiographic assessment of the right heart in adults: a report from the American Society of Echocardiography endorsed by the European Association of Echocardiography, a registered branch of the European Society of Cardiology, and the Canadian Society of Echocardiography, J. Am. Soc. Echocardiogr. 23 (2010) 685–713 (quiz 786-688).
[16] R.M. Lang, M. Bierig, R.B. Devereux, et al., Recommendations for chamber quantification: a report from the American Society of Echocardiography's guidelines and standards committee and the chamber quantification writing group, developed in conjunction with the European Association of Echocardiography, a branch of the European Society of Cardiology, J. Am. Soc. Echocardiogr. 18 (2005) 1440–1463.
[17] M.A. Quiñones, C.M. Otto, M. Stoddard, et al., Recommendations for quantification of Doppler echocardiography: a report from the Doppler quantification task force of the nomenclature and standards Committee of the American Society of Echocardiography, J. Am. Soc. Echocardiogr. 15 (2002) 167–184.
[18] B.J. Kircher, R.B. Himelman, N.B. Schiller, Noninvasive estimation of right atrial pressure from the inspiratory collapse of the inferior vena cava, Am. J. Cardiol. 66 (1990) 493–496.
[19] G.C. Kane, H. Maradit-Kremers, J.P. Slusser, C.G. Scott, R.P. Frantz, M.D. McGoon, Integration of clinical and hemodynamic parameters in the prediction of long-term survival in patients with pulmonary arterial hypertension, Chest 139 (2011) 1285–1293.
[20] P. Peduzzi, J. Concato, A.R. Feinstein, T.R. Holford, Importance of events per independent variable in proportional hazards regression analysis. II. Accuracy and precision of regression estimates, J. Clin. Epidemiol. 48 (1995) 1503–1510.
[21] R.L. Benza, D.P. Miller, M. Gomberg-Maitland, et al., Predicting survival in pulmonary arterial hypertension: insights from the registry to evaluate early and long-term pulmonary arterial hypertension disease management (REVEAL), Circulation 122 (2010) 164–172.
[22] G.E. D'Alonzo, R.J. Barst, S.M. Ayres, et al., Survival in patients with primary pulmonary hypertension. Results from a national prospective registry, Ann. Intern. Med. 115 (1991) 343–349.
[23] V. Fuster, P.M. Steele, W.D. Edwards, B.J. Gersh, M.D. McGoon, R.L. Frye, Primary pulmonary hypertension: natural history and the importance of thrombosis, Circulation 70 (1984) 580–587.
[24] R.J. Raymond, A.L. Hinderliter, P.W. Willis, et al., Echocardiographic predictors of adverse outcomes in primary pulmonary hypertension, J. Am. Coll. Cardiol. 39 (2002) 1214–1219.
[25] L.M. Wright, N. Dwyer, D. Celermajer, L. Kritharides, T.H. Marwick, Follow-up of pulmonary hypertension with echocardiography, JACC Cardiovasc. Imaging 9 (2016) 733–746.
[26] T.C. Yeo, K.S. Dujardin, C. Tei, D.W. Mahoney, M.D. McGoon, J.B. Seward, Value of a Doppler-derived index combining systolic and diastolic time intervals in predicting outcome in primary pulmonary hypertension, Am. J. Cardiol. 81 (1998) 1157–1161.
[27] D. Giavarina, Understanding Bland Altman analysis, Biochem. Med. (Zagreb) 25 (2015) 141–151.
[28] A. Bellofiore, E. Dinges, R. Naeije, et al., Reduced haemodynamic coupling and exercise are associated with vascular stiffening in pulmonary arterial hypertension, Heart 103 (2017) 421–427.
[29] J. Sanz, A. Garcia-Alvarez, L. Fernandez-Friera, et al., Right ventriculo-arterial coupling in pulmonary hypertension: a magnetic resonance study, Heart 98 (2012) 238–243.
[30] M.J. Brewis, A. Bellofiore, R.R. Vanderpool, et al., Imaging right ventricular function to predict outcome in pulmonary arterial hypertension, Int. J. Cardiol. 218 (2016) 206–211.
[31] S. Ghio, M. Guazzi, A.B. Scardovi, et al., Different correlates but similar prognostic implications for right ventricular dysfunction in heart failure patients with reduced or preserved ejection fraction, Eur. J. Heart Fail. 19 (2017) 873–879.
[32] L. Bosch, C.S.P. Lam, L. Gong, et al., Right ventricular dysfunction in left-sided heart failure with preserved versus reduced ejection fraction, Eur. J. Heart Fail. 19 (12) (2018) 1664–1671.
[33] S. Ghio, S. Pica, C. Klersy, et al., Prognostic value of TAPSE after therapy optimisation in patients with pulmonary arterial hypertension is independent of the haemodynamic effects of therapy, Open Heart 3 (2016), e000408.
[34] S. Ghio, C. Klersy, G. Magrini, et al., Prognostic relevance of the echocardiographic assessment of right ventricular function in patients with idiopathic pulmonary arterial hypertension, Int. J. Cardiol. 140 (2010) 272–278.
[35] L. Chen, C.M. Larsen, R.J. Le, et al., The prognostic significance of tricuspid valve regurgitation in pulmonary arterial hypertension, Clin. Respir. J. 12 (4) (2018) 1572–1580.
[36] S.H. Hsiao, S.K. Lin, W.C. Wang, S.H. Yang, P.L. Gin, C.P. Liu, Severe tricuspid regurgitation shows significant impact in the relationship among peak systolic tricuspid annular velocity, tricuspid annular plane systolic excursion, and right ventricular ejection fraction, J. Am. Soc. Echocardiogr. 19 (2006) 902–910.
[37] E.A. Fender, C.J. Zack, R.A. Nishimura, Isolated tricuspid regurgitation: outcomes and therapeutic interventions, Heart (2017) https://doi.org/10.1136/heartjnl-2017-311586.
[38] R. Badagliacca, A. Raina, S. Ghio, et al., Influence of various therapeutic strategies on right ventricular morphology, function and hemodynamics in pulmonary arterial hypertension, J Heart Lung Transplant 37 (3) (2018) 365–375.
[39] S. Ghio, M. D'Alto, R. Badagliacca, et al., Prognostic relevance of pulmonary arterial compliance after therapy initiation or escalation in patients with pulmonary arterial hypertension, Int. J. Cardiol. 230 (2017) 53–58.
[40] N. Al-Naamani, I.R. Preston, N.S. Hill, K.E. Roberts, The prognostic significance of pulmonary arterial capacitance in pulmonary arterial hypertension: single-center experience, Pulm. Circ. 6 (2016) 608–610.
[41] G.R. Stevens, A. Garcia-Alvarez, S. Sahni, M.J. Garcia, V. Fuster, J. Sanz, RV dysfunction in pulmonary hypertension is independently related to pulmonary artery stiffness, JACC Cardiovasc. Imaging 5 (2012) 378–387.
[42] K.W. Prins, S.L. Archer, M. Pritzker, et al., Interleukin-6 is independently associated with right ventricular function in pulmonary arterial hypertension, J Heart Lung Transplant 37 (3) (2018) 376–384.
[43] T. Kind, G.J. Mauritz, J.T. Marcus, M. van de Veerdonk, N. Westerhof, A. Vonk-Noordegraaf, Right ventricular ejection fraction is better reflected by transverse rather than longitudinal wall motion in pulmonary hypertension, J. Cardiovasc. Magn. Reson. 12 (2010) 35.
[44] K.E. Farsalinos, A.M. Daraban, S. Unlu, J.D. Thomas, L.P. Badano, J.U. Voigt, Head-to-head comparison of global longitudinal strain measurements among nine different vendors: the EACVI/ASE inter-vendor comparison study, J. Am. Soc. Echocardiogr. 28 (2015) 1171–1181 (e1172).

Anlage I

Right ventricular function correlates of right atrial strain in pulmonary hypertension: a combined cardiac magnetic resonance and conductance catheter study.

Tello K, Dalmer A, Vanderpool R, Ghofrani HA, Naeije R, Roller F, Seeger W, Wiegand M, Gall H, Richter MJ. Am J Physiol Heart Circ Physiol. 2020 Jan 1;318(1):H156-H164

Am J Physiol Heart Circ Physiol 318: H156–H164, 2020.
First published November 22, 2019; doi:10.1152/ajpheart.00485.2019.

RESEARCH ARTICLE | *Integrative Cardiovascular Physiology and Pathophysiology*

Right ventricular function correlates of right atrial strain in pulmonary hypertension: a combined cardiac magnetic resonance and conductance catheter study

Khodr Tello,[1] Antonia Dalmer,[1] Rebecca Vanderpool,[2] Hossein A. Ghofrani,[1,3,4] Robert Naeije,[5] Fritz Roller,[6] Werner Seeger,[1] Merle Wiegand,[1] Henning Gall,[1] and Manuel J. Richter[1]

[1]*Department of Internal Medicine, Justus Liebig University Giessen, Universities of Giessen and Marburg Lung Center, German Center for Lung Research, Giessen, Germany;* [2]*Division of Translational and Regenerative Medicine, University of Arizona, Tucson, Arizona;* [3]*Department of Pneumology, Kerckhoff Heart, Rheuma and Thoracic Center, Bad Nauheim, Germany;* [4]*Department of Medicine, Imperial College London, London, United Kingdom;* [5]*Erasme University Hospital, Brussels, Belgium; and* [6]*Department of Radiology, Justus Liebig University Giessen, Universities of Giessen and Marburg Lung Center, German Center for Lung Research, Giessen, Germany*

Submitted 27 August 2019; accepted in final form 15 November 2019

Tello K, Dalmer A, Vanderpool R, Ghofrani HA, Naeije R, Roller F, Seeger W, Wiegand M, Gall H, Richter MJ. Right ventricular function correlates of right atrial strain in pulmonary hypertension: a combined cardiac magnetic resonance and conductance catheter study. *Am J Physiol Heart Circ Physiol* 318: H156–H164, 2020. First published November 22, 2019; doi:10.1152/ajpheart.00485.2019.—The functional relevance of right atrial (RA) function in pulmonary hypertension (PH) remains incompletely understood. The purpose of this study was to explore the correlation of cardiac magnetic resonance (CMR) feature tracking-derived RA phasic function with invasively measured pressure-volume (P-V) loop-derived right ventricular (RV) end-diastolic elastance (E_{ed}) and RV-arterial coupling [ratio of end-systolic elastance to arterial elastance (E_{es}/E_a)]. In 54 patients with severe PH, CMR was performed within 24 h of diagnostic right heart catheterization and P-V measurements. RA phasic function was assessed by CMR imaging of RA reservoir, passive, and active strain. The association of RA phasic function with indexes of RV function was evaluated by Spearman's rank correlation and linear regression analyses. Median [interquartile range] RA reservoir strain, passive strain, and active strain were 19.5% [11.0–24.5], 7.0% [4.0–12.0], and 13.0% [7.0–18.5], respectively. E_{es}/E_a was 0.73 [0.48–1.08], and E_{ed} was 0.14 mmHg/mL [0.05–0.22]. RV diastolic impairment [RV end-diastolic pressure (EDP) and E_{ed}] was correlated with RA phasic function, but E_a and E_{es} were not. In addition, RA phasic function was correlated with inferior vena cava diameter. In multivariate linear regression analysis, adjusting for key P-V loop indexes, E_{ed} and EDP remained significantly associated with RA phasic function. We conclude that RA phasic function is altered in relation to impaired diastolic function of the chronically overloaded right ventricle and contributes to backward venous flow and systemic congestion. These results call for more attention to RA function in the management of patients with PH.

NEW & NOTEWORTHY There is growing awareness of the importance of the right atrial (RA)-right ventricular (RV) axis in pulmonary hypertension (PH). Our results uncover alterations in RA phasic function that are related to depressed RV lusitropic function and contribute to backward venous return and systemic congestion in chronic RV overload. Assessment of RA function should be part of the management and follow-up of patients with PH.

coupling; feature tracking; pulmonary hypertension; right atrial strain; right ventricular diastolic function

INTRODUCTION

Pulmonary hypertension (PH) is characterized by an increase in afterload, which induces progressive right ventricular (RV) remodeling with increased contractility (to maintain RV-arterial coupling) and diastolic stiffening, eventually leading to RV dilatation and clinical right heart failure (28, 34). RV failure is the leading cause of mortality in PH (18). PH and RV failure also lead to changes in right atrial (RA) size, function, and pressure, which are associated with a poor prognosis (15, 26, 27, 35). A recent two-dimensional echocardiographic speckle-tracking study suggested that RA reservoir and passive conduit functions are impaired in severe PH independently of RA size and pressure, likely reflecting RV failure and overload (26). Thus, the impact of RV failure on the right atrium is an essential part of the pathophysiology of PH, and the assessment of RA function appears essential to a better understanding of RV function in PH.

Awareness of the importance of the RA-RV axis in PH is growing. Several echocardiographic speckle tracking studies have reported on RA deformation and function in patients with PH (3, 7, 32), and RA reservoir function has been suggested to play a key role in the progression of PH (3, 7, 32). Cardiac magnetic resonance (CMR) imaging remains the reference imaging modality in patients with PH (6, 13, 37). Accordingly, it has also been recently applied to feature-tracking assessment of RA phasic function (19). However, the functional relevance of imaging studies of RA function remains incompletely understood.

Therefore, the purpose of the present study was to relate CMR imaging of RA function to invasively measured pressure-volume (P-V) relationships of the right ventricle including gold-standard determinations of contractility [measured as end-systolic elastance (E_{es})], afterload [measured as arterial elas-

Address for reprint requests and other correspondence: K. Tello, Dept. of Internal Medicine, Justus-Liebig-Univ. Giessen, Klinikstrasse 32, 35392 Giessen, Germany (e-mail: khodr.tello@innere.med.uni-giessen.de).

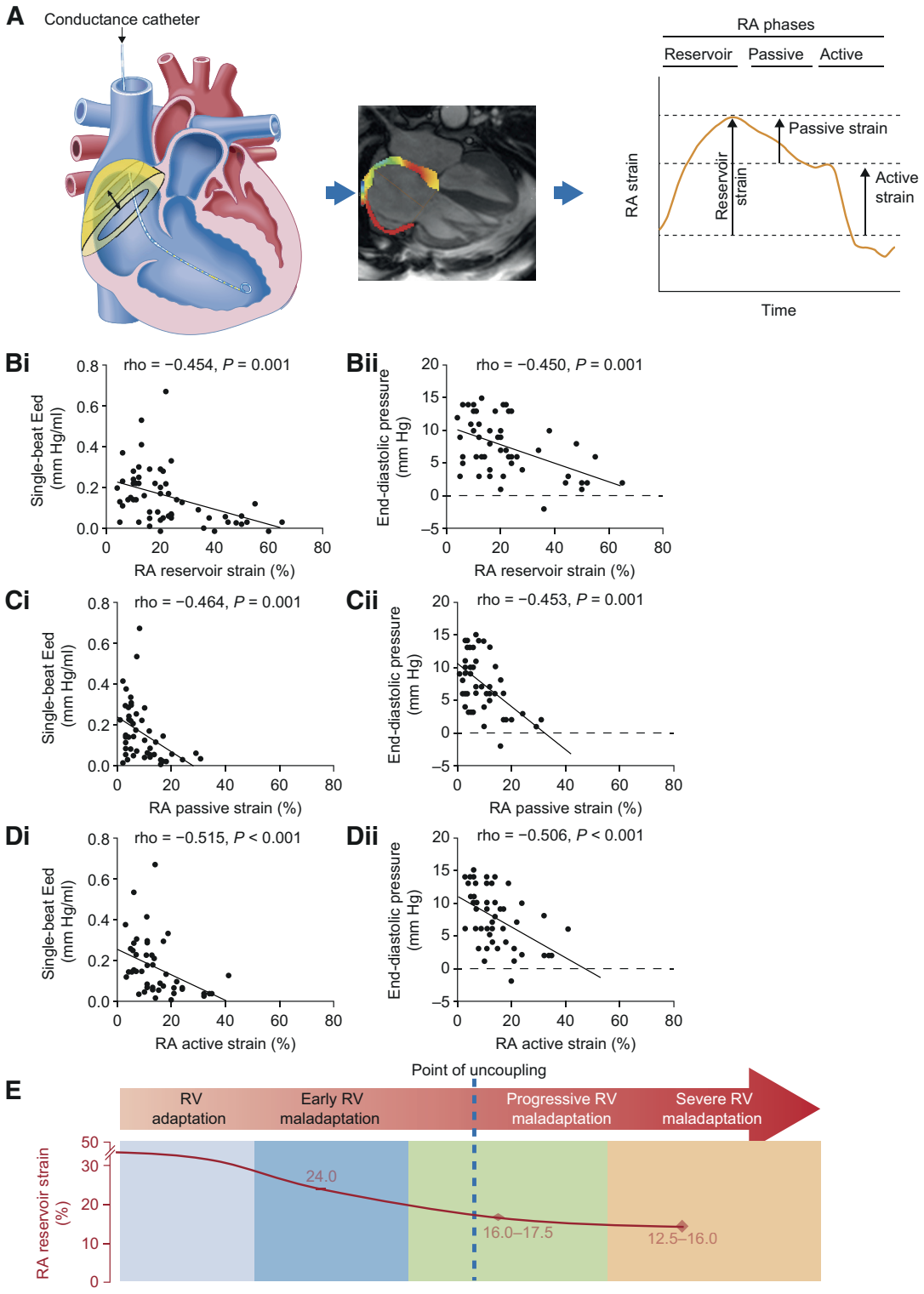

Fig. 1. Association of cardiac magnetic resonance (CMR) right atrial (RA) phasic function with right ventricular (RV) diastolic function derived from pressure-volume loop measurements. Schematic illustration of CMR-derived RA strain assessment in combination with pressure-volume catheterization, and an example of CMR feature tracking of RA reservoir, passive, and active strain (*A*). Correlation of CMR RA reservoir strain (*B*), passive strain (*C*), and active strain (*D*) with end-diastolic elastance (E_{ed}; *Bi*, *Ci*, and *Di*) and end-diastolic pressure (*Bii*, *Cii*, and *Dii*; in each panel, $n = 49–54$ patients). Spearman's rank was used to measure associations between variables (trend lines were least-squares fits of straight-line models). Progressive RV maladaptation is accompanied by decreasing RA reservoir strain [*E*; concept adapted from Vonk Noordegraaf et al. (45)]. The initial level of RA reservoir strain (before RV adaptation and maladaptation) was estimated on the basis of previous publications (14, 24). Values for RA reservoir strain during RV adaptation and maladaptation were based on median values obtained after stratification by E_{ed} and the end-systolic elastance-to-arterial elastance ratio (E_{es}/E_a) tertiles (Supplemental Fig. S1 and Supplemental Tables S1 and S2; all Supplemental Material is available at https://dx.doi.org/10.17504/protocols.io.8wjhxcn).

Table 1. *Patient characteristics and pulmonary hemodynamics*

	Value
Patients, *n*	54
Male/female, *n/n*	27/27
Age, yr	55 ± 14
PH subtype, *n* (%)	
Idiopathic pulmonary arterial hypertension	37 (68.5)
Heritable pulmonary arterial hypertension	1 (1.9)
Pulmonary arterial hypertension associated with	
Human immunodeficiency virus infection	2 (3.7)
Portal hypertension	3 (5.6)
Connective tissue disease	3 (5.6)
Congenital heart disease	1 (1.9)
Pulmonary arterial hypertension with overt features of venous/capillary involvement	2 (3.7)
Chronic thromboembolic PH	5 (9.3)
WHO functional class, *n* (%)	
I	3 (5.6)
II	19 (35.2)
III	29 (53.7)
IV	3 (5.6)
Right heart catheterization	
Mean pulmonary arterial pressure, mmHg	45 ± 14
Right atrial pressure, mmHg	7 ± 3
Pulmonary vascular resistance, Wood units	6.8 [4.4–10.1]
Cardiac index, $L \cdot min^{-1} \cdot m^{-2}$	2.8 ± 0.7
Pulmonary arterial wedge pressure, mmHg	9 ± 3
Treatment, *n* (%)	
Phosphodiesterase type 5 inhibitor	27 (50)
Endothelin receptor antagonist	32 (59.3)
Soluble guanylate cyclase stimulator	19 (35.2)
Selexipag	4 (7.4)
Prostanoid	13 (24.1)
Combination therapy, *n* (%)	
Therapy naïve	5 (9.3)
Monotherapy	17 (31.5)
Dual therapy	16 (29.6)
Triple therapy	15 (27.8)
Laboratory	
BNP, pg/mL	102 [38–333]
Echocardiography	
Inferior vena cava diameter,* cm	1.9 ± 0.5

Values are means ± SD or medians [interquartile range], unless otherwise specified; *n* = no. of patients. BNP, B-type natriuretic peptide; PH, pulmonary hypertension; WHO, World Health Organization. *Here, *n* = 46 patients.

tance (E_a)], and diastolic stiffness [measured as end-diastolic elastance (E_{ed})] as previously described by our group (38, 43).

METHODS

Study design and patients. The analysis included consecutive patients with pulmonary arterial hypertension (PAH) and chronic thromboembolic PH who were prospectively enrolled into the Right Heart I study (ClinicalTrials.gov identifier: NCT03403868) and the Giessen PH Registry (9) between January 2016 and December 2018. Patients with atrial flutter or fibrillation were excluded. Diagnoses were made according to current guidelines (8) and updated recommendations (36), and each diagnosis was assessed by a multidisciplinary board including pulmonologists and radiologists before enrollment. The study population included a proportion of previously published patients (29, 38–42). P-V/Swan-Ganz catheterization was performed 1 day after CMR imaging. B-type natriuretic peptide (BNP) was measured in all patients with a commercially available, fully automated, two-site sandwich immunoassay (ADVIA Centaur BNP Test; Siemens Healthineers, Erlangen, Germany). Diameter of the inferior vena cava was measured as recommended (16). All patients were treated with targeted PH medications on the basis of clinical grounds and best standard of care. The investigation conforms with the principles of the Declaration of Helsinki and was approved by the ethics committee of the Faculty of Medicine at the University of Giessen (approval no. 108/15). Written informed consent was provided by all participating patients.

CMR imaging. CMR imaging of RV and left ventricular volumes was performed with the Avanto 1.5-T scanner system [gradient strength and slew rate: SQ-Engine (45 mT/m at 200 $T \cdot m^{-1} \cdot s^{-1}$); Siemens Healthineers, Erlangen, Germany].

RA myocardial feature tracking was performed off-line on the basis of balanced steady-state free precession cine images using dedicated software (cvi[42]; Circle Cardiovascular Imaging, Calgary, AB, Canada).

RA strain analysis was based on the four-chamber view only. Endocardial contours were drawn manually in end-systolic images with subsequent automatic tracking of the endocardial contour throughout the cardiac cycle. The quality of automatic tracking was checked. In case of insufficient automated border tracking, manual adjustments were made to the initial contour, and the algorithm was repeated. Segments were not excluded from the analysis, since contour drawing and tracking were not hindered by the right atrial appendage or the presence of a Eustachian valve in our cohort. Tracking was repeated three times, and averages were used for analysis as described in a comparable study (47). To test intraobserver and interobserver reproducibility of RA reservoir strain, 10 randomly sampled analyses were repeated twice by the same observer and by a second observer, respectively. As previously described (19), RA total reservoir strain and RA active strain were assessed by measuring the corresponding peak strains (Fig. 1*A*). RA passive strain was calculated as the difference between RA total reservoir strain and RA active strain.

RA maximum and minimum volumes were assessed at ventricular systole and diastole, respectively, using cvi[42] software. From these measurements, RA total emptying fraction was calculated as (RA maximum volume − RA minimum volume)/RA maximum volume.

Right heart catheterization. We inserted a Swan-Ganz catheter via the internal jugular vein using an 8-F introducer sheath. We assessed pressures continuously and recorded cardiac index as the average of

Table 2. *Pressure-volume loop and CMR measurements*

	Value
Pressure-volume loop measurements	
E_a, mmHg/mL	0.75 [0.46–1.01]
E_{es}, mmHg/mL	0.55 [0.33–0.76]
E_{es}-to-E_a ratio	0.73 [0.48–1.08]
E_{ed}, mmHg/mL	0.14 [0.05–0.22]
End-systolic pressure, mmHg	66 ± 23
End-diastolic pressure, mmHg	8 ± 4
CMR measurements of right atrium	
RA reservoir strain, %	19.5 [11.0–24.5]
RA passive strain,* %	7.0 [4.0–12.0]
RA active strain,* %	13.0 [7.0–18.5]
RA total emptying fraction,† %	35 ± 14
RA maximum volume indexed to BSA,† mL/m^2	58.9 [46.6–90.0]
RA minimum volume indexed to BSA,† mL/m^2	36.2 [27.5–60.2]
CMR measurements of right ventricle	
RV EDV indexed to BSA, mL/m^2	116.9 ± 40.0
RV end-diastolic mass indexed to BSA, g/m^2	41.1 ± 18.0
RV mass-to-volume ratio, g/mL	0.4 ± 0.1
RV ejection fraction, %	39.3 [27.2–48.2]
Left ventricle	
LV ejection fraction,‡ %	62.8 [56.3–68.1]

Values are means ± SD or medians [interquartile range]. BSA, body surface area; CMR, cardiac magnetic resonance; E_a, arterial elastance; EDV, end-diastolic volume; E_{ed}, end-diastolic elastance; E_{es}, end-systolic elastance; LV, left ventricular; RA, right atrial; RV, right ventricular. *Here, *n* = 49 patients; †*n* = 53 patients; ‡*n* = 48 patients.

three to five measurements (taken using the direct or indirect Fick method as available). We calculated pulmonary vascular resistance (PVR) as [mean pulmonary arterial pressure (mPAP) − pulmonary arterial wedge pressure]/cardiac output (8).

P-V catheterization. We obtained and analyzed P-V loops as described previously (38). Briefly, we positioned a 4-Fr P-V catheter (CA-41063; CD Leycom, Zoetermeer, The Netherlands) in the RV apex and used an intracardiac analyzer (Inca; CD Leycom) to display P-V loops in real time. We calculated E_a as the ratio of end-systolic pressure (ESP) to stroke volume and used the RV single-beat method to calculate E_{es} (4). RV-arterial coupling was defined as the ratio of E_{es} to E_a (E_{es}/E_a). We calculated diastolic stiffness β by fitting a nonlinear exponential curve $P = \alpha(e^{\beta V} - 1)$ through three points on the diastolic portion of the P-V loops using a custom MATLAB program, and we obtained E_{ed} from the relationship $dP/dV = \alpha\beta \times e^{\beta \times EDV}$ at calculated end-diastolic volumes (EDV; α is a curve-fit parameter; 44). When the P-V loops showed a clear overlap, we chose a single beat for extrapolation to a sinusoidal curve and for analysis of E_{ed}. Volume measurements were calibrated with CMR imaging data.

Statistical analyses. Statistical analysis and presentation followed the Guidelines in Cardiovascular Research article by Lindsey et al.

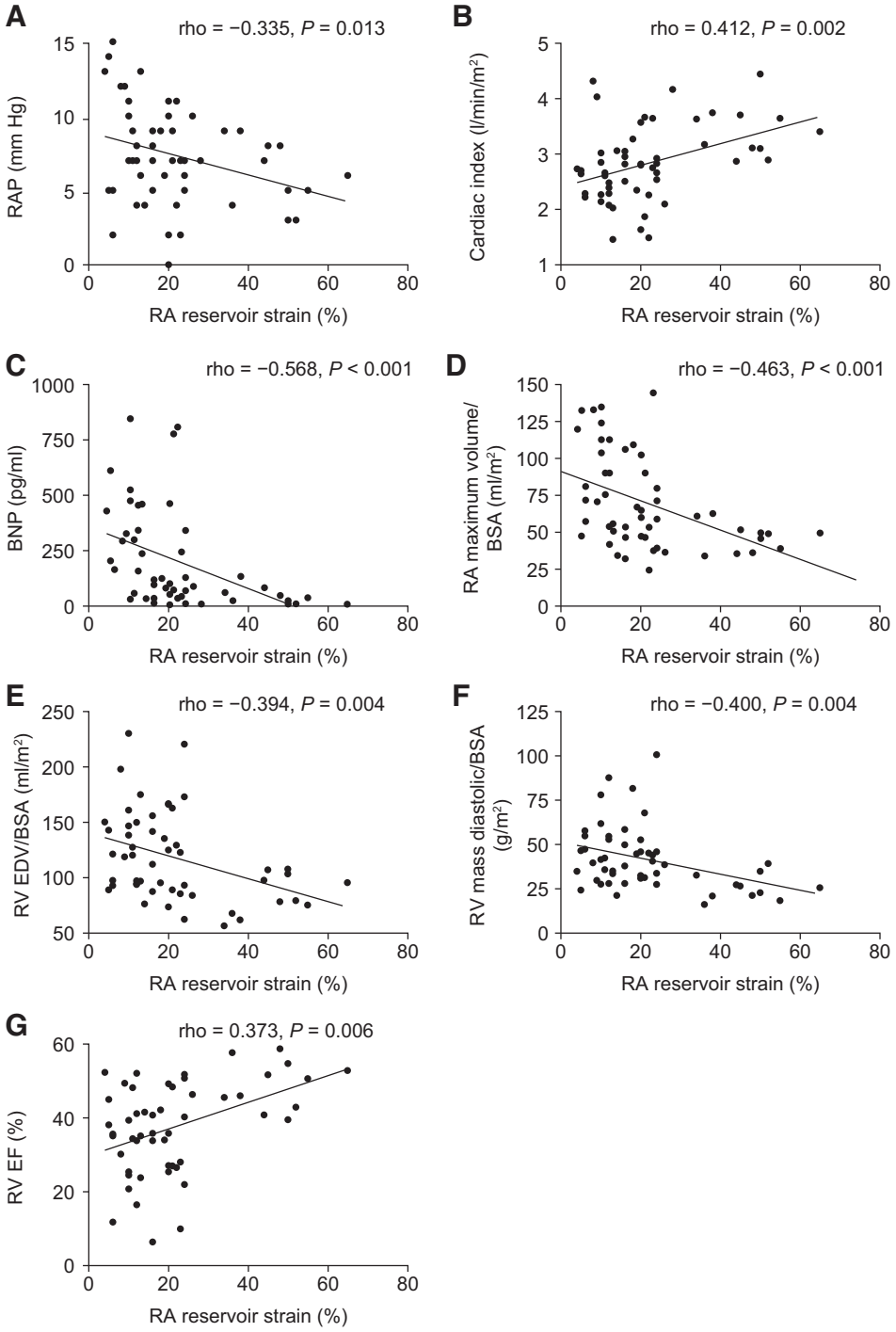

Fig. 2. Correlation of cardiac magnetic resonance imaging-derived right atrial (RA) reservoir function with pulmonary hemodynamics, B-type natriuretic peptide (BNP) levels, RA volume, and right ventricular (RV) function, dilatation, and hypertrophy. RA reservoir strain was correlated with right atrial pressure (RAP; *A*), cardiac index (*B*), BNP levels (*C*), RA maximum volume indexed to body surface area (BSA; *D*), RV end-diastolic volume (EDV) indexed to BSA (*E*), RV end-diastolic mass indexed to BSA (*F*), and RV ejection fraction (EF; *G*). In each panel, $n = 53$ to 54 patients. Spearman's rank was used to measure associations between variables (trend lines were least-squares fits of straight-line models).

(20). We determined adherence to a Gaussian distribution using the Kolmogorov-Smirnov test and visual assessment of histograms. Spearman's rank was used to measure associations between variables (trend lines were least-squares fits of straight-line models). We used univariate and multivariate linear regression analysis with RA phasic function as the dependent variable to determine the association with P-V loop parameters. Multivariable analyses were adjusted to all P-V loop parameters with $P < 0.05$ in univariate analysis (31). Multicollinearity was assessed using the variance inflation factor. Nonnormally distributed parameters were natural log transformed for linear regression analysis and rechecked by visual assessment of histograms. For all analyses, $P < 0.05$ was considered statistically significant. SPSS version 23.0 (IBM, Armonk, NY) was used for statistical analyses.

RESULTS

Patients. In total, 54 patients with PH were included; most of the patients had idiopathic PAH, and the majority presented in World Health Organization (WHO) functional class III (Table 1). Pulmonary hemodynamics showed precapillary PH. A substantial proportion of the patients were receiving dual or triple combination targeted PH therapy. Five patients with incident PH without specific pulmonary vascular therapy were included, one of whom had chronic thromboembolic PH (CTEPH) that was judged operable; this patient was referred for pulmonary endarterectomy surgery. The remaining four patients with CTEPH were previously judged inoperable by the local CTEPH board, had already received soluble guanylate cyclase stimulators, and were reevaluated for balloon pulmonary angioplasty.

P-V loop measurements (Table 2) showed impaired RV-arterial coupling [E_{es}/E_a was substantially lower than the optimal ratio, which is considered to be 1.5–2.0 (12)]. CMR imaging-derived RA and RV measurements (Table 2) showed RA enlargement and a high RV EDV (indicating RV dilatation) and decreased RV ejection fraction (EF) compared with values reported in healthy individuals (25). The intraclass correlation coefficient for agreement between the different observers was 0.86 (95% confidence interval: 0.417–0.970; $P = 0.05$) with a coefficient of variation of 11% regarding the RA reservoir strain measurement.

Association of CMR RA phasic function with RV function and biomarkers. RA reservoir strain, passive strain, and active strain were significantly correlated with P-V loop-derived measurements of RV diastolic function [E_{ed} and end-diastolic pressure (EDP); Fig. 1, *B–D*], but no association with RV contractility (E_{es}) or afterload (E_a) or mPAP was observed (data not shown). Figure 1*E* presents our findings regarding worsening RA reservoir function in the context of the current pathophysiological concept of progressive RV maladaptation leading to RV failure [adapted from previous work by Vonk Noordegraaf and colleagues (45, 46)].

In addition, RA reservoir strain showed significant correlations with RA pressure (RAP), cardiac index, BNP, and RA maximum volume (Fig. 2, *A–D*). Moreover, significant correlations with RV dilatation (RV EDV), RV hypertrophy (RV end-diastolic mass), and RV EF were observed (Fig. 2, *E–G*). We observed significant correlations of RA passive strain with RAP (rho = −0.368; $P = 0.009$), cardiac index (rho = 0.389; $P = 0.006$), BNP (rho = −0.455; $P = 0.002$), RA maximum volume (rho = −0.405; $P = 0.004$), RV EDV (rho = −0.337; $P = 0.020$), RV end-diastolic mass (rho = −0.463; $P = 0.001$), and RV EF (rho = 0.482; $P = 0.001$). Of note, we also observed significant correlations of RA active strain with RAP (rho = −0.307; $P = 0.032$), cardiac index (rho = 0.426; $P = 0.002$), BNP (rho = −0.512; $P < 0.001$), RA maximum volume (rho = −0.556; $P < 0.001$), RV EDV (rho = −0.454; $P = 0.001$), RV end-diastolic mass (rho = −0.477; $P = 0.001$), and RV EF (rho = 0.455; $P = 0.001$). In addition, significant associations of RA reservoir strain (rho = 0.317; $P = 0.032$) and RA active strain (rho = 0.404; $P = 0.008$) with left ventricular EF were observed. RA reservoir strain, passive strain, and active strain were all significantly associated with the diameter of the inferior vena cava (Fig. 3).

Determinants of RA phasic function. In univariate linear regression analysis, the B-coefficient indicated that an increase in E_{ed} and EDP was significantly associated with a reduction of RA reservoir strain. In the corresponding multivariate model, we found that increased EDP was independently associated with reduced RA reservoir strain (Table 3). In addition, an increase in E_{ed}, EDP, and ESP and a decrease in E_{es}/E_a were

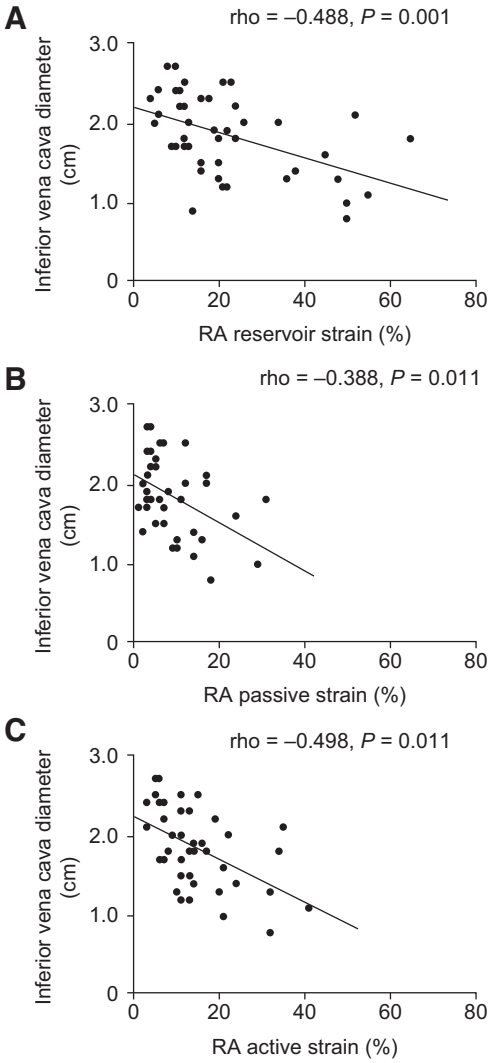

Fig. 3. Correlation of right atrial (RA) reservoir strain (*A*), RA passive strain (*B*), and RA active strain (*C*) with inferior vena cava diameter (in each panel, $n = 46$ patients). Spearman's rank was used to measure associations between variables (trend lines were least-squares fits of straight-line models).

Table 3. *Pressure-volume loop determinants of RA phasic function in univariate and multivariable linear regression analysis*

	RA Reservoir Strain		RA Passive Strain		RA Active Strain	
	B-coefficient (95% CI)*	*P*	B-coefficient (95% CI)*	*P*	B-coefficient (95% CI)*	*P*
Univariate						
E_a, mmHg/mL	−4.80 (−12.39 to 2.79)	0.210	−3.39 (−7.11 to 0.34)	0.074	−2.57 (−7.43 to 2.29)	0.292
E_{es}, mmHg/mL	3.06 (−3.50 to 9.61)	0.353	2.27 (−0.93 to 5.47)	0.160	2.48 (−1.62 to 6.58)	0.229
E_{es}-to-E_a ratio	5.42 (−0.38 to 11.21)	0.066	4.13 (1.32 to 6.95)	0.005	3.81 (0.07 to 7.55)	0.046
E_{ed}, mmHg/mL	−7.84 (−11.68 to −4.00)	<0.001	−3.49 (−5.40 to −1.58)	0.001	−4.76 (−7.16 to −2.36)	<0.001
ESP, mmHg	−9.34 (−19.80 to 1.12)	0.079	−5.60 (−10.84 to −0.37)	0.037	−5.77 (−12.56 to 1.01)	0.094
EDP, mmHg	−11.21 (−16.30 to −6.12)	<0.001	−5.93 (−8.26 to −3.61)	<0.001	−5.87 (−9.18 to −2.56)	<0.001
Multivariate†						
E_{ed}, mmHg					−3.25 (−6.50 to −0.001)	0.050
EDP, mmHg	−7.46 (−14.21 to −0.70)	0.031	−4.67 (−7.96 to −1.37)	0.007		

CI, confidence interval; E_a, arterial elastance; EDP, end-diastolic pressure; E_{ed}, end-diastolic elastance; E_{es}, end-systolic elastance; ESP, end-systolic pressure; RA, right atrial. *Unstandardized coefficients. †Adjusted with backward stepwise selection for pressure-volume loop parameters with $P < 0.05$ in univariate analysis.

significantly associated with a reduction of RA passive strain in univariate analysis. In a multivariate model with RA passive strain as the dependent variable, we found that an increase in EDP was independently associated with a reduction of RA passive strain (Table 3). Moreover, an increase in E_{ed} and EDP and a decrease in E_{es}/E_a were also significantly associated with a reduction of RA active strain in univariate analysis. In multivariate analysis, we found that increased E_{ed} was independently associated with reduced RA active strain (Table 3).

DISCUSSION

The present results show that in the setting of chronic pressure overload, RA phasic performance assessed with CMR feature tracking is predominantly altered in relation to RV diastolic function. Our data suggest that impairment of RV lusitropic function directly influences RA deformation, which in turn may be a cause of increased backward venous flow.

Untreated PH is a progressive disease, with the chronic pressure overload resulting in RV failure and maladaptation characterized by inappropriate RV hypertrophy, dilatation, fibrosis, remodeling, and impairment of both systolic and diastolic function (28, 45). The effect of progressive RV dysfunction on RA phasic performance remains incompletely understood and is therefore among the research areas open for exploration by advanced imaging of the right heart combined with state-of-the-art invasive functional assessment, as recently mentioned by an American Thoracic Society Research Statement (18). Our study provides further insights into this topic as we directly measured load-independent RV function via the acquisition of RV P-V loops with the assessment of E_{ed} as a measure of RV diastolic stiffness (33, 44), E_a as a lumped parameter of afterload (43), E_{es} as a marker of load-independent contractility (43), and E_{es}/E_a to describe RV-arterial coupling (43).

Impairment of RA phasic function was predominantly related to alterations of RV lusitropy rather than RV contractility or coupling as assessed by invasive measurements of P-V relationships. In the course of pulmonary hypertension, the right ventricle adapts either through homeometric adaptation (increased contractility) or through heterometric adaptation (increased volumes) to maintain stroke volume. At a certain threshold of E_{es}/E_a (recently shown to be 0.805), E_{es} decreases (with no further possibility to increase) and E_{ed} increases (38). Median [interquartile range] E_{es}/E_a in our present study was 0.73 [0.48–1.08]. Therefore, one of the possible explanations for the lack of association of E_{es}/E_a with RA strain parameters is that most of the patients had surpassed the "point of uncoupling" of 0.805.

Altered RA phasic function may be a cause and consequence of RV stiffness and increased EDP; the direction of causality is not clear. Similar to the right ventricle, the right atrium appears to respond to increased loading by both increased dimension and increased contractility to boost RV filling (10, 11) until excessive RA dilation and stiffness occurs, with subsequent RA-RV "uncoupling." Therefore, the observed association between RV diastolic stiffness and RA phasic function is consistent with the fact that RV myocardial stiffening leads to reduced passive inflow and a backward diastolic flow, impairing early diastolic filling and causing a large proportion of RV filling to be dependent on the final atrial contraction (2, 5). When atrial function is impaired, there is increased backward venous flow and subsequent deterioration of clinical signs of RV failure. Our data show significant correlations of RA phasic strain with RA size and inferior vena cava diameter, indicating that loss of reservoir function leads to backward venous flow. This is supported by recent data from Marcus et al., who measured load-independent RV parameters using a modified method without P-V loops and showed an association of backward venous flow during atrial contraction with RV diastolic stiffness (21). Although the main cause for venous backflow seems to be RV diastolic stiffness rather than RV-arterial uncoupling, the latter might contribute indirectly by first leading to elevation of RV volumes, with significant elevation of diastolic stiffness occurring as a second step.

Our findings are consistent with previous studies of RA strain demonstrating the prognostic relevance of RA reservoir function (14) and showing significant associations of RA

phasic function with RAP (assessed via echocardiography; 48), disease severity (WHO functional class; 22), and outcome (1, 3). Of note, we also observed a significant association with left ventricular EF. However, the extent to which alterations in RA phasic function might contribute to ventricular interdependency (23) deserves further investigation.

The present results are also consistent with a previous demonstration of impaired echocardiography-derived RA reservoir function (longitudinal strain) that was not correlated with mPAP or PVR in patients with PAH (26). However, a study in pediatric patients with PAH reported significant associations of echocardiography-derived RA reservoir function with PVR and mPAP as well as echocardiography-derived systolic parameters (tricuspid annular plane systolic excursion, fractional area change, and RV reservoir strain; 15). The reasons for these discrepancies are difficult to assess but may be further elucidated by more robust CMR imaging studies.

Limitations. We used a single-beat method rather than a multibeat method to estimate E_{ed}, E_{es}, and E_a. It is unclear whether this would affect the results, as the single-beat method was recently validated against the multibeat method (30). The sample size precluded meaningful race- and sex-specific analysis but was reasonable given the demanding methodology. The study population showed a near-equal distribution between women and men. Interestingly, our cohort is quite comparable to that of the Swedish Pulmonary Arterial Hypertension Registry, which has been published recently (17). Absence of female predominance in the present study may be related to sample size and yet-unclear evolution of referral biases (17). Diastolic echocardiographic indexes of ventricular function were not assessed and need further evaluation since echocardiography is more accessible than CMR in most PH centers. Also, information of RV function is provided by longitudinal RV shortening; the association of RA and RV feature tracking deserves further investigation in dedicated studies. Our limited sample size affected the regression analysis. The lack of a control group is another limitation to our study.

Of note, our analyses were performed with CMR feature tracking of the RA in the four-chamber view as previously published by other groups (19, 47). However, higher reliability and validity may have been achieved with a second plane in analyzing RA strain. Furthermore, there is a lack of standardization of the terms used to describe RA function. We used the terms "active," "passive," and "reservoir" strain, whereas some groups use "booster," "conduit," and/or "total" strain as corresponding terms (14, 19). Standardization of the methods and nomenclature would contribute to a better understanding of RA strain.

Conclusion. In the setting of chronic pressure overload, impaired RV diastolic function appears to be the dominant determinant of altered RA phasic performance, which in turn contributes to backward venous flow and systemic congestion. These observations call for improved therapeutic strategies targeting the RA-RV axis.

ACKNOWLEDGMENTS

For the manuscript, editorial assistance was provided by Claire Mulligan (Beacon Medical Communications Ltd., Brighton, UK).

GRANTS

This work was funded by the Excellence Cluster Cardio-Pulmonary System and by Deutsche Forschungsgemeinschaft (German Research Foundation) Projektnummer 268555672, Sonderforschungsbereich 1213, Project B08. Editorial assistance was funded by the University of Giessen.

DISCLOSURES

K. Tello has received speaking fees from Actelion and Bayer. H. A. Ghofrani has received consultancy fees from Bayer, Actelion, Pfizer, Merck, GSK, and Novartis; fees for participation in advisory boards from Bayer, Pfizer, GSK, Actelion, and Takeda; lecture fees from Bayer HealthCare, GSK, Actelion, and Encysive/Pfizer; industry-sponsored grants from Bayer HealthCare, Aires, Encysive/Pfizer, and Novartis; and sponsored grants from the German Research Foundation, Excellence Cluster Cardiopulmonary Research, and the German Ministry for Education and Research. R. Naeije has relationships with drug companies including AOPOrphan Pharmaceuticals, Actelion, Bayer, Reata, Lung Biotechnology Corporation, and United Therapeutics. In addition to being an investigator in trials involving these companies, relationships include consultancy service, research grants, and membership of scientific advisory boards. W. Seeger has received speaker/consultancy fees from Pfizer, Bayer Pharma AG, United Therapeutics, and Liquidia. H. Gall has received fees from Actelion, AstraZeneca, Bayer, BMS, GSK, Janssen-Cilag, Lilly, MSD, Novartis, OMT, Pfizer, and United Therapeutics. M. J. Richter has received support from United Therapeutics and Bayer; speaker fees from Actelion, Mundipharma, Roche, and OMT; and consultancy fees from Bayer. None of the other authors has any conflicts of interest, financial or otherwise, to disclose.

AUTHOR CONTRIBUTIONS

K.T., H.A.G., W.S., H.G., and M.J.R. conceived and designed research; K.T., A.D., F.R., W.S., M.W., H.G., and M.J.R. performed experiments; K.T., A.D., R.V., H.A.G., R.N., F.R., W.S., H.G., and M.J.R. analyzed data; K.T., A.D., R.V., H.A.G., R.N., F.R., W.S., M.W., H.G., and M.J.R. interpreted results of experiments; K.T. and M.J.R. prepared figures; K.T., A.D., R.V., H.A.G., R.N., F.R., W.S., M.W., H.G., and M.J.R. drafted manuscript; K.T., A.D., R.V., H.A.G., R.N., F.R., W.S., M.W., H.G., and M.J.R. edited and revised manuscript; K.T., A.D., R.V., H.A.G., R.N., F.R., W.S., M.W., H.G., and M.J.R. approved final version of manuscript.

REFERENCES

1. **Alenezi F, Mandawat A, Il'Giovine ZJ, Shaw LK, Siddiqui I, Tapson VF, Arges K, Rivera D, Romano MM, Velazquez EJ, Douglas PS, Samad Z, Rajagopal S.** Clinical utility and prognostic value of right atrial function in pulmonary hypertension. *Circ Cardiovasc Imaging* 11: e006984, 2018. doi:10.1161/CIRCIMAGING.117.006984.
2. **Andersen S, Nielsen-Kudsk JE, Vonk Noordegraaf A, de Man FS.** Right ventricular fibrosis. *Circulation* 139: 269–285, 2019. doi:10.1161/CIRCULATIONAHA.118.035326.
3. **Bhave NM, Visovatti SH, Kulick B, Kolias TJ, McLaughlin VV.** Right atrial strain is predictive of clinical outcomes and invasive hemodynamic data in group 1 pulmonary arterial hypertension. *Int J Cardiovasc Imaging* 33: 847–855, 2017. doi:10.1007/s10554-017-1081-7.
4. **Brimioulle S, Wauthy P, Ewalenko P, Rondelet B, Vermeulen F, Kerbaul F, Naeije R.** Single-beat estimation of right ventricular end-systolic pressure-volume relationship. *Am J Physiol Heart Circ Physiol* 284: H1625–H1630, 2003. doi:10.1152/ajpheart.01023.2002.
5. **Burlew BS, Weber KT.** Cardiac fibrosis as a cause of diastolic dysfunction. *Herz* 27: 92–98, 2002. doi:10.1007/s00059-002-2354-y.
6. **Crowe T, Jayasekera G, Peacock AJ.** Non-invasive imaging of global and regional cardiac function in pulmonary hypertension. *Pulm Circ* 8: 2045893217742000, 2018. doi:10.1177/2045893217742000.
7. **Fukuda Y, Tanaka H, Ryo-Koriyama K, Motoji Y, Sano H, Shimoura H, Ooka J, Toki H, Sawa T, Mochizuki Y, Matsumoto K, Emoto N, Hirata K.** Comprehensive functional assessment of right-sided heart using speckle tracking strain for patients with pulmonary hypertension. *Echocardiography* 33: 1001–1008, 2016. doi:10.1111/echo.13205.
8. **Galiè N, Humbert M, Vachiery JL, Gibbs S, Lang I, Torbicki A, Simonneau G, Peacock A, Vonk Noordegraaf A, Beghetti M, Ghofrani A, Gomez Sanchez MA, Hansmann G, Klepetko W, Lancellotti P, Matucci M, McDonagh T, Pierard LA, Trindade PT, Zompatori M, Hoeper M.** 2015 ESC/ERS Guidelines for the diagnosis and treatment of pulmonary hypertension: The Joint Task Force for the Diagnosis and Treatment of Pulmonary Hypertension of the European Society of Cardiology (ESC) and the European Respiratory Society (ERS): Endorsed by: Association for European Paediatric and Congenital Cardiology (AEPC),

International Society for Heart and Lung Transplantation (ISHLT). *Eur Respir J* 46: 903–975, 2015. [Erratum in *Eur J Respir* 46: 1855–1856, 2015.] doi:10.1183/13993003.01032-2015.

9. **Gall H, Felix JF, Schneck FK, Milger K, Sommer N, Voswinckel R, Franco OH, Hofman A, Schermuly RT, Weissmann N, Grimminger F, Seeger W, Ghofrani HA.** The Giessen Pulmonary Hypertension Registry: survival in pulmonary hypertension subgroups. *J Heart Lung Transplant* 36: 957–967, 2017. doi:10.1016/j.healun.2017.02.016.
10. **Gaynor SL, Maniar HS, Bloch JB, Steendijk P, Moon MR.** Right atrial and ventricular adaptation to chronic right ventricular pressure overload. *Circulation* 112, *Suppl*: I212–I218, 2005. doi:10.1161/CIRCULATIONAHA.104.517789.
11. **Gaynor SL, Maniar HS, Prasad SM, Steendijk P, Moon MR.** Reservoir and conduit function of right atrium: impact on right ventricular filling and cardiac output. *Am J Physiol Heart Circ Physiol* 288: H2140–H2145, 2005. doi:10.1152/ajpheart.00566.2004.
12. **Hsu S.** Coupling right ventricular-pulmonary arterial research to the pulmonary hypertension patient bedside. *Circ Heart Fail* 12: e005715, 2019. doi:10.1161/CIRCHEARTFAILURE.118.005715.
13. **Jaijee S, Quinlan M, Tokarczuk P, Clemence M, Howard LS, Gibbs JS, O'Regan DP.** Exercise cardiac MRI unmasks right ventricular dysfunction in acute hypoxia and chronic pulmonary arterial hypertension. *Am J Physiol Heart Circ Physiol* 315: H950–H957, 2018. doi:10.1152/ajpheart.00146.2018.
14. **Jain S, Kuriakose D, Edelstein I, Ansari B, Oldland G, Gaddam S, Javaid K, Manaktala P, Lee J, Miller R, Akers SR, Chirinos JA.** Right atrial phasic function in heart failure with preserved and reduced ejection fraction. *JACC Cardiovasc Imaging* 12: 1460–1470, 2019. doi:10.1016/j.jcmg.2018.08.020.
15. **Jone PN, Schäfer M, Li L, Craft M, Ivy DD, Kutty S.** Right atrial deformation in predicting outcomes in pediatric pulmonary hypertension. *Circ Cardiovasc Imaging* 10: e006250, 2017. doi:10.1161/CIRCIMAGING.117.006250.
16. **Kiely DG, Levin D, Hassoun P, Ivy DD, Jone PN, Bwika J, Kawut SM, Lordan J, Lungu A, Mazurek J, Moledina S, Olschewski H, Peacock A, Puri GD, Rahaghi F, Schafer M, Schiebler M, Screaton N, Tawhai M, Van Beek EJ, Vonk-Noordegraaf A, Vanderpool RR, Wort J, Zhao L, Wild J, Vogel-Claussen J, Swift AJ.** Statement on imaging and pulmonary hypertension from the Pulmonary Vascular Research Institute (PVRI). *Pulm Circ* 9: 2045894019841990, 2019. doi:10.1177/2045894019841990.
17. **Kjellström B, Nisell M, Kylhammar D, Bartfay SE, Ivarsson B, Rådegran G, Hjalmarsson C.** Sex-specific differences and survival in patients with idiopathic pulmonary arterial hypertension 2008–2016. *ERJ Open Res* 5: 00075-2019, 2019. [Erratum in *ERJ Open Res* 5: 00075-2019-ERR, 2019]. doi:10.1183/23120541.00075-2019.
18. **Lahm T, Douglas IS, Archer SL, Bogaard HJ, Chesler NC, Haddad F, Hemnes AR, Kawut SM, Kline JA, Kolb TM, Mathai SC, Mercier O, Michelakis ED, Naeije R, Tuder RM, Ventetuolo CE, Vieillard-Baron A, Voelkel NF, Vonk-Noordegraaf A, Hassoun PM; American Thoracic Society Assembly on Pulmonary Circulation.** Assessment of right ventricular function in the research setting: knowledge gaps and pathways forward. an official American Thoracic Society Research Statement. *Am J Respir Crit Care Med* 198: e15–e43, 2018. doi:10.1164/rccm.201806-1160ST.
19. **Leng S, Dong Y, Wu Y, Zhao X, Ruan W, Zhang G, Allen JC, Koh AS, Tan RS, Yip JW, Tan JL, Chen Y, Zhong L.** Impaired cardiovascular magnetic resonance-derived rapid semiautomated right atrial longitudinal strain is associated with decompensated hemodynamics in pulmonary arterial hypertension. *Circ Cardiovasc Imaging* 12: e008582, 2019. doi:10.1161/CIRCIMAGING.118.008582.
20. **Lindsey ML, Gray GA, Wood SK, Curran-Everett D.** Statistical considerations in reporting cardiovascular research. *Am J Physiol Heart Circ Physiol* 315: H303–H313, 2018. doi:10.1152/ajpheart.00309.2018.
21. **Marcus JT, Westerhof BE, Groeneveldt JA, Bogaard HJ, de Man FS, Vonk Noordegraaf A.** Vena cava backflow and right ventricular stiffness in pulmonary arterial hypertension. *Eur Respir J* 54: 1900625, 2019. doi:10.1183/13993003.00625-2019.
22. **Meng X, Li Y, Li H, Wang Y, Zhu W, Lu X.** Right atrial function in patients with pulmonary hypertension: a study with two-dimensional speckle-tracking echocardiography. *Int J Cardiol* 255: 200–205, 2018. doi:10.1016/j.ijcard.2017.11.093.
23. **Naeije R, Badagliacca R.** The overloaded right heart and ventricular interdependence. *Cardiovasc Res* 113: 1474–1485, 2017. doi:10.1093/cvr/cvx160.
24. **Padeletti M, Cameli M, Lisi M, Malandrino A, Zacà V, Mondillo S.** Reference values of right atrial longitudinal strain imaging by two-dimensional speckle tracking. *Echocardiography* 29: 147–152, 2012. doi:10.1111/j.1540-8175.2011.01564.x.
25. **Petersen SE, Aung N, Sanghvi MM, Zemrak F, Fung K, Paiva JM, Francis JM, Khanji MY, Lukaschuk E, Lee AM, Carapella V, Kim YJ, Leeson P, Piechnik SK, Neubauer S.** Reference ranges for cardiac structure and function using cardiovascular magnetic resonance (CMR) in Caucasians from the UK Biobank population cohort. *J Cardiovasc Magn Reson* 19: 18, 2017. doi:10.1186/s12968-017-0327-9.
26. **Querejeta Roca G, Campbell P, Claggett B, Solomon SD, Shah AM.** Right atrial function in pulmonary arterial hypertension. *Circ Cardiovasc Imaging* 8: e003521, 2015. doi:10.1161/CIRCIMAGING.115.003521.
27. **Raymond RJ, Hinderliter AL, Willis PW IV, Ralph D, Caldwell EJ, Williams W, Ettinger NA, Hill NS, Summer WR, de Boisblanc B, Schwartz T, Koch G, Clayton LM, Jöbsis MM, Crow JW, Long W.** Echocardiographic predictors of adverse outcomes in primary pulmonary hypertension. *J Am Coll Cardiol* 39: 1214–1219, 2002. doi:10.1016/S0735-1097(02)01744-8.
28. **Ren X, Johns RA, Gao WD.** Right heart in pulmonary hypertension: from adaptation to failure. *Pulm Circ* 9: 2045894019845611, 2019. doi:10.1177/2045894019845611.
29. **Richter MJ, Grimminger J, Krüger B, Ghofrani HA, Mooren FC, Gall H, Pilat C, Krüger K.** Effects of exercise training on pulmonary hemodynamics, functional capacity and inflammation in pulmonary hypertension. *Pulm Circ* 7: 20–37, 2017. doi:10.1086/690553.
30. **Richter MJ, Peters D, Ghofrani HA, Naeije R, Roller F, Sommer N, Gall H, Grimminger F, Seeger W, Tello K.** Evaluation and prognostic relevance of right ventricular-arterial coupling in pulmonary hypertension. *Am J Respir Crit Care Med*. 2019 Sep 20. doi:10.1164/rccm.201906-1195LE.
31. **Rose L, Prins KW, Archer SL, Pritzker M, Weir EK, Misialek JR, Thenappan T.** Survival in pulmonary hypertension due to chronic lung disease: Influence of low diffusion capacity of the lungs for carbon monoxide. *J Heart Lung Transplant* 38: 145–155, 2019. doi:10.1016/j.healun.2018.09.011.
32. **Sakata K, Uesugi Y, Isaka A, Minamishima T, Matsushita K, Satoh T, Yoshino H.** Evaluation of right atrial function using right atrial speckle tracking analysis in patients with pulmonary artery hypertension. *J Echocardiogr* 14: 30–38, 2016. doi:10.1007/s12574-015-0270-4.
33. **Sanz J, Kariisa M, Dellegrottaglie S, Prat-González S, Garcia MJ, Fuster V, Rajagopalan S.** Evaluation of pulmonary artery stiffness in pulmonary hypertension with cardiac magnetic resonance. *JACC Cardiovasc Imaging* 2: 286–295, 2009. doi:10.1016/j.jcmg.2008.08.007.
34. **Sanz J, Sánchez-Quintana D, Bossone E, Bogaard HJ, Naeije R.** Anatomy, function, and dysfunction of the right ventricle: JACC state-of-the-art review. *J Am Coll Cardiol* 73: 1463–1482, 2019. doi:10.1016/j.jacc.2018.12.076.
35. **Sato T, Tsujino I, Ohira H, Oyama-Manabe N, Ito YM, Yamada A, Ikeda D, Watanabe T, Nishimura M.** Right atrial volume and reservoir function are novel independent predictors of clinical worsening in patients with pulmonary hypertension. *J Heart Lung Transplant* 34: 414–423, 2015. doi:10.1016/j.healun.2015.01.984.
36. **Simonneau G, Montani D, Celermajer DS, Denton CP, Gatzoulis MA, Krowka M, Williams PG, Souza R.** Haemodynamic definitions and updated clinical classification of pulmonary hypertension. *Eur Respir J* 53: 1801913, 2019. doi:10.1183/13993003.01913-2018.
37. **Stam K, van Duin RW, Uitterdijk A, Cai Z, Duncker DJ, Merkus D.** Exercise facilitates early recognition of cardiac and vascular remodeling in chronic thromboembolic pulmonary hypertension in swine. *Am J Physiol Heart Circ Physiol* 314: H627–H642, 2018. doi:10.1152/ajpheart.00380.2017.
38. **Tello K, Dalmer A, Axmann J, Vanderpool R, Ghofrani HA, Naeije R, Roller F, Seeger W, Sommer N, Wilhelm J, Gall H, Richter MJ.** Reserve of right ventricular-arterial coupling in the setting of chronic overload. *Circ Heart Fail* 12: e005512, 2019. doi:10.1161/CIRCHEARTFAILURE.118.005512.
39. **Tello K, Dalmer A, Husain-Syed F, Seeger W, Naeije R, Ghofrani HA, Gall H, Richter MJ.** Multibeat right ventricular-arterial coupling during a positive acute vasoreactivity test. *Am J Respir Crit Care Med* 199: e41–e42, 2019. doi:10.1164/rccm.201809-1787IM.
40. **Tello K, Dalmer A, Vanderpool R, Ghofrani HA, Naeije R, Roller F, Seeger W, Dumitrescu D, Sommer N, Brunst A, Gall H, Richter MJ.** Impaired right ventricular lusitropy is associated with ventilatory ineffi-

ciency in PAH. *Eur Respir J* 54: 1900342, 2019. doi:10.1183/13993003.00342-2019.

41. **Tello K, Dalmer A, Vanderpool R, Ghofrani HA, Naeije R, Roller F, Seeger W, Wilhelm J, Gall H, Richter MJ.** Cardiac magnetic resonance imaging-based right ventricular strain analysis for assessment of coupling and diastolic function in pulmonary hypertension. *JACC Cardiovasc Imaging* 12: 2155–2164, 2019. doi:10.1016/j.jcmg.2018.12.032.
42. **Tello K, Richter MJ, Axmann J, Buhmann M, Seeger W, Naeije R, Ghofrani HA, Gall H.** More on single-beat estimation of right ventriculoarterial coupling in pulmonary arterial hypertension. *Am J Respir Crit Care Med* 198: 816–818, 2018. doi:10.1164/rccm.201802-0283LE.
43. **Tello K, Seeger W, Naeije R, Vanderpool R, Ghofrani HA, Richter M, Tedford RJ, Bogaard HJ.** Right heart failure in pulmonary hypertension: diagnosis and new perspectives on vascular and direct right ventricular treatment. *Br J Pharmacol*. 2019 Sep 13. doi:10.1111/bph.14866.
44. **Vanderpool RR, Puri R, Osorio A, Wickstrom K, Desai A, Black S, Garcia JG, Yuan J, Rischard F.** Surfing the right ventricular pressure waveform: methods to assess global, systolic and diastolic RV function from a clinical right heart catheterization. *Pulm Circ*. 2019 Apr 29. doi:10.1177/2045894019850993.
45. **Vonk Noordegraaf A, Chin KM, Haddad F, Hassoun PM, Hemnes AR, Hopkins SR, Kawut SM, Langleben D, Lumens J, Naeije R.** Pathophysiology of the right ventricle and of the pulmonary circulation in pulmonary hypertension: an update. *Eur Respir J* 53: 1801900, 2019. doi:10.1183/13993003.01900-2018.
46. **Vonk Noordegraaf A, Westerhof BE, Westerhof N.** The relationship between the right ventricle and its load in pulmonary hypertension. *J Am Coll Cardiol* 69: 236–243, 2017. doi:10.1016/j.jacc.2016.10.047.
47. **von Roeder M, Kowallick JT, Rommel KP, Blazek S, Besler C, Fengler K, Lotz J, Hasenfuß G, Lücke C, Gutberlet M, Thiele H, Schuster A, Lurz P.** Right atrial-right ventricular coupling in heart failure with preserved ejection fraction. *Clin Res Cardiol*. 2019 May 3. doi:10.1007/s00392-019-01484-0.
48. **Wright LM, Dwyer N, Wahi S, Marwick TH.** Association with right atrial strain with right atrial pressure: an invasive validation study. *Int J Cardiovasc Imaging* 34: 1541–1548, 2018. doi:10.1007/s10554-018-1368-3.

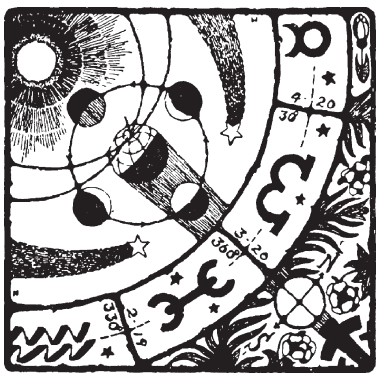

Danksagung

Ohne die Unterstützung zahlreicher Personen hätte diese Arbeit in dieser Form nicht realisiert werden können. Für die vielfältig erfahrene Hilfe möchte ich mich an dieser Stelle sehr herzlich bedanken.

Mein besonderer Dank gilt Prof. Dr. Werner Seeger für die jederzeit großartige Unterstützung, für die vielfältige und hilfreiche Beratung und die motivierenden Worte in schwierigen Zeiten der Erarbeitung der Forschungsergebnisse. Allen Patienten, die an den Studien teilgenommen haben, die verlängerte Untersuchungszeiten in Kauf genommen und teilweise zusätzliche invasive Untersuchungen im Sinne der Forschung haben durchführen lassen, gebührt unendlicher Dank und größter Respekt.

Für die klinische Ausbildung, die Grundlage der Forschungsarbeit ist, bedanke ich mich herzlich bei Prof Dr Hans-Dieter Walmrath. Prof Dr Ardeschir Ghofrani, Dr Manuel Richter und PD. Dr. Dr. Henning Gall haben zu jederzeit mit Rat und Tat zur Lösung aufkommender Probleme beigetragen.

Für die besondere Organisation der Untersuchungen sei Susanne Wissgott gedankt, die zusätzlich für die gute Betreuung der Patienten gesorgt hat.

Der größte Dank gebührt meiner Frau Silke. Ohne die unermüdliche Unterstützung, das Verständnis und die ausserordentlich gute Beratung wäre diese Arbeit nicht zustande gekommen.